The role of tetraspanins in multinucleated giant cell formation induced by *Burkholderia thailandensis*

A thesis submitted in partial fulfilment of the requirements for the degree of
Doctor of Philosophy

By:

Atiga Mohamed Elgawidi

Department of Molecular biology and Biotechnology

The University of Sheffield

February 2016

Summary

The tetraspanins are a superfamily of transmembrane proteins with a wide distribution in multicellular organisms. Tetraspanins have been involved in many cellular functions including adhesion, migration and the immune response. Tetraspanins are considered as cell membrane organizers and their function is likely to be due the ability to interact with cell membrane proteins. These interactions lead to them forming a large extended network known as tetraspanin enriched microdomains (TEM) or the tetraspanin web. There is growing evidence for the role of some tetraspanins in various fusion events including sperm-egg fusion, viral-cell fusion and monocyte fusion.

Monocyte/macrophage fusion is associated with chronic inflammation and is thought to be important for immune defence. Monocyte fusion leading to multinucleated giant cell formation (MNGC) has been linked with the pathogenesis of *Burkholderia pseudomallei* a causative agent of melioidosis disease, a severe invasive disease endemic in south Asia and North Australia. However the mechanism of *B.p*-induced MNGC formation is unclear.

The role of tetraspanins in MNGC formation has been demonstrated previously. Antibodies to CD9 and CD81 enhanced the fusion of con A stimulated peripheral blood monocytes and the deletion of CD9/CD81 resulted in enhanced MNGC formation in vivo and in vitro. In addition recombinant proteins of tetraspanin large extracellular domain (EC2) of CD9 inhibited MNGC formation, suggesting that CD9 and CD81 are negatively regulating monocyte fusion (Takeda et al., 2003). These finding were confirmed by our research group, who also reported that CD63 is involved in this process as anti CD63 antibodies and CD63 EC2 proteins inhibited Con A-stimulated monocyte fusion whereas CD151 EC2 and CD82 EC2 had no effect (Parthasarathy et al., 2009).

This thesis describes attempts made to investigate the role of tetraspanins in MNGC formation induced by *B.thailandensis*, a non-pathogenic species that is closely related to *B.pseudomallei* and widely used as a model to study *B.p* features. Using antibodies to tetraspanins, recombinant EC2 proteins, and tetraspanin deficient cell lines we found that tetraspanins are involved in *B.thailandensis*-induced cell fusion. Our data is partly in line with previous findings: antibodies to CD9 and CD81 enhanced MNGC formation, whereas CD9 EC2 and CD63 EC2 proteins inhibit fusion. In contrast with other results mentioned above, we found that CD81 EC2 proteins also inhibited *B.t*-induced fusion. The deletion of CD9 and CD82 resulted in an enhanced MNGC formation, confirming that CD9 negatively promotes *B.t*-induced cell fusion and suggesting the involvement of CD82 in this process. Further investigation revealed that the absence of tetraspanins could affect the expression level of other cell surface molecules that have been implicated in fusion at the protein level but not at the gene level, which may be relevant to their role as cell membrane organisers. The role of some of these molecules in *B.t*-induced fusion was also investigated in this study.

Several studies showed that *Burkholderia* induced MNGC formation is facilitated by bacterial effectors, which bring the plasma membrane of infected cells to very close position where they can spread from one cell to another. It is likely that the bacteria regulate this process by affecting the expression of host cell membrane molecules including tetraspanins.

Acknowledgments

Abbreviations

ADAM	A disintegrin and metalloproteinase
APCs)	antigen-presenting cells
B.c	*Burkholderia cepacia*
B.m	*Burkholderia mallei*
B.p	*Burkholderia pseudomallei*
B.t	*Burkholderia thailandensis*
BCC	Burkholderia cepacia complex
BimA	Burkholderia invasion/intracellular motility A
BoaA	Burkholderia oligomeric adhesin A
BopE	T3SS-3 secreted effector proteins
C3b	Complement factor
CHAPS	3-[(3-cholamidopropyl) dimethylammonio]-1-propane sulphonate
CD9P-1	Immunoglobulin superfamily member
DAP12	Signaling adaptor protein
DC-SIGN	Dendritic Cell-Specific Intercellular adhesion molecule-3-Grabbing Non-integrin
DC-STAMP	Dendritic cell-specific transmembrane protein
EC1	A small extracellular loop
EC2	A large extracellular loop
FBGCs	Foreign body giant cells
FIV	Feline immunodeficiency virus
gp120	HIV-envelope protein
GPCR	G-protein coupled receptor
HCV	Hepatitis C virus
HCV-E1 and E2	HCV envelope proteins
HisF	Histidine
HIV	Human immunodeficiency virus
HPV	Human alpha-papilloma virus
HTLV-1	Human T cell leukaemia virus
ICAM-1	Intercellular adhesion molecular
IFN-γ	Interferon gamma
IL-13	Interleukin-13
IL-4	Interleukin-4
KO	Knockout
LC3	Autophagy marker protein
LGCs	Langhans' giant cells
LPS	Bacterial lipopolysaccharide
M1	Classic 1-activated macrophage
M2	Classic 2-activated macrophage
MCSF	Macrophage colony stimulating factor

MHC	Major histocompatibility complex
MIP	Macrophage inflammatory proteins
MMP-9	Matrix metalloproteinase
MNGC	Multinucleated giant cell
MOI	Multiplicity of infection
NK	Natural killer cell
NOD2	Refers to the nucleotide-binding oligomerization domain-containing protein 2
OD	Optical density
OPG	Osteoprotegerin
PabB	Para-aminobenzoate
PBE	The plant-associated beneficial and environmental
PCA	Principal component analysis
PE	Parasitized erythrocytes
pilA	*B.p* type IV pilin
PM	Plasma membrane
PRRSV	Porcine Reproductive and Respiratory virus
PS	Phosphatidylserine
PS	Phosphatidylserine
PSG	Pregnancy-specific glycoprotein
PTP-PEST /PTPN12	Cytoplasmic protein tyrosine phosphatase
PurM, PurN	Purine
PXXC	Proline, Xaa, Xaa, cysteine
Pyk2	protein tyrosine kinase
RANKL	Receptor activator of NF-kB ligand
RIN	RNA integrity number
RpoS	*B. pseudomallei* (RNA polymerase sigma factor
STAT	Signal transducer and activator of transcription
T3SS	Type III secretion system
T3SS-3	Type III secretion system cluster 3
T6SS	The type VI secretion system
T6SS-1 Hcp	B. pseudomallei T6SS-1 Hcp protein
TCR	T cell receptor
TCR	T cell receptor
TEM	Tetraspanin enriched microdomains
Th1	Type 1 T helper lymphocytes
Th2	Type 2 T helper lymphocytes
TLR	Toll like receptors
TNF	Tumor-necrosis factor
TRAP	Tartrate-resistant acid phosphatase
UPEC	Uropathogenic *Escherichia coli*
WT	Wild-type

αMβ2, αXβ2,   Integrin proteins
α5β1,αVβ1,α3β1

Contents

Tables and figures

Tables

Figures

Chapter 1 Introduction

1.1 The tetraspanin protein superfamily

Tetraspanins are a superfamily of transmembrane glycoproteins expressed on cell surfaces and intracellular membranes of multiceluar organisms. Different members of the tetraspanins are expressed in nearly all cell types (Hemler, 2003). Tetraspanins have an important role in cell functions such as proliferation, activation, and mobility (Seigneuret et al., 2001, Figdor and van Spriel, 2010, Boucheix et al., 2001), the generation of immune responses, membrane dynamics and fusion, cell migration and invasion (Shearer et al., 1992, Delaguillaumie et al., 2002, Hemler, 2003).

The first member of the superfamily was identified in 1988 as melanoma-associated antigen ME491 (CD63), which had no significant sequence homology with other proteins at the time (Hotta et al., 1988). Later, ME491 was reported to have a similar sequence to the Sm23 protein of the human pathogen *Schistosoma mansoni,* and also to the target of anti-proliferation, TAPA-1 (CD81), first identified on human lymphoma cell lines, and to the B-lymphocyte antigen CD37 (Oren et al., 1990, Classon et al., 1990). Since then, many different members with variable functions and distributions have been discovered and the tetraspanin superfamily has grown to include 33 members in humans, 34 in mouse, 37 in Drosophila, 20 in *Caenorhabditis elegans,* and more than 17 members of the tetraspanin superfamily are expressed in plants (Garcia-Espana et al., 2008, Huang et al., 2005, Todres et al., 2000). The fact that tetraspanin genes have been conserved in animals from nematodes to human cells, suggests that tetraspanin proteins have retained their structure during evolution and play an essential role in cell development (Maecker et al., 1997).

Based on phylogenetic analysis the tetraspanin superfamily can be divided into four subfamilies: the CD family, the CD63 family, the uroplakin family, and the RDS family (Garcia-Espana et al., 2008).

1.1.1 Tetraspanin Structure

Tetraspanins are generally small proteins (25-30 KDa) composed of four hydrophobic transmembrane domains (TM1; TM2; TM3; TM4) forming two extracellular loops of unequal sizes, a small extracellular loop (EC1), which contains 20-28 amino acids and a large extracellular loop (EC2), which contains 76-131 amino acids. The extracellular domains are punctuated by a small intracellular loop, and flanked by short cytoplasmic tails: the C- and N- termini consisting typically of about 19 amino acids or less (Wright and Tomlinson, 1994, Maecker et al., 1997).

Tetraspanins contain highly conserved residues present in both the extracellular and intracellular regions, although intracellular domains are reported to be conserved to a greater extent among species compared to the extracellular domains. For instance, the analysis of CD9, CD81, CD151 and TM4SF2/A15 showed a 43-58% identity in EC1 and EC2, compared to a 72-83% identity in intracellular domains between humans and zebra fish. The large extracellular loops have the greatest sequence diversity between tetraspanin members, and contain important functional sites. In addition almost all of the monoclonal antibodies to tetraspanins recognize EC2 (Stipp et al., 2003).

The most important feature that differentiates tetraspanins from other proteins which contain four transmembrane domains is that tetraspanins contain several highly conserved amino acid residues that are characteristic of their structure and functions. Several cysteine residues in the transmembrane or intracellular regions are considered to be palmitoylation sites, which are important for tetraspanin-tetraspanin complex formation. In addition, there are highly conserved amino acid residues such as asparagine in TM1 and glutamic acid or glutamine in TM3 and TM4, which are thought to be important in stabilising interactions between the TM domains (Wright and Tomlinson, 1994, Maecker et al., 1997). Some tetraspanins also contain a tyrosine-containing sorting motif (YXXØ, where X is any amino acid and Ø is a hydrophobic amino acid) in the C-terminal cytoplasmic domain that may be involved in internalisation or targeting to intracellular vesicles such as lysosomes (Berditchevski and Odintsova, 2007). All tetraspanins also have four cysteine residues in the large extracellular domain, which are essential for disulphide bridge formation and thus for the correct folding of the EC2 region. Two of these are in the highly conserved cysteine-cysteine-glycine motif (C-C-G) found in all family members and the proline, Xaa, Xaa, cysteine (PXXC) motif in found in about 95% of tetraspanins (Levy et al., 1991, Boucheix and Rubinstein, 2001) Figure (1.1.1).
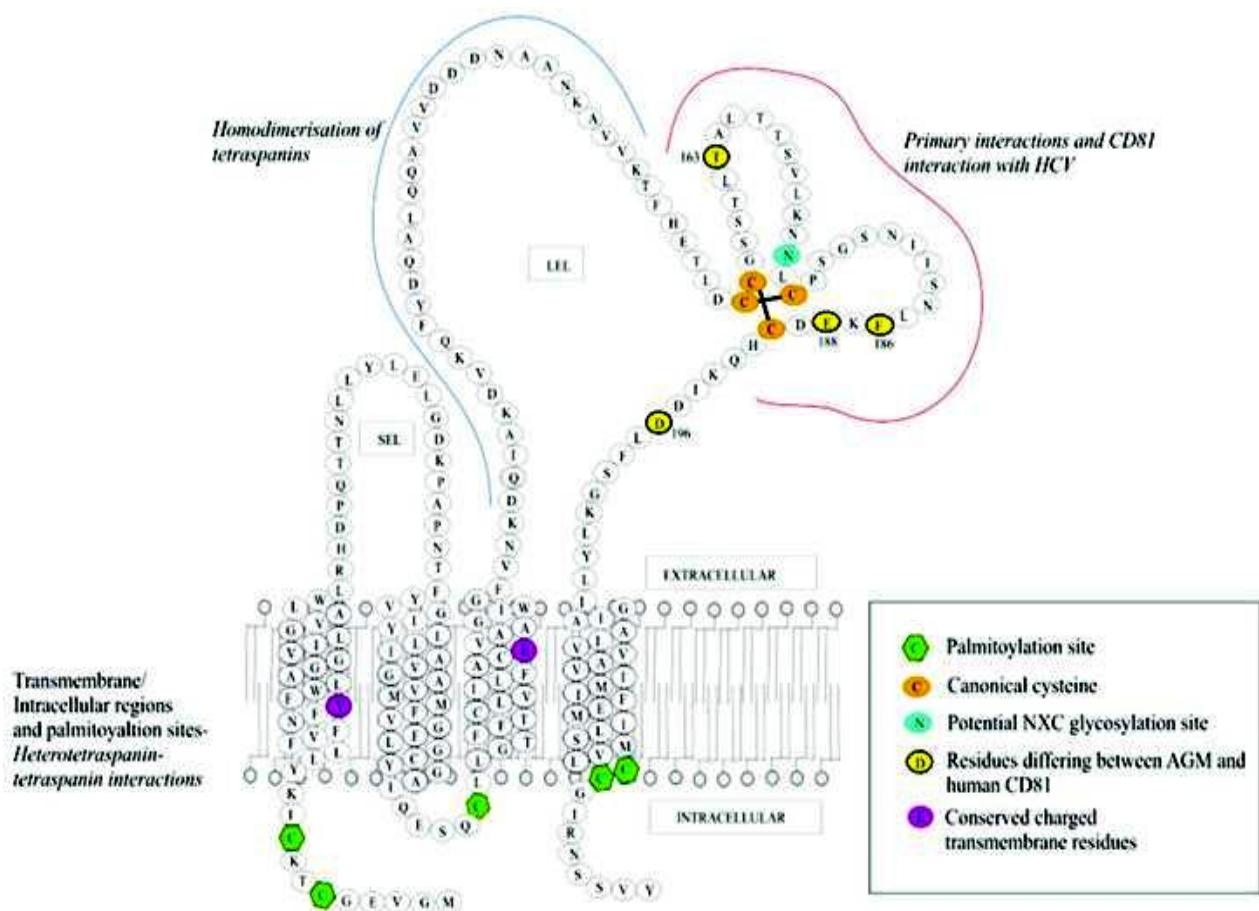
Figure 1.1.1 General structure of a tetraspanin. Tetraspanins consist of four transmembrane helices (1-4), a large EC2 domain and a small EC1 domain, short cytoplasmic N and C termini and a small putativde intracellular loop between transmembran helices 2 and 3. (adapted from a figure provided by Dr P. Monk, Dept. of Infection and Immunity, University of Sheffield).

1.1.1.1 The extracellular domain EC2

Kitadokoro and co-workers have resolved the crystal structure of the large extracellular domain of CD81 at 1.6 Å resolution using recombinant His-tagged human CD81-EC2 (Kitadokoro et al., 2001) figure 1.1.2. *h*CD81-EC2 is organized in a homodimeric structure, consisting of 176 residues and 194 solvent molecules per asymmetric unit. Each subunit in the dimer is composed of five α-helices (A, B, C, D and E), with a short helical segment which covers residues Leu162–Ala164. The α-helices A and E are antiparallel and form the stalk of a mushroom-shaped molecule, with a head subdomain (∼60 residues) that is basically composed of the last two turns of the α helix A, B, C and D-helices and their intervening segments, and the DE loop. There are several specific interactions that stabilize the subunit fold of *h*CD81. The stalk region is held together by hydrophobic contacts along the A- and E-helices and by two salt bridges. The antiparallel pairing of the N- and C-

terminal α-helices allows the two termini of the expressed *h*CD81-LEL to be close to each other (Kitadokoro et al., 2001). The head subdomain is stabilized by the two tetraspanin-invariant disulfide bridges, that are constructed from two adjacent (156 and 157) cysteine residues and extend approximately in opposite directions within the domain, connecting the C-terminal region of the B-helix (Cys156) to the first turn of the E-helix (Cys190), and the BC segment (Cys157) to the CD loop (Cys175). The head sub-domain is also stabilized by the Gly158 and Pro176 residues, which establish specific backbone conformations that accommodate the structure of Cys157–Cys175 disulfide bonds on the CD loop (Kitadokoro et al., 2001).
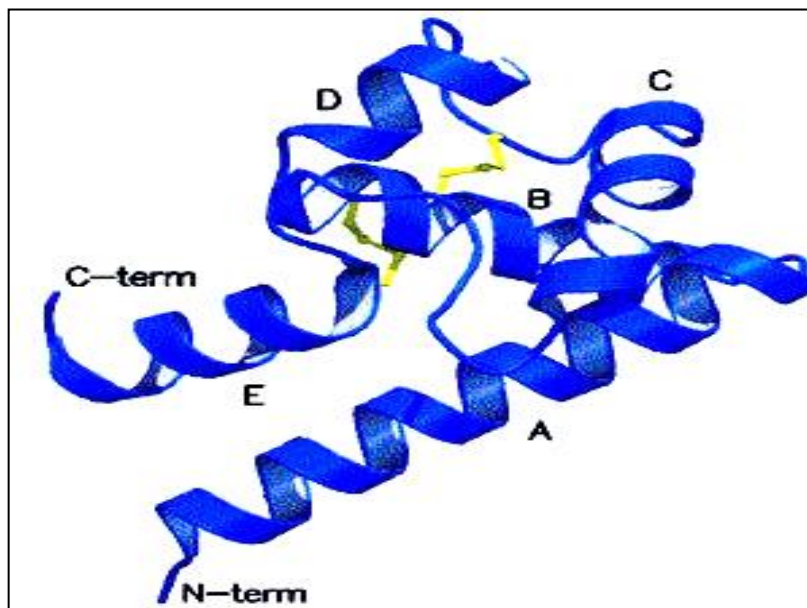
Figure 1.1.2 structure of large extracellular domain EC2 of CD81.
The five alpha helices (A to E). The two disulphide bridges are in yellow. (Kitadokoro et al., 2001)

The CD81 EC2 structure was used as a template for predicting the structure of other tetraspanin EC2s (Seigneuret et al., 2001). This structural comparison study revealed that the CD81 EC2 structural features are conserved partially among tetraspanins. The EC2 is essentially organized in two subdomains: the first subdomain, despite significant sequence diversity, seems to have a structurally conserved fold. A second subdomain, which has higher heterogeneity, is extremely variable in size, secondary structure and fold. The variable subdomain is integrated within the conserved subdomain and their relative topology is controlled by the presence of disulfide bridges. These variable regions are thought to be implicated in tetraspanin interactions, while the conserved region may control dimerisation (Seigneuret et al., 2001). This study also showed that, some tetraspanins have six or eight conserved cysteine residues in EC2 domain forming four disulphide bonds (Seigneuret et al., 2001). Recent NMR study of CD81EC2 suggests that helix D form a highly dynamic loop conformation which is important in CD81/HCV glycoprotein E2 interaction (Rajesh et al., 2012).

1.1.2 Tetraspanin-enriched microdomains (TEMs)

Although tetraspanins are widely expressed in a range of cell and tissue types, their direct functional contributions have not yet been well-classified, and they do not have conventional ligands. However, through the interactions with other membrane proteins, tetraspanins form an extended network termed tetraspanin-enriched microdomains (TEMs) which enable tetraspanins to contribute to many cell functions (Hemler, 2014). There is a huge list of proteins that can be co-immunoprecipitated with tetraspanins including integrins, immunoglobulin superfamily members (for example CD2, CD3, CD4, CD8, MHC proteins), growth factors (e.g. HB-EGF), structural proteins (e.g. claudin), adaptor molecules (e.g. syntenin), signalling molecules (e.g. phosphatidylinositol PI-4- kinase), proteoglycans (e.g. syndecan, CD44) and complement-regulatory proteins (e.g. CD21, CD46). Through these interactions, tetraspanins can be involved in cell processes such as adhesion, invasion, migration, signalling, infection and cell membrane fusion (Hemler, 2005, Boucheix and Rubinstein, 2001). The structure of TEMs is dynamic and their composition and cellular localization is subject to change in response to cell stimulation (Charrin et al., 2009). The size and the structure of TEMs are variable and depend on cell function (Barreiro et al., 2008, Yanez-Mo et al., 2009). The interaction of tetraspanins with vascular cell adhesion protein 1 (VCAM-1) and intercellular adhesion molecular (ICAM-1) on the epithelial cells was found to be important to facilitate their adhesion properties (Barreiro et al., 2008). More advanced and recent technique showed that the possibility of visualization of individual tetraspanin web using super resolution microscopy provide better understanding of molecular mechanism of functions that are promoted by tetraspanins and their protein partners (Zuidscherwoude et al., 2015).

TEM complexes can be classified into three categories depending on their strength and stability in different detergents: primary, or direct interactions, and indirect actions, which may be secondary or tertiary (Boucheix et al., 2001, Tarrant et al., 2003). (Figure 1.1.3).
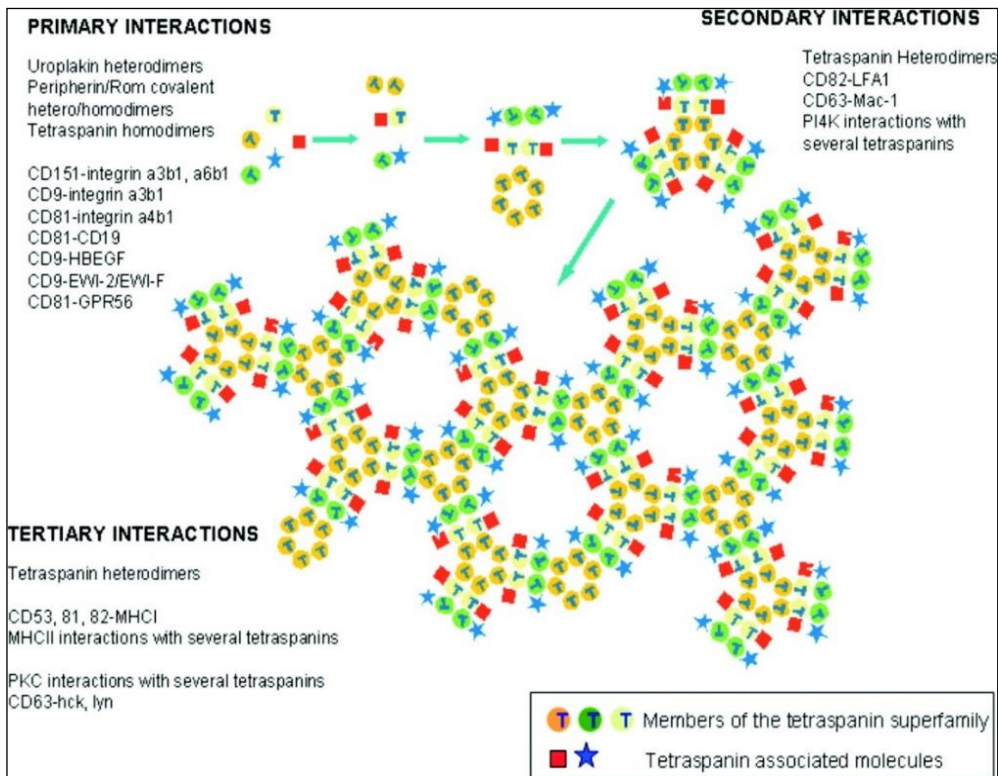
Figure 1.1.3 Interactions of tetraspanins within the tetraspanin web.
(adapted from (Martin et al., 2005))

Class 1 primary interactions are formed by the aggregation of tetraspanin and non-tetraspanin molecules (Boucheix et al., 2001). Some tetraspanins have the ability to associate with different partners in different cell types. For instance, CD81 interacts with the B-lineage-specific molecule CD19 in B cells, whereas in T cells CD81 associates with CD4 and CD8 (Todd et al., 1996). Primary interactions are strong and stable in strong hydrophobic detergents such as Triton X-100 and 1% NP-40. They are also direct, as demonstrated by chemical cross-linking. Such interactions are commonly formed with Ig proteins and integrins (for example CD151 and α3β1 integrins) (Yauch et al., 2000).

Class 2 secondary association involves indirect interactions between tetraspanin members, for instance the associations of CD9, CD81 and CD63 to form hetrobimolecular complexes with a wide range of effects on cell functions (Berditchevski et al., 1996). Secondary interactions are stable in mild detergents such as 1% Brij96 or 1% Brij97 and are stabilised by the presence of divalent cations (Charrin et al., 2002). Palmitoylation sites are normally required in these interactions (Berditchevski et al., 1996, Charrin et al., 2002), as their loss affects tetraspanin associations with other proteins, subcellular distribution, and protein stability during biosynthesis and cell morphology.

In class 3 tertiary interactions, tetraspanins are associated indirectly with additional proteins forming complexes that are disrupted in detergents such as TritonX-100 but retained in mild detergents such as CHAPS (Levy and Shoham, 2005).

1.1.3 Tetraspanin distributions

Some tetraspanins have wide cell and tissue distributions, whereas others are restricted to specific tissues. For example, CD9 has been shown to be expressed in a variety of cell types such as macrophages, eosinophils, basophils, fibroblasts and epithelial cells (Kotha et al., 2008) and its contributions to processes such as cell morphology, adhesion and fusion have been demonstrated (Hemler, 2005, Boucheix et al., 2001). However, tetraspanins such as uroplakins UP1a and UP1b are localised in the urothelium (Sun et al., 1996). In addition, TSSC6, which was detected in embryogenesis in primitive blood cells, is only expressed in haematopoietic cells (Robb et al., 2001). Whilst many tetraspanins are found on the plasma membrane, some are also intracellular. CD63, known as a mainly intracellular tetraspanin, is strongly expressed in platelet lysosomes (Azorsa et al., 1991), in Weibel-Palade bodies of endothelial cells (Vischer and Wagner, 1993) and in the azurophil granules of neutrophil granulocytes (Kuijpers et al., 1991). CD63 has therefore been shown to play an essential role in trafficking. Tetraspanin CD151 is also found in the endosomes of endothelial cells (Sincock et al., 1999). Tetraspanins CD37, CD53, CD63, CD81 and CD82 are expressed in major histocompatibility (MHC) class II-enriched compartments (MIIC) of B lymphocytes (Escola et al., 1998).

1.1.4 Tetraspanin interactions and associated functions

Tetraspanin interactions with partner molecules produce functional units that regulate cell activities and roles in many different cell processes have been identified. The association between CD151 and α3β1 and α6β4 integrins are implicated in regulating cell morphology, adhesion and migration (Karamatic Crew et al., 2004). Many other tetraspanins have been shown to associate to integrins (Hemler, 2003), and their involvement in cell adhesion, migration and invasion is likely to related to very many studies that suggest a role in cancer (Rappa et al., 2015, Hemler, 2014).The full description of all cell function thought to involve tetraspanin is outside the scope of this introduction but their roles in processes relevant to the thesis will be described.

Tetraspanins have been identified as general immune modulators that mediate immune responses through interactions with B cell receptors CD4, CD8, integrins and MHC molecules (van Spriel and Figdor, 2010). In addition to cell function, tetraspanins are involved in infectious diseases caused by bacteria, viruses and fungi (Mollinedo et al., 1997).

1.1.4.1 The role of tetraspanins in immune response

Through their interactions tetraspanins have been implicated in both the innate and adaptive immune responses. Studying mice deficient in CD9 (Le Naour et al., 2000), CD37 (Knobeloch et al., 2000), CD81 (Miyazaki et al., 1997), CD151 (Wright et al., 2004) revealed that, despite leucocytes growing normally in these mice, their functions were affected, particularly in relation to pattern recognition, antigen presentation by DCs and subsequent T-cell activation (Jones et al., 2011b).

Leukocyte-specific tetraspanin CD37 has been found to functionally interact with C-type lectin dectin-1; a pattern-recognition receptor essential for pathogen binding and uptake. CD37 controls dectin-1 stabilization in APC membranes and macrophages of CD37-deficient mice showed decreased dectin-1 membrane levels and increased dectin-1 internalization, whereas transfection of CD37 into a macrophage resulted in increased dectin-1 surface expression. This interaction also controls cytokine production as the absence of CD37 resulted in an increase of dectin-1-induced IL-6 production. This is thought to be the reason for the resistance to *Candida albicans* in CD37 deficient mice (Meyer-Wentrup et al., 2007).

It has been shown that CD9 regulates the response of macrophages upon stimulation with bacterial lipopolysaccharide (LPS). The disruption of CD9 with monoclonal antibody (mAb) treatment, small interfering RNA transfection, or gene knockout in RAW264.7 cells or bone marrow-derived macrophages results in increased pro-inflammatory cytokine production. On macrophages, CD9 expression was shown to interfere with the LPS-induced signaling mediators TLR-4 and CD14. In CD9 knockout macrophages, the expression of CD14 and TLR4 localization into the lipid raft, and their complex formation, were increased in response to LPS. In addition, deletion of CD9 in mice increased macrophage infiltration and TNF-alpha (tumour necrosis factor-alpha) production in the lung after intranasal administration of LPS *in vivo* (Suzuki et al., 2009).

Major histocompatibility complex (MHC) proteins are cell surface molecules whose main function is to bind to peptide fragments derived from pathogens and display them on the cell surface for recognition by the T cell receptor (TCR) on T-cells thus initiating the adaptive immune cell response. The interaction of MHC I and MHC II with tetraspanins CD9, CD37, CD81, CD53, CD63, CD81 and CD82 has been characterized (Szollosi et al., 1996, Schick and Levy, 1993, Angelisova et al., 1994, Engering and Pieters, 2001). These interactions were suggested to indicate an important role for tetraspanins in peptide trafficking and its association with MHC on the cell surface which is an essential step for T cell activation.

The interaction of CD81 with B cell co-receptors CD19 and CD21 is found to be important for B cell activation; the expression of CD81 is essential for CD19 expression as CD81-/- mice showed reduced surface expression of CD19 and reduction in B cell activity (Tsitsikov et al., 1997, Miyazaki et al., 1997, Maecker and Levy, 1997). A complete absence of CD19 expression was also found in an antibody deficiency patient whose CD19 gene was normal but had a mutation in the CD81 gene (van Zelm et al., 2010).

Kaji and co-workers demonstrated that CD9 interacts with Fcγ receptors on macrophages and thus is involved in macrophage activation and function (Kaji et al., 2001). CD9 has been also suggested to be involved in IL-6-regulated chemotaxis and activation of human and mouse mast cells and it is likely to be the primary IL-6 receptor on the surface of human mast cell line HMC-1 (Qi et al., 2006).

1.1.4.2 The role of tetraspanins in bacterial infections

1.1.4.2.1 *Corynebacterium diphtheria*
The involvement of tetraspanins in the pathogenesis of bacterial infections was reported for the first time in diphtheria bacterial toxin binding and sensitivity (Iwamoto et al., 1994). Diphtheria is caused by the bacterium *Corynebacterium diphtheria* that produces the diphtheria toxin DT, a cellular protein synthesis inhibitor (Pappenheimer, 1977). CD9 interacts with pro heparin-binding EGF-like growth factor (proHB-EGF), a diphtheria toxin

receptor on host cells (Mitamura et al., 1992). Via this interaction CD9 may regulate DT binding and endocytosis (Iwamoto et al., 1994).

1.1.4.2.2 Uropathogenic *Escherichia coli* (UPEC)

Tetraspanins have also been implicated in uropathogenic *Escherichia coli* (UPEC) pathogenesis which causes urinary tract infections, the most common form of urinary infections. Type I fimbriae *E. coli* target bladder epithelial cells associated with uroplakins (Wu et al., 1996). It has been found that uroplakin 1a (TSPAN21) and uroplakin 1b (TSPAN 20) are the major proteins in the urothelium, acting as the binding sites for *E.coli* on host cells via the interaction with FimH, the lectin expressed in Type I fimbriae *E. coli* (Zhou et al., 2001, Xie et al., 2006). Internalized UPEC are found in CD63 positive vesicles within the bladder epithelium cells by which mechanism bacteria avoid elimination during voiding (Bishop et al., 2007).

1.1.4.2.3 *Listeria monocytogenes*

Listeria monocytogenes is a food-borne bacterial pathogen that causes listeriosis in pregnant women and meningitis in newborns. Tham and co-workers suggested a role for tetraspanins in bacterial invasion by this species. CD9, CD63 and CD81 were found to be recruited to the bacterial entry site upon infection with *Listeria*. Depletion of CD81 levels by siRNA resulted in inhibited bacterial uptake and impaired the activation and co-localization of PI4KIIalpha, a type II phosphatidylinositol-4-kinase that promotes *Listeria* uptake (Pizarro-Cerda et al., 2007)) to the bacterial entry site. This data suggested that CD81 may act as a membrane organizer that facilitates *Listeria* entry (Tham et al., 2010).

1.1.4.2.4 *Chlamydia infection*

Chlamydia is an obligate intracellular bacterium, causing diseases such as sexually transmitted infections and eye infections. After the infection, internalized *Chlamydia* can replicate and migrate in host cells within vacuoles known as inclusion bodies. Upon *Chlamydia* infection, CD63 was found to mobilize from multivesicular bodies to assemble in *Chlamydia* inclusion bodies. Even though whole anti-CD63 antibodies interrupted this trafficking and reducing *Chlamydia* growth in host cells, siRNA knock down of CD63 and anti-CD63 Fab fragments showed no effect. This data suggested that results obtained from the divalent whole antibody were due to disruption of CD63-partner protein interactions (Beatty, 2006, Beatty, 2008).

1.1.4.2.5 Tetraspanin mediated adherence of multiple bacterial strains

Green and co-workers demonstrated that tetraspanins mediate the adhesion of several bacterial species to human epithelial cells including *Staphylococcus aureus, Neisseria lactamica, Neisseri meningitides, Escherichia coli* and *Streptococcus pnemoniae*. Bacterial adhesion was blocked or reduced by the pre-treatment of epithelial cells with CD9, CD63 and CD151 antibodies or recombinant proteins of the EC2 domains of these tetraspanins. Blocking of tetraspanins had a lesser effect on the adhesion of Opa and pili mutant of *Neisseria meningitides* strains. These data suggested that tetraspanins are involved in

bacterial adhesion via their association with partner proteins which may include bacteria-specific receptors thereby providing adhesion platforms for multiple bacterial strains (Green et al., 2011).

1.1.4.3 The role of tetraspanins in fungal infections

As mentioned previously, tetraspanin CD37 has been reported to play an essential role in the immune response to *Candida albicans* infection. CD37-/- mice are evidently better protected from infection than wild-type (WT) mice, due to increased levels of IL-6 and *C. albicans*-specific IgA antibodies in CD37-/- mice. However adoptive transfer of CD37-/- serum resulted in protection in WT mice. This suggested that CD37 regulates the anti-fungal immune response by inhibiting IgA responses (van Spriel et al., 2009). Also as described before, CD37 was shown to be important for the cell surface expression and stability of Dectin-1, a C-type lectin which is a pattern-recognition receptor essential for pathogen binding and uptake by antigen-presenting cells (APCs) (Meyer-Wentrup et al., 2007). The interaction between CD37 and Dectin-1 regulates Dectin-1-mediated IL-6 secretion in response to *Toxoplasma gondii* infection (Yan et al., 2014). Other tetraspanins have been shown to have a role in the immune response against fungi via their interactions with fungal receptors such as CD9/CD151-α5b1 integrin in *Histoplasma capsulatum* infection and CD9/CD81-TLR4 receptor for *C. albicans* (van Spriel and Figdor, 2010).

CD82 and CD63 have also been suggested to be involved in fungal and host cell interactions. The dynamic rearrangement and specific recruitment of CD82 and CD63 to phagosomes of fungal-infected dendritic cells has been observed, including in infections with *Cryptococcus neoformans, Candida albicans* and *Aspergillus fumigatus*, as well as bacterial pathogens such as *Staphylococcus aureus* and *Escherichia coli* (Artavanis-Tsakonas et al., 2011).

1.1.4.4 The role of tetraspanins in parasitic infections

Plasmodium sporozoites, the causative agent of malaria disease, are transmitted from the insect to the mammalian host, which is an obligatory stage of the life cycle. Within hepatocytes, Plasmodium sporozoites develop in a membrane-bound vacuole, and differentiate into merozoites which then infect erythrocytes and cause the disease. Tetraspanin CD81 has been shown to be required on hepatocytes for human *Plasmodium falciparum* and rodent *Plasmodium yoelii* sporozoite infection. *P. yoelii* sporozoites are able to infect CD81-deficient mouse hepatocytes *in vivo* and *in vitro*, and anti-mouse and anti-human CD81 antibodies suppressed the hepatic development of *P. yoelii* and *P. falciparum*, respectively.

CD81 was linked to sporozoite entry into hepatocytes via formation of a parasitophorous vacuole (Silvie et al., 2003). Transfection with CD81 was not sufficient to allow infection in Hep G2, a *P. falciparum*-resistant cell line, even though this cell line was permissive for *P. yoelii* infection, suggesting that CD81 has an indirect role in *P. falciparum* host tropism (Silvie et al., 2006b). The Silvie group also demonstrated that CD81 is functionally linked with cholesterol during infection by malaria parasites, which is thought to be facilitated by TEMS (Silvie et al., 2006a). Yalaoui et al demonstrated that a region of 21 amino acid

residues at the junction between the A and B α helices of CD81 EC2 is crucial for plasmodium infection (Yalaoui et al., 2008).

1.1.4.5 The role of tetraspanins in viral infection

1.1.4.5.1 Hepatitis C virus

The role of tetraspanins in viral infections was first demonstrated for CD81 in Hepatitis C virus (HCV) infection (Pileri et al., 1998). HCV is an enveloped RNA virus belonging to the *Flaviviridae* family that causes hepatic disease, often progressing to cirrhosis and hepatocellular carcinoma. E1 and E2, a heterodimer of HCV envelope proteins are involved in virus binding and entry into host cells (Op De Beeck et al., 2004). HCV-E2 interacts specifically with CD81 EC2 (Pileri et al., 1998).

Although CD81 is required for HCV-E2 binding, CD81-E2 alone has been shown to be not sufficient for HCV infection (Flint et al., 1999). It is suggested that HCV entry is regulated by co-receptors including CD81, scavenger receptor class B member1 (SR-B1) (Grove et al., 2007), the tight junction protein claudin-1 (CLDN1) (Evans et al., 2007), occludin (Ploss et al., 2009), Dendritic Cell-Specific Intercellular adhesion molecule-3-Grabbing Non-integrin (DC-SIGN), liver/lymph node-specific intracellular adhesion molecules-3 grabbing non-integrin L-SIGN, Low-Density Lipoprotein Receptor LDLR, heparin sulphate, proteoglycans and the asialoglyco protein receptor (van Spriel and Figdor, 2010). After binding to the host cell, HCV enters into the cytoplasm by endocytosis and acid-dependent fusion (Meertens et al., 2006). It has been reported that CD81-HCV binding plays a role in HCV intercellular trafficking (Masciopinto et al., 2004). Despite CD81 being associated with HCV in intercellular tight junctions, CD81 was not found to be required for cell-cell transmission of HCV (Witteveldt et al., 2009, Timpe and McKeating, 2008). It has been found that HCV entry activates the PI3K-AKT signaling pathway that is involved in cell growth and metabolism. This activation was regulated by the interaction between the HCV E2 envelope protein and its co-receptors, CD81 and claudin-1 (Liu et al., 2012). By utilizing high-affinity anti-human CD81 monoclonal antibodies, recent data showed that CD81 is essential for HCV infection and virus spreading *in vivo*, and these antiCD81 antibodies may have potential as broad-spectrum antiviral agents for the prevention and treatment of HCV infection (Ji et al., 2015).

1.1.4.5.2 Human immunodeficiency virus (HIV)

HIV-1 virus belongs to the *Retroviridae* family of viruses; HIV is responsible for acquired immune deficiency syndrome (AIDS). The virus initially targets CD4^{+} T cells, and antigen-presenting cells such as dendritic cells and macrophages. Viral infection mediated by the interaction of viral envelope gp120 protein with CD4 is followed by its interaction with CCR5 or CXCR4 co-receptors on target cells. The fusion of viral envelope and host cell membrane is regulated by gp41 protein and viral RNA is then injected into host cells (Dalgleish et al., 1984, Freed and Martin, 1995). Tetraspanins have been shown to be involved in HIV-1 infection at different levels. These include the strong expression of CD63 in binding structures and newly generated sites of HIV-1 in H9T cells (Meerloo et al., 1992), the concentration of CD81 and CD9 at the infection synapse between infected cells (Nydegger et al., 2006, Weng et al., 2009, Krementsov et al., 2009), the ability of recombinant tetraspanins (CD53, CD63, CD81, CD82 and CD151) and anti-CD63 antibodies to inhibit HIV-1 infection (von Lindern et al., 2003, Ho et al., 2006) as well as the ability of tetraspanins CD9 and CD81 to associate with CD4 and other receptors of HIV-1 and mediate

viral cell to cell transmission (Gordon-Alonso et al., 2006). These all suggest that tetraspanins are important in the binding, entry, release and transmission of HIV-1 in target cells.

1.1.4.5.3 Human T cell leukaemia virus

Human T cell leukaemia virus (HTLV-1) belongs to the *Retroviridae* family (*Deltaretro virus genus*) which infects CD4+ve and CD8+ve T cells and is associated with human T cell leukaemia (Goncalves et al., 2010). HTLV-1 Gag protein, which is essential for viral assembly and release (Heidecker et al., 2004), is reported to interact with the tetraspanin CD82 on both surfaces of the plasma membrane of T cells (Heidecker et al., 2004, Mazurov et al., 2006, Pique et al., 2000). Subsequently, CD82 has been suggested to play an important role in HTLV-1 assembly and transmission. Other tetraspanins reported to be co-localised with Gag proteins include CD53, CD81, CD82 and CD231 on the plasma membrane of Jurkat T cells (Mazurov et al., 2006).

1.1.4.5.4 Porcine Reproductive and Respiratory virus

PRRSV (family *Arteriviride*, genus *Arterivirus*) causes respiratory and reproductive disease in swine. CD151 has been reported to interact with three untranslated regions of PRRSV RNA (Shanmukhappa et al., 2007), which suggests it is critical for the viral replication process (Cao et al., 1992, Meulenberg et al., 1998). It has therefore been suggested that CD151 plays a role in PRRSV replication, which may confirmed by the ability of CD151 antibodies to completely block virus infection (Shanmukhappa et al., 2007).

1.1.4.5.5 Feline immunodeficiency virus

FIV (family *Retroviridae*, genus *Lentivirus*) is associated with an AIDS-like syndrome in domestic cats. Anti-CD9 antibodies inhibit feline T cell infection with FIV through the inhibition of virus release, but not virus entry. CD9 is therefore involved in virus life-cycle processes rather than in virus entry. Moreover, CD9 antibodies have no effect on the infection of 3201 cells, which do not express CD9, whereas the ectopic expression of CD9 on these cells enhances infection with FIV. This suggests that CD9 is directly involved in virus infections (Willett et al., 1997).

1.1.4.5.6 Human alpha-papilloma virus

HPV is associated with benign warts on epithelia and with cervical carcinoma (Doorbar, 2006). Following the attachment of virus cells to a membrane, HPV16 is associated with CD63 and CD151, leading to virus entry into the host cell. CD63 and CD151-specific antibodies inhibit HPV16 infection, confirming the role of these tetraspanins in these processes (Spoden et al., 2008).

1.1.4.6 The role of tetraspanins in fusion

Cell fusion is a critical process in a number of physiological and pathological conditions, including fertilization, development, bone and muscle homeostasis, and the response to certain pathogens and foreign materials. Cell fusion is a cell membrane event that includes the interaction between plasma membrane molecules of the fusing cells and the incorporation of the plasma membranes. Membrane fusion processes can occur in cell-cell fusion, intracellular vesicle fusion (a basic process for protein trafficking and exocytosis), and in viral infection. Tetraspanins CD9, CD81 and CD63 have been shown to be involved in various membrane fusion processes including sperm-egg fusion, myoblast fusion and virus syncytium formation.

1.1.4.6.1 Sperm-egg fusion

In the process of fertilization, the essential biological event is the fusion of the sperm and the egg. The sperm penetrates the zona pellucida after binding on to it and gains entry into the perivitelline space. At this region the adhesion of the sperm plasma membrane to the egg plasma membrane occurs. Adhesion usually precedes the fusion of the sperm and the egg and is necessary for the fusion (Talbot et al., 2003). The tetraspanin CD9 is the only egg membrane protein that has been shown to be essential for fertilisation. Anti-CD9 antibodies showed strong inhibition of sperm-egg fusion. CD9-/- mouse oocytes, but not sperm, showed severely reduced sperm–egg fusion (Miyado et al., 2000b, Le Naour et al., 2000, Kaji et al., 2002), whereas the injection of human or murine CD9 mRNA into CD9-/- mouse oocytes restored fusion competence (Kaji et al., 2002). CD9 is also concentrated in oocyte microvilli, a structure on oocytes that captures sperm and brings it into contact with the oocyte's plasma membrane (Runge et al., 2007) which suggests that CD9 is involved in adhesion processes. Sperm injected directly into the cytoplasm of CD9-/- oocytes yielded normal development (Miyado et al., 2000b). CD81 and CD151 are also involved in sperm-egg fusion, as the injection of CD81 in CD9-/- mice restored the fertilisation up to 50%, which suggests that CD81 has the ability to compensate for the function of CD9 in sperm-egg fusion, whereas CD151 antibodies led to a partial inhibition of fusion (Kaji et al., 2002). Deletion of the CD81 gene in mice reduced female fertility by about 40%. CD9 and CD81 double knock-out mice were completely infertile, which indicated that CD9 and CD81 together promote sperm-egg fusion (Rubinstein et al., 2006). It has been also shown that human CD9EC2 recombinant protein has inhibitory effects on sperm-egg binding whilst a mutated version of CD9EC2 had no effect, which suggests the importance of two disulphide bonds in the structure and function of CD9 (Higginbottom et al., 2003). Recently, a study suggested that CD9 and CD81 work independently upon fusion of sperm and oocyte as CD9 and CD81 are expressed separately in the oocytes membrane as confirmed by immunocytochemical and electron microscopic analysis (Ohnami et al., 2012).

1.1.4.6.2 Myoblast formation

Fusion of myoblasts is a crucial stage of myogenesis, the process of formation of the muscular component. During development, myoblasts initiate expression of the muscle specific genes. Then there is fusion of these mononucleate myoblasts to form the nascent multinucleate myoblasts which later form the myotubes and the myofibres. By the process of maturation these myofibers specific groups of muscles are formed. A crucial role for CD9

and CD81 in myoblast fusion has been demonstrated; Charrin and co-works reported that CD9 and CD81 have important roles in the restitution of normal muscle during the muscle regeneration. Mice lacking either CD9 or CD81 showed abnormal muscle regeneration due to a distinct and quick myofiber formation. The association of both tetraspanins with the immunoglobulin superfamily member CD9P-1 may have functional significance. *In vitro*, increased rates of myoblast and myotubes fusion was seen in the absence of CD9-1 or both CD9 and CD81 (Charrin et al., 2013).

1.1.4.6.3 HIV-mediated syncytium formation

Infection with HIV-1 results in cell-cell fusion and formation of syncytia which may indicate a way of virus spreading and escape from humoral immune responses. This fusion is found to be mediated both by viral proteins and host cell surface molecules.

Roles for CD9 and CD81 in cell-cell fusion induced by HIV-1 were demonstrated. Anti-tetraspanin antibodies enhance the syncytia formation mediated by HIV-1 envelope proteins and viral entry in human T lymphoblasts. CD9 and CD81 knock-down resulted in increased viral entry and syncytia formation, whereas CD9 and CD81 over expressing cells were less susceptible to HIV-envelop-mediated syncytia formation, suggesting that CD9 and CD81 facilitate syncytia formation mediated by gp120/CD4 interaction (Gordon-Alonso et al., 2006). Recently data showed that CD9 and CD63 arrest HIV-1-induced cell fusion at a particular stage of the fusion process (the transition from hemifusion to pore opening), and that may be due to their interaction with viral or host cell factors that regulate pore stability and/or extension (Symeonides et al., 2014).

1.1.5 Multinucleated giant cell (MNGC) formation

Multinucleated giant cells (MNGCs) are cells formed by the fusion of monocytes or macrophages at sites of inflammation. They are believed to increase the ability of cells to digest and reabsorb large extracellular infectious agents and are thus involved in immune defence. MNGCs are also important in bone remodelling and are associated with osteoporosis, inflammatory diseases and tumours (Han et al., 2000). The phenotypes of the MNGCs vary and depend on the local environment and the chemical and physical (size) nature of the inducing agent or the agent which the MNGCs and their monocyte/macrophage precursors are going to act against. It has been argued that MNGCs are a feature of granulomatous inflammation associated with chronic infections; for example tuberculosis, fungal infection and HIV, as reviewed in (Kumar et al., 2013)). However, the exact role of MNGCs in infection remains unknown. Although it has been suggested that MNGCs may limit the cell-cell spread of infection, they may cause inflammatory damage in infected tissues (Byrd, 1998).

1.1.5.1 Types of multinucleated giant cell formation

1.1.5.1.1 Langhans giant cells

Langhans' giant cells (LGCs) are seen in infective granulomatous diseases such as tuberculosis (TB) and schistosomiasis (reviewed in (Sandor et al., 2003)). LGCs are also

associated with sarcoidosis which is a granulomatous disorder of unknown etiology (Anderson, 2000). The production of cytokines and chemokines by *Mycobacterium tuberculosis*-infected lung macrophages stimulates the recruitment of macrophages, lymphocytes, and dendritic cells to the infected area and this cellular aggregation is named a granuloma; a major histopathological feature of tuberculosis. Within granuloma, macrophages differentiate into epithelioid cells or fuse to form LGCs (Lay et al., 2007). Granulomas are thought to suppress the infection in a localized area thus preventing bacterial spread; mice that lose the ability to form evident granulomas exhibited highly elevated bacterial loads (Saunders et al., 1999). The diagnostic feature of LGCs is the presence of a relatively small number of nuclei (<20), arranged in a circular peripheral or horse shoe shaped arrangement within the giant cell. For the formation of LGCs, interferon-γ (IFN-γ) induction of the monocyte-macrophage fusion is thought to be required (Gasser and Most, 1999). The glycolipids of the mycobacterial envelope (DIMs and LM) are pro-inflammatory, which induces macrophage aggregation and fusion of granuloma macrophages into multinucleated giant cells. The entire process is mediated through a Toll-Like Receptor 2-dependent, Disintegrin and metalloproteinase domain-containing protein 9 (ADAM9) and integrin β1- mediated pathway (Puissegur et al., 2007).

In latent tuberculous, mycobacteria can penetrate into organs and tissues and persist there for decades before a possible activation of the tuberculous process followed by the development of active disease (Parrish et al., 1998). Analysis of granulomas from mice with latent TB infection showed that active acid-fast bacteria can be found in macrophages, dendritic cells and multinucleated LGCs (Ufimtseva, 2015). Recently, a study demonstrated that CD40-CD40 ligand interaction and the cytokine IFN-γ that is secreted by T cells are required for monocyte fusion and LGC formation. The authors also reported the involvement of Dendritic cell-specific transmembrane protein (DC-STAMP) in LGC formation as DC-STAMP was shown to be up-regulated in LGC formation and knockdown of DC-STAMP inhibited LGC formation (Sakai et al., 2012).

1.1.5.1.2 Foreign body giant cells

Foreign body giant cells (FBGCs) are spotted at the tissue-material interface of medical devices implanted in tissue *in vivo*, and are thought to remain there for the lifetime of the device. FBGCs have been implicated in biodegradation of such devices. The characteristic feature of FBGCs are that they are larger cells than LGCs with greater numbers of nuclei (>20) arranged in an irregular manner throughout the cytoplasm of the giant cell. The induction and characteristics of FBGC formation at the device-tissue interface depends on the nature of the biomaterial and the surface area. Flat surfaces encapsulated within a thin (one or two cells in thickness) layer of macrophages and FBGCs can be seen in breast implants, whereas fabrics applied as vascular grafts stimulate high densities of FBGCs (Anderson, 2000). The significant importance of interleukin-4 in FBGC formation was demonstrated using recombinant human lymophokines. With freshly isolated human monocytes, interleukin-4 (IL-4) induced very large FBGCs with a high rate of macrophage fusion (more than 72%) (McNally and Anderson, 1995). Type 2 T helper lymphocytes (Th2) are thought to play a role in the fusion of macrophages at the tissue-material interface, due to their capacity to secrete IL-4 and IL-13, another cytokine that is implicated in FBGC formation (DeFife et al., 1997). β1 and β2 integrin receptor families have been implicated in the adhesion processes during IL-4-induced FBGC formation (McNally and Anderson,

2002). The specific alpha partners to the β1 and β2 integrins including αMβ2, αXβ2, α5β1>αVβ1>α3β1, and α2β1 have also been identified as FBGC mediators (McNally et al., 2007). Studies of FBGC formation using genetically modified mice or cells derived from them have confirmed the requirement for matrix metalloproteinase MMP-9, and DC-STAMP in this process (MacLauchlan et al., 2009, Yagi et al., 2005).

1.1.5.1.3 Osteoclasts

Osteoclasts are cells involved in physiological bone remodelling, a process controlled by the coordinated effort of bone-forming by osteoclasts and bone-resorbing by osteoclasts (Charles and Aliprantis, 2014). Imbalance in bone remodelling leads to bone disorders e.g. osteoporosis, an increased osteoclast activity which is also seen in rheumatoid arthritis and bone tumours, or a decrease in osteoclast activity leading to the accumulation of dense, but brittle, bones (Boyle et al., 2003, Segovia-Silvestre et al., 2009, Jones et al., 2011a).

The osteoclast is a tissue-specific macrophage induced by the differentiation and then fusion of myeloid precursor cells at or near the bone surface. Osteoclasts contain between 5 and 10 nuclei and multinucleation is an essential process in the differentiation of osteoclasts, since mononucleotide macrophages cannot perform the resorption of bone effectively and efficiently (Vignery, 2005). The osteoclast is formed by the induction of the cytokines macrophage colony stimulating factor (MCSF) and receptor activator of NF-kB ligand (RANKL) synthesized by osteoblasts and/or osteocytes. RANKL interacts with its receptor RANK or with osteoprotegerin (OPG) which is produced by osteoblasts (Teitelbaum, 2006). OPG is a soluble protein that blocks osteoclast formation *in vitro* and bone resorption *in vivo* (Simonet et al., 1997) and the balance between RANKL and OPG production leads to normal bone remodeling. RANKL production is enhanced by osteoclast-stimulating agents such as parathyroid hormone and TNF-α. RANKL triggers the expression of integrin $\alpha_v\beta_3$ which is absent on macrophage precursors but highly expressed by osteoclasts and considered as the osteoclast phenotype marker. The RGD (Arg-Gly-Asp) tripeptide sequence is recognized by $\alpha_v\beta_3$ integrin in several extracellular matrix macromolecules such as osteopontin, as well as fibronectin, vitronectin, and fibrinogen. Along with the increased osteoclast expression of $\alpha_v\beta_3$, mammalian osteoclasts also express $\alpha_2\beta_1$, a collagen-laminin receptor, and $\alpha_v\beta_1$, another vitronectin receptor (Teitelbaum, 2006, Brodbeck and Anderson, 2009). The mechanism of how osteoclasts form remains unclear, despite several cell surface molecules having been demonstrated to be involved. Yagi and co-workers reported that DC-STAMP is essential of osteoclast formation; in DC-STAMP–deficient mice osteoclast formation was completely abrogated, while osteoclast multinucleation was restored by retroviral introduction of DC-STAMP. Defects in osteoclast multinucleation in DC-STAMP-/- mice led to reduced bone resorbing activity, leading to osteopetrosis (Yagi et al., 2005). A role for tetraspanin CD9 in osteoclast formation has been reported and CD9 expression was enhanced by RANKL on the RAW264.7 macrophage cell line. Targeting CD9 using siRNA suppressed osteoclast formation and the distribution of CD9 into lipid raft microdomains was reported in RANKL-treated cells but not in untreated cells. This suggested the importance of CD9 and its distribution in lipid rafts during osteoclastogenesis (Ishii et al., 2006).

1.1.5.1.4 Multinucleated giant cells in cancer

Fusion of somatic cells is one of the primary theories of cancer etiology (Wang et al., 2012). Several types of cancer cell are fusogenic, for instance, melanoma cells fuse with

macrophages (Rachkovsky et al., 1998) and breast cancer cells fuse with endothelial cells (Mortensen et al., 2004). Tumour cells can fuse with themselves as well as with other somatic cells such as monocytes, to enhance metastasis, chromosomal aberration and epigenetic regulation (Duelli and Lazebnik, 2003).

1.1.6 Macrophage activation

Monocytes migrate from the blood into tissues where they are differentiated into macrophages. Macrophages are present in all organs and tissues, usually in sites where they are likely to be needed in defence against foreign entities (reviewed in (Martinez et al., 2009)). In tissues, macrophages differ in their function and morphology, depending on particular environmental stimuli, giving rise to their tissue-specific names. For instance in bone (osteoclasts), in lung (alveoli), in brain (microglia), in connective tissue (histiocytes), in liver (Kupffer cells), spleen (littoral cells), in kidney (mesangial phagocytes) in joints (synovial A cells) (Gordon and Taylor, 2005, Gordon et al., 2014).

Macrophages play an important role in both the innate and adaptive immune responses. Besides their function in defence against foreign entities, macrophages are responsible for eliminating host cells, dead cells and cellular debris. Macrophages are activated by direct contact with pathogens or their products, proteins of the complement or the blood coagulation system and host tissue breakdown. In the innate immune response, macrophages phagocytise and eliminate foreign bodies and secrete chemokines, cytokines, and growth factors which recruit other immune cells to inflammatory sites (Mosser and Edwards, 2008). In the adaptive response, macrophages function as antigen-presenter cells (APCs). They express on their surface MHCI and MHCII molecules, which can interact with T cell receptors on T helper and T cytotoxic cells that can lead to the activation of these cells. The activation of T helper cells leads to differentiation to either Th1 or Th2 cells. Macrophages also express receptors that can bind to antibodies (Fc receptors) thus they can uptake antigens that have been coated with antibodies (Mosser and Edwards, 2008).

According to its mediators, the activation of macrophages has been classified into two pathways; a classic M1 and alternative M2. Interferon gamma (IFN-γ) and tumor-necrosis factor (TNF) (which is produced by APCs) are associated with M1 activation. IFN-γ is produced by Th1 and other cells such as natural killer (NK) cells and macrophages. The M2 pathway is mediated by interleukin IL-4 and IL-13 which are mainly produced by Th2 cells (Helming and Gordon, 2009, Martinez and Gordon, 2014). Mosser and Edwards reported that activated macrophages can be grouped into three populations with regard to their distinct homeostatic activities; immune regulation, host defence and wound healing. These population can be produced in response to either innate or adaptive immune signals (Mosser and Edwards, 2008).
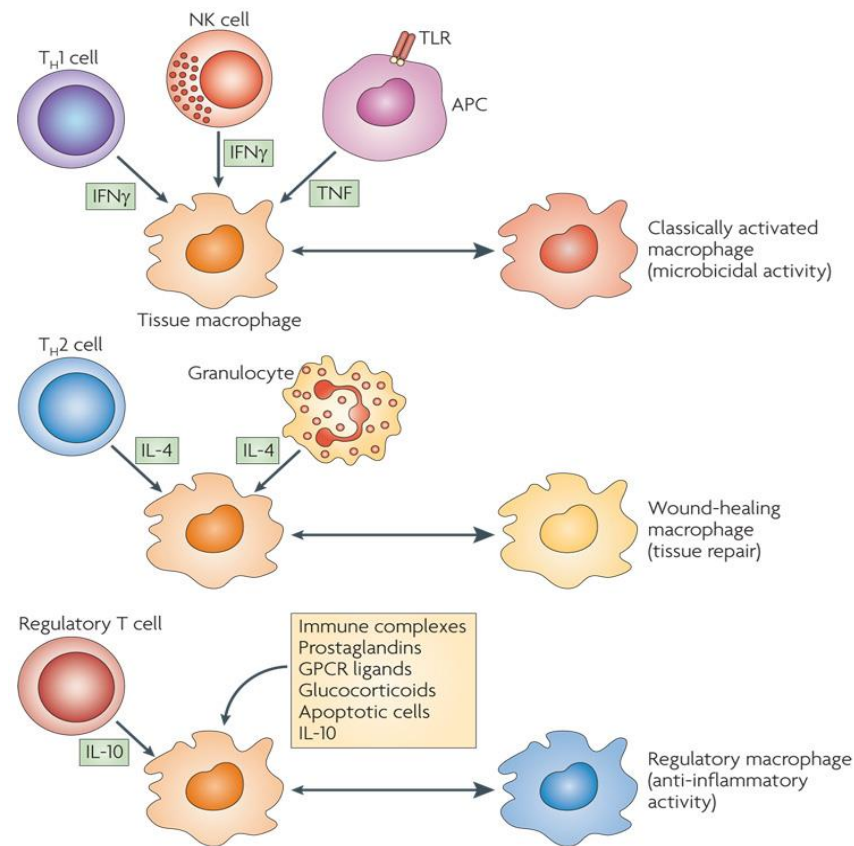
Figure 1.1.4 macrophage activation.

Macrophages function differently according to their responses to the immune cell that induces their production; classically activated macrophages are generated in response to TNF which is secreted by APCs, and IFNγ which can be produced during an adaptive immune response by Th1 cells or during an innate immune response by NK cells. Classically activated macrophages have been implicated in microbicidal activity. Wound-healing (alternatively activated) macrophages are generated in response to IL-4, which is produced in adaptive immune response by Th2 cells or in innate immune responses by granulocytes. Wound-healing macrophages are involved in tissue repair processes. Regulatory macrophages arise in response to diverse stimulatory factors, including immune complexes, prostaglandins, G-protein coupled receptor (GPCR) ligands, glucocorticoids, apoptotic cells or IL-10. Regulatory macrophages produce high levels of IL-10 to suppress immune responses. Adapted from (Mosser and Edwards, 2008).

As mentioned previously, with the regard to macrophage fusion, IL-4 and IL-13 are major stimuli that are associated with macrophage fusion *in vivo* and *in vitro*. Both IL-4 and IL-13 can bind to the common IL-4 receptor α chain, which then activates a common mechanism for macrophage fusion by up-regulation of the expression of receptors that may be essential participants in macrophage fusion (DeFife et al., 1997, Helming and Gordon, 2007). An example is the activation of signal transducer and activator of transcription 6 (STAT-6) pathway, which regulates the expression of fusion mediators such as DC-STAMP and E-cadherin; STAT-deficient mice showed significant inhibition of FBGC formation and

also marked inhibition in the expression of DC-STAMP and E-cadherin (Helming and Gordon, 2007, Moreno et al., 2007, Yagi et al., 2007). In contrast, STAT-1 is considered an inhibitor of multinucleation; its expression is up-regulated in STAT-6-/- mice and STAT-1-/-mice exhibit accelerated FBGC formation which suggested that both members regulate each other and control FBGC formation (Miyamoto et al., 2012).

Whilst IL4 and IL13 are associated with FBGC formation (from M2 actifated macrophages), IFN-γ is associated with the formstion of langhans cells (from M1 activated macrophages). This is covered in review by (Anderson, 2000).

1.1.7 Mechanism of macrophage fusion

Although the activation of macrophages to be induced to form giant cells or osteoclasts by cytokines IL-4 and RANKL, respectively, are well defined, the mechanism of the fusion processes are still not well-characterized. However, previous studies have described the involvement of several membrane proteins, such as CD44, CD47, CD98, macrophage fusion receptors, P2X$_7$ receptors, ADAMs and integrins, in these processes (Han et al., 2000), as well as DC-STAMP as previously mentioned (Ohgimoto et al., 1995)(Yagi et al 2005) . It has been suggested that cell fusion involves sequential events: the activation of macrophages enhances up-regulation of fusion mediators, resulting in fusion-competent macrophages, then the cells move toward each other (chemotaxis), followed by cell-cell attachment, cytoskeleton rearrangements and membrane fusion (Helming and Gordon, 2009). Recent data demonstrated that the cytoplasmic protein tyrosine phosphatase PTP-PEST (also known as PTPN12) is involved in these events. PTP-PEST is necessary for macrophage fusion *in vivo* and *in vitro*; cell fusion into MNGC was markedly inhibited in IL-4-stimulated PTP-PEST deficient macrophages, in RANKL-stimulated macrophages (osteoclasts), and following foreign body implantation in mice. PTP-PEST controls phosphorylation of protein tyrosine kinase Pyk2 and its adaptor paxillin, a key regulator of cell adhesion, migration and spreading. The absence of PTP-PEST therefore resulted in specific hyperphosphorylation of these molecules, thus the ability of macrophages to migrate in response to cytokines, undergo cell-cell adhesion and cytoskeleton rearrangement was suppressed (Rhee et al., 2013).

Another signalling pathway was shown by Helming and co-workers who identified that signaling through the transmembrane protein signaling adaptor protein DAP12 (DNAX activating protein of 12 kD), its associated receptor TREM-2 (triggering receptor expressed by myeloid cells 2), and the downstream protein tyrosine kinase Syk is crucial for cytokine-stimulated macrophage fusion. The loss of DAP12 results in defects in MNGC and FBGC formation *in vivo* and *in vitro*, while over-expression of DAP12 enhances MNGC formation. DAP12 is involved in programming of macrophages through the regulation of gene and protein expression of molecules that regulate cell fusion such as DC-STAMP, MMP9 and cadherin to induce a fusion-competent state (Helming et al., 2008).

Cytoskeleton rearrangement controls cell shape and cell migration. Shilagardi and co-workers reported the importance of cytoskeleton rearrangement in MNGC formation. Actin cytoskeleton rearrangement was essential for cell fusion, as the actin cytoskeleton supplies an active driving force for cell-cell fusion by establishing membrane protrusions that are required and sufficient to control fusion promoted by fusogenic proteins (Shilagardi et al., 2013) .

It has been proposed that cell fusion may involve a mechanism similar to phagocytosis (cellocytosis) figure 1.1.5 A. After the adhesion of one macrophage to another, one cell takes the lead and internalises the other macrophage which is then coated by two plasma membranes. Once these two membranes have been recycled, the cytoplasm and organelles of the internalized and host cells become integrated (Vignery, 2005). A phagocytic mechanism of macrophage fusion was also supported by evidence provided by McNally and Anderson. They proposed that cell fusion is promoted by endoplasmic reticulum-mediated phagocytosis, with ER markers such as calnexin and calregulin co-localized at fusion interfaces and on cell surfaces during FBGC formation in IL4-stimilated macrophages. The inhibition of ER components resulted in FBGC formation inhibition and reduced mannose receptor expression, which is known as a FBGC regulator (McNally et al., 1996, McNally and Anderson, 2005).

Another proposed mechanism for macrophage fusion was suggested by Takito and co-workers (figure 1.1.5 B). The fusion stages of multinucleated osteoclast formation were analysed using time-lapse confocal microscopy of RANKL-stimulated RAW264.7 cells transfected with EGFP–actin (Takito and Nakamura, 2012, Takito et al., 2012). The attachment of two macrophages is followed by a delay before fusion and this delay is thought to be required for forming of a temporary actin superstructure named the zipper-like structure at the contact site. This structure disappears from a small area where the site of fusion was initiated and with time the gap is expanded in parallel with plasma membrane deformation following membrane fusion, resulting in the fusion of podosome belts of distinct osteoclasts (Takito and Nakamura, 2012).

A)
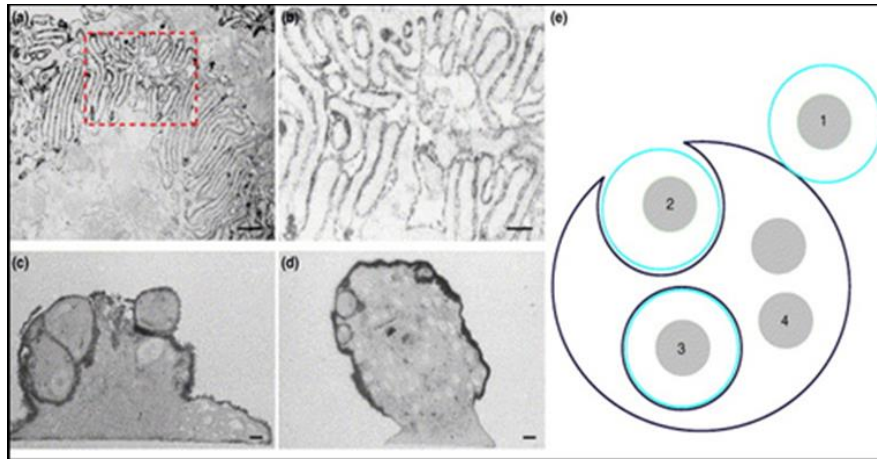
B)
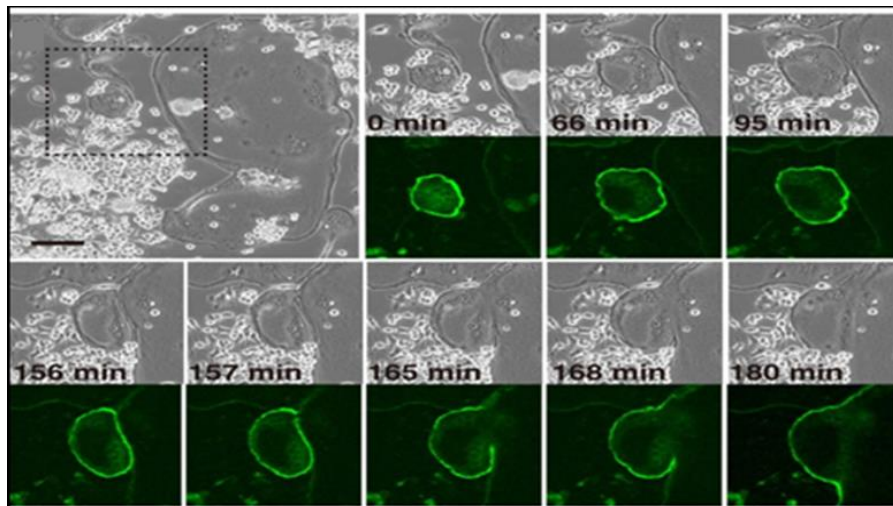
Figure 1.1.5 mechanism of monocyte/macrophage fusion.

(A) Macrophage fusion involving phagocytosis (cellocytosis): a) interdigitations of the plasma membrane initiated between fusing macrophages, b) higher-magnification of area labelled by red dotted line in a, c) internalized cell but not fused, d) multinucleated alveolar macrophage contains a large number of nuclei, e) the cellocytosis model describing MNGC formation (Vignery, 2005).

(B) Time lapse confocal microscopy images indicate the fusion between EGFP-positive and EGFP-negative osteoclasts (Takito et al., 2012). The gray panel shows phase contrast images, the green panel shows fluorescence images. All images have been captured from the same field. Two cells come into close contact, a small gap present in EGFP-fluorescence indicates the disappearance of cell membrane in this region and this gap is increased with time until the fluorescence completely disappears from the contact area and the two cells are fused.

1.1.8 Tetraspanins in Multinucleated giant cell formation

The role of tetraspanins CD9 and CD81 in MNGC formation was demonstrated by Takeda and co-workers. Expression of CD9 and CD81 and their complex formation with β1 and β2 integrins was up-regulated when monocytes were cultured under normal conditions. However, under fusogenic conditions in the presence of Con A (a lectin that indirectly induces fusion), up-regulation of CD9 and CD81 was inhibited, whereas CD63 up-regulation was enhanced (Takeda et al., 2003). CD9 and CD81 null mice showed enhanced formation of MNGCs *in vitro* and *in vivo*, whilst CD9/CD81 double–null mice showed spontaneous development of MNGCs in the lungs and enhanced osteoclastogenesis in the bones. Moreover, anti-CD9 and anti-CD8 antibodies enhanced the fusion of monocytes (Takeda et al., 2003). Overall, while CD9 and CD81 are required in fusion events such as the fusion of gametes, myoblast fusion and viral infections, CD9 and CD81 basically seem to prevent monocyte fusion. These findings were confirmed using tetraspanin antibodies and a range of recombinant tetraspanin EC2 domains to understand their role in the formation of MNGCs. This study showed that anti-CD63 antibodies and recombinant CD63EC2 protein inhibited MNGC formation. CD63 is suggested to play a direct role in this process, whilst CD9 has a direct negative role in formation and CD81 has an indirect negative role as its EC2 had no effect on the formation of MNGCs (Parthasarathy et al., 2009).

By contrast, in osteoclast formation, CD9 has been found to be highly expressed in osteoclast cells in bone tissue that induced osteoporosis as well as at sites of bone erosion in arthritic lesions (Iwai et al., 2008). Another study suggested that CD9 is strongly expressed in osteoclasts and that anti-CD9 antibody significantly inhibited multinucleated osteoclast formation and strongly stimulated the activation of p44/42 mitogen-activated protein kinase (MAPK). CD9 has therefore been suggested to enhance the progress of osteoclastogenesis via the negative regulation of the concentration and duration of p44/42MAPK activation at a particular level (Yi et al., 2006).

1.2 *Burkholderia*

The phylogenetically well-defined and diverse genus *Burkholderia* contains approximately 100 species and they occupy different ecological niches (Ginther et al., 2015). *Burkholderia* species have been organised into four groups, the B. pseudomallei group, the *Burkholderia* cepacia complex (BCC), the plant-associated beneficial and environmental (PBE) group and 'others (Suarez-Moreno et al., 2012, Choudhary et al., 2013). Most *Burkholderia* species are soil commensals and phytopathogens and rarely affect the human population. *Burkholderia mallei* (*B.m*) and *Burkholderia pseudomallei* (*B.p*), however, are primary pathogens affecting humans and animals, and causing glanders and melioidosis, respectively (Galyov et al., 2010). In addition *Burkholderia cepacia* complex contains 18 closely related species some of which affect cystic fibrosis patients (Mahenthiralingam et al., 2002).

1.2.1 Melioidosis disease

1.2.1.1 *Burkholderia pseudomallei* (*B.p*), route of infection, Incubation period

B. pseudomallei is an oxidase-positive, Gram-negative (Dance et al., 1989), motile, non-spore forming, aerobic bacillus (Wiersinga et al., 2006) that exhibits different colony morphology depending on the medium type. *B.p* is a facultative intracellular bacterial organism and the etiological agent of melioidosis in humans and animals which is endemic in parts of Southeast Asia and north Australia (Dance, 1991, Cheng and Currie, 2005). It is a saprophytic organism and can be isolated from niches like water, moist soil and rice paddies. *B.p* infection is acquired through cutaneous inculcation, inhalation and aspiration in individuals exposed to environments containing *B.p*. Most cases present as septic shock associated with severe pneumonia (Wiersinga et al., 2006). The incubation period of the disease commonly ranges from one to 10 days. However, long incubation periods spanning several years are seen in recrudescent melioidosis, and an incubation period of up to 62 years has been recorded before the occurrence of clinical manifestations after exposure to *B.p* (Ngauy et al., 2005).

1.2.1.2 Characteristic of melioidosis disease, diagnosis, treatment and prevention

B.p infection is diverse and can occur as localized infection, pulmonary infection, blood stream infection or disseminated infection (Wiersinga et al., 2006). Melioidosis has a variety of manifestations and produces a range of clinical symptoms, including seropositive subclinical conditions, and rapidly worsening septicaemia (Puthucheary et al., 1992). The patient may die within 48 hours of developing septic shock symptoms and melioidosis is responsible for 20% of all community-acquired septicaemias and 40% of sepsis-related mortality in northern Thailand (Wiersinga et al., 2006). The rates of morbidity and mortality are higher in patients with chronic pulmonary disease, diabetes mellitus, renal dysfunction and compromised immune systems (Limmathurotsakul et al., 2010). The clinical features of the disease include dissemination of the bacteria to distant sites resulting in septic shock. Infective organisms that are in the dormant state in the host can be triggered, leading to acute and fatal disease, particularly when the immune response is depressed (Currie et al., 2000). *B.p* can be isolated on the Ashdown medium. Various additional methods that have been employed for the isolation and the identification of the organism and the diagnosis of melioidosis include gas-liquid chromatography analysis of bacterial fatty acid methyl esters (GLC-FAME), agglutinating antibody test and polymerase chain reaction (Wiersinga et al., 2012).

It is difficult to eradicate the infection due to the slow fever clearance time requiring prolonged antibiotic therapy and a very high relapse rate. Recurrent disease rate is reported to occur in approximately 6–13% of cases, due to relapse rather than reinfection, especially when occurring within a year of primary infection (Currie et al., 2000). The treatment protocol for melioidosis is different from other infectious diseases. There is an initial intensive therapy with ceftazidime or meropenem for at least 14 days, followed by an eradication therapy with trimethoprim-sulphamethoxazole for at least 3 months. Alternative therapies are sought in cases of allergy to penicillin (Chaowagul et al., 2005). Resistance to antibiotics is a major cause for concern while treating this disease; the main

antibiotic resistance mechanisms include enzymatic inactivation of the antibiotic, target deletion and efflux from the cell (Schweizer, 2012, Chantratita et al., 2011). Currently, there is no vaccine against melioidosis. However, research is being carried out to develop vaccines and possible candidates include whole killed cells, live attenuated cells, plasmid DNA, and dendritic cell vaccines. Peacock et al. have reviewed recent efforts for vaccine development (Peacock et al., 2012).

1.2.1.3 *Burkholderia pseudomallei* pathogenesis

The pathogenesis of this organism is mainly by the process of host cell invasion and escape from endocytic vesicles followed by intracellular multiplication and formation of actin tails and membrane protrusions resulting in cell to cell spreading. *B. pseudomallei* induce host cell fusion leading to multinucleated giant cell (MNGC) formation (Kespichayawattana et al., 2000, Harley et al., 1998). It is also able to induce apoptotic death in infected host cells (Suparak et al., 2005).

Several *B.p* virulence factors have been identified including pili, flagella, capsule, bacterial lipopolysacchride (LPS), and type III (TTSS/T3SS) and type VI (T6SS) secretion system (Allwood et al., 2011, Galyov et al., 2010, Zughaier et al., 1999).

1.2.1.3.1 *Burkholderia pseudomallei* adhesion

Infection with this organism begins at the epithelial cell layer of either mucosal surfaces or abraded skin. The attachment of *B. pseudomallei* to human pharyngeal epithelial cells is reported to be controlled by the bacterial capsule, a thin polysaccharide layer that coats the bacteria (Ahmed et al., 1999). The *B.p* capsule has been shown to be an essential virulence factor. For instance, the addition of purified capsule results in an increase in the virulence of a capsule mutant strain in the Syrian hamster model of acute melioidosis (Reckseidler-Zenteno et al., 2005). It has been suggested that the asialogangliosides GM1 and GM2 are part of the receptor complex for *B. pseudomallei* on human pharyngeal epithelial cells (Gori et al., 1999). However, the receptor for adhesion and the exact mechanism of initial attachment remain unclear. The *B.p* capsule is considered as a virulence factor due to its crucial role in suppressing the immune response against the bacterium. Production of the *B.p* capsule enhances resistance to phagocytosis by reducing complement factor C3b binding to the bacterial surface thereby downregulating complement activation (Reckseidler-Zenteno et al., 2005). Flagellum-mediated adhesion was found to be important in *B.p* infection of the amoeba *Acanthamoeba astronyxis* but has no effect on mammalian cell infection(Haiko and Westerlund-Wikstrom, 2013). The *B.p* type IV pilin (pilA) has been implicated in the adhesion and the invasion. A pilA deletion resulted in decreased adhesion to human epithelial cells and reduction in the virulence in the nematode and the murine models (Essex-Lopresti et al., 2005). The adhesins BoaA (Burkholderia oligomeric coiled-coil adhesin A) and BoaB (Burkholderia oligomeric coiled-coil adhesin B) have been shown to be involved in *B.p* adhesion to epithelial cell lines as A549 and Hep2 (Figure 1.2.1) (Balder et al., 2010).

1.2.1.3.2 Internalization and colonization

It has been demonstrated that the internalization of *B.p* is promoted by its virulence factor the type III secretion system cluster 3, known also as *Burkholderia* secretion apparatus (bsa), and it is essential for the virulence of *B.p* in animal models (Stevens et al., 2003, Stevens et al., 2004, Warawa and Woods, 2005). Notably *B.p* contains three T3SS clusters;

T3SS-1, T3SS-2 T3SS-3, that are thought to promote the interaction of *B.p* with variable hosts (Sun and Gan, 2010). TTSSs are protein complexes, consisting of about 20 different subunits that assemble into a syringe-like structure spanning both membranes of Gram-negative bacteria, and inject effector proteins through the plasma membrane and into the host cell cytoplasm (Gong et al., 2015, Haraga et al., 2008, Mueller et al., 2008). The exact mechanism of invasion by *B.ps* remains unknown but it has been reported that *B. p* enters epithelial cells by a mechanism regulated by the Bsa T3SS-3 and one of its secreted effector proteins, *bopE*, as mutation of *bopE* resulted in suppressed bacterial invasion of epithelial cells (Stevens et al., 2003). However, by utilizing a photothermal nanoblade to deliver *B.t* directly into cytosol, French and co-workers reported that T3SS-3 is required for escape from endosomes, but not for bacterial invasion (French et al., 2011). Intracellular *B.p* is initially seen in the vacuoles and later in the cytoplasm, where the bacteria can replicate (Puthucheary and Nathan, 2006, Inglis et al., 2000, Harley et al., 1998).

The type VI secretion system (T6SS) is also used by Gram-negative bacteria to infect and survive within host cells, and it has also been hypothesised that the T6SS forms needle-like appendages to export effectors proteins directly into target cells (Miyata et al., 2013). T6SS has been implicated in *B.p* uptake and intracellular survival in phagocytic and non-phagocytic cells, as reviewed in (Miyata et al., 2013). It is also involved in *B.p*-induced cell fusion leading to MNGC formation (see section 1.2.1.3.3 for more detail)(Schwarz et al., 2014, Shalom et al., 2007).

Once *B.p* effectors enter the cell, they alter the host cellular processes in order to promote bacterial survival and colonization. The exact mechanism of the secondary spread of *B. pseudomallei* is not well characterized, although invasion of macrophages would allow *B.p* to spread via the lymphatic system to the spleen and other organs. Cullinane and co-workers reported that the induction of autophagy (a potent host cell defence pathway against intercellular pathogens) in response to *B.p* infection was increased or inhibited by treatment with pharmacological stimulators or inhibitors, respectively. However, *B.p* can actively evade this pathway and this is likely to be related to and promoted by the activity of the T3SS-3 effector, BopA. Intracellular survival of *B.p* decreased in a BopA mutant and *B.p* was shown to co-localise with the autophagy marker protein LC3, while inhibition of autophagy resulted in increased intracellular viability of the *B. pseudomallei bopA* mutant (Cullinane et al., 2008). Once *B. pseudomallei* escape from the entry vacuole and are free in the cytosol, they are able to induce their own propulsion by polymerizing actin at one bacterial pole by the activity of BimA protein. The actin-based motility of the pathogen was eliminated by mutation of *bimA* and restored by re-introducing the wild-type gene (Benanti et al., 2015, Stevens et al., 2005b). (Figure 1.2.2).
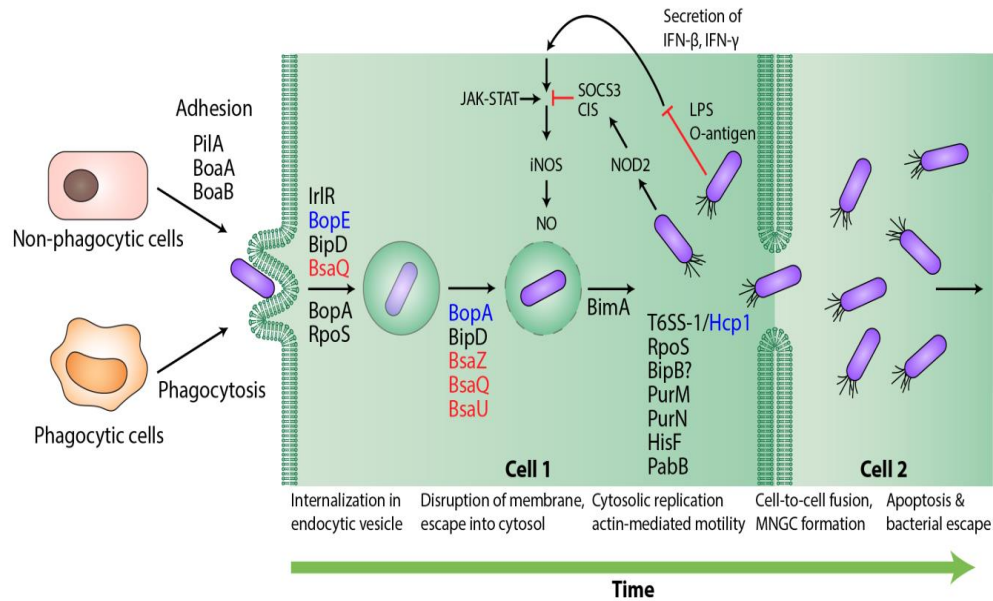
Figure 1.2.1 A diagram to illustrate selected steps of the _B.p_ life cycle within infected cells. _B. pseudomallei_ PilA protein and the adhesions BoaA and BoaB facilitate invasion of non-phagocytic cells. The uptake steps in non-phagocytic cells are controlled by the Bsa T3SS structural proteins BipD (translocator), BsaQ (structural component), and BopE (effector). The IrlRS two-component signal transduction system is suggested to regulate the expression of other essential gene(s) implicated in internalization. In phagocytic cells, the Bsa T3SS putative effector BopA and the alternative sigma factor RpoS promote bacterial uptake. Escape from the endocytic vesicle is facilitated by Bsa T3SS structural proteins BsaZ, BsaQ, and BsaU, the translocator protein BipD and the putative effector BopA. Once in the cytosol _B.p_ can replicate and move by actin-based motility in a BimA-dependent manner. _B. pseudomallei_ capsule only weakly triggers IFN secretion resulting in reduced iNOS expression. B. pseudomallei up-regulates the expression of suppressor of cytokine signaling 3 (SOCS3) and cytokine-inducible Src homology 2-containing (CIS) proteins that prevent the Janus kinases–signal transducers and activators of transcription (JAK–STAT) signaling pathway. Proteins involved in purine (PurM, PurN), histidine (HisF), and para-aminobenzoate (PabB) biosynthetic pathways are important for intracellular replication and survival, while the B. pseudomallei T6SS-1 Hcp protein and the alternative sigma factor RpoS are implicated in inducing cell-to-cell fusion andMNGC formation. NOD2 refers to the nucleotide-binding oligomerization domain-containing protein 2. Green arrows show progression of time. Inhibitory interactions are shown by red T-bar arrows whilst secretion system components are in blue, translocators in black and structural components in red (Allwood et al., 2011). The role of additional factors is shown that are not discussed in the text.

1.2.1.3.3 Cell to cell transmission (or 'spread'), cell fusion and multinucleated giant cell MNGC formation

Burkholderia pseudomallei are highly capable of intercellular spreading via membrane protrusions which extend onto neighbouring cells and via which the bacteria travel by actin-

mediated motility, this notable feature of *B. pseudomallei* leads to the induction of cell fusion and MNGC formation, enabling the bacterium to spread from cell to cell. (Benanti et al., 2015, Stevens et al., 2005b, Kespichayawattana et al., 2000, Sitthidet et al., 2011). This survival capability is thought to be responsible for the relapse of the disease, and may also be involved in *B. pseudomallei* pathogenicity as MNGC are found in tissues of patients with melioidosis (including the lung, kidney and spleen), which provides useful diagnostic evidence (Wong et al., 1995).

In tissue culture models, *B.p* can induce MNGC formation in phagocyte and non-phagocyte cell lines (Harley et al., 1998). Following multinucleated giant cell formation and cell to cell spread, the organism induces apoptotic cell death of the infected host cell (Kespichayawattana et al., 2000). The apoptotic changes that are seen include; condensed and fragmented nuclei, DNA ladder formation, cleavage of the DNA-repairing enzyme PARP and translocation of membrane phosphatidylserine (PS) from the cytoplasmic side to the external surface, which is typical for cells undergoing apoptotic change (Lengwehasatit et al., 2008). Another typical feature of apoptosis which is peripheral chromatin condensation can be demonstrated in *B. pseudomallei*-infected cells using transmission electron microscopy (Kespichayawattana et al., 2000). At present, several specific bacterial factors have been shown to be involved in *B.p*-induced cell fusion leading to MNGC formation.

The role of the Bsa T3SS effector protein, BipB in the cell biology and virulence of *B.p* has been reported by Suparak and co-workers. Mutation of *bipB* reduced MNGC formation and cell-to-cell transmission of bacteria and promoted apoptosis of the J774A.1 macrophage cell line. The *bipB* mutant was also significantly debilitated following intranasal challenge of BALB/c mice where the *bipB* mutant showed a significant reduction in virulence, which could be completely recovered by complementation with a functional *bipB* gene (Suparak et al., 2005).

Utaisincharoen and colleagues demonstrated a role for *B. pseudomallei* RpoS (RNA polymerase sigma factor) protein in *B.p*-induced cell fusion. RpoS is a global regulatory factor known to control the expression of a large number of chromosomal genes involved in resistance to stress conditions. The *B. pseudomallei rpoS* null mutant was comparable to the wild type in terms of its ability to survive and replicate within macrophages, but incapable of stimulating MNGC formation (Utaisincharoen et al., 2006). *B.p rpoS* has been also implicated in the regulation of cell death in mouse macrophages since the *B.p* RpoS mutant failed to induce cytotoxicity in a mouse macrophage cell line (RAW 264.7) (Lengwehasatit et al., 2008).

B. pseudomallei encodes six T6SSs referred to as T6SS-1 to T6SS-6 (Schell et al., 2007; Shalom et al., 2007). It should be noted that the names assigned to each T6SS in *B.p* and *B.m*, and the names of some of the component subunits, differs between the two research groups. The nomenclature of Shalom et al., 2007 will be used here. It has been demonstrated that T6SS-5 (referred to as the 'cluster 1' T6SS by Schell et al., 2007) T6SS is related to the contractile tail of certain types of bacteriophage, such as T4, and that it is comprised of four main components: the tail tube (consisting of stacked rings of Hcp (TssD) with a tail spike located at the tip (consisting of a trimer of VgrG (TssI)), a contractile sheath (consisting of polymerised TssB and TssC, also referred to as VipA and VipB), a baseplate complex (consisting of TssE, -F and -G, and possibly TssA) and a membrane complex that includes TssJ, -L and -M. TssK may be a baseplate protein or it may link the baseplate to the cell membrane complex (Durand et al., 2014, Schell et al., 2007, Shalom et al., 2007).

T6SS-5 has an important role in *B.p* virulence. Firstly, it was shown to be upregulated upon infection of RAW cells (Shalom et al., 2007). Moreover, investigation of *B. pseudomallei hcp* gene deletion mutants (*Δhcp1* to *Δhcp6*) showed that only the *Δhcp-5* (*tssD-5*) mutant (Δhcp1 according to Schell et al. 2007) was attenuated for virulence in a Syrian hamster model (Burtnick et al., 2011). Although inactivation of *hcp5* had no effect on *B.p* uptake by a mouse macrophage cell line, it showed delayed intracellular growth and reduced levels of actin-based motility and was unable to induce cell fusion and MNGC formation in this cell line. The defect in MNGC formation might explain the reduction in intracellular growth, as the fusion of *B.p*-infected MNGC with uninfected cells provides nutrients that are required for bacterial growth (Burtnick et al., 2011). The T6SS-5 tail-spike protein, VgrG5 (TssI-5), has been implicated in cell membrane fusion during intercellular spread by *B.p* and its close relative *B. thailandensis* as MNGC formation was inhibited in *B.p* 340 and *B.t* E264 *ΔvgrG5* mutant-infected cells figure 1.2.2 (Toesca et al., 2014). Schwarz et al reported that VgrG-5 production is specifically activated during host cell infection, and VgrG-5 C-terminal domain is essential for the virulence, as vgrG-5ΔCTD mutant was avirulent in mice and unable to induce cell fusion (Schwarz et al., 2014).

Boddey and co-workers demonstrated that *B.p lfpA* mRNA (lactonase family protein A) expression is dramatically up-regulated in bacteria during infection of the RAW264.7 cell line compared to bacteria growing in the absence of RAW264.7 cells. *lfpA* was found to promote the expression of the osteoclast (a type of MNGC) markers, calcitonin receptor (CTR), cathepsin K (CTSK) and tartrate-resistant acid phosphatase (TRAP), as mutation of *lfpA* significantly inhibited the expression of these markers. This data suggested that *B.p* are able to stimulate several host cells factors involved in membrane fusion processes (Boddey et al., 2007).

 The role of several host cell surface molecules in *B.p*-induced MNGC formation in the human macrophage cell line U937 has been identified by utilizing monoclonal antibodies. Antibodies specific to a fusion regulatory protein (CD98), E-selectin (CD62E), integrin-associated protein (CD47), and E-cadherin (CD324) could almost completely suppress *B.p*-induced MNGC formation, while monoclonal antibodies against ICAM-1 (CD54), LFA-1 (composed of CD11a and CD18) and CD172a partially inhibited MNGC formation (Suparak et al., 2011). Flow cytometry analysis revealed that the expression levels of adhesion molecules CD47 and CD98 increased on U937 cells in response to *B.p* infection, whereas no significant increases in surface expression of CD62E or CD324 were detected suggesting that *B.p*-induced fusion is associated with up-regulation of CD47 and CD98, the mechanism by which these molecules facilitate *B.p* cell fusion in unknown, however it is likely to promote cell attachment and enable close contact for cell membranes, also it is possible that *B.p* induce the fusion by regulating the expression of these molecules (Suparak et al., 2011).
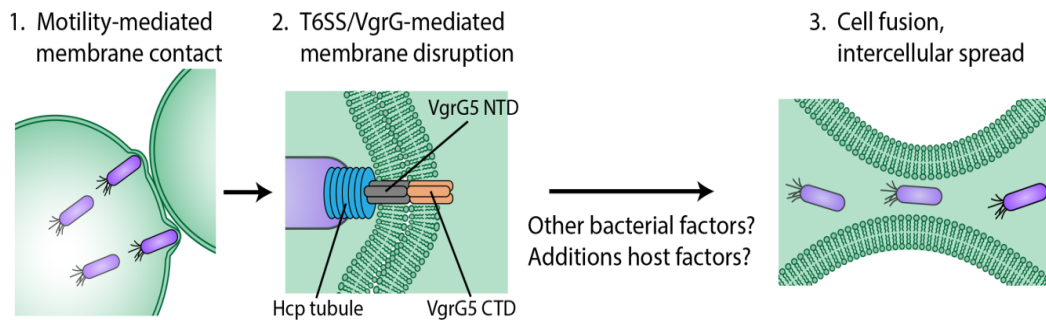
Figure 1.2.2 A hypothetical model of *Burkholderia pseudomallei*-induced cell fusion. *B. pseudomallei* stimulates the formation of MNGCs to promote intercellular spread once sufficient bacterial replication has occurred within an infected cell. A possible explanation of the mechanism of *B.p*-induced cell fusion could be that the lateral flagella or actin polymerization provide movement thereby facilitating the contact between bacteria and the plasma membrane (PM), which brings adjacent host membranes into close apposition. A close contact with the membrane activates contraction of the T6SS-5 sheath and VgrG5 is inserted across the infected and adjacent cell membranes , inducing a region of localized disturbance of lipid bilayers and creating a disordered hemifusion zone that leads to membrane fusion (Toesca et al., 2014).

1.2.1.4 Host cell response and inflammation

The immune status of a patient can have an effect on the onset and advancement of melioidosis and the diverse outcomes of the disease are basically correlated with the way in which the host immune system responds (Gan, 2005). The acute melioidosis of the BALB/c mice resulting in hyper-production of pro-inflammatory cytokines leads to an inappropriate cellular response including release of reactive oxygen species (ROI) and stimulation of autophagy which leads to increased replication and intracellular survival of the bacterium. Thus this response fails to eliminate the infection and contributes instead to tissue destruction and multiple organ failure. In contrast, in the chronic condition the immune response is less exaggerated, with a small increase in cytokine levels which triggers macrophages and allows *B.p* phagocytosis, thus allowing time for an adaptive immune response to occur (Koo and Gan, 2006, Ulett et al., 2002, Tan et al., 2008).

Toll like receptors (TLRs) are one of the critical innate immune signaling mechanisms that have a significant role in *B.p* defence. TLRs recognise conserved molecular patterns associated with pathogens and set into motion an inflammatory immune response. Wiersinga and colleagues found that the monocytes and granulocytes of melioidosis patients exhibited up-regulated TLR2 and TLR4 expression and mRNA levels. In addition, these TLRs can be activated by *B.p in vitro* (Wiersinga et al., 2007). West et al. showed that TLR2 and TLR4 can be stimulated by heat-killed *B.p.*, TLR4 can also be activated by *B.p* lipopolysaccharide (LPS) and lipid A thus these *B.p* molecules are TLR4 ligands (West et al., 2008). They also reported that cytokine TNF-α (tumour necrosis factor-alpha) and MIP (macrophage inflammatory proteins) production by macrophages stimulated with *B. pseudomallei* LPS or lipid A was entirely dependent on TLR4 as TLR4-/- cells failed to produce these cytokines (West et al., 2008).

Infection with *B.p* activates neutrophils and macrophages. Activated neutrophils are rapidly recruited to the lungs in response to *B.p* infection and reduction of these cells results in an acute and severe melioidosis. This increased susceptibility was associated with a suppression of the early pro-inflammatory cytokine response in the lungs (Easton et al., 2007). Within macrophages, *B.p* can remain viable due to a reduced level of lysosomal fusion and *B.p* survival in macrophages is likely to be responsible for chronic melioidosis (Puthucheary and Nathan, 2006).

One of the mechanisms by which B.p avoid killing by macrophages is the failing in activation of inducible oxide Synthase (iNOS), the expression of iNOS is induced by IFN-β (interferon-beta) and other cytokines. Failure of *B.p*-infected macrophages to produce sufficient level of these cytokines may be due to the lipopolysacchride (LPS) of *B.p* which differs from the LPS of other Gram-negative bacteria that stimulate the production of IFN-β and consequently induce significant levels of iNOS (Arjcharoen et al., 2007, Jacobs and Ignarro, 2001, Utaisincharoen et al., 2001). It has been reported that in *B.p*-infected macrophages the bacteria can suppress the activation of nitric oxide Synthase (iNOS) by activating two negative regulators; SOCS3 (suppressor of cytokine signalling 3) and CIS, a cytokine-inducible src homology 2 protein. Intracellular *B. pseudomallei* activate these regulators through intercellular receptors that are unknown (Ekchariyawat et al., 2005).
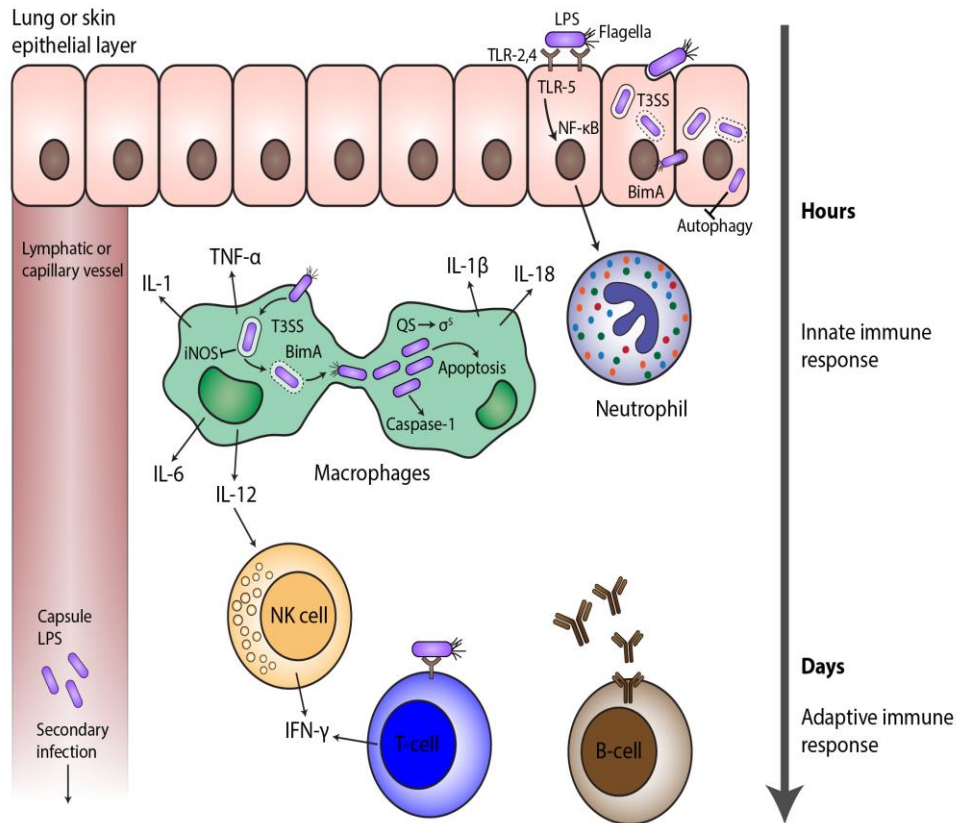
Figure 1.2.3 *Burkholderia pseudomallei* **pathogenesis**. From its ecological niches, *B.p* is transmitted to epithelial cells of the skin or lungs, where it initiates binding, likely via the bacterial capsule and type IV pili. Following invasion of epithelial cells, the T3SS3 effectors promote vacuolar escape and intracellular movement by utilizing BimA-mediated actin polymerization and inhibit killing by autophagy. TLR2 and TLR4 are activated by *B. pseudomallei* lipopolysaccharide (LPS) and/or flagella, leading to induction of innate immune cells including neutrophils, natural killer cells (NK) and macrophages. These cells are responsible for the pro-inflammatory cytokine release that causes host tissue damage seen in acute melioidosis, providing an additional intracellular niche for the replication of *B. pseudomallei*. Once bacterial replication within macrophages reaches a critical threshold, as determined by the action of regulatory factors such as QS molecules and RpoS, *B. pseudomallei* escapes via induction of apoptosis. Secondary spread can be facilitated by lymphatic vessels, with bacteria possibly carried within macrophages, or via the capillary vessels, with bacterial serum resistance mediated by the capsule and LPS. As the *B.p* infection progresses, the host mounts an adaptive immune response with T cells recruited in response to IFN-γ production allowing a cell mediated immunity (CMI) response, and B cells producing antibodies (Lazar Adler et al., 2009).

1.2.2 *Burkholderia thailandensis* as an alternative model for *Burkholderia pseudomallei* studies

The related species *B. thailandensis* was considered to be an avirulent biotype of *B.p* as most characteristics in both species are very similar (Brett et al., 1998, Anuntagool et al., 1998). However, in 1998 a 16S rDNA phylogenetic analysis demonstrated genotypic and phenotypic dissimilarities between two related species of *Burkholderia*, *B.p* 1026b, a virulent clinical isolate, and *B.p*-like E264, an environmental isolate, which was then named *B. thailandensis* (Brett et al., 1998).

B.p and *B.t* have the ability to invade, survive and replicate in a range of phagocytic and non-phagocytic cells (Kespichayawattana et al., 2004, Charoensap et al., 2009) and exhibit a particular intracellular life cycle (Wiersinga et al., 2006, Galyov et al., 2010). After uptake and escape from endosomes, they are able to replicate in the cytoplasm and induce plaque formation and cell fusion (Charoensap et al., 2009, Kespichayawattana et al., 2004). However, a difference in the rates of invasion, adherence capacity, growth and resistance to phagocytosis in some cell types is suggested to relate to the ability of *B.p* to produce an exopolysaccharide capsule (Reckseidler-Zenteno et al., 2005, Kespichayawattana et al., 2004). The notable difference between *B.p* and *B.t* is the ability of *B.t* to assimilate L-arabinose, whereas *B.p* lacks the entire arabinose assimilation operon (Lertpatanasuwan et al., 1999, Haraga et al., 2008), which may be responsible the virulence of *B.p* (Moore et al., 2004) . *B.p* is considered to be at least 10^6-fold more virulent than *B.t* in BALB/C mice(Ulett et al., 2001). The infection dose of *B.p* ranges from 50 to 50,000 cfu (colony forming units) in murine models (Titball et al., 2008).

Although *B.t* is considered to be non-pathogenic for humans, infected patients with similar symptoms to melioidosis have been reported in Thailand and the United States (Chen and Folch, 2006, Lertpatanasuwan et al., 1999, Brett et al., 1997). *B.t* has been shown to be lethal in the model system *Caenorhabditis elegans* (*C. elegans)* (O'Quinn et al., 2001). In addition, an inhalation challenge on mice with *B.t* caused severe infections that may be dependent on one or more virulence factors shared with *B.p* (Galyov et al., 2010). Intranasal challenge models with doses higher than 10^4 cfu of *B.t* showed that *B.t*-infected mice were killed by *B.p* disease phenotypes, despite *B.t* having been shown to be less virulent than *B.p* (Titball et al., 2008). Moreover, the inhalation of *B.t* in C56BL/6 mice induced lung pathologies similar to those stimulated by *B.p* (Wiersinga et al., 2008).

Bsa T3SS is considered to be a virulence encoding region which promotes the ability of *B.p* to escape from endocytic vesicles replicate and spread to other cells. This region is conserved to a large extent between *B.p* and *B.t* (Haraga et al., 2008). However, it has also been noted that the *B.t* Bsa T3SS is negatively regulated by incubation in a medium containing L-arabinose, which may affect the virulence of this bacteria (Moore et al., 2004). Furthermore, the absence of a gene cluster which regulates capsular polysaccharide production may also contribute to the reduced virulence of *B.t* (Reckseidler et al., 2001). These findings are suggestive of similar pathogenesis factors of the two species in animal models, which leads to the possibility of using *B.t* as an alternative infection model to study the behaviour of *B.p* and understand the pathogenesis of melioidosis.

Proteome analysis of *B.p* and *B.t* highlighted the expression of 14 hypothetical proteins of unknown function in *B.p* but not in *B.t* (Arjcharoen et al., 2007). The crystallography study of some these proteins revealed the structure of protein, which identified as *Burkholderia*

lethal factor 1 (BLF1) (Cruz-Migoni et al., 2011). Recombinant BLF1 is toxic and kills mice and cultures of macrophages, in addition, a partial in-frame deletion of the gene encoding BLF1 resulted in 100-fold less potent at killing mice (Cruz-Migoni et al., 2011). BLF-1 promotes deamidation of glutamine-339 of the translation initiation factor eIF4A, abolishing its helicase activity and inhibiting translation (Cruz-Migoni et al., 2011).

1.3 The aim and brief description of this study

As mentioned previously, there has been extensive research that showed the involvement of tetraspanins in cell fusion, an important process in health and disease. Takeda and co-workers, as well as our own group, demonstrated a role for tetraspanins in the fusion of monocytes/macrophages using mainly the model of con A-stimulation (Takeda et al 2003, Parthasarathy 2009 et al and Fanaei 2013). The role of tetraspanins in membrane fusion events which are associated with viral infectivity and spread has been widely studied. However, currently there is no research on the role of tetraspanins in cell fusion mediated by bacteria.

As discussed above, certain members of the *Burkholderia* genus have been shown to promote cell fusion leading to multinucleated giant cell formation, including *Burkholderia pseudomallei* the causative agent of melioidosis, and the closely related but non-pathogenic species *Burkholderia thailandensis*. The ability of the bacteria to induce cell fusion and MNGC formation has been associated with melioidosis pathogenesis. *Burkholderia* cell-cell spread and MNGC formation suggested to be controlled by its type VI secretion system; however the involvement of host cell factors in MNGC formation processes remains poorly understood. A Previous study shows that *B.p*-induced cells fusion can be inhibited by monoclonal antibodies to host cell surface molecules, and suggests the contribution of several cell membrane molecules in this process (Suparak et al., 2011).

Therefore we hypothesised a possible role for tetraspanins (a superfamily of cell membrane proteins) in monocyte/macrophage fusion induced by *Burkholderia*, and the aim was:

To investigate the role of tetraspanins in MNGC formation induced by *Burkholderia thailandensis.*

Initially the conditions under which *B.thailandensis* induces multinucleated giant cell formation in mouse macrophage cell lines were investigated as well as in human monocytic/macrophage cell lines. The possible role of tetraspanins on *B.thailandensis*-induced MNGC formation was investigated utilizing specific anti-tetraspanin antibodies, recombinant proteins corresponding to the large extracellular domains of tetraspanins (EC2) and synthetic peptides representing the EC2 domain. Further investigation was carried out using tetraspanin mutant cell lines.

To try to further explain the results that were achieved the expression levels of tetraspanins and other cell surface molecules in response to *B.thailandensis* infection were investigated. The expression levels of these molecules in the absence of certain tetraspanins were also studied. In addition, the project aimed to investigate *B.t* and host cell interactions using EM microscopy as well as investigating *B.t* and tetraspanin colocalization in MNGC using confocal microscopy. We further investigated the gene expression profiles of mouse macrophages lacking the tetraspanin CD9 by microarray analysis.

Chapter 2 Materials and Methods

2.1 Materials

2.1.1 General buffers and reagents

Ultrapure water was prepared using the Purite Neptune System (Scientific Laboratory Supplies Limited). This was used for the preparation of all buffers and solution unless otherwise stated. Bacteria culture media, buffers, glassware, tips and reagents were sterilised by autoclaving at 121°C, 15 psi for 20 min. Antibodies, antibiotics and other laboratory reagents were filter sterilised using 0.2 µm disposable filters (Sartorius).

2.1.1.1 Buffers and solution

General buffers and solutions used in this study are listed in table 2.1.1

Buffer	Preparation
BBN (washing/dilution)	0.1% sodium azide, 0.2% BSA(bovine serum albumin) Dissolved in BSS, stored at 4°C
BSS (balanced salt solution)	43.36g (NaCl), 1.83g (KCl), 8.19g (D-sorbitol), 3.00g ($K_2HPO_4 3H_2O$), O.7g (KH_2PO_4) and 12.09g HEPES. All dissolved in 4.8L ddH_2O, pH was adjusted to 7.2-7.4 using 1M (NaOH) then the final volume was adjusted to 5L, filter-sterilised and stored at 4°C
PBS (phosphate buffer saline) 10x	80g (NaCl), 2g (KCl), 11.5g (Na_2HPO_4), 2g (KH_2PO_4). Dissolved in 1L H_2O
M9 salts 10x	60g (Na_2HPO_4), 30g (KH_2PO_4), 5g (NaCl0, 10g (NH_4Cl). Dissolved in 1L dd H_2O, autoclaved and stored at room temp.
PFA (Paraformaldehyde solution) 4%	4g paraformaldehyde were dissolved in 50ml of dd$H_2$0 plus 1ml 1M (NaOH) in a glass bottle by heating in a H2O bath for 1hr at 60°C. This was left to cool, then 10ml of 10x PBS was added, the pH adjusted to 7.4, then topped to 100 mls with ddH2O and it was filter sterilized and stored at 4°C.
Con A (Sigma) stock solution	Dissolved to 1mg/ml in BSS, filter-sterilised and stored in aliquots at -20°C
Propidium Iodide 1mg/ml solution(Sigma)	1/1000 diluted in PBS
Lysis buffer (Triton X-100)	0.1% in PBS
Giemsa solution (Sigma)	0.6% w/v
Acid /ethanol	5% acetic acid(v/v), 5% dH_2O, 90% ethanol(v/v)

HBSS (modified)	No Mg2+, Ca2+, no phenol red (Lonza)
Blocking buffer (Western blot)	5% w/v semi-skimmed milk powder made in 1x TBS buffer, 0.15% Tween 20
Blotting buffer (10x)no methanol	30.3g Tris, 144 glycine, made up to 1 L
Blotting buffer (1x)	100 ml 10x blotting buffer, 200ml 10x blotting buffer, 200ml methanol, made up to 1L with water
SDS-PAGE running buffer (10x)	30g Tris-base, 144g glycine, 10g SDS, made up to 1L water
SDS-PAGE stacking gel buffer (4x)	6.06g Tris-base, 4ml 10% w/v SDS, pH adjusted to 6.8 and made up to 100ml in water stored at 4°C
SDS-PAGE separating gel buffer (4x)	18.17g Tris-base, 4ml 10% w/v SDS, pH adjusted to 8.8 and made up to 100ml in water stored at 4°C
Tris buffer saline tween 20 (TBST)	8.8g NaCl, 0.2 KCl, 3g Tris-base, 500µl Tween 20, pH adjusted to7.4 and made up 1L water

Table 2.1.1 Buffers and solutions.

2.1.1.2 Electrophoresis gel materials

Gel	Composition
SDS-PAGE separating gel (12.5%)	2.5ml water, 3ml 30% acrylamide, 1.9ml separating buffer(4x), 112µl 10% ammonium persulphate (made up in water) 5µl TEMED
SDS-PAGE stacking gel (5%)	1ml water, 300µl 30% acrylamide, 444µl stacking buffer(4x), 28µl 10% ammonium persulphate (made up in water) 5µl TEMED

Table 2.1.2 Electrophoresis gel

2.1.1.3 SRB assay buffers and solutions

Reagent	preparation
0.4% w/v SRB solution	40mg of sulforhodamine B salt (Sigma, cat. no S9012) in 10ml of 1% acetic acid solution
50% Trichloroacetic acid solution (TCA)	50g Trichoroacetic acid was dissolved in 80ml water, and the final volume was adjusted to 100ml with water and was stored at 4°C
Unbuffered Tris-base (10mM) 1	1.21g Tris-base was dissolved in 95ml water and pH adjusted to 10.5, final volume 100ml

Table 2.1.3 Reagent and solution for SRB assay

2.1.2 Antibodies

The primary antibodies, isotype controls and secondary antibodies used for immunofluorescent studies, fusion assays and Western blots are summarised in Tables (2.1.4), (2.1.5) and (2.1.6) respectively.

2.1.2.1 Primary antibodies

Antibody	Target antigen	specificity	Label	Conc. Used	source	Cat. NO	Isotype
Mouse anti-human CD9 (602.29)	CD9	Human	-	10µg/ml	Prof. Andrews Dept.of BMS, Univ. of Sheffield	NA	Mouse IgG1
Mouse anti human(H5C6)	CD63	Human	-	10µg/ml	In house	NA	Mouse IgG1
Mouse anti human CD37	CD37	Human	-	10µg/ml	Abcam	ab 76522	Mouse IgG1
Mouse anti human CD53	CD53	Human	-	10µg/ml	Serotec	ACA723F	Mouse IgG1
Mouse anti-human CD151 (14.A2)	CD151	Human	-	10µg/ml	Prof. Leonie Ashman University of Newcastle, Australia	NA	Mouse IgG1
Mouse anti human CD81	CD81	Human	-	10µg/ml	Serotec	MCA1847 T	Mouse IgG1
Mouse anti human CD82	CD82	Human	-	10µg/ml	Serotec	Mac1311	Mouse IgG1
Rat anti-mouse CD9	CD9	Mouse	-	10µg/ml	Serotec	MCA2749	Rat IgG2b
Hamster anti-mouse CD81	CD81	Mouse	-	10µg/ml	Serotec	MCA1846	IgG1
Anti-mouse CD63	CD63	Mouse	-	10µg/ml	Biolegend	143902	Rat IgG2a,κ
Rat anti-mouse CD47	CD47	Mouse	-	10µg/ml	Biolegend	127502	Rat IgG2a,κ
Rat anti-	CD98	Mouse	-	10µg/ml	Biolegend	128202	Rat

							IgG2a,κ
mouse CD98							
Rat anti-mouse/human CD44	CD44	Mouse/human	-	10μg/ml	Biolegend	103002	Rat IgG2b,κ
Rat anti-mouse CD200	CD200	Mouse	-	10μg/ml	Biolegend	123802	Rat IgG2a,κ
Rat anti - mouse CD206	CD206	Mouse	-	10μg/ml	Biolegend	141702	Rat IgG2a,κ
Rat anti - mouse CD172a	CD172a	Mouse	-	10μg/ml	Biolegend	144002	Rat IgG1,κ
anti-mouse CD36	CD36	Mouse	-	10μg/ml	Biolegend	102602	Armenian Hamster IgG
Rat anti-mouse CD324	CD324	Mouse	-	10μg/ml	Biolegend	147302	Rat IgG1,κ
Anti-DC-STAMP	DC-STAMP	Mouse /Human	-	10μg/ml	MILLIPORE	MABF39	IgG2a,κ
PE anti-mouse/rat/human MCP1	MCP1	Mouse/rat/human	PE	10μg/ml	Biolegend	505904	Armenian Hamster IgG

Table 2.1.4 Primary antibodies

2.1.2.2 Isotype controls

Isotype	Label	Conc. used	Source	Cat. No
Mouse IgG1, κ (clone JC-1)	-	10μg/ml	In house	NA
PE Armenian hamster IgG	PE	10μg/ml	Biolegend	400908

Rat IgG2a,κ	-	10µg/ml	Biolegend	400502	
Rat IgG2b,κ	-	10µg/ml	Biolegend	400602	
Armenian Hamster IgG	-	10µg/ml	Serotec	MCA2356	
Mouse IgG1,κ	-	10µg/ml	Biolegend	400101	
Mouse IgG2a,κ	-	10µg/ml	Biolegend	401501	

Table 2.1.5 The isotype control

2.1.2.3 Secondary antibodies

Antibody	Target antigen	Label	Conc. used	Source	Cat. No
anti-mouse IgG	Mouse IgG	FITC	1:250	Sigma	F-2653
anti-hamster IgG	Hamster IgG	FITC	1:100	Bio RAD	MCA 2357
anti-rat IgG	Rat IgG	FITC	1:350	Sigma	F-9387
Alexa Fluor® 546 Phalloidin	Rat IgG	Alexa Fluor	1:200	Life science	A22283
Goat anti-Rat HRP	Rat	HRP	1:5000	abcam®	Ab97057

Table 2.1.6 Secondary antibodies

2.1.3 Recombinant tetraspanin proteins

The GST-fusion proteins of the tetraspanin large extracellular domains (EC2) of CD9, CD63, CD81, CD151 and Tspan 2 were constructed and purified in the laboratory by co-workers Marzieh Fanaei, John Palmer and Ibrahim Yaseen as described in detail by Higginbottom and co-workers (Higginbottom et al., 2003) and in sections 2.2.4.1 -2.2.4.3 .

2.1.4 Bacteriology work

2.1.4.1 Bacteriological reagent

Media and other reagents used for bacteriological work are summarized in Table 2.1.7.

Media	Preparation
LB (Luria-Bertani) Broth	10g tryptone, 5g yeast extract, 10g NaCl. Dissolved in 1L H_2O pH adjusted to 7, and autoclaved
LB Agar	10g tryptone, 5g yeast extract, 10g NaCl, 15g bacteriological agar. Dissolved in 1L dd H_2O, pH adjusted to 7, and autoclaved
M9 Minimal Agar	0.5g glucose, 1.5g bacteriological agar. Dissolved in 90ml H_2O, autoclaved then 10ml M9 salts, 0.1ml 1M $MgSO_47H_2O$, 0.1ml 0.1M $CaCl_2$ (sterile) were added
Kanamycin solution	A stock solution was made at 25mg kanamycin/ml in H_2O and then was filter sterilized and stored at -20°C
Amikacin solution	A stock solution was made at 25mg amikacin /ml in H_2O and then was filter sterilized and stored at -20°C
Chloramphenicol solution	A stock solution was made at 34mg chloramphenicol /ml in ethanol and then was filter sterilized and stored at -20°C

Table 2.1.7 Bacterial reagents

2.1.4.2 *Burkholderia thailandensis* strains

E264 an environmental isolate, sequenced strain (Brett et al., 1998, Yu et al., 2006).

CDC2721121 clinical isolate from Louisiana, abbreviated as CDC272 (Glass et al., 2006)

Current stocks of both strains were kind gifts from the laboratory of Professor Richard Titball, Biosciences, University of Exeter.

2.1.4.3 Fluorescent protein-encoding plasmids

PIN 25 (GFP) plasmid and PIN29 (DS Red) plasmid (INSERT REFERENCE – SEE BELOW) were used for labelling the bacteria and these were obtained from Dr Mark Thomas (Dept. Infection and Immunity, Medical School, University of Sheffield) (Vergunst et al., 2010).

2.1.6 Mammalian cell culture work

2.1.6.1 Mammalian cell lines

J774.2 This is a mouse BALB/c monocyte/macrophage cell line that was recloned from J774.1 the original ascites and solid tumour [118, 119]. These cells were obtained from Prof H. Harris and Dr R.Sutherland (Sir William Dunn School of Pathology Oxford).

RAW 264.7 This is a mouse BALB.c monocyte/macrophage cell line that was established from ascites of a tumour induced in a male mouse by intraperitoneal injection of Abselon Leukaemia virus (A-MuLV) [120, 121]. Current stocks were from Dr Peter Grabowski (Medical School, University of Sheffield), obtained from the American Type Culture Collection (ATCC).

U937 cells This is a human histiocytic lymphoma cell line with monocytic characteristics (Sundstrom and Nilsson, 1976). They were originally obtained from Dr. Jim Gallagher (Dept. Human Metabolism, Medical School, University of Sheffield).

THP-1 cells This is a human monocytic cell line derived from a patient with acute monocytic leukaemia (Tsuchiya et al., 1980). These were obtained from ECACC.

Mutant cell lines and their corresponding wild-type

CD9WT and CD9KO cells These are macrophage cell lines derived from CD9 knockout and the corresponding wild type C57BL/6 mice (Ha et al 2005). CD9-/- mice were generated in which the CD9 gene was disrupted by gene targeting in embryonic stem (ES) cells using homologous recombination. The recombination was confirmed by southern DNA blot and absence of CD9 was verified by flow cytometry analysis and immunohistochemistry as described by the authors (Le Naour et al., 2000, Ha et al., 2005). Peritoneal mouse macrophages were transformed using J2 transforming retrovirus (Ha et al 2005). These cells were kindly provided by Dr. Gabriela Dveksler, Dept. Pathology. Uniformed Services University of Health Sciences, Bethesda, MD, US.
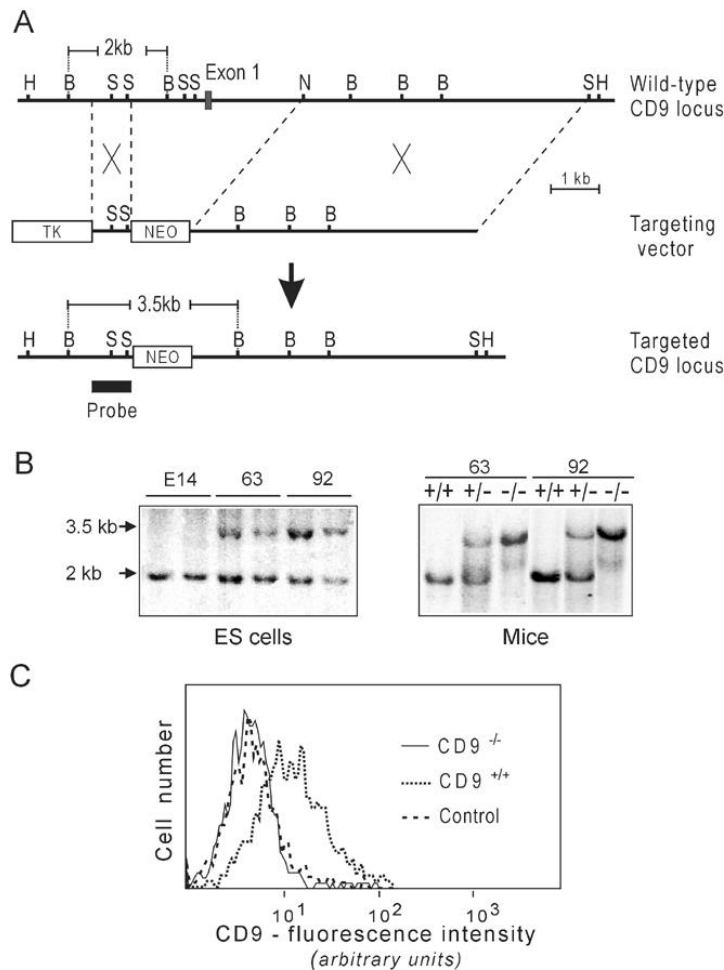
CD82WT and CD82KO cells These are mouse macrophage cell line derived from and CD82-/- and the corresponding wild type C57BL/6 mice. CD82 was deleted by homologous recombination-based gene targeting in (ES) cells and deletion of CD82 was confirmed by Southern blot and PCR analysis (Risinger et al., 2014, Wei et al., 2014). These cells were kindly provided by Professor Jatin Vyas, Division of Infectious Disease, Massachusetts General Hospital, Boston.

2.1.6.2 Media

- Dulbecco's Minimal Essential (DMEM) 4.5 g/l Glucose Medium (Gibco).
- Dulbecco's Minimal Essential Medium (DMEM) GlutaMAX™ media (Gibco).
- RPMI 1640 medium (Gibco).
- Foetal Calf Serum (FCS) (Biowest).
  The media were purchased ready-made as 1x solution, FCS was added to a final concentration of 10%.

2.1.6.3 Cell culture solutions and reagent

- Cell dissociation solution (CDS).
- Phorbol 12-Myristate 13-acetate (PMA)(Sigma P1585). Stock solution was prepared in DMSO (Sigma D2650) at 50-100μg/ml, filter sterilised and stored in aliquots at -

20°C. The solution was diluted 1/10 in fresh DMSO prior to use at final concentrations of 20-50ng/ml in tissue culture medium.

- Poly-L-lysine solution (Sigma P4707), 0.01% sterile-filtered in water, stored at 4°C.
- 2×10^{-3} M 2-Mercaptoethanol (14µl neat 2-ME was diluted to 10ml with 0.15M NaCl, 1ml of this solution was added to 9ml of saline to make the 2×10^{-3} M stock, which was filter sterilised and stored in aliquots at -20°C).
- Trypan blue with colour intensity 23850. The solution was prepared by dissolving 0.2g trypan blue in 100ml 0.013M citrate buffered saline.
- Freezing Mixture was 90% FCS, 10% dimethyl sulphoxide (DMSO), protected from the light and stored at 4°C or in aliquots at -20°C.
- CelLytic™ M Mammalian Cell Lysis/Extraction Reagent (Sigma C2978).
- Protease Inhibitor Cocktail (Sigma P8340) stored in aliquots at -20°C.

2.1.6.4 Mountants

- DPX Mountant for histology (Sigma 44581).
- Vectashield mountant with DAPI (Vector Labs H-1200)

2.1.7 Laboratory equipment and instrumentation

Equipment	Supplier
Flow cytometry	Becton Dickinson (BD)FACS Calibre LSR II (BD)
Class I Microbiological safety cabinet	WALKER
Class II Microbiological safety cabinet	BioMAT²
Microscopes	Eclipse E400 (fluorescence) (Nikon) CK40 (light) (Olympus) A1+ Confocal imaging system (Nikon)
Incubators	BIOHIT LTE laboratory thermal equipment LTD
SDS-PAGE and Western blotting equipment	Biorad Mini-PROTEAN Tetra Cell and Mini-Transblot Module

Table 2.1.8 Laboratory equipment.

2.1.8 General laboratory consumables

Consumable	Supplier

Cell culture dishes	Corning Inc
Petri dishes	Sterilin
12x75mm FACS tubes	Elkay
Lab-Tek II chamber slides	Nalgene Nunc International
Multi well plates	Corning Inc
25cm cell scraper	Sarstedt
Microscope slides	Thermo Scientific
Spectrophotometer cuvettes	Sarstedt
Universal tubes	Sarstedt
0.5/1.5ml tubes	Eppendorf
gloves	Glovco powder free nitrile
Pipette tips	Starlabs
Aluminium foil	Aluchef
Cryovials	Nunc
Pasteur pipettes	Mexcel
Parafilm	Sigma-Aldrich

Table 2.1.9 laboratory consumables.

2.1.9 Software

- **GraphPad Prism 6** Statistical analysis software was used for data analysis.
- **Lucia G Immunofluorescence software** was used for Image processing.
- **Cell Quest Pro Flow cytometry software** was used for data acquisition and analysis.
- **Flow Jo software:** was used for Flow cytometry data analysis.
- **NIS-Elements confocal software** was used for capturing the images.
- **Image J and Fiji software:** were used for image analysis.
- **QLUCORE software:** was used for microarray data analysis**.**

2.2 Methods

2.2.1 Tissue culture methods

2.2.1.1 Growth conditions

Cell lines were cultured in standard tissue culture flasks at 37°C under different CO_2 concentration; 8% (J774 and RAW264.7) or 5% (THP1, U937, CD9WT, CD9KO, CD82WT and CD82KO) in a humidified atmosphere. Cells were harvested and subcultured depending on the type of the cells.

J774.2 cells were cultured in DMEM+2mM glutamine + 4.5g/l glucose with 10% FCS. Once cells were confluent the medium was removed and the adherent cells were harvested with 10ml medium using a cell scraper and cells were split 1:6 to 1:13 using fresh medium.

RAW264.7 cells were cultured in DMEM with GlutaMAX +10% FCS. Cells were harvested and subculture the same as J774 cells.

THP1 cells were cultured in RPMI medium + 50µM 2-mercaptoethanol+ 10% FCS. Cells were harvested by centrifugation at 400g for 5 minutes, and then were resuspended in 10 ml of medium. Cells were split 1:3 to 1:10 in medium and incubated as described above.

U937 cells were cultured in RPMI medium 10% FCS. Cells were harvesting and subcultured the same as THP1.

CD9 WT and CD9KO cells were cultured in DMEM+2mM Glutamine + 4.5g/l glucose + 10% FCS. Once cells were about 80% confluent the medium was removed and the adherent cells were harvested with 10ml medium using a cell scraper and cells were split 1:3 to 1:10 using fresh medium.

CD82 WT and CD82KO cells were cultured in RPMI medium 10% FCS. Once cells were confluent the medium was removed and cells were harvested with 10ml medium using a cell scraper and cells were split 1:3 to 1:6 using fresh medium.

2.2.1.2 Cell counting and viability measurement

Cells were counted using an Improved Neubauer haemocytometer. The viability of growing cells was tested by trypan blue exclusion after incubation at 1:5 for 3 min.

2.2.1.3 Cell freezing

When new batches of cells were growing well in log phase with good viability (>90%) (1-5x10^{6}cell /ml), an appropriate volume of suspension was centrifuged for 5 min, at 400g. The supernatant was discarded and the pellet was placed on ice, then resuspended with freezing mixture then 1ml of cell suspension was transferred into each chilled freezing vial (labelled with the cell line and the date). The vials then transferred to a biological freezing plug for gradual chilling (1°C per minute) in the vapour phase of a liquid nitrogen dewar for 1.5 hr. After that the vials were a placed in a storage cane and transferred to liquid nitrogen.

2.2.1.4 Cells thawing

The vials were removed from liquid nitrogen and agitated under the hot tap until nearly thawed, then wiped with tissue soaked in ethanol and placed on ice. The contents were transferred quickly to a chilled universal tube standing on ice. 9 ml of pre-warmed medium (no FCS) was added, the mixture was centrifuged at 200g for 5min, the supernatant was discarded and the cells were resuspended with appropriate medium containing 10%FCS and placed into new culture flask. The viability and cell growth were monitored over the next few days.

2.2.2 Stimulation of U937 and THP1 with phorbol 12-myristate 13-acetate (PMA)

Cells were pelleted and resuspended at a cell density of 0.3×10^6/ml in RPMI medium + 50µM 2-mercaptoethanol+ 10% FCS for THP1 cells and RPMI medium 10% FCS for U937 cells. Phorbol ester (PMA) was added at final concentration 160 nM. Cells were incubated for 72hr.

2.2.3.1 Immunofluorescence for cells grown on slides

The cells were harvested using medium and the suspension was diluted to 0.7×10^5/ml and 0.5ml was dispensed into the wells of a Lab-Tek™ chamber slide (each slide has 8 chambers) and incubated overnight. The cells were washed once with HBSS, fixed and permeabilized with acetone (0.5 ml/chamber) for 5 min. at RT. Cells were then washed twice with 1x PBS followed by a third wash for 10 minutes in a tank of PBS with stirring. Cells were incubated with 100µl of primary antibody or isotype control (10µg/ml in BBN) for 45-60 minutes. Cells were washed with 1x PBS 3 times as before. Cells were incubated with 100µl/chamber of appropriate secondary- labelled antibody for 30 min, at room temperature under humid conditions in the dark. The slides then were washed as before with PBS. The nuclei were staining by adding 100µl/chamber propidium iodide (1µg/ml diluted with PBS) for 3 minutes at RT. Slides were washed with PBS as described previously. The plastic chamber compartments were removed according to manufacturer's instructions. Remaining PBS was removed from each section by using a Pasteur pipette before adding small drop of mountant to each. The slides were covered with a large size coverslip and sealed using nail varnish and stored at 4°C in the dark until examined by fluorescence microscopy.

2.2.3.2 Assessment of antigen expression by flow cytometry

2.2.3.2.1 Detection of surface antigen expression

For estimation of the expression level of surface antigen the experiment was carried out using live cells with high viability (>90%) at 4°C to avoid capping, internalisation and shedding of the antigen. Cells were harvested and counted and resuspended in BBN. The suspension was centrifuged for 5 minutes at 400g, the supernatant was discarded and the cells were resuspended with cold BBN at $0.5 \text{-} 1 \times 10^6$/ml. The suspension was dispensed in 1ml aliquots in round bottomed plastic test tubes (FACS tubes) and centrifuged at 400g for 5 minutes. Cells were washed twice with cold BBN by centrifugation. Cell pellets were incubated with 50µl of primary antibody (10µg/ml in BBN unless otherwise stated) for 1hr on ice. Cells then were washed twice with BBN with centrifugation at 400g for 5min. 50µl labelled secondary antibody was added to the cell pellet and incubated for 1hr in the dark on ice, and then washed as before. For analysis by flow cytometry cells were resuspended with 0.3ml BBN and stored on ice until sampled. Flow cytometry was carried out using a FACS LSRII machine at the Medical School Flow Cytometry Facility, University of Sheffield. Data analysis was carried out using Flow Jo software.

2.2.3.2.2 Detection of surface and intracellular antigen

In these experiments cells were fixed and permeabilized using a permeabilization kit (Life Science GAS-003) which allows access of antibody to intracellular targets. Cells were harvested, washed and transferred into FACS tubes as described above (2.2.3.1.1). At this

step tubes were separated into two groups; in the first group samples were fixed (for surface staining only) and in the second group cells were fixed and then permeabilized (for surface and intercellular staining). Cells were fixed with 50μl reagent A (fixative) for 15 minutes at RT. Cells were washed twice with BBN and 50μl of primary antibody or isotype control and either reagent B (for permeabilization) or 50μl BBN (or fixed cells only) were added for 30 minutes. Cells were washed twice with BBN and incubated with 50μl of FITC-labelled secondary antibody and either reagent B or 50μl BBN (for fixed cells only) for 30 minutes in dark. Cell were washed twice and resuspended in 300μl of 2% paraformaldehyde solution (PFA) and stored at 4°C in the dark before FACS analysis.

2.2.3.2.3 Flow cytometry gating strategy
Initially, the negative control sample (unstained cells with viability > 98%) was used to adjust the forward lights scatter and side scatter then the cell population of interest was gated to include for further analysis.

2.2.3.2.4 Controls
- Negative control (unstained cells).
- Negative control (cells stained with labelled secondary antibody only).
- Isotype control (cells incubated with isotype control flowed by staining with secondary labelled antibody).

2.2.4 Production of recombinant GST-EC2 of tetraspanins
The recombinant proteins corresponding to the large extracellar domains (EC2s) of tetraspanins were produced in our laboratory for studying tetraspanin functional activities. The glutathione S-transferase (GST) gene fusion system was used to produce GST-EC2 proteins as described previously (Higginbottom et al., 2003), with DNA corresponding to the tetraspanin EC2 regions cloned into the pGEX-KG expression vector (Guan and Dixon, 1991). The next section describes the method in more detail. These proteins were produced by other laboratory members.

2.2.4.1 Recombinant protein GST-EC2 production
Protein expression was carried out in *E.coli* Rosetta-gami B (DE3) pLysS (Novagen). The transformation was performed as instructed by the manufacturer, with minor modifications. Aliquots of competent cells (10μl) were defrosted on ice for 5minutes. 1μl of tetraspanin expression plasmid (1ng/μl stock) was added to the cells, mixed by gentle swirling and incubated for 5 minutes on ice. The DNA was transformed into *E.coli* by heat shock for 30 seconds in water bath at 42°C. Cells were then incubated immediately on ice for 2 minutes. 190μl SOC medium was added and cells were incubated for an hour at 37°C with shaking (250rpm). 25-100μl of the culture was plated on LB agar selection plates supplemented with antibiotics (Table 2.1.7), and incubated at 37°C overnight. Single colonies from overnight plates were inoculated into 5ml selective (antibiotic-containing) LB broth overnight at 37°C with shaking (250rpm). Aliquots of 1ml from the culture were inoculated into 500ml LB antibiotic selective media and cultured overnight at 37°C with shaking (100rpm). The optical density of the bacterial culture was measured and the culture was diluted with LB to reach an OD_{600} of 0.6-0.8. The expression of recombinant protein was then induced by culture with 0.1mM IPTG for 4 hours at 37°C with shaking (250rpm). The

cultures were pelleted by centrifugation at 4,500g for 20 minutes at 4°C. The supernatant was discarded and pellets were stored at -80°C.

2.2.4.2 Recombinant protein GST-EC2 extraction and purification

Frozen pellets were defrosted on ice and resuspended gently in 1x ice-cold PBS buffer (5-10ml PBS/g of bacteria pellet) containing 1 in 100 v/v dilution of Halt Protease Inhibitor Cocktail (Thermoscientific). The bacterial suspension was split into chilled universal tubes and sonicated (each tube was sonicated at an amplitude of 15 microns for two 10 second bursts and this was repeated for 5-6 rounds then tubes were placed in a beaker containing 50% ice-water. Lysed bacteria were centrifuged at 24,000g at 4°C for 20 minutes to pellet insoluble cell debris. The supernatant was transferred into a fresh chilled Falcon tube, and purified immediately or stored at -80°C until purification. Recombinant protein was purified using glutathione-Sepharose beads (G4B, GE Healthcare). The supernatant was mixed with about 1.33ml (100µl/g of bacteria ballet) of glutathione beads, incubated at RT for 1hr or overnight at 4°C with gentle rotation on a blood mixer. Beads were pelleted by centrifugation at 500g at 4°C for 5 minutes. The supernatant was discarded and the beads were then washed in 5 bead volumes of ice-cold 1x PBS and centrifuged as before. This was repeated twice more. Beads then were resuspended in 25mM glutathione elution buffer (about 0.5-1ml/g of original bacterial pellet) and incubated at RT with gentle rotation on blood mixer to elute the recombinant protein. Beads were centrifuged and the supernatant was transferred into a fresh ice cold tube (the first elution). Beads were resuspended again in elution buffer (the volume this time was half that used in the first time) and incubated as before. Beads were then pelleted and the supernatant was transferred into fresh ice-cold microfuge tubes (the second elution). Tubes were stored at -80°C unless used immediately. The protein concentration of the first and second elutions was estimated spectrophotometircally by Bradford assay and samples with the same protein concentration were mixed. Protein samples were run on SDS-PAGE gels and subjected to Coomassie staining to visualise all proteins present or subjected to Western blot using conformation-sensitive antibodies to confirm correct folding of the GST-EC2 tetraspanins as described previously (Parthasarathy et al 2009).

2.2.4.3 Reduction of LPS contamination by Triton X-114

In some cases, steps were taken to reduce potential LPS contamination of the recombinant GST-EC2 proteins using the method described in (Reichelt et al., 2006). Following incubation of bacterial cell lysate with GST-Sepharose beads for 2hr, the tubes were centrifuged and the supernatant was discarded. The beads were placed on ice for 5 minutes then incubated with 50 bead volumes of ice-cold 0.1%v/v Triton X-114/PBS at 4°C for 2 minutes with rotation on a blood mixer. The tubes were centrifuged at 500g for 5 minutes at 4°C, and the pelleted beads were washed three times with 20 volumes of PBS. Recombinant GST-tagged protein was eluted from the beads as described in 2.2.4.2.

2.2.5 Sodium Dodecyl Sulphate-Polyacrylamide Gel Electrophoresis (SDS-PAGE)

12.5% separating gels and 5% stacking gels were prepared as described in Table 2. The protein samples were mixed with the loading buffer (4x reducing for Coomassie staining and 2x non-reducing for Western blot) and were boiled for 15 minutes. 16µl of protein

sample and 7μl of standard protein marker (All Blue Precision Plus, Biorad, 161-0373) were loaded into the gel. Gels were first run at low voltage (60-70v) to let the sample cross the stacking gel (for ~30 minutes), then the voltage was set to 100v for 60-90 minutes.

2.2.6 Western Blotting

Once the protein samples had run on SDS-PAGE, it was transferred from the gel to nitrocellulose membrane (Hybond ECL, Amersham) for immunoblotting. A gel sandwich was assembled containing sponge, blotting paper, the SDS-PAGE gel, nitrocellulose membrane and these were all soaked in blotting buffer. The sandwich was then placed in a blot module with the nitrocellulose membrane at the anode side. An ice pack was also placed in the module and the module was filled with blotting buffer. The protein was transferred at 250mA for 2hr. The membrane was removed from the cassette and placed in blocking buffer at 4°C overnight to block non-specific protein binding sites.

2.2.7 Nitrocellulose membrane-probing

Appropriate primary antibodies and isotype controls were prepared in blocking buffer. The membranes were washed with dH$_2$O to remove the excess blocking buffer and then were washed with TBST for 5 minutes 2 times. Membranes were washed with dH$_2$O and were incubated with primary antibodies for 1-2hr at RT with rocking. The membranes were washed once with dH$_2$O and the with TBST 3 times each for 5 minutes with rocking. Secondary HRP-labelled antibodies were also prepared in blocking buffer at appropriate concentration and incubated with the membranes for 1hr with rocking. The membranes were washed for 25 minutes with TBST with several changes of buffer. Membranes were then incubated with SuperSignal West Pico chemiluminescent substrate (Thermo Scientific). Membrane were placed in a cassette and exposed to CL-Xposure X-ray film (Pierce) for varying times. The exposed film was immersed in developing solution for 30 seconds until the appearance of the bands, then washed with tap water, and immersed in fixative solution for 30 seconds, washed with water and left to dry.

2.2.8 Microbiology Methods

2.2.8.1 Bacteria growth condition

B.t E264 and *B.t* CDC272 were stored using minimal agar plates (M9-glucose agar). The bacteria were streaked on the agar, incubated at 37°C for 48hrs and then the plates were stored at 4°C.

2.2.8.2 Bacterial glycerol stock

Bacteria were cultured overnight in LB broth at 37C° with shaking. 700μl of culture was added to 300μl of 50% glycerol (final concentration 15%). The mixture was transferred into labelled cryovial tubes and mixed using a vortex mixer and tubes were stored at -80C°.

2.2.8.3 Estimation of viable bacteria

The number of viable bacteria was estimated by culturing a tenfold serial dilution of growth culture on LB agar plates. The number of bacteria was assessed using the Miles and Misra method (Miles et al., 1938). The relationship between bacteria numbers and optical density (OD) of the culture was determined and accordingly the number of the bacteria in the

culture at OD~ 0.4 at 600 nm was (~ 1×10^8/ml), and cultures at this OD were used in the following assays.

2.2.8.4 Labelling of *Burkholderia* with fluorescent protein-encoding plasmids

Burkholderia strains were inoculated in 6ml of LB broth and incubated overnight at 37°C whilst shaking and an extra empty culture (no plasmid) was used as a control. The culture was transferred into four 1.5ml micro-centrifuge tubes and centrifuged at 22289g for 2 minutes at RT. The supernatant was discarded and the pellet was gently re-suspended in 1 ml sterile 300mM sucrose solution, the resuspended pellets were centrifuged as before for 1 minute and this step was repeated for 2 minutes. The pellets in four tubes were resuspended with 100µl of 300mM sucrose solution sequentially with the same 100µl. 100µl of this suspension was transferred into a 2 mm-gap electroporation cuvette and 500ng of appropriate vector DNA (2.1.2.3) was add. The pulse was applied using the automated bacteria *P. aeruginosa* setting in the Bio-Rad gene pulser (25µF, 200Ω, 2.5kV). Immediately, 1ml of LB was added and the culture then transferred into a universal tube and incubated at 37°C for 2hr with shaking. 10-fold serial dilutions were made and 50-100µl of selected dilutions were spread onto antibiotic-containing selection plates and incubated at incubated at 37°C for 24hr. The success of transformation was confirmed using fluorescence microscopy.

2.2.9 Multinucleated giant cell formation assay

2.2.9.1 Stimulation of cells with Concanavalin A (Con A)

The cells were treated with Con A in an attempt to induce cell fusion and MNGC formation. Con A is a carbohydrate binding lectin and is a well-known mitogen which stimulates monocytes to form multinucleated giant cells (MGCs) in vitro (Takeda et al., 2003, Parthasarathy et al., 2009)). J774.2 and RAW264.7 cells were resuspended to 0.7×10^4 and 1.4×10^4 /ml with medium. 0.5ml aliquots of suspension were dispensed into the wells of Lab-Tek™ chamber slides. The cells were cultured overnight, and then the medium was removed from the chambers. 0.5ml of medium containing Con A at various final concentrations (10, 20, 50, and 100) µg/ml was added to the cells growing in the chambers. The dilutions were made up using sterile culture medium and each was tested in duplicate. As a control an equivalent volume of BSS was added to the medium for each dilution. Slides were then incubated for 72hr.

2.2.9.2 Staining and analysis of cell lines treated with Con A

Con A-stimulated cells were fixed and stained as described in 2.2.3.1. The primary antibody was mouse anti-actin (unlabelled monoclonal antibody, clone NH3 produced "in house") and the secondary was FITC-labelled anti-mouse IgG antibody. Images were captured with x20 objective of Nikon Eclipse E400 immunofluorescence microscope.

2.2.10 *Burkholderia thailandensis*-induced multinucleated giant cell assays

2.2.10.1 *Burkholderia* uptake and intercellular survival assay

Initially, an optimization trial for a suitable multiplicity of infection (MOI) was carried out. Mammalian cells were seeded at 2 x 10^5 cells/ml in 24-well plates and cultured overnight. An overnight culture of bacteria was washed with 1X PBS twice with centrifugation, and the pellet was resuspended with LB medium to OD ~ 0.4, and then diluted with tissue culture medium to reach an appropriate number of bacteria. Cells were infected at a multiplicity of infection (MOI) of 3, 5, 10, 50, and 100. The cell monolayers were incubated at 37C°, 5%CO$_2$ for 2h, the cells then washed with PBS and incubated with media containing 500µg/ml kanamycin for an additional 2hr to eliminate extracellular bacteria. As a negative control, cells were treated with cytochalasin D for 1hr prior to infection to prevent bacteria uptake; also the supernatant from the cells was examined for viable bacteria. Cells then were washed with 1x PBS and lysed in 0.01% Triton x-100 in PBS for 5 min. The lysis mixture was diluted and a selection of dilutions were plated on LB agar plates and incubated for 28hr at 37C° and the numbers of colonies (CFU/ml) were counted.

2.2.10.2 Optimization of *Burkholderia thailandensis*-induced multinucleated giant cell formation assays

Although MNGC formation is of interest to our group and fusion assays have been widely performed by previous researchers in the laboratory, where human monocytes were induced to fuse using various reagents, the present study was the first time that bacteria had been used. Therefore attempts to optimize the conditions for *Burkholderia*-induced cell fusion were made, using variations of the methods described by Wand and co-workers (Wand et al 2011). Cells were infected with bacteria using varied conditions. Cells were cultured into 24-well plates directly or in 24-well plates containing glass coverslips. Cells were infected at MOIs of 1, 3 and 10 for 30, 60 or 120 minutes and to suppress growth of extracellular bacteria kanamycin alone or with in combination with amikacin at concentrations of 100, 250 and 500µg/ml were investigated. According to the results of the optimization experiments, the MOI of 3:1 and 2hr infection with f kanamycin and amikacin (at 500µg/ml for each) were chosen as the optimal conditions for the *B.t-induced* cell fusion assay. After an appropriate time post-infection cells were washed with 1x PBS and fixed using acid/ethanol (5% acetic acid (v/v), 5% dH$_2$O and 90% ethanol (v/v)) for 30minutes at RT. Cells were washed with PBS and stained with Giemsa solution (0.1% solution w/v) for 30 minutes at RT, then washed with dH$_2$O and allowed to dry. Images were captured with Nikon light microscope using the 40X objective.

2.2.10.3 Evaluation of multinucleated giant cell formation

Images were analysed using Image J software. Images of 10 random fields captured at 400x magnification were analysed and cells with 3 nuclei or more were present were considered to be MNGCs. Data from all 10 fields/well were combined, and then the percentage of MNGCs and the average MNGC size were calculated using following formula (Parthasarathy et al., 2009).

$$Percent\ of\ MNGCs\ (fusion\ index)$$
$$= \frac{number\ of\ nuclei\ in\ giant\ cells}{total\ number\ of\ nuclei\ counted} x100$$

$$MNGC\ size = \frac{number\ of\ nuclei\ in\ giant\ cells}{number\ of\ giant\ cells}$$

2.2.10.5 Effects of tetraspanins on *Burkholderia thailandensis*-induced multinucleated giant cell formation

2.2.10.5.1 Effects of a short incubation with tetraspanin reagents on *B.t*-induced MNGC formation

Cells were seeded at $2x10^5$/ml in 96 well plates (100µl/well) overnight. Cells were washed twice with PBS and incubated in presence or absence of (10µl/ml) anti tetraspanin antibodies or matching isotype controls or 500nM of recombinant proteins or GST for 1hr. Cells were then washed with PBS and infected at MOI of 3:1 and MNGC formation performed as described in 2.2.6.2.

2.2.10.5.2 Effects of a long incubation of tetraspanin reagents on *B.t*-induced MNGC formation

Cells were cultured into 96 well plates as previously. Cells were infected with *B.t* strains at MOI of 3:1 as described in 2.2.6.1. After 2hr post infection cells were washed with PBS twice and were incubated with antibiotics in the presence or absence of tetraspanin reagents. At an appropriate time cells were fixed stained and MNGC formation was quantified as described in section 2.2.6.3.

2.2.10.6 Effects of other reagents on B.t-induced MNGC formation

The role of other (non-tetraspanin) cell surface molecules in *B.t*-induced MNGC formation was investigated using appropriate specific monoclonal antibodies (Table 2.1.3). Monolayer of cells were cultured in 96 well plates as described above and cells were pre-treated with the 10µg/ml antibodies or their matching isotype controls for 1hr post infection and then the MNGC assay was performed as described in 2.2.6.2. The effects of pre-treatment with different concentrations of LPS (10, 50, 100, 200ng/ml) were similarly investigated as described in 2.2.6.2.

2.2.11 Effect of GST-EC2 tetraspanins on cell number 2.2.10.1 Sulforhodamine B (SRB) assay

The sulforhodamine B (SRB) is a rapid, sensitive, and inexpensive method used for measuring the cellular protein content colorimetrically and it was primarily developed as an assay for testing anticancer drugs (Skehan et al., 1990). Here the SRB assay was adopted for investigating any possible effects of GST-EC2 tetraspanin on cell number (i.e. on cell proliferation or viability).

2.2.11.1 Calibration of cell number vs optical density

J774 cells were harvested by scraping, counted and diluted to 2×10^5/ml in medium. 100µl cells were plated (20,000 cells) in the wells of a 96 well plate, and then serially diluted 2-fold across the plate (some wells were incubated with just medium to measure the background optical density). These were incubated for 2hr at 37°C in CO_2. Cells were fixed by layering 50µl of ice cold 50% TCA on the top of the medium to a final concentration of 10% TCA and incubated for 5 minutes at RT then for 1hr at 4°C. The plate was washed 5 times with tap water, and allowed to dry. Cells were stained with 100µl of 4% sulforhodamine B sodium salt (Sigma, S9012-5G) dissolved in 1% acetic acid for 30 minutes. The SRB was removed and the plate was rinsed 4 times with 1% acetic acid (to remove unbound dye) and allowed to dry. Cell bound dye was solubilised with 100µl of 10mM unbuffered Tris base (pH 10.5) for 5 minutes using a gyratory shaker. The OD at 570 nm was measured using ELISA plate reader.

2.2.11.2 Effect of short incubation of GST-EC2 tetraspanins

Cells were cultured in 96 well plates as before. Cells were incubated in the presence or absence of GST-EC2 tetraspanin/GST at concentrations of 100, 500 or 1000nM for 1hr. cells were then washed 2 times with PBS and incubated with medium for about 14 hr, then fixed with TCA and the SRB assay was carried out as described above.

2.2.11.3 Effects of long incubation of GST-EC2 tetraspanins

In this experiment cells were incubated in the presence or absence of GST-EC2 tetraspanin/GST at concentrations 100, 500 or 1000nM for 72hr and then fixed with TCA and the SRB assay was carried out as described above.

2.2.12 Effect of CD9 and CD82 deficiency on *Burkholderia thailandensis* behaviour

The role of tetraspanins in *B.t*-induced cell fusion was also investigated in cells lines lacking tetraspanin CD9 or CD82 (2.1.6.1.). (The work with CD82 cells was carried out in part by Jocelyn an undergraduate project student in this Department).

2.2.12.1 Effect of CD9 or CD82 deficiency on B.t uptake

The effect of CD9 or CD82 deletion on *B.t* uptake were investigated using kanamycin protection assay as described in 2.2.6.1. Briefly, *B.t* invasion rate in these cells was determined at different MOIs and at different times post infection and comparing to the corresponding wild-type cells.

2.2.12.2 Effect CD9 or CD82 deficiency on B.t-induced MNGC formation.

The effect of CD9 or CD82 deletion on B.t-induced cell fusion was investigated as described previously in 2.2.6.2. A time course assay was also performed in CD9KO cells compared to corresponding wild-type cells, in which MNGC formation was assessed at different time points (8, 11, 14, 17, 20, and 23) hr post-infection as described in 2.2.6.2.

2.2.12.3 Effect CD9 or CD82 deficiency on the expression level of cell surface molecules

The expression levels of cell surface membrane molecules by C9KO and CD82KO cells in comparison with the corresponding WT cells was determined by FACS analysis as described in section 2.2.3.2. Cells were harvested and prepared for FACS analysis as described previously and cells were incubated with 10µl of primary antibodies directed to CD9, CD36, CD44, CD47, CD63, CD98, CD200, CD206, DC STAMP or appropriate isotype control (Table 2.1.5). After 1hr incubation cells were washed twice with BBN and were then incubated with appropriate secondary antibody (2.1.6).

2.2.13 Gene expression profiling of CD9 WT and CD9KO cells

2.2.13.1 RNA extraction

Total RNA from CD9KO and CD9WT cells was extracted using RNeasy®Mini RNA ISOLATION KIT (Qiagen-70022) according to manufacturer's instruction. Briefly, cells were harvested (~ $1x10^7$) and pelleted. Cells were lysed with 600µl of buffer RLT containing guanidine isothiocyanate and 1 volume of 70% ethanol was added to the lysate and mixed well by pipetting. 700ul of the sample was transferred to an RNeasy spin column placed in a 2ml collection tube and centrifuged at 8000g for 15 seconds. The flow-through was discarded and the column was washed with 700µl of RW1 buffer (containing guanidine salt+ phenol to remove molecules such as proteins and fatty acids) with centrifugation as before. The flow-through was discarded and the sample was washed twice with 500µl RPE buffer and centrifuged at 8000g for 5 seconds and 2 minutes respectively. The RNA sample was then dissolved with 30-50µl nuclease free water and stored at -80°C.

All subsequent steps were performed with the collaboration with Dr Paul Heath, Sheffield Institute for Translational Neuroscience University of Sheffield.

2.2.13.2 RNA evaluation

2.2.13.2.1 Evaluation of RNA quality
The quality of RNA samples was evaluated by determining its A_{260}/A_{280} ratio of absorbance using a NanoDrop spectrophotometer.

2.2.13.2.2 Evaluation of RNA integrity and quantity
Integrity and the quantity of extracted RNA was evaluated using the Agilent 2100 Bioanalyzer (an automated bio-analysis machine using microfluidics technology that provides an automated and reproducible electrophoretic separations (Mueller et al., 2000)) and RNA LabChip (Agilent RNA 6000 Nano Kit) according to manufacturer's instruction.

Gel preparation 550µl of RNA gel matrix was transferred into a spin filter and centrifuged at 1500g for 10 minutes at RT, 65 µL of filtered gel were aliquoted into 0.5 ml RNase-free microcentrifuge tubes and stored at 4°C.

Gel-Dye Mix RNA dye concentrate was allowed equilibrating to RT for 30 minutes, and then mixed by vortexing for 10 seconds. 1µl of dye was mixed with 65µl aliquots of filtered gel with vortexing then the mixture was centrifuged at 13000g for 10 minutes at RT.

Loading the Gel-Dye Mix RNA A chip was placed into the priming station and 9µl of gel-dye mix was loaded in the well-marked G. 5µl of RNA marker was loaded in 12 sample wells. 1µl of prepared ladder was loaded in the well that marked "ladder". 1µl of sample was loaded in each of 12 sample wells. The chip was replaced horizontally in the vortexer and vortexed for 1 minute at 2400 rpm. The chip was then run in the Agilent 2100 Bioanalyzer instrument within 5 minutes.

2.2.13.3 Preparing control RNA

An RNA positive control was used to insure that the reagents are working effectively and was prepared using RNA from HeLa cells (1mg/ml) that was included with the kit. On ice, 2µL of the Control RNA was dispensed in 78µl of nuclease-free water for a total volume of 80µl (25ng/µl).

2.2.13.4 Preparing Poly-a RNA controls

The poly-A RNA kit contains four exogenous poly-adenylated prokaryotic positive controls that monitor the whole target preparation. Their resultant signal intensities on GeneChip arrays provide a sensitive indicator of the labelling reaction efficiency. The Eukaryotic GeneChip probe array contains probe sets for several *B. subtilis* genes that are absent in eukaryotic samples (lys, phe, thr, and dap). Poly-A control stock was diluted with the Poly-A control dilution buffer. To prepare the Poly-A RNA dilutions for 100ng of total RNA:2µl of Poly-A RNA control stock was added to 38µl of the buffer for the first dilution (1:20).2µl of first dilution was added to 98µl of the buffer for the second dilution (1:50). 2µl of second dilution was added to 98µl of the buffer for the third dilution (1:50).2µl of third dilution was added to 18µl of the buffer for the fourth dilution (1:20).

2.2.13.5 Preparing total RNA/ POLY-A RNA control mixture

1µl of total RNA was added to 2µl of the fourth dilution of Poly-A RNA control and 2µl of nuclease-free water.

2.2.13.6 Synthesis First-strand cDNA

For preparing the first-strand master mixture (for each sample), on ice and in nuclease-free tube 4µL of 3' first-strand buffer were added to 1µl of 3' first-strand enzyme and mixed by gently vortexing. The tubes were centrifuged briefly to collect the mixture at the bottom.

- On ice, 5µl of total RNA and Poly-A RNA mixture were added with mixing and centrifugation as before. The first-strand synthesis reaction was incubated at 42°C for 2hr in a thermal cycler using the first-strand cDNA synthesis program.
- After the incubation tubes were centrifuged briefly to collect the first-strand cDNA at the bottom of the tube and incubated on ice for 2minutes. Then synthesis second-strand cDNA proceeded immediately.

2.2.13.7 Synthesis second-strand cDNA

For preparing the second-strand master mixture (for each sample), on ice and in a nuclease-free tube, 13µl of nuclease-free water, 5µl 3' second-strand buffer and 2µl 3' second-strand enzyme were mixed and centrifuged as before.

On ice, 20µl of second-strand master mix was transferred to each 10µl first-strand cDNA. The second-strand synthesis reaction was incubated at 16°C for 1hr and for 10 minutes at 65°C in a thermal cycler using the second-strand cDNA synthesis program.

After incubation tubes were centrifuged briefly as before and replaced on ice for 2 minutes and then synthesis of labelled aRNA was performed immediately.

2.2.13.8 Synthesis labeled aRNA by in vitro transcription

To prepare IVT master mixture (for each sample), at room temperature in a nuclease-free tube 4µl of 3' IVT biotin label, 20µl IVT buffer and 6µL IVT enzyme were mixed and centrifuged briefly as before.

30µl of the mixture was added to each 30µl of second-strand cDNA sample and mixed then centrifuged. The tubes were then incubated at 40°C for 16hr in a thermal cycler using the In vitro Transcription aRNA synthesis program.

After the incubation tubes were centrifuged briefly and replaced on ice before purifying the labeled aRNA or alternatively stored at -20°C.

2.2.13.9 aRNA purification

100µl of purification beads were added to each (60µl) aRNA sample and mixed by pipetting up and down. The mixture was then transferred to a well of a U-bottom plate and mixed by pipetting up and down 10 times then incubated for 10 minutes at RT. The plate was then moved to a magnetic stand to capture the purification beads for 5 minutes and the supernatant was discarded. Beads were washed with 200µl of 80% ethanol wash solution to each well and incubated for 30 seconds then the supernatant was discarded. This was repeated 2 times more. Beads were allowed to dry for 5minutes.To elute aRNA, the plate was removed from the magnetic stand, 50µl of preheated (65°C) nuclease-free water was added to each well and incubated for 1 minute, then the samples were mixed by pipetting up and down 10 times.The plate was replaced on the magnetic stand for 5 minutes. The supernatant which contains eluted aRNA was transferred to a nuclease-free tube and stored at -20°C.

2.2.13.10 Quantitation and expected yield of aRNA

The concentration of aRNA was determined by measuring the absorbance of 2µl of the sample at 260nm using a NanoDrop spectrophotometer, aRNA size distribution was analysed using an Agilent Bioanalyzer and RNA6000 nano kit loaded with 300ng of aRNA per well.

2.2.13.11 Fragmentation of labeled aRNA

The aRNA fragmentation mixture was prepared on ice by mixing 15µg? (in 32µl) of labeled aRNA with 8µl 3' fragmentation buffer and centrifuged briefly. The fragmentation reaction was incubated for 35 minutes at 94°C in a thermal cycler using the fragmentation program. The tubes were centrifuged and replaced on ice. The size of aRNA fragments was

determined by running a 300ng sample on an Agilent bioanalyzer using an RNA6000 Nano kit.

2.2.13.12 Array Hybridization

The array hybridization was carried out using the GeneChip$^{®}$ Mouse Genome 430 2.0 Array Kit (Affymetrix 900495). The array was allowed to equilibrate to room temperature. Meanwhile, hybridization cocktail for single probe array was prepared by mixing 12.5µg (33.3µl) of fragmented and labeled aRNA, 4.2µl of control oligonucleotide B2 (3nM), 12.5µl of 20x hybridization control, 125µl of 2x hybridization mix, 25µl of DMSO and 50µl nuclease-free water. The hybridization cocktail was incubated at 99°C for 5minutes then at 45°C for 5 minutes in a thermal cycler using the hybridization cocktail program. The array was dehydrated with 200µl of Pre-Hybridization mixture and incubated with 60 rpm rotation for 10-30 minutes at 45°C. The hybridization cocktail was centrifuged for 5 minutes to collect any insoluble material from the hybridization mixture. The pre-hybridization mix was extracted from the array and the appropriate volume of the clarified hybridization cocktail was loaded into the array and the array was then incubated with rotation at 60 rpm for 16hr at 45°C.

2.2.12.13 Array washing and scanning

After the incubation the hybridization cocktail mixture was extracted from the array chip, and the array was filled with wash buffer and allowed to equilibrate to RT. The array chip was then stained and washed using the Affymetrix Fluidics System 450, and scanned using a GeneChip 30007G scanner.

2.2.14 Effect of *Burkholderia* infection on the expression of tetraspanins and other cell surface molecules

The expression levels of cell surface membrane proteins by uninfected and infected J774 were measured by FACS analysis. Cells were cultured in 12 well plates at $1x10^6$/well for 2hr to allow cell adhesion. Cells were cultured without/with *B.t CDC* 272 for 2hr. Bacteria were then removed and cells were washed with PBS twice and cultured with antibiotics. At 3 or 9hr post-infection cells were harvested and prepared for FACS analysis as described in 2.2.3.2 using appropriate primary antibodies and matching isotype controls and appropriate FITC-labelled secondary antibodies shown in Tables 2.1.4, 2.1.5 and 2.1.6 respectively.

2.2.15 confocal microscopy

Cells were seeded on glass coverslips placed into 24-well plates at 2x105 /well and cultured at 37°C. Cells were infected with *Burkholderia* strains transformed with florescent plasmid pIN25 (GFP) or pIN29 (DS Red) at MOI of 3 as already described in 2.2.6.1. At appropriate time points cells were washed 3 times with PBS and fixed with 4% paraformaldehyde for 15 minutes at RT. Cells were washed 3 times with PBS for 5 minutes each. Cells were covered with 0.1% sodium azide in PBS and plates were kept in foil at 4°C until staining. For staining, cells were permeabilized with 0.1% Triton X-100 in PBS for 30 minutes at RT then washed 3 times with PBS as before. Cells were incubated with 1x bovine serum albumin (BSA) in HBSS for 10 minutes for preventing nonspecific binding. Cells were incubated with

appropriate concentrations of primary antibody (Table 2.1.4) for 1hr at RT. cells were washed with PBS 3 times as before and incubated with 1% BSA for 10 minutes. Cells were then incubated with appropriate concentrations of matching FITC-labelled secondary (Table 2.1.6) antibodies for 30 minutes at RT. Cells were then washed 3 times with PBS. The coverslips were removed and mounted onto microscopy slides using Vectashield mounting medium containing DAPI. Samples were analysed using a Nikon A1 confocal microscopy or widefield Deconvolution Delta vision microscope.

2.2.16 EM microscopy

Cells were harvested and centrifuged and the supernatant was then discarded. The tubes were placed on ice and were processed by the EM Unit, Department Biomedical Science.

Specimens were fixed as a pellet in 3% glutaldehyde/0.1M phosphate buffer overnight, washed in buffer and dehydrated in ethanol, cleared in epoxypropane (EPP) and infiltrated with a 50/50 araldite resin:EPP mixture overnight on a rotary mixer. This mixture was replaced twice over 8 hours with fresh araldite resin mixture before embedding and curing at 60° C for 48-72 hours. Ultrathin sections, approximately 85nm thick, were cut on a Reichert Ultracut E ultramicrotome on 200 mesh copper grids and stained for 30 mins with saturated aqueous uranyl acetate followed by staining with Reynold's lead citrate for 10 mins. Sections were examined using a Transmission Electron Microscope at an accelerating voltage of 80Kv. Electron micrographs were recorded using a Gatan digital camera.

Chapter 3

Burkholderia thailandensis infection and multinucleated giant cell formation in monocyte/macrophage cell lines

3.1 Introduction

3.1.1 MNGC formation: a feature of melioidosis

Burkholderia pseudomallei (B.p) is a gram negative bacteria that causes melioidosis; an endemic disease in Southeast Asia and north Australia. Melioidosis produces a variety of clinical symptoms ranging from seropositive subclinical conditions to rapidly severe septicemia. *B.p* is highly resistant to a range of antibiotics and there is no vaccine against melioidosis. *B p* infects a range of cell types, is able to avoid killing by macrophages and is also able to promote cell fusion and induce multinucleated giant cell (MNGC) formation (Wong et al., 1995)

MNGCs are formed by monocyte/ macrophage fusion as an immune response to foreign bodies or pathogenic microorganisms in inflammation sites associated with chronic infection including tuberculosis, fungal infection and HIV (Anderson, 2000). MNGCs are suggested to enhance the ability of cells to digest and eliminate large components (Han et al., 2000), and may eliminate cell to cell spread of infection (Byrd, 1998). By contrast MNGC formation induced by *B.p* is thought to be important in cell: cell spread. In addition *B.p* can remain inactive but viable for a long time within MNGCs, which are thought to be a feature of *B.p* pathogenicity since these cells were observed in tissues of melioidosis patients (Ngauy et al., 2005). Known bacterial factors and unknown host effectors promote *B.p*-induced cell fusion. *Burkholderia pseudomallei* virulence factors such as motility protein Bim A, the cluster 3 type III secretion system (T3SS-3), and the cluster 1 type VI secretion system (T6SS-1) are thought to play important roles in macrophage invasion and fusion leading to MNGC formation (Shalom et al., 2007, Suparak et al., 2005); however the exact mechanism of *B.p*-induced cell fusion is unclear.

3.1.2 *Burkholderia thailandensis* non-pathogenic species used for studying *B.pseudomallei* life cycle

Burkholderia thailandensis (*B.t*) is a gram-negative environmental saprophyte bacterium that was identified as a non-pathogenic biotype of *Burkholderia pseudomallei*, due to the similarity in their morphological and biochemical characteristics (Brett et al., 1997, Anuntagool et al., 1998). Brett and co-workers in 1998 reported significant genotypic and phenotypic differences between the two organisms that led to the classification of a new species of *Burkholderia* named *thailandensis* (Brett et al., 1998). Nevertheless, *B.pseudomallei* and *B.thailandensis* express nearly identical virulence factors that include type III, type VI secretion systems and lipopolysacchride LPS (Brett et al., 2003, Haraga et al., 2008, Heiss et al., 2012, Shalom et al., 2007). In addition, *B.p* and *B.t* share the ability to invade and replicate within a range of phagocytic or non-phagocytic cell lines and promote actin polymerization to facilitate intracellular motility, cell-cell spread and multinucleated

giant cell formation (Kespichayawattana et al., 2000, Stevens et al., 2005b, Kespichayawattana et al., 2004, Stevens et al., 2005a). Therefore *B.thailandensis* is considered very useful as a model for studying certain aspects related to *B.pseudomallei* pathogenicity.

In this study two strains of *B.thailandensis* were used: *B.t* E264 environmental isolate strain (Brett et al., 1998); *B.t* CDC272 clinical isolate strain (Glass et al., 2006). Both strains have been shown to infect a variety of eukaryotic cell lines and promote multinucleated giant cell formation (Harley et al., 1998, Wand et al., 2011, French et al., 2011).

3.1.3 Cell line models for studying *B.thailandensis*- induced MNGC formation

Several cell lines were used in this study. We started with the J774.2 mouse macrophage cell line that was re-cloned from the original ascites and solid tumour J774.1 (Ralph and Nakoinz, 1975). RAW 264.7, a mouse macrophage cell line which was established from an ascitic tumour induced in a mouse by intraperitoneal injection of Abselon leukaemia virus cells (Ralph and Nakoinz, 1977) was also used. These cells have an efficient growth rate so they can be obtained in high numbers, which may be required for some assays. They are also adherent cells which is useful in MNGC formation assays. In addition these cells have been used as a model in *Burkholderia*-induced fusion studies (Suparak et al., 2005, Utaisincharoen et al., 2006), so they are good candidates for investigating the role of tetraspanins in *B.t*-induced cell fusion.

Other cell lines used in this study were human monocytic cell lines, which should have characteristics similar to human monocytes or macrophages. In addition there are more antibodies available for human tetraspanins that could be used to investigate the effect of tetraspanins in *B.t*-induced cell fusion. U937 a human monocytic cell line that was derived from the pleural effusion of a histiocytic lymphoma patient has the phenotype of an immature monocyte or monoblast (Sundstrom and Nilsson, 1976). Previous data showed that U937 cells can be stimulated to fuse by *B.pseudomallei* (Suparak et al., 2011). The THP1 cell line, which is also a human monocytic cell line derived from a patient with acute monocytic leukaemia (Tsuchiya et al., 1980), was also used. THP1 has been widely used to study monocyte and macrophage function and regulation (recently reviewed by (Chanput et al., 2014). U937 and THP1 both can be stimulated to differentiate with phorbol 12-Myristate 13-acetate (PMA). However differentiated THP1 cells behave more like native monocyte-derived macrophages compared to other human monocytic cell lines, such as HL-60, U937, KG-1, or HEL cell lines (Auwerx, 1991).

3.2 Aims

The aims of the work described in this Chapter were

- To investigate the expression level of tetraspanins on cell lines used in this project.
- To optimise the method of multinucleated giant cells formation induced by *Burkholderia thailandensis* using different cell lines.

3.3 Results

3.3.1 The expression of tetraspanin on cells under study

In order to study the role of tetraspanins on *B.t*-induced MNGC formation, and to choose suitable cell lines for this study, the expression level of tetraspanins on different cell lines was tested by flow cytometry and FACS analysis.

3.3.1.1 Expression of tetraspanins on mouse macrophage cell lines

Currently monoclonal antibodies to mouse tetraspanins are limited for almost all of the tetraspanin proteins. Therefore only the level of tetraspanins CD9, CD63 and CD81 was tested on mouse macrophage cell lines J774.2 and RAW264.7 by flow cytometry as described in section (2.2.3.2.1). More than 80% of J774.2 and RAW264.7 cells expressed CD9 and CD81 on their surface, with high levels for CD9. A low surface expression level of CD63 was detected on RAW cells, whereas no CD63 was detected on J774.2 cells figures (3.3.1) (3.3.2). As it is known that CD63 is mainly expressed in intracellular membranes, the intracellular expression of CD63 was checked by FACS in fixed and permeabilized cells as mentioned in (2.2.3.2.2). However, only weak expression was detected in J774.2 and RAW264.7 cells (figure 3.3.3).

A   B
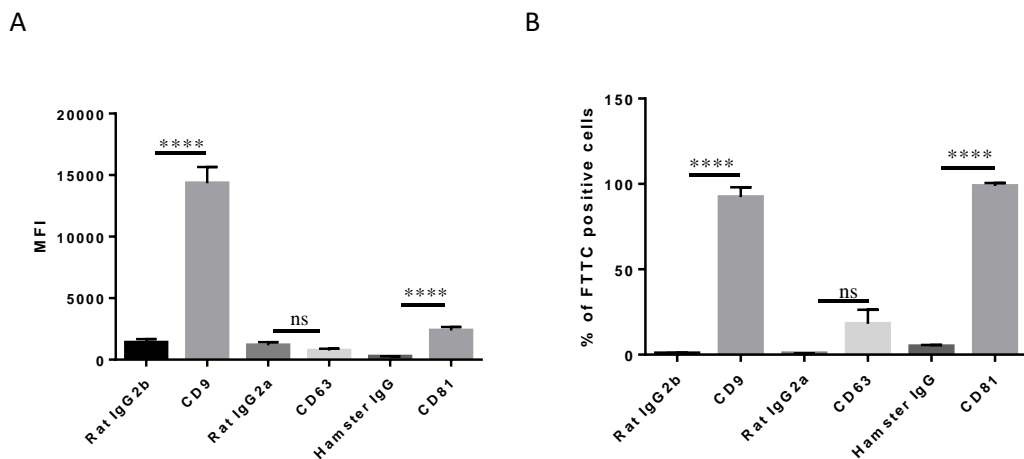
Figure 3.3.1 Surface expression of tetraspanins on J774 cells. Tetraspanins surface expression was tested by FACS analysis as described in section (2.2.3.2.1). Primary anti tetraspanin antibodies were used (anti-CD9, anti-CD63 and anti-CD81), with isotype controls (rat IgG2b, rat IgG2a, hamster IgG) as appropriate. Secondary antibodies were anti rat-IgG-FITC antibody or anti hamster IgG-FITC antibody. The experiment was done twice in duplicate and the significance of differences was measured by unpaired t-test where ****is significant at P < 0.0001. (A) MFI= Median fluorescent intensity, (B) percentage of FITC positive cells.
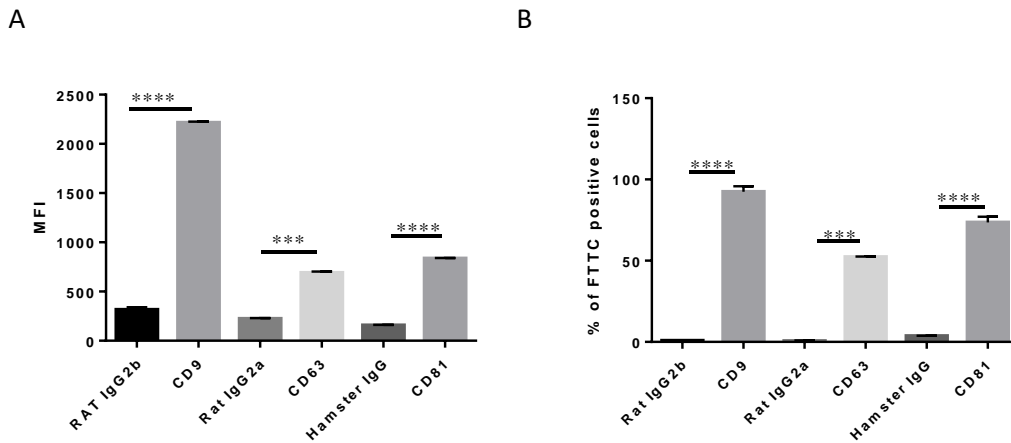
Figure 3.3.2 Surface expression of tetraspanins on RAW264.7 cells. Tetraspanin surface expression was tested by FACS analysis as described in section (2.2.3.2.1). Antibodies and controls were as described for Figure 3.3.1. The experiment was done twice in duplicate and the significance of differences was measured by unpaired t-test where ****is significant at P < 0.0001, ***is significant at P < 0.0005. (A) MFI= Median fluorescent intensity, (B) percentage of FITC positive cells.
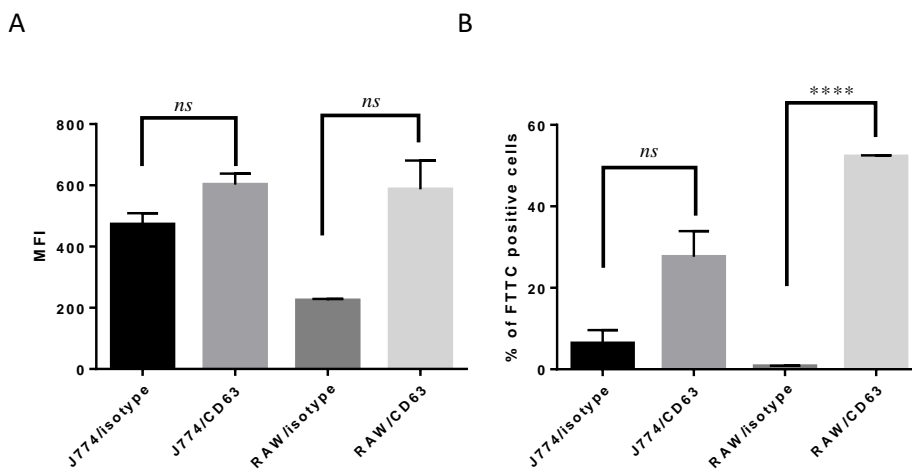
Figure 3.3.3 Total expression of tetraspanin CD63 on J774.2 and RAW 264.7 cells. Cells were fixed and permeabilized before staining as described in section (2.2.3.2.2). Primary antibody anti-CD63 with corresponding rat IgG2a isotype control and secondary anti-rat IgG-FITC antibody were used. (A) MFI= Median fluorescent intensity, (B) percentage of FITC positive cells. The experiment was done twice in duplicate and the significance of differences was measured by unpaired t-test where ****is significant at P < 0.0001. (A) MFI= Median fluorescent intensity, (B) percentage of FITC positive cells.
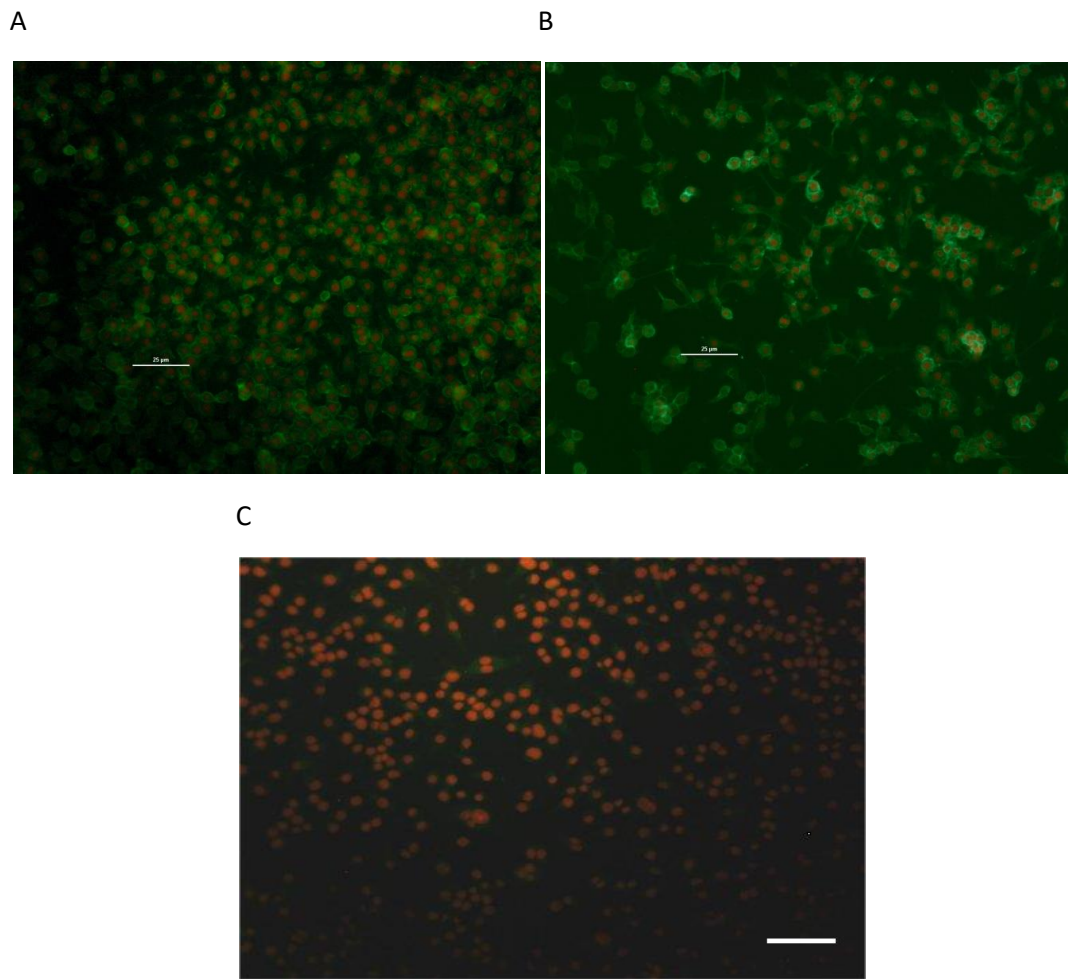
Figure 3.3.4 Expression of CD9 by fluorescence microscope. Cells were grown in Lab-Tek™ chamber slides overnight then fixed and stained as described in (2.2.3.1), using antibodies as described in Figure 3.3.1, Nuclei were stained with with propidiun iodide (red). Slides were imaged using a Nikon Eclipse E400 fluorescence microscope using the 20x objective. (A) CD9 on J774.2 cells, (B) CD9 on RAW264.7 cells (C) J774 4.2 Cells stained with isotype control. Scale bar 25µm.

3.2.1.2 Expression of tetraspanins on human monocytic cell lines.

3.2.1.2.1 Expression of tetraspanins on THP1 cells (unstimulated and stimulated)

The expression of tetraspanins on unstimulated and stimulated THP1 was examined. Cells were stimulated with phorbol ester as described in section (2.2.2). There was a visible change in cell morphology as shown in figure (3.3.5), and a change from suspension growing into adherent cells as observed with the microscope. These changes were also detected by flow cytometry in the form of an increase in forward scatter and side scatter (Figure 3.3.6 A). The level of tetraspanins in stimulated cells was compared to unstimulated cells. There was a significant increase in the expression levels of CD9, CD53, CD63 and CD81 in stimulated cells compared to unstimulated (Figure 3.3.6 B).
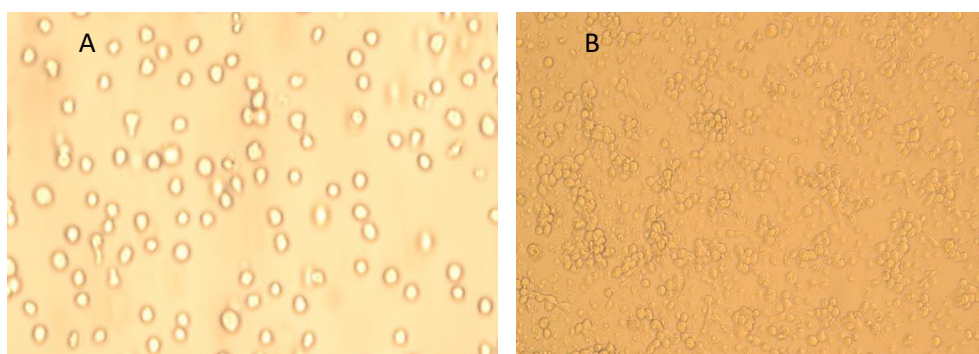
Figure 3.3.5 Light microscopic images of human monocytic cell line THP1. Cells were cultured in 24 well plates and stimulated with PMA for 72hr as described in (2.2.2). (A) Unstimulated THP1 (B) stimulated THP1. The images were captured with a Nikon inverted microscope using the 20x objective.

A
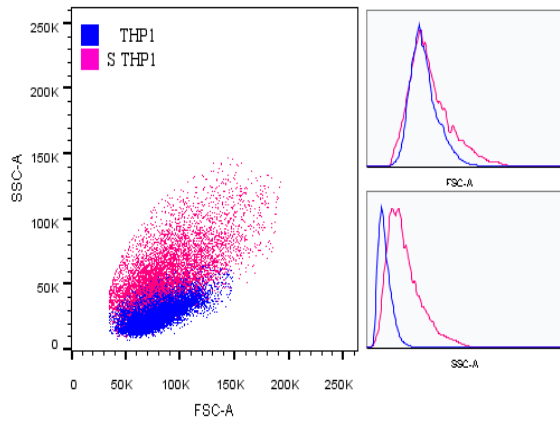
B
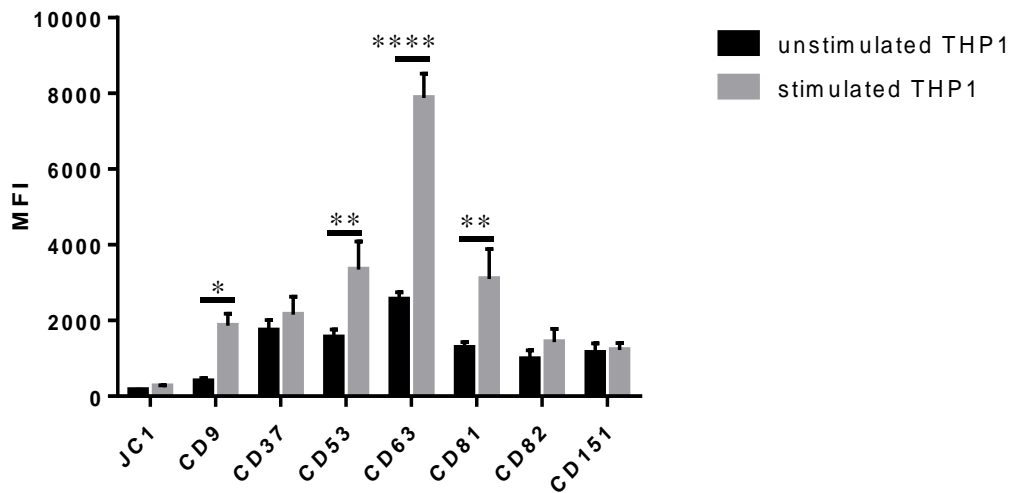
Figure 3.3.6 Surface expression of tetraspanins on THP1 cells. Cells were stimulated with PMA as described in section (2.2.2). The expression of tetraspanins was tested on unstimulated and stimulated THP1 using primary antibodies anti-CD9, anti-CD37, anti-CD53, anti-CD81, anti-CD82, anti-CD151, IgG JC1 isotype control and the secondary was anti-mouse IgG FITC. (A) Scatter plots showing the change in size of stimulated THP1 compared with unstimulated THP1, and overlay histogram of FSC and SSC of unstimulated and stimulated THP1. (B) Expression of tetraspanins on unstimulated cells compared to stimulated cells. The experiment was performed three times in duplicate and the significance was determined by using two-way ANOVA with Holm-Sidak's multiple comparisons test. MFI=median fluorescent intensity.

3.2.1.2.2 Expression of tetraspanins on U937 cells (unstimulated and stimulated):

The expression of tetraspanins on the monocytic cell line U937 was investigated. Cells were stimulated with PMA and the level of tetraspanins was measured by FACS analysis as described in section (2.2.3.2.1). Stimulated U937 changed from growing in suspension to adherent clumps of cells and their morphology also changed (Figure 3.3.7. A B). This was

confirmed by flow cytometry, with an increase in cell granularity and size (Figure 3.3.8 A). There was a significant increase in the expression levels of CD9 and CD82 in stimulated U937 compared to unstimulated U937. The level of CD151 significantly decreased in stimulated U937 cells Figure (3.3.8 B). Other tetraspanins showed no significant change in expression.
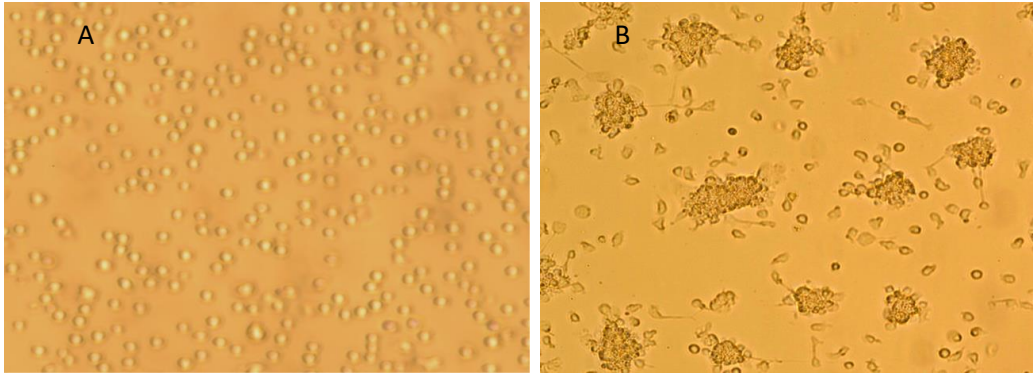
Figure 3.3.7 Light microscopic images of human monocytic cell line U937. Cells were cultured into 24 well plates in the presence of PMA for 72hr as described in (2.2.2). (A) Unstimulated U937 (B) stimulated U937. The images were captured with a Nikon inverted microscope using the 20x objective.

A
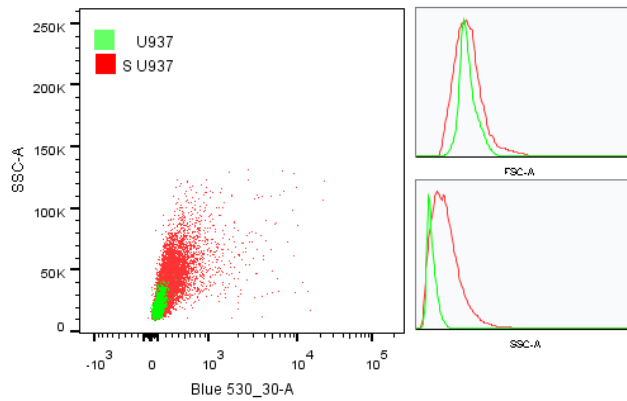
B
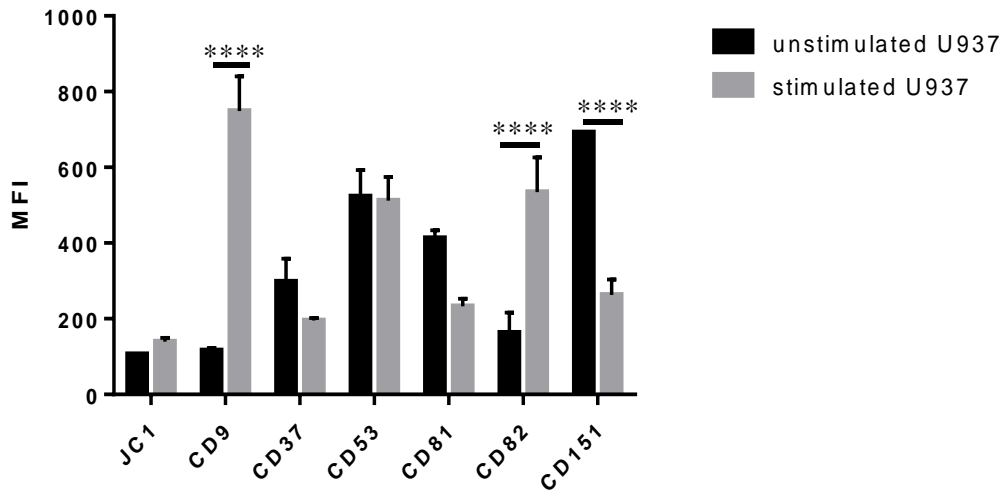
Figure 3.3.8 Surface expression of tetraspanins on unstimulated U937 and stimulated U937. Cells were stimulated with PMA as described in section (2.2.2). The expression of tetraspanins was tested on unstimulated and stimulated U937 using antibodies as described in Fig. 3.3.6. (A) Scatter plots showing the change in size of stimulated U937 compared with unstimulated U937, and overlay histogram of FSC and SSC of unstimulated and stimulated cells. (B) The expression of tetraspanins on unstimulated and stimulated cells. The experiment was performed three times in duplicate and the significance was determined by using two-way ANOVA with Holm-Sidak's multiple comparisons test. MFI=median fluorescent intensity.

3.2.2 *Burkholderia thailandensis* uptake

This section shows the results of optimising the conditions of the *Burkholderia thailandensis* uptake assay in a various cell lines. Two isolated strains of *B.thailandensis*; *B.t* CDC and *B.t* E264 were used in this study, and their ability to infect was tested in macrophage cell lines J774.2 and RAW264.7 as well as in human monocytic cell lines THP1 and U937.

3.2.2.1 *Burkholderia thailandensis* uptake by mouse macrophage cell lines J774.2 and RAW264.7

A kanamycin protection assay was used to estimate the number of intracellular bacteria in infected cells as described in (2.2.10.1). For negative controls, cells were treated with cytochalasin D for 1hr prior to infection, to prevent uptake.

As shown in Figure 3.3.9, *B.t* CDC272 and *B.t* E264 were able to infect J774.2 and RAW cells. J774.2 cells were more susceptible to the infection compared to RAW264 cells. The *B.t* CDC strain was shown to be more virulent than *B.t* E264. The results also show that the number of intracellular bacteria increased when using a higher MOI. A statistically significant increase in number of intracellular bacteria was found in cells infected at MOI of 10:1 compared to cells infected at MOI of 3:1. There were no intracellular bacteria evident in cells treated with cytochalasin D.
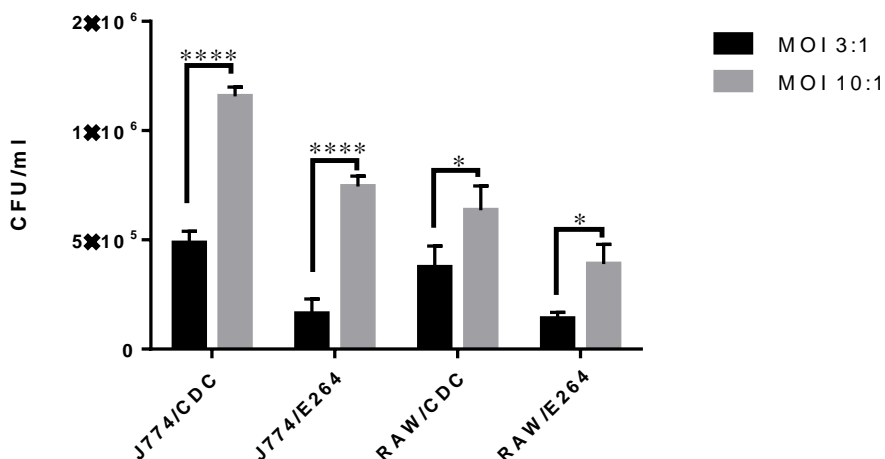
Figure 3.3.9 *Burkholderia thailandensis B.t* **CDC272 and** *B.t* **E264 uptake by J774.2 and RAW264.7 cell lines**. Cells were infected at multiplicity of infection (MOI) 3:1 or 10:1 as described in section (2.2.10.1). The number of intracellular bacteria was measured after 4hr post infection. The experiment was performed three times in duplicate. Statistical analysis was done using two-way ANOVA with Holm-Sidak's multiple comparisons test ****$p<0.0001$. CFU= colony-forming unit.

3.2.2.2 *Burkholderia thailandensis* uptake by human monocytic cell lines THP1 and U937

The invasion rate of *B.t* CDC272 and *B.t* E264 inhuman monocytic cell lines THP1 and U937 was investigated as described in (2.2.10.1). THP1 and U937 cells were stimulated with PMA at 50ng/ml as described in (2.2.2). Unstimulated and stimulated cells were infected with *B.t* CDC272 or *B.t* E264 at an MOI of 10 and the number of intracellular bacteria detected after 4hr post infection. The results showed that both strains can infect unstimulated and stimulated THP1 and U937 cells. There was a slight increase in *B.t* uptake within stimulated

cells compared to unstimulated cells. U937 cells were more susceptible to the infection than THP1 cells. This suggested that the *B.t* invasion and survival are cell type dependent to some extent. The CDC272 strain again appeared more virulent figure (3.3.10).

A
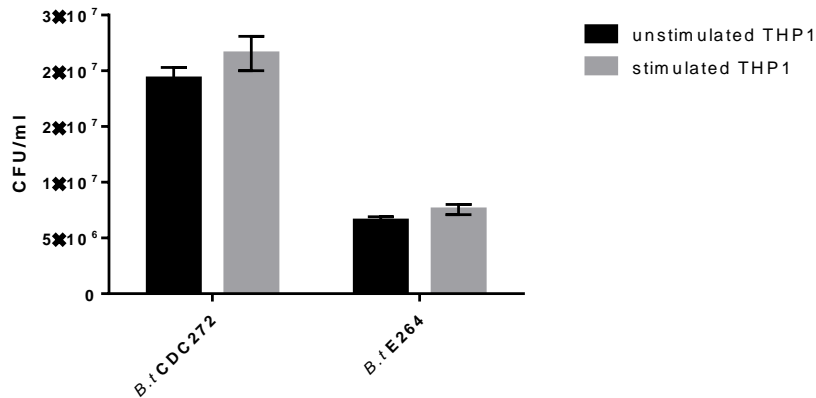
B
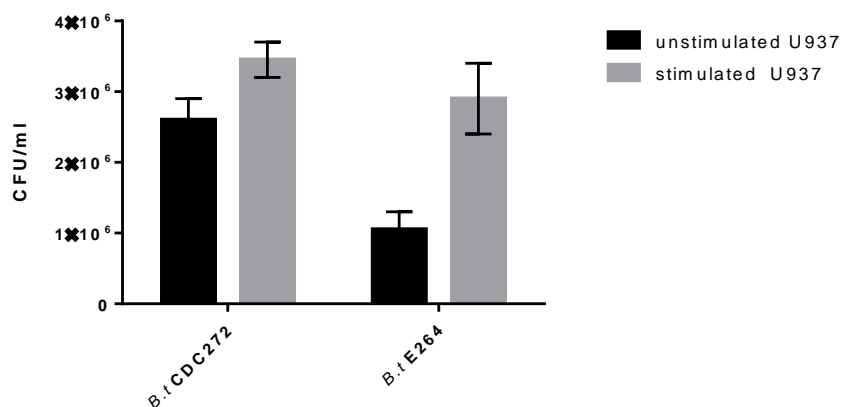
Figure 3.3.10 *Burkholderia thailandensis B.t* **CDC272 and** *B.t* **E264 uptake by human monocytic cells lines THP1 and U937**. Cells were stimulated with PMA for 72hr as described in section (2.2.2). Unstimulated cells and stimulated cells were infected with *B.t* CDC272 or *B.t* E264 at an MOI of 10:1. The number of intracellular bacteria was tested after 4hr post infection in unstimulated and stimulated cells.

3.2.3 Optimizing the conditions for the *B.t*-induced multinucleated giant cell formation assay.

In order to establish optimal MNGC formation, various different assay conditions were initially tested. Experiments using different macrophage cell densities, MOIs, and infection times were carried out. We started with J774.2 and RAW cells. Cells were cultured on cover slips in 24 well plates at 2, 3, 4 or 5 x10^5 cells/ml and cultured overnight. Cells were infected with *B.t* CDC or *B.t* E264 at MOIs of 1, 3 or10 as described in (2.2.10.2). Cells were fixed and stained with fluorescent stain or with Giemsa as described in (2.2.9.2) and (2.2.10.2) respectively. The rate of MNGC formation was estimated as described in (2.2.10.3) for in 10 fields of view for each sample (coverslip) using light microscopy. MNGC formation was

measured as fusion index (the percentage of the number of nuclei in MNGCs relative to the total number of nuclei in all cells) and MNGC size (the number of nuclei in MNGCs relative to the number of MNGCs. The results showed that using a lower MOI was more efficient in generating MNGC formation. Using an MOI of 10 caused cell death and detachment from the slide surface; therefore very few cells were found on the cover slips. According to the results shown in Figure 3.3.11 an MOI of 3:1 was chosen as the optimal condition for the MNGC formation assay.

A
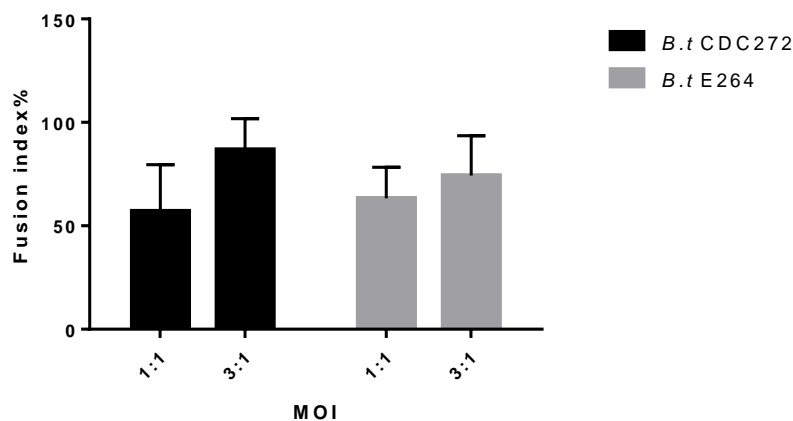
B
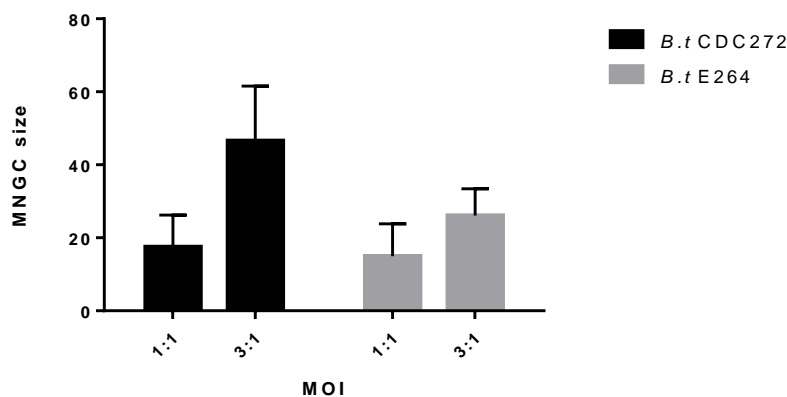
Figure 3.3.11 Multinucleated giant cell (MNGC) formation induced by *B.t* CDC272 and *B.t* E264 in the macrophage cell line RAW264.7. Cells were infected at MOI 1:1 or 3:1 as described in section (2.2.10.2). Cells were fixed and stained with Giemsa. Fusion index and size of MNGCs were calculated as described in section (2.2.6.3).

A suitable time for optimal MNGC formation and the best concentration of antibiotics to kill any extracellular bacteria were also checked. Cells were infected for 2hr at an MOI of 3:1 and incubated with medium containing 250, 500 or 1000 µg/ml kanamycin alone or in combination with amikacin at 250, 500 or 1000 µg/ml. At different time points cells were fixed and stained as described in (2.2.10.2). The results showed that MNGC formation increased with time. RAW cells which were infected with *B.t* CDC272 showed extremely large MNGC after 24 hr post infection whereas almost of all J774 cells were dead by this time. Therefore 16hr post infection and 500µg/ml of kanamycin and 500µg/ml of amikacin

were chosen as the optimal conditions for *B.t*-induced MNGC formation. 500µg/ml (kanamycin and amikacin) showed no effect on macrophage cell viability after 24 hr incubation as checked with trypan blue dye.
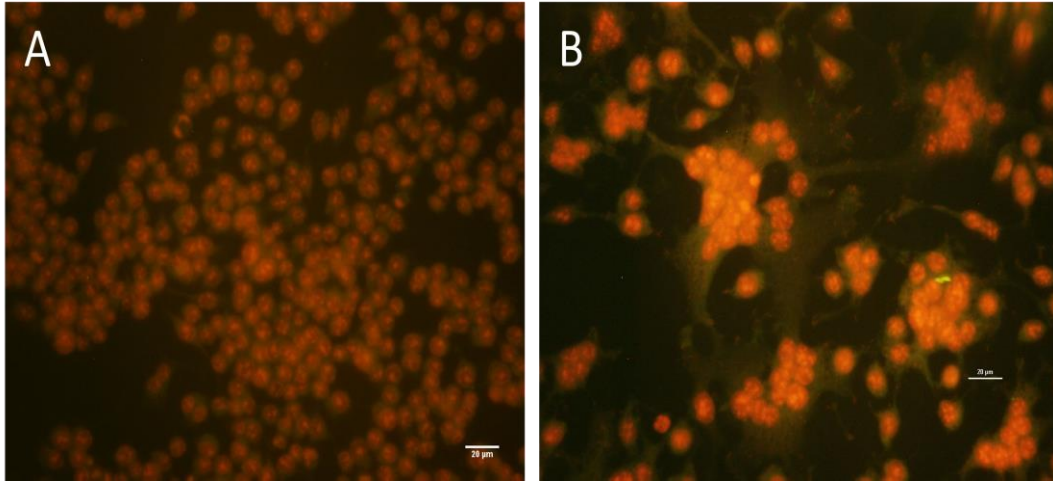
Figure 3.3.12 *Burkholderia thailandensis* **induced cell fusion in mouse macrophage cell line J774.** The images show the nuclei in uninfected cell (A) and in B.t-E264 infected cells (B). Cells were infected as described in 2.2.10.2. Cells were fixed and the Nuclei were stained with propidium iodide (red). The images were captured with a Nikon Eclipse E400 fluorescence microscope (green channel) using the 40x objective, scale bar= 20µm.

A
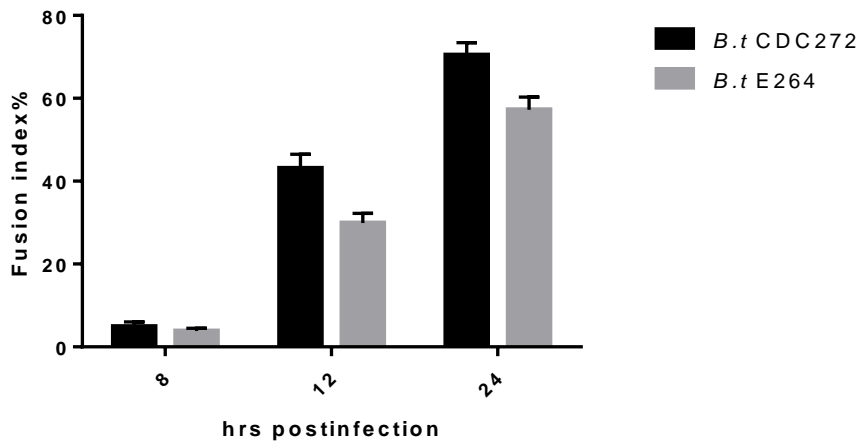
B
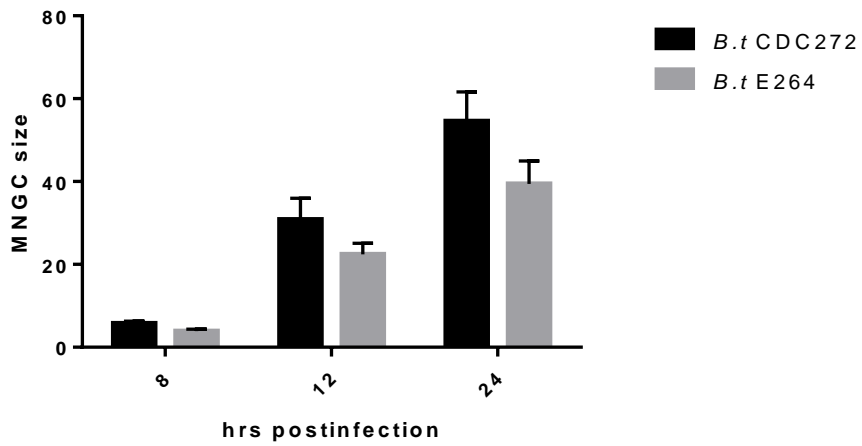
Figure 3.3.13 MNGC induced by _B.t_ CDC272 and _B.t_ E264 in the macrophage cell line RAW264.7. Cells were infected as described in section (2.2.10.2), fixed at 8, 12 and 24 hr post infection and stained with Giemsa. Fusion index (A) and MNGC size (B) were calculated as was mentioned in (2.2.10.3) in 10 fields of view.
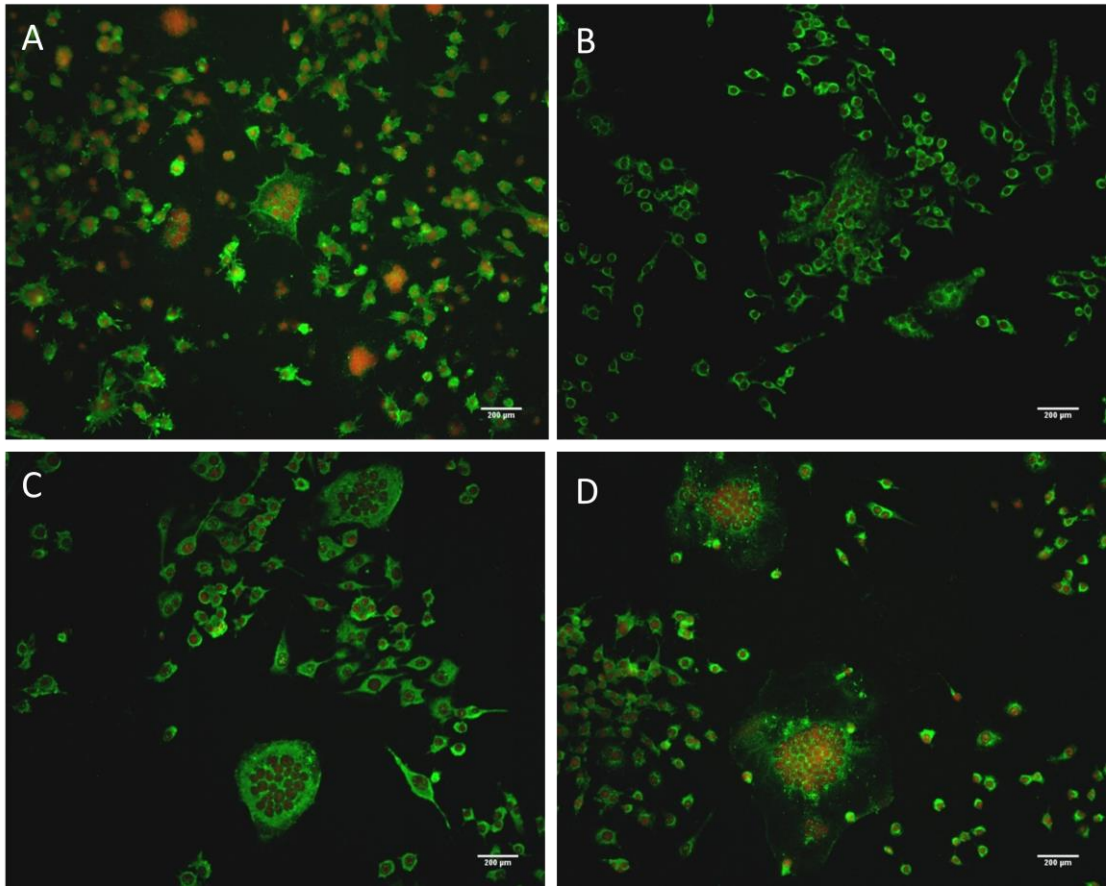
Figure 3.3.14 Immunofluorescence images of multinucleated giant cells. RAW 264.7 cells were cultured on cover slips in 24 well plates overnight and then infected with *B.t* E264 as described in (2.2.10.2). Cells were fixed at 8, 12, 16, 24 hr post infection (A, B, C, D) respectively. Cells were stained using mouse anti- actin antibody followed by anti-mouse Ig-FITC (green). Nuclei were stained with propidiun iodide (red). The images were captured with a Nikon Eclipse E400 fluorescence microscope using 20 x objectives, scale bar= 25µm.
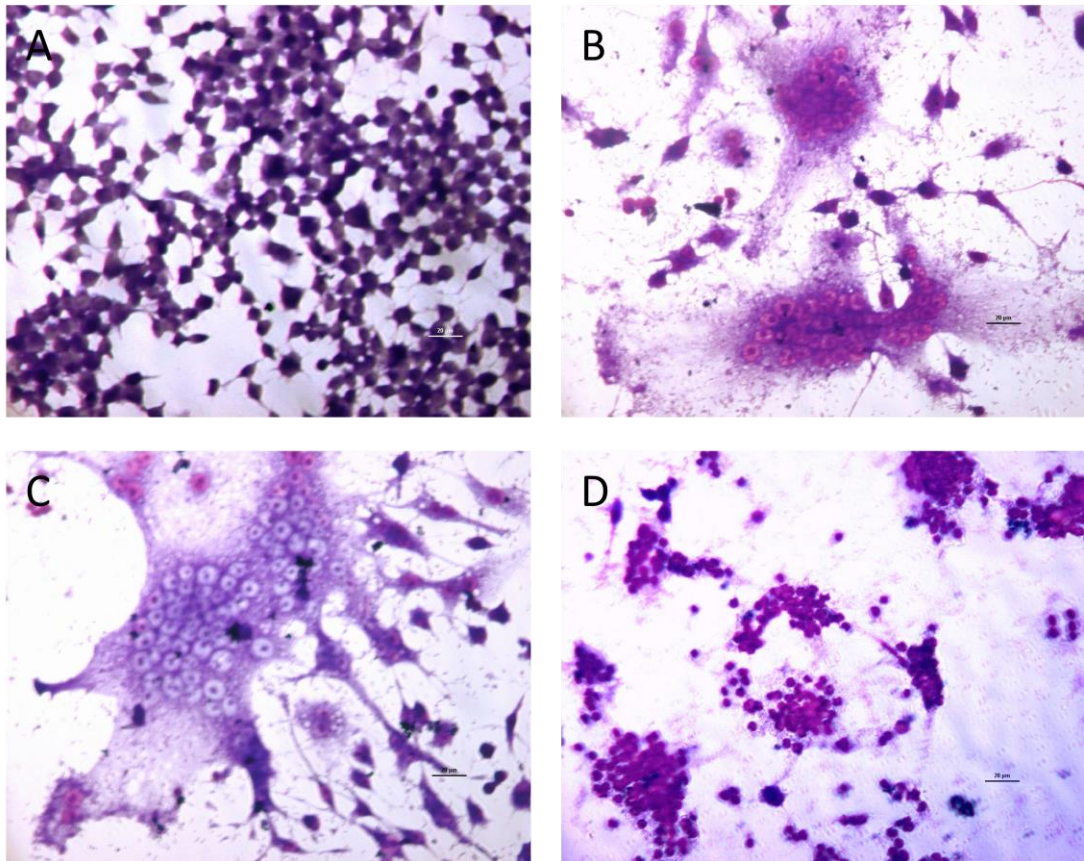
Figure 3.3.15 B. thailandensis induced MNGC formation inRAW264.7. Cells were infected as described above and fixed and stained with Geimsa. (A) uninfected cells (B) cells infected with B.t CDC272 (C) cells infected with B.t E264 D) necrotic B.t-infected cell (loss of cell membrane). Images were captured using by light microscopy using the 40x objective, scale bar 20μm.

3.3.4 Multinucleated giant cells formation in human monocytic cell lines THP1 and U937

Many attempts were made to induce cell fusion and MNGC formation in human cell lines THP1 and U937 using *Burkholderia thailandensis B.t* CDC and *B.t* E264, since more antibody reagents are available for human tetraspanins. Various conditions were used: unstimulated and PMA-stimulated THP1 and U937 were cultured in 24 well plates pre-coated or not with poly L lysine (to enhance adhesion), on glass cover slips or directly in the wells of 24-well plates. Cells were infected with *B.t* strains at different MOIs and at different time points. All the conditions that were used showed that *B.t* strains were not capable of inducing sufficient and distinct MNGC formation within THP1 and U937. PMA-stimulated U937 cells formed clumps, as described in 3.2.1.2., and consequently it was difficult to distinguish whether the cells fused or not. In an attempt to overcome this, after stimulation cells were harvested with cell dissociation solution, washed 3X with PBS and re-plated before infecting with *B.t.* However, under these conditions the cells were growing poorly and no MNGCs formation were noted. A few MNGC were observed within THP1 cells, however almost all of cells appeared to undergo apoptosis after 9hr post infection.

Because of the poor results obtained with *B.t*-induced MNGC formation in human monocytic cell lines, investigations on the role of tetraspanins on *B.thailandensis*-induced cell fusion was carried out using the mouse macrophage cell lines J774.2 and RAW264.7.

3.4 Discussion

3.4.1 Tetraspanins are expressed on different monocyte/macrophage cell lines

The expression levels of different tetraspanins were investigated on cells used in this study by flow cytometry analysis. Currently, monoclonal anti-mouse tetraspanin antibodies are limited, therefore the expression of only three members of tetraspanins have been investigated: CD9, CD63 and CD81. High levels of CD9 and CD81 were detected on both mouse macrophage cell lines RAW264 and J774; therefore these cells were good candidates for this study as the role of both tetraspanins in several cell fusion events has been identified (Takeda et al., 2003, Charrin et al., 2013). To take advantage of the fact that more monoclonal antibodies against human tetraspanin are available, we included two human monocyte cell lines in this project; U937 and THP1. The level of tetraspanins CD9, CD37, CD53, CD63, CD81, CD82 and CD151 were examined on these cells before and after differentiation upon stimulation with PMA. In U937 only CD9 and CD82 were upregulated upon differentiation whereas in THP1 expression of almost all tetraspanins was upregulated. This may be because THP1 are generally more differentiated than U937 and exhibit a morphology of normal monocyte-derived-macrophages compared with U937 (Tsuchiya et al., 1980), as also noted from the observation of cell morphology under the microscope.

3.4.2 *Burkholderia thailandensis* infection

As it mentioned previously, *Burkholderia thailandensis* is very closely related to *Burkholderia pseudomallei* and is widely used as a model to study *B.p* behaviour. Two *Burkholderia thailandensis* isolates were chosen for this project, the clinical isolate *B.thailandensis* CDC272, which were isolated from pleural wound (Glass et al., 2006) and the environmental isolate *B.thailandensis* E264 that have not been associated with human disease (Brett et al., 1998, Yu et al., 2006). The intracellular survival of bacteria in monocyte/macrophage cell lines was investigated using a modified protection assay (Wand et al., 2011). Both strains were able to internalize and survive within all cell lines used in this study. This result was in agreement with previous work that showed that *Burkholderia* species such as *B.pseudomallei*, *B.mallei*, *B.cepacia* and *B.thailandensis* have the ability to invade and survive within various cell lines derived from several species of mammal, and that is consistent with the observation of broad *B.p*-affected tissues found in patients with melioidosis (Harley et al., 1998). Notably, the number of intracellular *B.t* CDC272 at 4 hrs post infection was higher than the numbers of intracellular *B.t* E264. In agreement with this result, CDC strains (CDC 272 and CDC301) were shown to have an increased ability to grow and replicate within macrophages compared to E264. This may due to differences in bacterial behaviour within host cells rather than a variation in bacterial suitability, because there was no differences in the growth rates of these strains when they were cultured in free antibiotic medium (Wand et al., 2011, Sim et al., 2010).

The number of intracellular bacteria increased according to increased MOIs used in the infection assay. The J774 cell line was shown to be more susceptible to the infection than the RAW264.7 cell line, probably because each cell line regulates bacterial uptake (phagocytosis) differently. Other cells were used in this study represent human monocytes;

THP1 and U937. These cells are known to be more mature after stimulation with reagent such as PMA (Hattori et al., 1983). The results indicated that the *B.t* infection rate was increased upon stimulation by PMA, which is likely to be due to the enhanced phagocytosis capacity of PMA-stimulated cells, or possibly in contrast due to the efficiency of unstimulated cell to digest and eliminate the intracellular bacteria compared with PMA-stimulated cells.

3.4.3 *Burkholderia thailandensis* induced cell fusion in mouse macrophage cell lines.

The first basic step in this study was to establish a MNGC formation assay. We started with mouse macrophages as these cells have an efficient growth rate and they are adherent cells which is useful for MNGC formation assays. In addition these cells have been used as a model in *Burkholderia*-induced fusion studies (Suparak et al., 2005, Utaisincharoen et al., 2006). Although both J774 and RAW are mouse macrophages, their responses to *B.thailandensis* infection is different. MNGC formation was observed early in J774 and these cells also showed rapid morphological change and programmed cell death which may due to the susceptibility of these cells to the infection resulting in a rapid intracellular bacterial life cycle (escaping from phagosomes, replication and cell-cell spreading). By contrast, RAW264 cells appeared to be relatively more resistant to the infection; however extremely large giant cells were observed in *B.t*-infected RAW264 cell. In a comparable study utilizing several environmental and clinical isolates of *Burkholderia* and different cell lines including phagocytic and non-phagocytic cell lines, *B.pseudomallei*-infected RAW264 showed the most rapid MNGC formation compared with other cells including J774 cells and this was thought to be due to increased bacterial load within these cells (Harley et al., 1998).

In order to find the most appropriate MNGC formation assay, different conditions were tested initially. It was important to control bacterial growth in order to delay apoptosis and cell death which causes cells to detach. A combination of kanamycin and amikacin was found to be effective in this assay and a sufficient cell viability rate was obtained under these conditions (Shalom et al., 2007). The results showed that using lower MOIs resulted in controlled progression to MNGC formation. As MNGC formation is increased over time leading to eventual cell death, the appropriate time for cell fixation and MNGC assessment was another important factor need to be considered.

3.4.4 *B.thailandensis* infected human monocyte/macrophage cell lines

Despite both *B.thailandensis* strains used in this study promoting cell fusion and MNGC formation in mouse macrophages cell lines, these bacteria was poorly promoted cell fusion and MNGC formation in the human monocyte/macrophage cell lines U937 and THP1. Diverse conditions were used including different MOIs, times of infection, PMA-stimulation and poly-lysine for enhancing cell adhesion; however there were no reasonable numbers of fusion events that could be assessed. In a comparable study, Harly and co-workers showed that several strains of both *B.p* and *B.t* were unable to induce cell fusion in the monocyte-like cell line U937, in this study unstimulated U937 grow in suspension were used, so the cells could not contact and adhere properly to each other to establish fusion process

leading MNGC formation (Harley et al., 1998). In contrast, Suparak and co-workers showed the ability of *B.pseudomallei* K96243 to induce MNGC formation in PMA-stimulated U937 cells; however the fusion rate in these cells was relatively low (Suparak et al., 2011). Differentiated THP1 more closely represent the morphology of normal monocyte-derived-macrophages than U937; however, very few cells were noted to form MNGC formation with 4 to 5 nuclei. Even when cells were incubated for 24hr, no improvement was noted. Although MNGC formation is induced by *Burkholderia*, the cell responses to infection by these bacteria may have different possible effects. Horton and co-workers showed that *B.p* and *B.t* infection of human monocyte-derived dendritic and macrophage cells dramatically declined by 12 hr post-infection and that bacteria were unable to survive and replicate within DC cells (Horton et al., 2012). It has been shown that viable bacteria are required for the fusion process as heat-killed *B.p* were unable to induce MNGC formation (Suparak et al., 2011). The long term survival and replication of *B.t* within THP1 and U937 was not investigated in this study (only viability 4hr post-infection was tested). Death of the bacteria might be one possible explanation for the inability of *B.t* to induce fusion in these cells; this explanation is consistent with results showing that the *B.t* strain UE5 had a decreased survival rate and failed to replicate after 16hr post infection within primary human monocyte-derived macrophages compared with *B.pseudomallei* strain 844, although the numbers of both organisms were similar in the early stages of growth(Charoensap et al., 2009).

According to these poor results with human monocytes the project was carried out thereafter using mouse macrophages cell lines.

Chapter 4

Effects of tetraspanins in *Burkholderia thailandensis*-induced multinucleated giant cells formation

4.1 Introduction

4.1.1 Molecules implicated in cells fusion and MNGC formation

As mentioned in Chapter 1, previous studies showed roles for several surface proteins in cell fusion and MNGC formation. Scavenger receptor CD36 contributes to macrophage fusion induced by the cytokines IL-4 and GM-CSF, as anti-CD36 antibody inhibits macrophage fusion (Helming and Gordon, 2009). Integrin-associated protein CD47 participates in cell fusion, as blocking CD47 by using monoclonal antibodies strongly inhibited formation of tartrate resistant acid phosphatase (TRAP) multinucleated osteoclasts in a murine cell culture system(Lundberg et al., 2007). Convincing evidence suggested a role for CD98, a fusion regulatory protein, in syncytiotrophoblast cell fusion; CD98 expression is up-regulated following cell fusion and when CD98 protein expression is inhibited by transfection with siRNAs to CD98, cell fusion was suppressed, whereas scrambled siRNAs had no significant effect (Kudo and Boyd, 2004). In contrast, anti-CD98 mAbs enhanced MNGC formation in the HIV gp160 gene-transfected CD4$^+$ U937 cell line (Ohgimoto et al., 1995). Dendritic cell–specific transmembrane protein DC-STAMP showed an essential impact in cell fusion. Considerable multinucleated giant cell formation was noted in osteoclasts derived from wild-type mice, whereas no fusion was produced in DC-STAMP$^{-/-}$ osteoclasts. In addition, MNFBGCs induced by implantation of foreign bodies were also inhibited in DC-STAMP$^{-/-}$ mice (Yagi et al., 2005). Antibodies against Intracellular adhesion protein ICAM-1 (CD54) as well as antibodies against the transmembrane adhesion molecule CD44 inhibit macrophage fusion (Sterling et al., 1998). In *Burkholderia pseudomallei*- induced cell fusion, antibodies specific to CD47, CD98 and E-cadherin (CD324) inhibit significantly U937 macrophage fusion, whereas antibodies against CD44, and CD14 (LPS receptor) have no effect in *B.p*-induced U937 fusion (Suparak et al., 2011). Previous studies have reported roles for tetraspanins in cell fusion and MNGC formation (Takeda et al., 2003, Parthasarathy et al., 2009), in HIV-induced syncytia formation, (Gordon-Alonso et al., 2006), sperm-egg fusion (Kaji et al., 2000) and myoblast fusion (Tachibana and Hemler, 1999).

Our research group and others showed the contribution of tetraspanins in MNGC formation by using recombinant proteins corresponding to the large extracellular domain EC2 of tetraspanins. EC2 proteins of CD9, CD81 and CD63 inhibit MNGC formation in con A-stimulated monocytes (Takeda et al., 2003, Parthasarathy et al., 2009). Therefore, it was of interest to investigate a possible role for tetraspanins in cell fusion induced by *Burkholderia*, which may enhance knowledge about MNGCs formation mechanism and melioidosis pathogenesis.

4.1.2 Functional studies of tetraspanins using specific antibodies

Monoclonal antibodies (mAbs) to cell surface proteins are powerful tools that have been widely used in research studies and in clinical diagnosis and therapy. Anti-tetraspanin

antibodies have been useful in identifying and characterising tetraspanins and also in studying their functions. MAbs have helped demonstrate roles for tetraspanins in cell-cell fusion. Some evidence suggested that CD9 positively regulates cell fusion, as anti-CD9 antibodies significantly inhibit sperm-egg fusion (Kaji et al., 2000) and anti-CD9 and anti-CD81 antibodies delayed myoblast fusion and induced early myotube degeneration (Tachibana and Hemler, 1999). By contrast, anti-CD9 and anti-CD81 antibodies enhanced monocyte fusion which suggested that CD9 and CD81 negatively regulate cell fusion and MNGC formation (Takeda et al., 2003, Parthasarathy et al., 2009). In addition, anti-CD9 and anti-CD81 enhance HIV-induced lymphocyte membrane fusion (Gordon-Alonso et al., 2006).

4.1.3 EC2 proteins in tetraspanin functional studies

The large extracellular domain of tetraspanins (EC2) is variable in length and amino acid sequence among tetraspanin members. This region is thought to be important for tetraspanin partner interactions, and consequently it facilitates tetraspanin functions. Recombinant proteins corresponding to tetraspanin extracellular domain EC2s are an alternative tool to mAbs that are used in determining tetraspanin functions. These proteins are usually expressed in *E.coli* as fusion proteins with glutathione S-transferase. These GST fusion proteins are soluble and stable so can be purified using non denaturing procedures (Smith and Johnson, 1988).

Tetraspanin EC2 proteins have been effectively used in functional studies that suggested the involvement of tetraspanins in various cell processes. Recombinant GST-CD9EC2 protein strongly inhibited sperm-egg fusion (Zhu et al., 2002), which has also been confirmed by Higginbottom et al using both mouse and human GST-CD9EC2 recombinant proteins (Higginbottom et al., 2003). Takeda and co-workers found that human GST-CD9EC2 inhibited monocyte fusion whereas murine GST-CD9EC2 showed no effect (Takeda et al., 2003). Parthasarathy and co-workers also showed that GST-CD9EC2 inhibited MNGC formation; however mouse GST-CD9EC2 which has 77% identity with human CD9EC2 had no significant effect on MNGC formation (Parthasarathy et al., 2009). In addition, they showed that recombinant GST-CD63EC2 inhibited MNGC formation, whereas GST-CD81EC2 had no effect. Recombinant EC2 proteins have also been used to demonstrate roles for tetraspanins in virus infection. An essential role for CD81 in hepatitis C virus binding was suggested, since GST-CD81EC2 significantly inhibited the binding of hepatitis C virus envelop glycoprotein E2 to CD81 expressed on human and rat cells (Higginbottom et al., 2000). The involvement of tetraspanins in human immunodeficiency virus infection was also demonstrated with GST-EC2 proteins of CD9, CD63, CD81 and CD151 inhibiting HIV infection of macrophages (Ho et al., 2006).

Tetraspanin EC2 fusion proteins that were used in this study were generated by other workers in the laboratory. Tetraspanin GST-EC2 production methods are described in detail by (Higginbottom et al., 2003)(Fanaei, 2013 PhD thesis).

4.2 Results

4.2.1 Effects of anti-tetraspanin antibodies in *B.t*-induced MNGC formation

Anti-tetraspanin antibodies are widely used in studying tetraspanin functions and interactions. However, there were few anti-tetraspanin antibodies against mouse tetraspanins, which were available at the date of performing these experiments. Therefore, only the effect of antibodies to tetraspanins CD9, CD63 and CD81 were tested on *B.thailandensis*-induced cell fusion in J774.2 and RAW264.7 cells. As shown previously, CD9 and CD81 are highly expressed on J774.2 and RAW264.7 cells, whereas CD63 was poorly expressed on these cells. However, it was of interest to include anti-CD63 antibody in this experiment, since anti-CD63 antibodies were previously shown to inhibit Con A-induced MNGC formation of human monocytes, which also express relatively low levels of CD63 (Parthasarathy et al. 2009). Isotype controls were also used to investigate a possible effect of nonspecific binding of antibodies. Also for a negative control, the effect of antibodies on non-infected cell was tested.

An antibody concentration of 10 µg/ml was used, as this is known to give saturating binding. After the treatment with antibodies as described in 2.2.10.5.1, cells were co-cultured with *B.t* CDC or *B.t* E264 at MOI of 3:1 as mentioned in 2.2.10.2. Cells were fixed and stained with Giemsa and the fusion index and MNGCs size determined as described in 2.2.10.3.

4.2.1.1 Effects of antibodies in B.t-induced MNGC formation in the J774.2 cell line

The effects of antibodies on MNGC formation induced by *B.t*-CDC 272 and *B.t* E264 in J774.2 cells are shown in figures 4.2.1 and figure 4.2.2 respectively. The data was normalized to the mean of non-antibody treated cells (control for each independent experiment) to compensate for the effect of the variation between the experiments.

Anti-CD9 antibody and anti-CD81 antibody strongly enhanced MNGC formation in cells infected either with *B.t* CDC272 or *B.t* E264. There was a dramatic increase in fusion index and MNGC size in cells treated with anti CD9 or anti CD81 antibodies compared to untreated cells or cells treated with isotype controls (rat IgG2b and hamster IgG respectively). There was no effect with cells treated with anti-CD63 in J774 cells, possibly because of the low level of CD63 on J774.2 cells. *B.t* CDC stimulated cells showed about a 2-fold increase in MNGC size in the presence of antibodies compared to those in control cultures.

There was no cell fusion in uninfected cells, which were incubated with medium containing 10µg/ml anti-tetraspanin antibodies, meaning that the antibodies themselves were unable to induce cell fusion and MNGC formation. However, they promote MNGC formation in *B.t* infected cells, as earlier cell fusion was noted in infected cells in the presence of antibodies compared to controls.

A
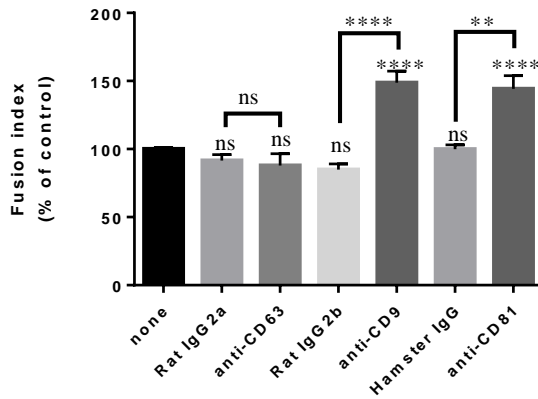
B
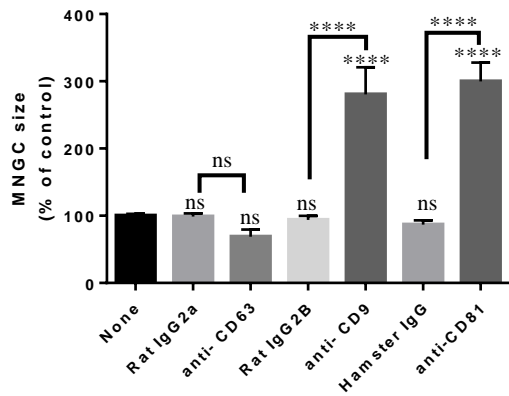
Figure 4.2.1 Effects of tetraspanin antibodies on *Burkholderia thailandensis* induced MNGC formation in the mouse macrophage cell line J774.2 (CDC 272 strain). Cells were cultured in 96 well plates overnight, and then incubated for 1hr in the presence or absence of antibodies at 10ug/ml (anti-CD9; anti-CD63 or anti-CD81) isotype controls: rat IgG2a, rat IgG2b, or hamster IgG. Cells then were infected with B. thailandensis CDC 272 as described in (2.2.8.1). Cells were fixed and stained with Giemsa. Fusion index (A) and MNGC size (B) was calculated from 10 fields of view per test as described in (2.2.6.3). The experiment was performed at least four times in triplicate. Data are normalized to non-antibody treated cells (control) and plotted as mean ± SEM. The significance of differences between antibody treated and non-treated cells and with isotype controls was tested using Ordinary one-way ANOVA with Holm-Sidak multiple comparison test. ***P<0.001, ****P< 0.0001, ns = not significant.

A
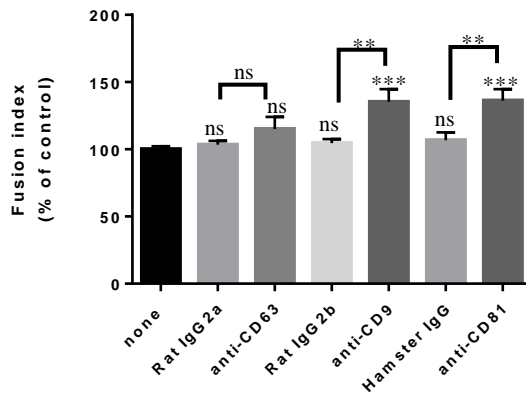
B
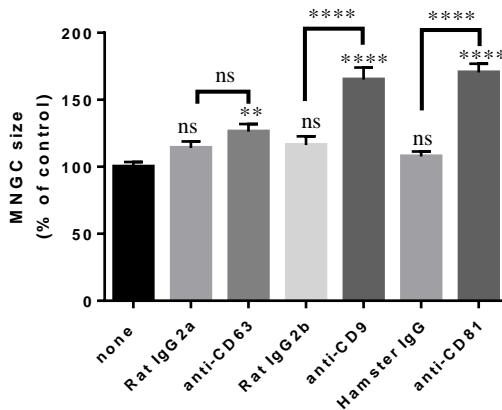
Figure 4.2.2 Effects of tetraspanin antibodies on *Burkholderia thailandensis* induced MNGC formation in the mouse macrophage cell line J774.2 (E264 strain). Cells were cultured, incubated with antibodies or isotype controls then infected with *B.thailandensis* E264 as described in Figure 3.3.14. (A) Fusion index (B) MNGC size. The experiment was performed at least four times in triplicate. Data are normalized to non-antibody treated cells (control) and plotted as mean ± SEM. Statistical analysis was performed as described in 3.1.14.

4.2.1.2 Effects of antibodies in B.t-induced MNGC formation in the RAW cell line

Similar results were obtained with the mouse macrophage cell line RAW264.7; anti-CD9 and anti-CD81 significantly enhance cell fusion and multinucleated giant cell formation induced by *B.t* CDC272 and *B.t* E264. There was a large increase of MNGCs in RAW cells treated with anti-CD9 or anti-CD81 (about 3- fold compared to untreated cells). The anti-CD63 antibody showed no effect compared to isotype effect. The data was normalized to non-antibody treated cells (control) to eliminate the effect of the variation between the experiments figures (2.2.3)(1.2.4).

A
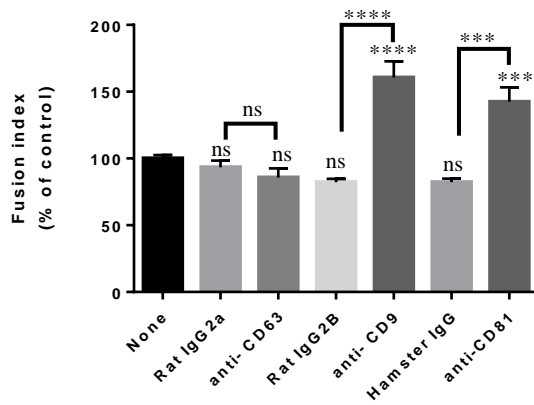
B
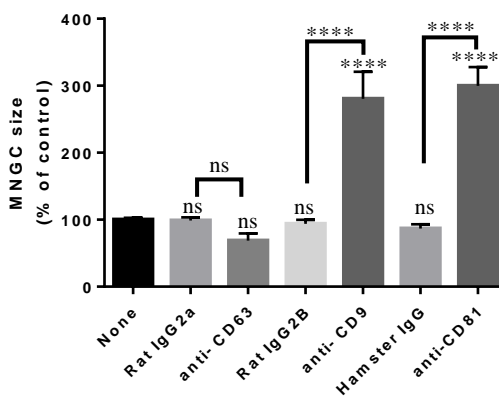
Figure 4.2.3 Effects of tetraspanin antibodies on *Burkholderia thailandensis* induced MNGC formation in mouse macrophage cell line RAW 264.7. Cells were cultured, incubated with antibodies or isotype controls then infected with *B.t.* CDC 272 as described in Figure 4.2.1. (A) Fusion index (B) MNGC size. The experiment was performed at least four times in triplicate. Data are normalized to non-treated cells (control) and plotted as mean ± SME. Statistical analysis was performed as described above.

A
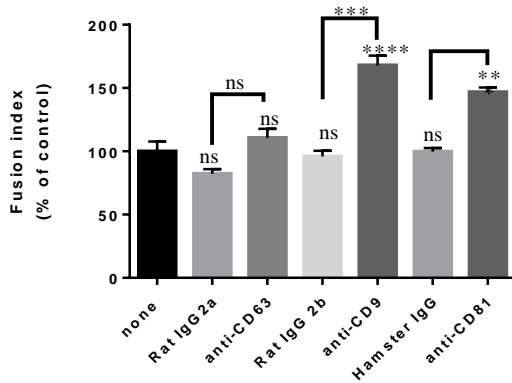
B
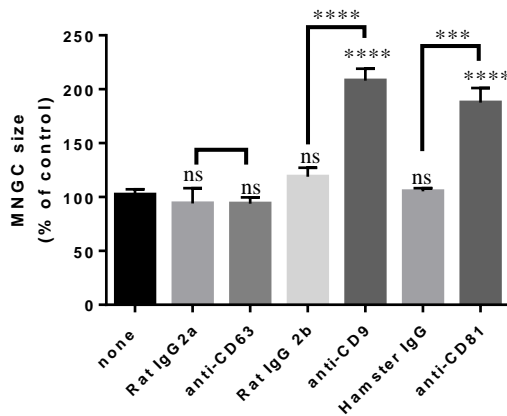
Figure 2.2.4 Effects of tetraspanin antibodies on *Burkholderia thailandensis* induced MNGC formation in mouse macrophage cell line RAW 264.7. Cells were cultured, incubated with antibodies or isotype controls then infected with *B.t.* E264 as described in Fig. 3.3.14. The experiment was performed at least four times in triplicate. Data are normalized to non-treated cells (control) and plotted as mean ± SEM. Statistical analysis was performed as described in Fig. 3.3.14.

4.2.1.3 Overnight treatment antibodies

Since pre-treatment for 1 hr with 10µg/ml anti-tetraspanin antibodies dramatically enhanced *B.t-* induced cells fusion, the effect of longer incubation of antibodies on *B.t-* induced MNGC formation was investigated. (In previous work from our group, the effect of anti-tetraspanin antibodies on Con A-induced MNGC formation was greater when antibodies were left in situ during the process (Parthasarathy et al 2009; Parthasarathy PhD Thesis University of Sheffield 2005)). J774 cells were infected as described previously with *B.t.* E264, cells were washed 3 times with PBS and incubated in medium contains antibiotics and in the presence or absence of 10µg/ml antibodies throughout the 16 hr incubation period. From the data shown in Figure 3.3.20, it appears that there was again a significant increase in MNGC formation in cells treated anti-CD9 and anti-CD81 antibodies compared

to untreated cells. Interestingly, anti-CD63 antibodies produced a slight but significant reduction in the amount of MNGC formation (Figure 4.2.5 A). The overnight incubation with antibodies also produced a significant enhancement in MNGC size, ~ 3-fold and ~ 2-fold in cells treated with anti-CD9 and anti-CD81 antibodies, respectively, compared to untreated cells. Anti CD63 antibodies showed no significant effect on this parameter (Figure 4.2.5 A).

A
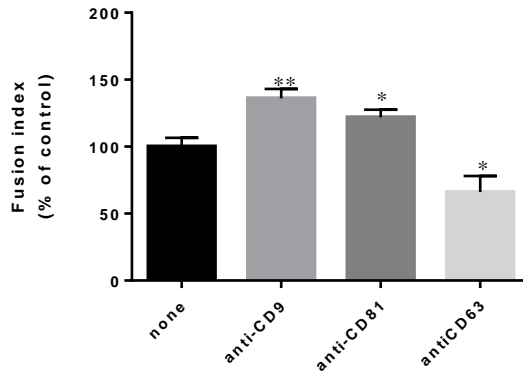
B
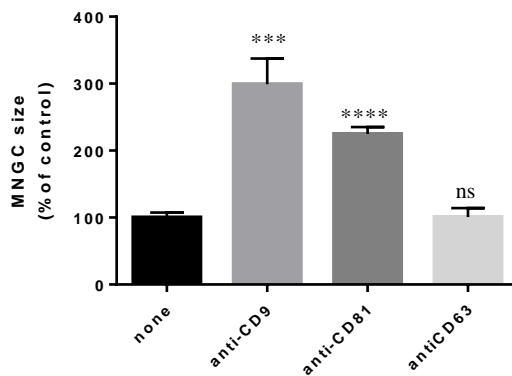
Figure 4.2.5 Effects of overnight treatment with anti-tetraspanin antibodies on *B.t*-induced MNGC formation in J774.2 cells. Cells were infected with B.t E264 as described in (2.2.8.2), and then cells incubated with medium contain 10μg/ml (anti-CD9, anti-CD63 or anti-CD81) and antibiotics as previously. (A) Fusion index, (B) MNGC size. The experiment performed twice in duplicate and significant differences between the non-treated cells and antibody treatment was tested by unpaired t test. ***P<0.001, ****P<0.0001, ns= Non-significant.

4.2.1.4 Effects of anti-tetraspanin antibodies on B.t uptake

Since the anti-tetraspanin antibodies affected *B.t*.-induced MNGC formation, their possible effects on the *B.t* uptake was investigated. Thus the effects of tetraspanin antibodies on *B.t* uptake were tested as described in (2.2.10.4). Briefly, a monolayer of J774 cells was treated with 10μg/ml of antibody or appropriate isotype control for 1 hr prior to infection. After infection, a kanamycin protection assay was used to determine the number of viable intracellular bacteria. The anti tetraspanin antibodies showed no effect on the invasion of J774 cells by *B.t* E264 in J774. There was a slight decrease in uptake of *B.t* CDC272 in anti-

CD9 and anti-CD81 treated J774 cells relative to non-antibody treated cells, but there was no effect compared with the isotype controls. This suggests that the tetraspanins CD9 and CD81 are involved in B.t-induced cells fusion at the stage where MNGCs are produced, rather than the initial infection (Figure 4.2.1.4).
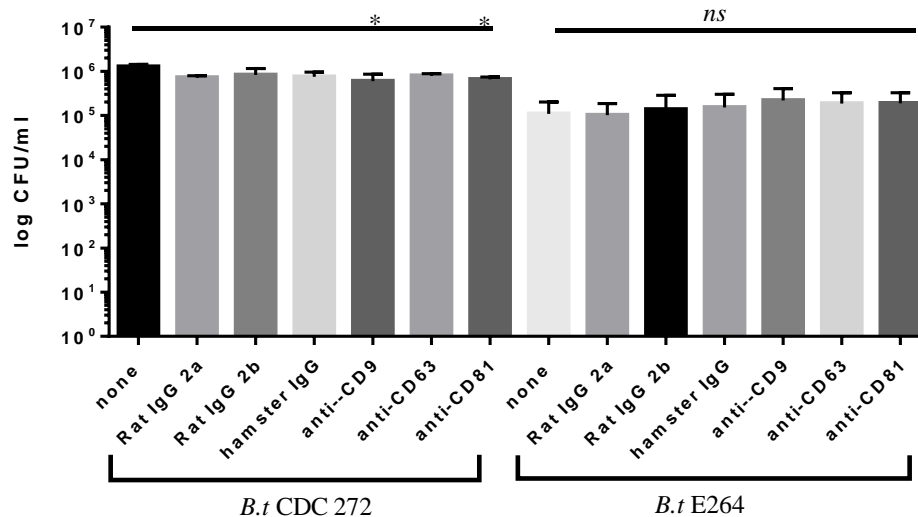
Figure 4.2.1.4 Effects of anti -tetraspanin antibodies on *Burkholderia thailandensis* uptake. Overnight cultures of J774 cells were incubated in presence or absence of 10μg/ml anti-tetraspanin antibody or appropriate isotype control for 1 hr prior to infection. The kanamycin protection assay was then curried out as described before. The experiment was performed twice in duplicate and significant differences were assessed using Ordinary one-way ANOVA with the Holm-Sidak multiple comparison test. *P<0.05 and ns= non significant.

4.2.2 Effects of recombinant tetraspanin EC2 proteins on *B.t*-induced MNGC formation

As described previously, recombinant proteins corresponding to the large extracellular domain EC2 of tetraspanin are other tools that have been used extensively in studying tetraspanin functions. It was therefore of interest to investigate the effects of these on MNGC formation induced by *Burkholderia thailandensis*. The EC2s used here were generated by other members of the group. The proteins were produced as fusion proteins with glutathione S-transferase (GST) in *E.coli* as described in (2.2.4). Therefore GST proteins were used as negative controls in EC2 protein experiments. Recombinant proteins produced in bacteria are contaminated with LPS. Some workers report that LPS interferes with Con A-induced MNGC formation (Takashima et al 1993; Marzieh Fanaei PhD thesis 2013), whereas others have found no effect (Parthasarathy, 2009). As a precaution, wherever possible, recombinant proteins that had been treated with triton X-114 to reduce LPS contamination (Reichelt *et al*. 2006) were included in these assays. These detergent-treated recombinant proteins are denoted by an "X" throughout.

4.2.2.1 Effects of GST-EC2 CD9 on *B.t*-induced MNGC formation

Given the strong effect of anti-CD9 antibody on B.t-induced MNGC formation, initial experiments were performed using CD9 EC2 expressed as a GST fusion protein**.**

4.2.2.1.1 Effects of pre-treatment of GST-EC2CD9 on *B.t*-MNGC formation

GST-CD9EC2 and GST proteins were expressed in *E.coli* strain Rosetta-gami as described in 2.2.4.The effects of these proteins on *B.t*-induced MNGC formation was investigated as described in (2.2.10.5.1). Briefly, J774.2 cells were cultured overnight in 96 well plates then treated with 500nM GST or GST-EC2CD9 for 1 hr before infection. Cells were fixed, stained and fusion index and MNGC size calculated as described previously.

Results in figures (4.2.6) and (4.2.7) show the effects of CD9 EC2 proteins on MNGC formation in J774.2 induced by *B.t* CDC272 and *B.t* E264 respectively. There was a highly significant inhibitory effect on fusion index on *B.t*-induced cells fusion in cells treated with GST-CD9 (detergent-treated or not) compared to either untreated cells or cells treated with GST proteins. The effects of the recombinant proteins on MNGC size was more variable depending on the strain of bacterium used and whether or not the proteins had been treated with detergent.

A
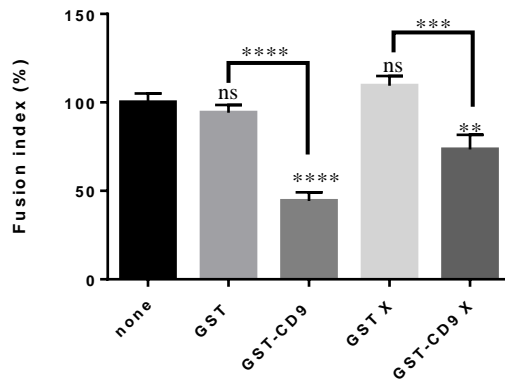
B
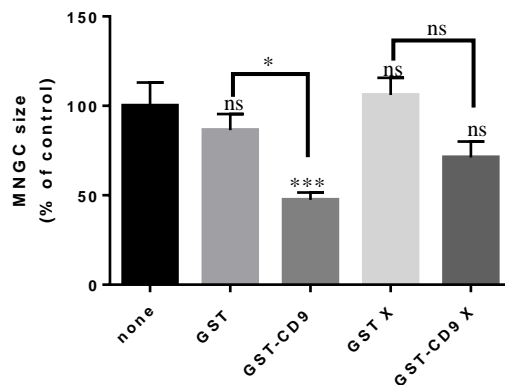
Figure 4.2.6 Effects of tetraspanin GST-CD9 proteins on *B. Thailandensis* CDC272- induced MNGC formation in J774.2 cells. Cells were cultured on 96 well plates overnight then incubated for 1hr with or without 500 n M GST-CD9 proteins or GST (control) before infection   as described in (2.2.10.5.1). Cells were fixed, stained with Giemsa and analysed as described in (2.2.10.2) and (2.2.10.3). (A) Fusion index (B) MNGC size. The experiment was performed at least four times in triplicate. Data are normalized to non-treated cells (control) and plotted as mean ± SEM. Statistical analysis was performed as described previously (Figure 3.3.14).

A

B

Figure 4.2.7 Effect of tetraspanin GST-CD9 proteins on *B. thailandensis* E264-induced MNGC formation in J774.2 cells. Cells were cultured, treated with or without GST proteins, infected with bacteria and analysed as described in Figure 4.2.7. (A) Fusion index (B) MNGC size.

4.2.2.1.2 Effects of overnight-treatment of GST-EC2CD9 on B.t-MNGC formation

Since pre-treatment of J774 cells with GST-CD9 proteins inhibited on B.t-induced cell fusion by >50%, the effect of a longer incubation with EC2 proteins was investigated. In this assay, following the infection with the bacteria, J774 cells were incubated in the presence of 500 nM recombinant protein. (GST; GST X; GST-CD9 or GST-CD9 X) and 500 µg/ml (kanamycin and amikacin) at 37C°. Cells were fixed and stained with Giemsa. Fusion index and MNGC size was calculated as shown in (2.2.10.3). Inhibition of fusion was observed (4.2.8) with a reduced fusion index for GSTEC2CD9 X compared to untreated and GST-X controls. However, there was also some inhibition with the GST control (for fusion index and MNGC size) and the GST-X control (for MNGC size), suggesting non-specific effects of the recombinant proteins during the longer incubation.

A
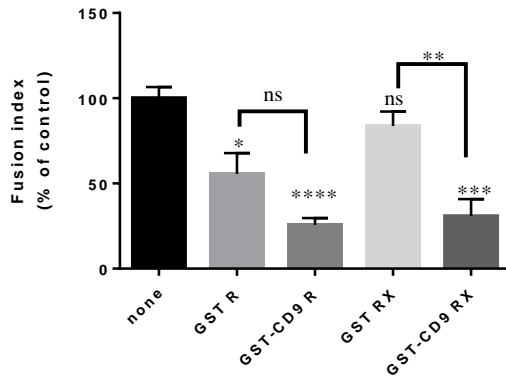
B
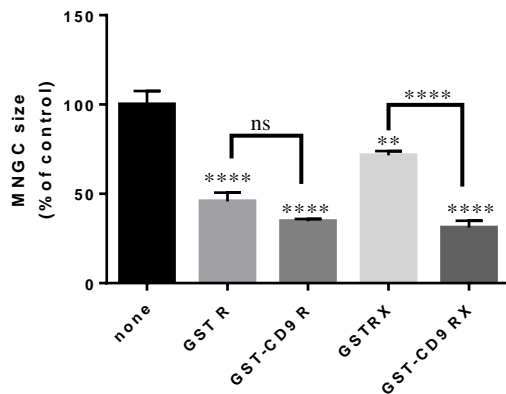
Figure 4.2.8 Effects of overnight treatment with GSTCD9EC2 proteins on *B.t*- induced MNGC formation in J774.2 cells. Cells were infected with *B.t* E264 as described previously then incubated for 16hr in the presence or absence of 500 n M of recombinant proteins. The experiment was performed twice in duplicate and differences between the non-treated and GST treated cells were analysed using unpaired t test. **P<0.005, ****P<0.0001, ns= Non-significant.

4.2.2.2 Effects of GST-EC2CD9 cysteine mutant on *B.t*-induced MNGC formation

Since pre-treatment with GST-EC2CD9 showed inhibitory effects on *B.t*-induced cells fusion, the effects of EC2CD9 mutants on *B.t*-induced cell fusion were also tested. GST-EC2CD9 proteins containing mutations at cysteine 153 (cysteine to alanine) and cysteine 152 (cysteine to alanine) were investigated. These mutants have been described previously (Higginbottom et al 2003) and are thought to be important for EC2 disulphide bond formation and conformation. Interestingly, the GSTEC2CD9 mutants showed a significant decrease in fusion index in cells infected with *B.t* CDC272 compared to control, but there was no effect in cells infected with *B.t* E264 (Figure 4.2.9).

A
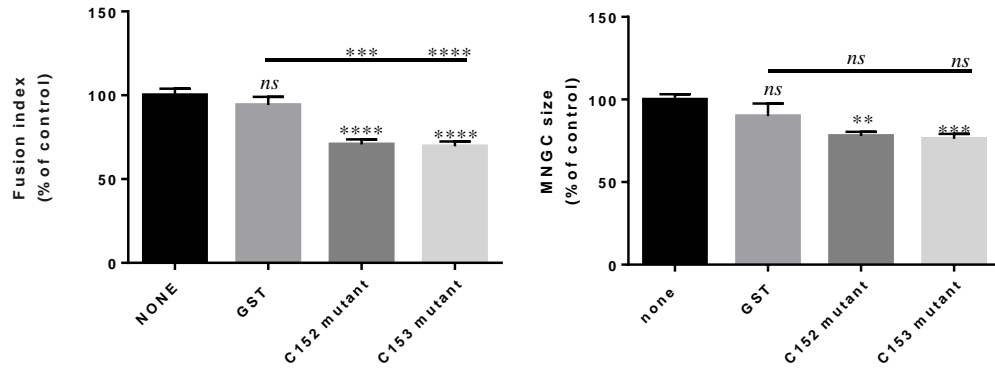
B
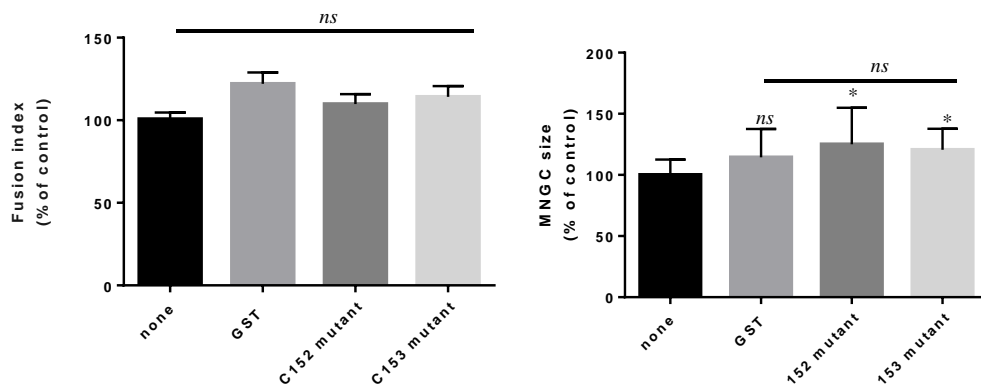
Figure 4.2.9 Effects of mutations of cysteine 152 and 153 in GSTEC2CD9 on MNGC formation induced by B.thailandensis. Cells were treated with mutant proteins for 1hr prior to infection as previously described. (A) J774 infected with B.t CDC272, (B) J774.2 infected with B.t E264. The experiment was performed twice in triplicate and results were analysed using Ordinary one-way ANOVA with Holm-Sidak's multiple comparison test. ***P<0.001 and ns= non significant.

4.2.2.3 Effects of CD9-derived peptides on *B.t*-induced MNGC formation

Synthetic peptides corresponding to different regions of the CD9 EC2 have previously been shown to have activity similar to the intact EC2 in some biological assays (Daniel Cozens, Jenny Ventress, personal communication). Since CD9 EC2 protein showed inhibitory effects in *B.t* induced MNGC formation, the effects of synthetic CD9-based peptides was also investigated. The peptides used are shown in Table 4.2.1 and Figure 4.2.10. This experiment aimed to identify the effective region of the EC2 CD9 protein that might promote cell fusion induced by *B.thailandensis*.

J774 cells were pre-treated with 50nM peptides for 1hr at 37C° and the MNGC formation assay performed as usual. From preliminary data shown in Figure (4.2.11), none of the peptides tested had any effects on *B.t* E264-induced cell fusion. Effects were seen with *B.t* CDC-infected cells or when peptides were incubated with cells after infection overnight (data not shown).

peptide	sequence
8001	Ser Lys His Asp Glue Val Ile Lys Glu Val Gln Glu Phe Tyr
8001 scrambled	Glu Glu Val lys Lys Phe Glu Ser Gln His Asp Ile Tyr Val
800	Glu Pro Gln Arg Glu Thr Leu Lys Ala Ile His Tyr Ala Leu Asn
800 scrambled	Ala Tyr Pro His Leu Glu Arg Asn Leu Glu Glu Ile Ala Lys Thr
810	Gly Pro Lys Lys Asp Val Leu Glu Thr Phe Thr Val Lys Ser
810 scrambled	Thr Ser Lys Glu Lys Leu Val Gly Pro Asp Thr Lys Val Phe

Table 4.2.1 CD9 EC2 derived peptide sequence.
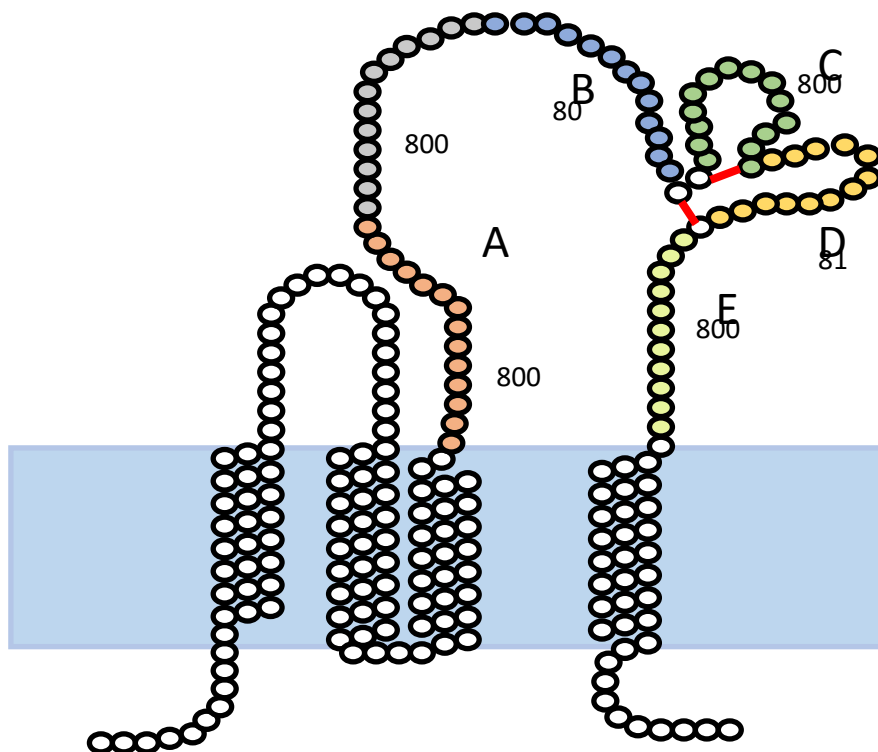
Figure 4.2.10 Synthetic peptides corresponding to different regions of CD9EC2. Peptide 8001 was designed to mimic a part of the A-helix region, 800 corresponds to part B of the head region and 810 corresponds to part of the sub loop D created by the disulphide bonds.

A
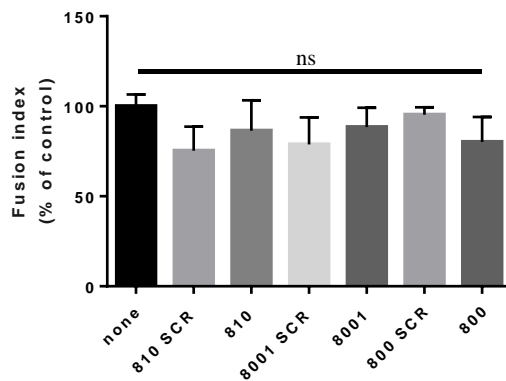
B
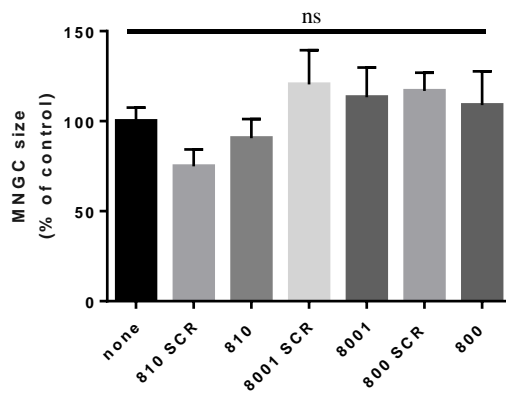
Figure 4.2.11 Effects of CD9-derived peptides on *B.t* E264-induced cells fusion. Cells were treated with peptides at final concentration 500nM for 1hr prior infection. (A) Fusion index, (B) MNGC The experiment was performed twice in duplicate.

3.2.2.4 Effects of GST-EC2CD9 on *Burkholderia thailandensis* uptake by the macrophage cell line J774

In this experiment we hypothesised that the inhibitory effects of CD9EC2 proteins on MNGC formation might be related to an effect on *B.t* uptake, since CD9EC2 has been shown to inhibit infection of human cells by some bacterial species (Green et al., 2011). Therefore the kanamycin protection assay was carried out to assess the number of intracellular bacteria in cells treated with GSTEC2CD9 proteins prior to infection. Briefly, J774 were incubated in presence or absence of 500 nM GST proteins (control) or GSTEC2CD9 proteins for 1hr, before the kanamycin protection assay was carried out as described before. The results showed that GST-CD9EC2 proteins did not have any effect on the invasion rate of *B.t* E264 compared to untreated cells, although GSTEC2CD9-X showed small but significant increase in infection compared to its negative control GST-X (Figure 4.2.12).
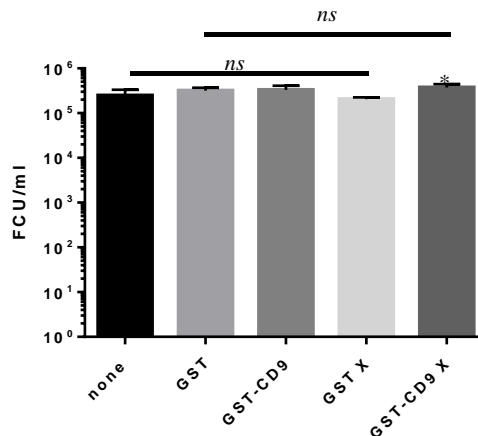
Figure 4.2.12 Effects of GSTEC2CD9 proteins on *B.t* E264 uptake by J774 cells. J774 cells seeded overnight in 24well plates were treated with EC2 protein for 1hr before infection and the kanamycin protection assay carried out as described in 2.2.6.1 to determine the number of viable intracellular bacteria. The experiment performed two times in duplicate and analysed using Ordinary one-way ANOVA with Holm-Sidak multiple comparison test. *P<0.05 and ns= non significant.

4.2.3 Effects of CD81EC2 and CD63EC2 on B.t-induced MNGC formation

To investigate the role of tetraspanin EC2 proteins on *B.t*-induced cell fusion, the effects of a range of GST-EC2 of CD63, CD81, CD151 and Tspan 2 proteins were tested (figure 4.2.13 and figure 4.2.14). As previously, these recombinant proteins had been generated by other members of the group (Marzieh Fanaei, John Palmer, Ibrahim Yaseen, and Arunya Jiraviriyakul). Note that detergent-treatment to remove LPS for some of these proteins was not possible, due to low yields and loss of protein following dialysis. However, in the case of CD63, a comparison was made with recombinant protein that had been produced in HEK293 mammalian cells (CD63M) which did not contain detectable endotoxin. J774 cells were treated with EC2 proteins for 1 hr before infection with *B.t* CDC272 or *B.t* E264, and then MNGC assay was carried out as described previously.

The results show that both GST- EC2CD63 proteins produced in bacteria and EC2CD63 produced in mammalian cells significantly inhibited MNGC formation induced by *B.t* CD272 and *B.t* E264 compared to controls. GST-EC2 CD81 showed an inhibitory effect on MNGC formation in cells infected with *B.t* CDC There was no significant difference in fusion index in cells treated neither with GST-EC2CD151 nor with GST-EC2 Tspan 2. There was a small effect noted in MNGC size in cells treated with GST-EC2 Tspan 2 compared with untreated cells but not with GST treated cells.
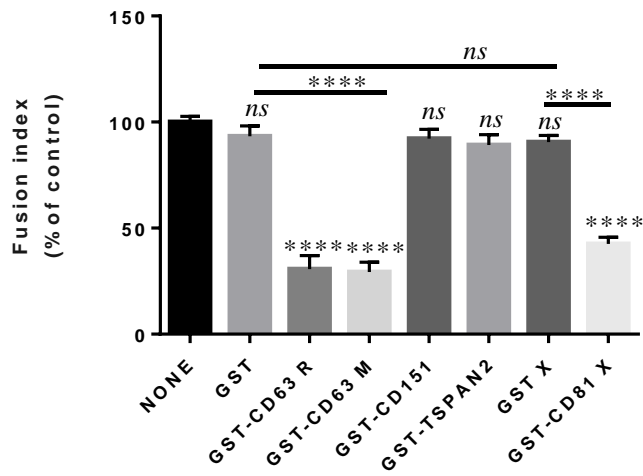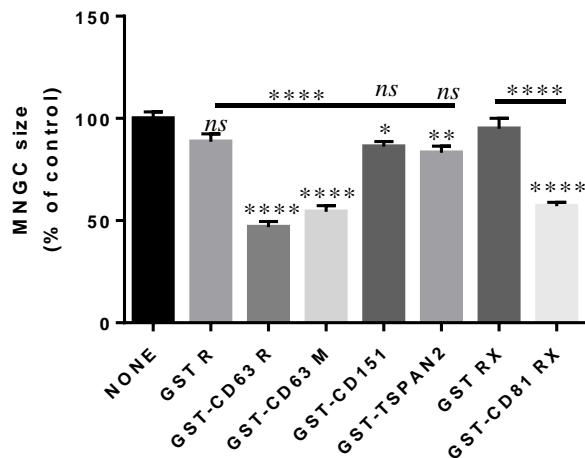
Figure 4.2.13 Effects of tetraspanin EC2 proteins on B. thailandensis CDC 272-induced MNGC in J774.2 cells. Cells were cultured, treated with or without recombinant proteins for 1hr, and then MNGC assay was performed as in 2.2.10.2 analysed as described in 2.2.10.3. The experiment was performed at least four in triplicate and analysed using Ordinary one-way ANOVA with Holm-Sidak multiple comparison test.
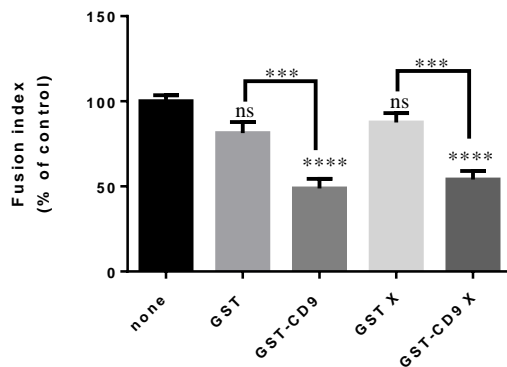
A
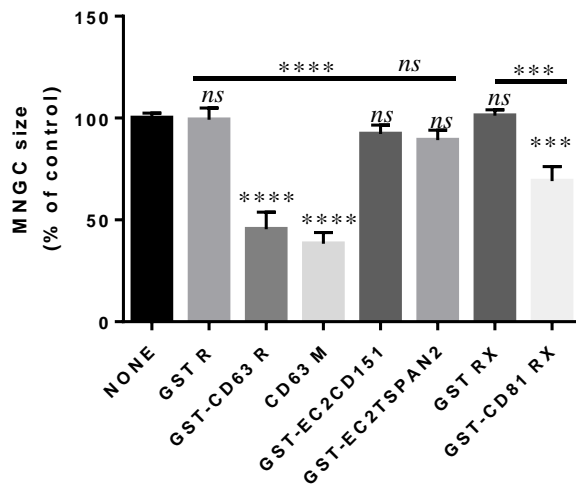
B
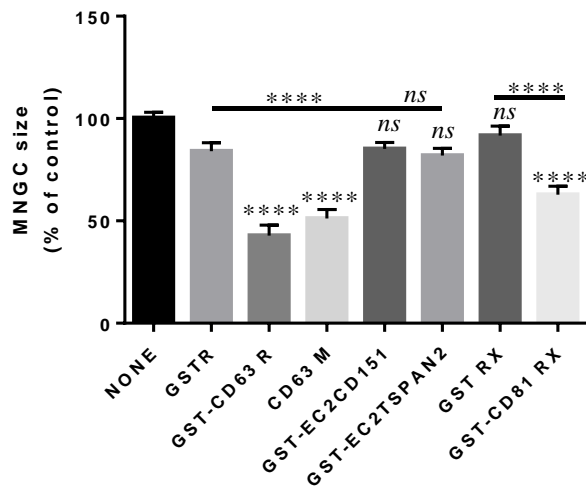
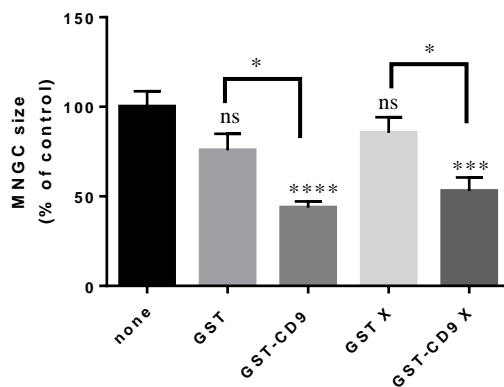**Figure 4.2.14 Effect of tetraspanin EC2 proteins on *B. thailandensis* E264-induced MNGC in J774.2 cells**. Cells were cultured, treated with or without recombinant proteins for 1hr, infected with bacteria and analysed as described in Figure 3.3.22. The experiment was performed at least four in triplicate and analysed using Ordinary one-way ANOVA with Holm-Sidak multiple comparison test.

4.2.4 Effects of bacteria lipopolysacchride (LPS) on B.t-induces MNGC formation.

As mentioned previously, the EC2 proteins that were used in this study produced in *E.coli*, and are likely to contain LPS, which some workers have reported that affects Con A-induced monocyte fusion and may contribute to the activity EC2proteins (Abe et al., 1984, Enelow et al., 1992, Lazarus et al., 1990, Takashima et al., 1993). Although a GST control, CD151EC2-GST and Tspan2EC2-GST (which had similarly been produced in bacteria) showed little or no effects, however the levels of LPS in preparations of recombinant proteins might vary. The effect of LPS on *B.t*-induced cell fusion was therefore investigated.

The effects of pre-treatment with LPS on MNGC formation induced by B.t were tested at different concentrations as indicated in Figures 4.2.15 and 4.2.16. The effect of LPS on non-infected was also tested. From the results it was observed that LPS had slight significant inhibitory effect on fusion index in cells infected with *B.t* CDC272 at concentrations 100, 50 and 10 ng/ml, whereas 200 ng/ml showed no significant effect. However there was no effect of LPS was noted for cells infected with *B.t* E264. In addition, small and very few MNGCs were formed in uninfected cells treated with LPS, suggested that LPS itself is capable of stimulating cell fusion.

A

B
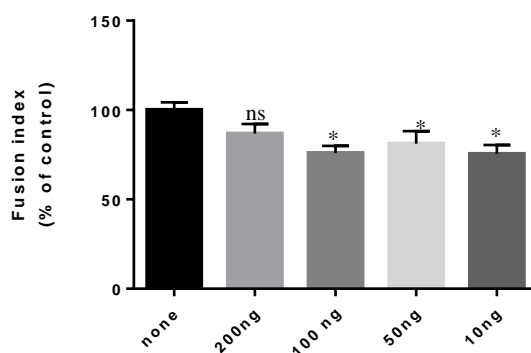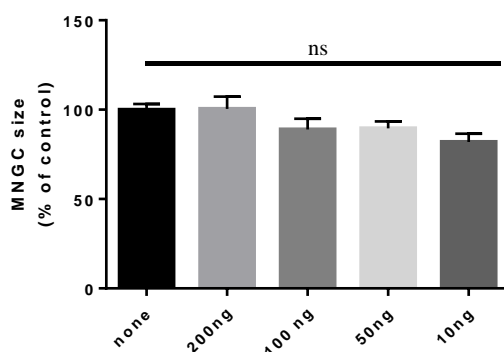
Figure 4.2.16 Effects of bacterial lipopolysacchride (LPS) on B.t CDC272-induced MNGC formation. Cells were incubated for 1hr in presence or absence of LPS at (200, 100, 50, 10) ng/ml. After washing, J774.2 cells were infected and MNGC assay was performed as in (2.2.10.2.1). (A) fusion index, (B) MNGC size The experiment was done three times in

duplicate and analysed using Ordinary one-way ANOVA with Holm-Sidak multiple comparison test.

A

B
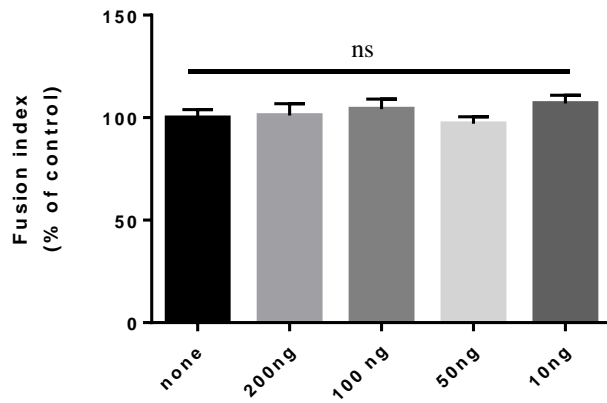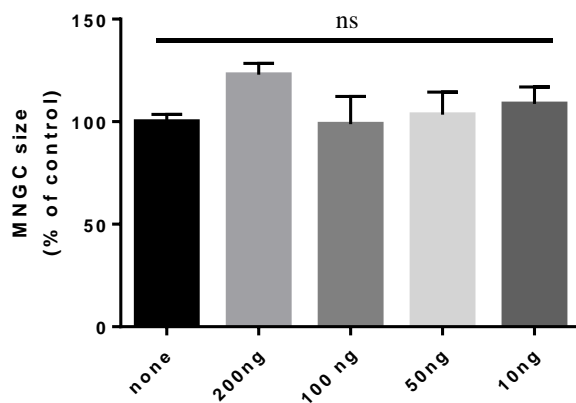
Figure 4.2.16 Effects of bacterial lipopolysacchride (LPS) on *B.t* –E264-induced MNGC formation. Cells were incubated with LPS and infected with bacteria as described in Figure 3.3.32 A) fusion index, (B) MNGC size. The experiment was done three times in duplicate and analysed as in Figure 4.2.16.

4.2.5 Effects of EC2 proteins on J774 cell number.

Since the GST-EC2 proteins of CD9, CD63 and CD81 showed significant inhibition of B.t induced cell fusion; possible adverse effects of these proteins on cell number were investigated using the sulforhodamine B (SRB) assay. This assay estimates cell number colorimetrically, using a dye that stains cellular protein and was originally developed as an assay for testing toxicity of anticancer drugs (Skehan et al., 1990).

4.2.5.1 Effects of pre-treatment with EC2 proteins on J774 cell number

In this assay cells were treated with tetraspanin EC2 proteins in the same way as that used to study their effect on *B.t*-induced MNGC formation i.e. cells were cultured overnight in 96 well plates, incubated in presence or absence of tetraspanin EC2 proteins for 1 hr, then washed twice with PBS and incubated overnight in medium. The cells were then fixed with TCA, and the SRB assay was performed as described in (2.2.11.2). The absorbance at 570 nm gives a measure of cellular protein, which is proportional to cell number, as described in 2.2.11.1 and figure 2.2.17. There was no significant effect on cell number on treatment with GST-EC2 proteins compared to untreated cells. This suggests that GST-EC2 of CD9, CD63 and CD81 proteins have no effects on J774 viability or proliferation under the conditions usually employed for the MNGC assay (figure 4.2.18).
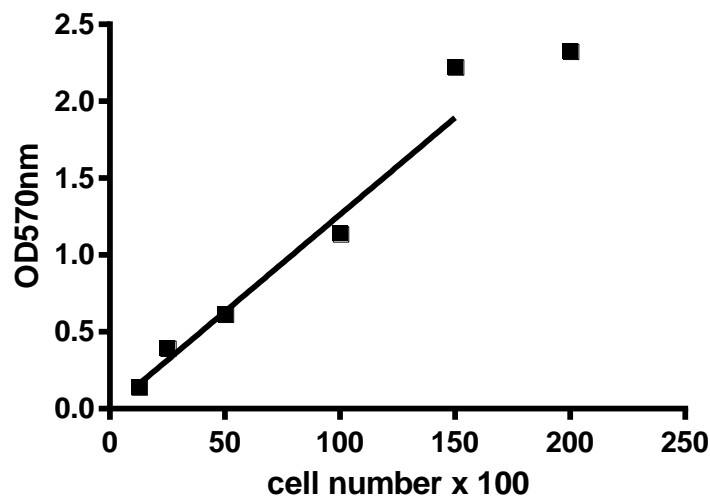
Figure 4.2.17 Standard curve for SRB assay for J774 macrophage cell line. Cell number was titrated as described in 2.2.11.1 (Dr Lynda Partridge, personal communication).
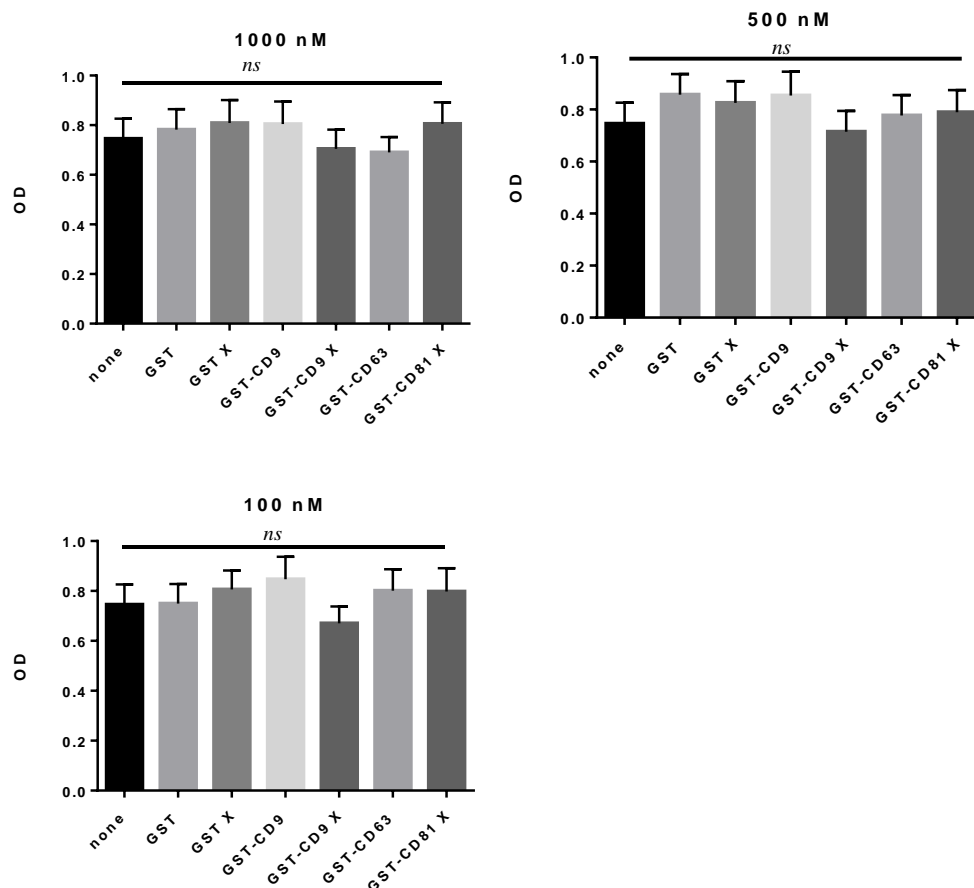
Figure 4.2.18 Effect of pre-incubation of recombinant EC2 proteins on cell number. J774 cells were cultured and treated with or without GST-EC2 proteins for 1hr as described for the MNGC assay then washed and incubated with medium overnight. Cells were fixed and SRB assay was performed as described in (2.2.11.2). The results are the mean of absorbance of 3 experiments performed in quadruplicate and were analysed by Ordinary one-way ANOVA with Holm-Sidak multiple comparison test.

4.2.5.2 Effects of long incubation with EC2 proteins on J774 number

Although pre-treatment with GST-EC2 of CD9, CD63 or CD81 under the conditions used for the MNGC assay showed no effect on cell number it was of interest to investigate the effect of a longer incubation with these proteins on the cells. Here, cells were incubated in the continuous presence or absence of GST-EC2 proteins for 72hr, before performing the SRB assay. The results showed that the GST-EC2s of CD9, CD63 and CD81 have a negative effect on cell number compared with untreated cells, whereas GST alone has no effect. These results indicated that the viability and/or proliferation of J774 are affected by long-term incubation with the GST-EC2 proteins (figure 4.2.19).
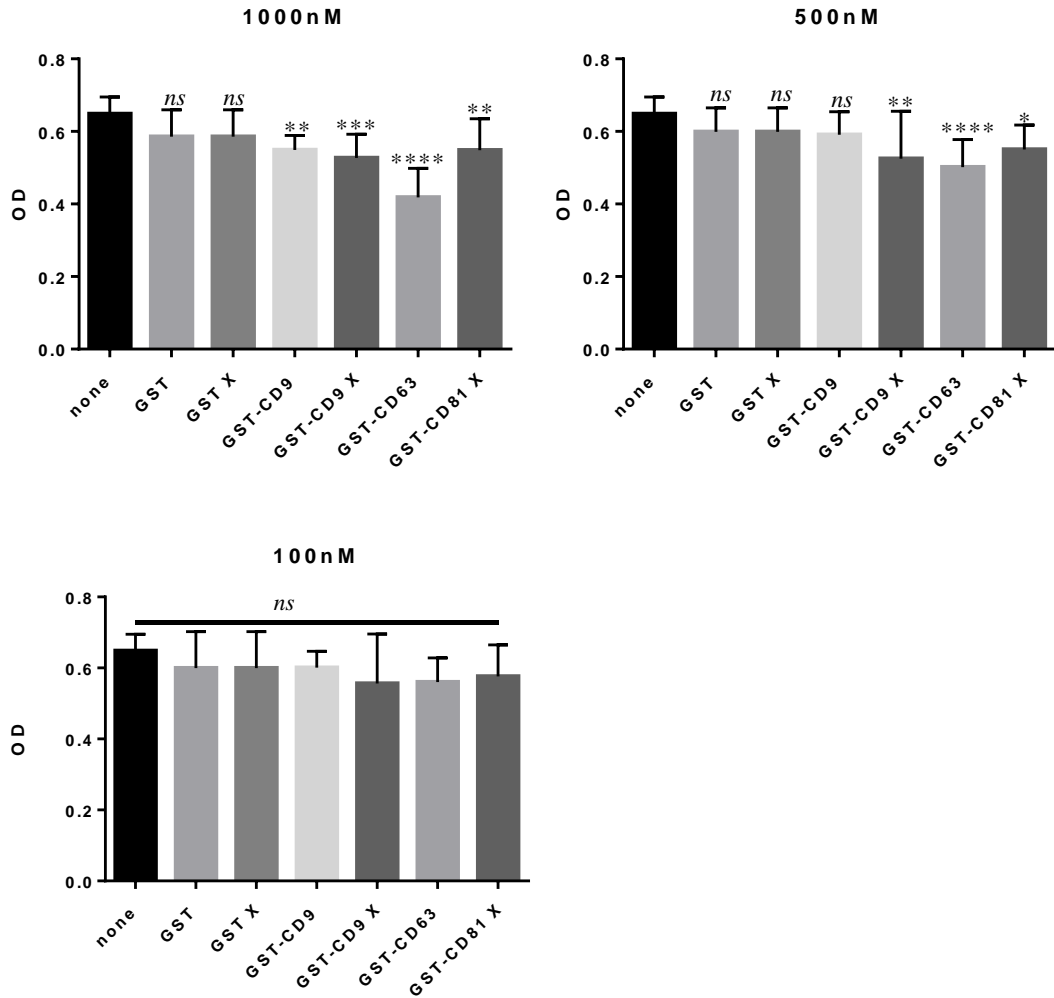
Figure 4.2.19 Effect of longer treatment with GST-EC2 proteins on cell number. J774 cells were cultured and incubated with or without GST-EC2 proteins continuously for 72 hr, before performing the SRB assay as described in (2.2.11.3). The results are the mean of absorbance of 3 experiments performed in quadruplicate and were analysed by Ordinary one-way ANOVA with Holm-Sidak multiple comparison test.

4.3. Discussion

The data presented in this chapter details the effects of anti tetraspanin antibodies and GST fusion proteins of large extracellular proteins (EC2s) on multinucleated giant cell formation induced by *Burkholderia thailandensis*.

4.3.1 Effects of monoclonal antibodies

The effect of a short incubation with anti CD9, anti CD63 or anti CD81 antibodies on *B.t*-induced MNGC formation was tested as described above. Briefly, cells were pre-treated with anti tetraspanin antibodies for 1hr at 37°C, and then the cells were washed to remove unbound antibodies before being infected with *B.thailandensis* and the MNGC assay was performed as described above. For controls, cells were treated with corresponding isotype controls to test the effect of any unspecific binding on *B.t*-induced MNGC formation and untreated cells were another control used in this study. The results revealed that anti-CD9 antibody and anti-CD81 antibody strongly enhanced MNGC formation in cells infected either with *B.t* CDC272 or *B.t* E264. There was a dramatic increase in fusion index and MNGC size in cells treated with anti CD9 or anti CD81 antibodies compared to untreated cells or cells treated with isotype controls. The effects of longer incubation of antibodies on *B.t*-induced MNGC formation were also investigated. Cells were infected with *B.thailandensis*, and then the cells were washed and incubated in the presence or absence of antibodies throughout the incubation period. There was again a significant increase in MNGC formation in cells treated anti-CD9 and anti-CD81 antibodies compared to untreated cells and the long incubation with antibodies also produced a significant enhancement in MNGC size. There was no cell fusion in uninfected cells, which were incubated with medium containing anti-tetraspanin antibodies, meaning that the antibodies themselves were unable to induce cell fusion and MNGC formation. However, they promote MNGC formation in *B.t* infected cells, as earlier cell fusion was noted in infected cells in the presence of antibodies compared to controls.

These results are in agreement with results showed by Takeda and co-workers (Takeda et al., 2003), and Parthasarathy and co-workers (Parthasarathy et al., 2009) that showed that anti CD9 and anti CD81 antibodies enhance Con A-induced monocyte fusion. Gordon-Alonso and co-workers reported similar enhanced effects of anti CD9 and anti CD81 on syncytia formation induced by HIV-1 envelope proteins (Gordon-Alonso et al., 2006), suggesting that CD9 and CD81 may modulate *B.thailandensis*-induced cell fusion by a comparable mechanism.

There was no effect observed with J774 and RAW264 cells pre-treated with anti-CD63 on *B.t*-induced cell fusion and MNGC formation, possibly because of the low level of CD63 on both cell lines as shown by FACS analysis in this study (Chapter 3). However notably, the long incubation with anti CD63 antibodies produced a slight but significant reduction in the amount of MNGC formation, but not on the size of MNG cells. There are contradictory results about the effects of anti CD63 on MNGC formation, as Parthasarathy and co-worker showed a significant inhibitory effect for anti CD63 on Con A-induced MNGC formation, whereas Takeda and co-worker reported that anti CD63 antibody has no effect (Takeda et al., 2003, Parthasarathy et al., 2009). These inconsistent results may be due to the effect of different parameters and methods used including antibodies and cell resources.

4.3.2 Effects of tetraspanin EC2 proteins

The effect of tetraspanins on *B.t*-induced MNGC formation in mouse macrophage cell lines was tested using human tetraspanins GST-EC2 (CD9, CD63, CD81, CD151 and Tspan2), the amino acid sequence of these tetraspanins has 77.38%, 67.32%, 77.53%, 88.07% and 87.01% identity with murine tetraspanins respectively. Figure 4.3.1 shows the alignment of the amino acid sequence of human EC2s with murine EC2s analysed using Clustalo-Omega. Taking advantage of the high degree of sequence identity these proteins were used to investigate their effects on *B.t*-induced MNGC formation in the mouse macrophage cell lines. It has been shown that the injection of human CD9 mRNA or mouse CD9 mRNA in CD9 KO oocytes restores their fusion ability (Zhu et al., 2002, Kaji et al., 2002). The EC2s of mouse and human CD9 differ by 18 residues, including nine non-conservative substitutions, indicating that certain changes of amino acids in mouse EC2 does not affect its functional activity (Zhu et al., 2002). It has also been reported that, human and murine GST-CD9 proteins both significantly inhibit murine sperm-oocyte fusion (Higginbottom et al., 2003).

```
CD9_HUMAN   SHKDEVIKEVQEFYKDTYNKLKTKDEPQRETLKAIHYALNCCGLAGGVEQFISDICPKKD
CD9_MOUSE   THKDEVIKELQEFYKDTYQKLRSKDEPQRETLKAIHMALDCCGIAGPLEQFISDTCPKKQ
            :********:********:**::************* **:***:** :****** ****:
CD9_HUMAN   VLETFTVKSCPDAIKEVFDNKFHI
CD9_MOUSE   LLESFQVKPCPEAISEVFNNKFHI
            :**:* ** **:**.***:*****


CD81_HUMAN  FVNKDQIAKDVKQFYDQALQQAVVDDDANNAKAVVKTFHETLDCCGSSTLTALTTSVLKN
CD81_MOUSE  ---KDQIAKDVKQFYDQALQQAVMDDDANNAKAVVKTFHETLNCCGSNALTTLTTTILRN
               *******************:*****************:****.:**:***::*:*
CD81_HUMAN  NLCPSGSNIISNLFKEDCHQKIDDLFSGK
CD81_MOUSE  SLCPSGGNILTPLLQQDCHQKIDELFSGK
            .*****.**:: *:::*********:*****


CD63_HUMAN  AGYVFRDKVMSEFNNNFRQQMENYPKNNHTASILDRMQADFKCCGAANYTDWEKIPSMSK
CD63_MOUSE  AGYVFRDQVKSEFNKSFQQQMQNYLKDNKTATILDKLQKENNCCGASNYTDWENIPGMAK
            *******:* ****:.*:***:** *:*:**:***::* : :****:******:**.*:*
CD63_HUMAN  NRVPDSCCINVTVGCGINFNEKAIHKEGCVEKIGGWLRKNV
CD63_MOUSE  DRVPDSCCINITVGCGNDFKESTIHTQGCVETIAIWLRKNI
            :*********:***** :*:*.:**.:****.*. *****:


CD151_HUMAN AYYQQLNTELKENLKDTMTKRYHQPGHEAVTSAVDQLQQEFHCCGSNNSQDWRDSEWIRS
CD151_MOUSE VYYQQLNTELKENLKDTMVKRYHQSGHEGVSSAVDKLQQEFHCCGSNNSQDWQDSEWIRS
            .*****************.***** ***.*:****:****************:*******
CD151_HUMAN QEAGGRVVPDSCCKTVVALCGQRDHASNIYKVEGGCITKLETFIQEHLR
CD151_MOUSE GEADSRVVPDSCCKTMVAGCGKRDHASNIYKVEGGCITKLETFIQEHLR
            ** .***********:** **:**************************


TSN2_HUMAN  GKGVAIRHVQTMYEEAYNDYLKDRGKGNGTLITFHSTFQCCGKESSEQVQPTCPKELLGH
TSN2_MOUSE  GKDVAIRHVQSMYEEAYSDYLKDRARGNGTLITFHSAFQCCGKESSEQVQPTCPKELPGH
            ** *******:******.******.:**********:***************** **
TSN2_HUMAN  KNCIDEIETIISVKLQL
TSN2_MOUSE  KNCIDKIETVISAKLQL
            *****:***:**.****
```

Figure 4.3.1 Alignment of extracellular domain EC2 amino acid sequence of human tetraspanins with their corresponding murine tetraspanins using Clustalo-Omega.

The GST-CD9, GST-CD63, GST-CD81 showed a strong and significant inhibitor effect on *B.t*-induced MNGC formation in both bacterial strains, but no effects were observed with GST-CD151 and GST-TSPAN-2. However, due to a lack of specific monoclonal antibodies to the mouse tetraspanins, it was not possible to determine if this might relate to low expression

levels of CD151 and Tspan-2 on the surface of the cells used here. Previous results obtained by Takeda and co-workers showed that GST-CD9 inhibited con A-induced MNGC formation (Takeda et al., 2003), Parthasarathy and co-workers also showed the GST-CD9 and GSTCD63 inhibited con-A induced MNGC formation while GST-CD81 and GST-CD151 had no effect (Parthasarathy et al., 2009), which was partly in line with results obtained in *B.t*-induced MNGC formation. In other consistent results, GST-CD9 (Zhu et al., 2002) and GST-CD81 have also been shown to inhibit sperm oocyte fusion (Zhu et al., 2002, Higginbottom et al., 2003).

Our data therefore suggest negative regulatory roles for CD9 and CD81 in *B.t*-induced MNGC formation as blocking of CD9 and CD81 resulted in enhancement of MNGC formation whereas binding of CD9EC2 and CD81EC2 to the cells disrupted *B.t*-induced MNGC formation. Despite a short incubation with anti-CD63 showing no effect, long incubation with the antibody as well as GST-CD63 pre-treatment resulted in inhibition MNGC formation. Notably CD63 showed a poor expression level on J774 cells, therefore the inhibition on MNGC formation could be due to interaction of CD63 EC2 with a molecule other than CD63, which could be another tetraspanin or another molecule of a different family. CD63 is known to interact with tetraspanins such as CD9, CD81, CD82 and CD151 and with other proteins including integrins such as β1 integrin, syntenini-1 and TIMP-1 (Berditchevski, 2001, Jung et al., 2006, Latysheva et al., 2006).

Since the recombinant proteins had been produced in the *E.coli*, it is likely that the proteins contain bacterial lipopolysaccharide (LPS) which may contribute to their activity. A recent study in our research group suggested that the functional activity of CD9 EC2 proteins (produced in bacteria) in con A-induced monocyte fusion may due to the activity of LPS contamination rather than the direct effect of EC2 itself. In that study the contribution of LPS to EC2 protein activity was elucidated by utilizing reduced LPS batches of the proteins, referred to as GST X and GST-CD9 X. The level of inhibitory effects of these proteins was significantly reduced compared to GST and GST-CD9. In addition there were no significant differences in the activity of boiled proteins compared to native proteins in MNGC assay (Marzieh Fanaei PhD thesis 2013). It has also been found that LPS could inhibit the monocyte fusion induced by Con A, which is thought to be due to LPS binding to receptors that are involved in cell-cell adhesion (Takashima et al., 1993). In contrast, other studies showed that bacterial cell wall proteins can stimulate MNGC formation such as muramy1 dipeptide (MDP) which can trigger epithelioid cell granulomas (Tanaka and Emori, 1980), and enhance Con A-induced monocyte fusion(Mizuno et al., 2001b). In a similar manner LPS has been found to enhance Con A-induced MNGC (Mizuno et al., 2001a). Previous findings in our group showed the ability of LPS to stimulate monocyte fusion and LPS treated cells produced a higher fusion rate compared to untreated cells in presence of Con A (Parthasarathy, PhD thesis 2005). Recently, an insignificant effect for LPS on Con A-induced fusion has been reported by our group (Hulme et al., 2014). Therefore, to determine the possible interference of LPS on recombinant protein activity, GST X and GST-CD9 X (where LPS levels were reduced by treatment with detergent, produced by Marzieh Fanaei) were used in the *B.t*-induced MNGC formation assay.

The results revealed that GST-CD9 and GST-CD9X both showed strong and highly significant inhibitory effects as shown by reduction in fusion in both *B.t* strains compared to the effect of GST and GST X respectively and there was no significant difference between the effects

of GST-CD9 and GST-CD9 X when cells pre-treated with these reagents before the infection. However long incubation with these proteins after the infection showed a significant inhibitory effect for GST-CD9, which was also observed with the GST control compared to untreated cells. This effect was reduced in GST X and a significantly reduced effect for GST-CD9 X was observed. The long incubation result was compatible with previous result showed inhibitory effect of GST on con A-induced MNGC formation where long incubations were used (M. Fanaei PhD thesis 2013). The effects that were observed in long incubations with GST-treated cells may therefore be due to LPS contamination.

It has been reported that human CD9 EC2 (where the GST tag has been removed) was slightly less active than GST-CD9 EC2, suggesting that GST contributes to the stability/activity of CD9 EC2 or that GST alone has weakly inhibitory effects in sperm-egg fusion (Higginbottom et al., 2003). However, Parthasarathy and co-workers reported similarly significant inhibitory effects for cleaved CD63 EC2, and highly purified his-tagged CD9 EC2 and CD63 EC2 compared to GST-CD63EC2 in Con A-induced cell fusion (Parthasarathy et al., 2009).

For further investigation, the effect of pure LPS on *B.t*-induced MNGC was tested. The effect of pre-treated of LPS at different concentrations was examined. A slight inhibition effect in fusion index was observed in cells infected with *B.t* CDC at low concentration, whereas 200ng showed no effect. However no effects noted with *B.t* E264-infected cells, suggesting that LPS has little contribution to the recombinant protein activity and the inhibition in *B.t*-induced MNGC formation is due to the EC2 proteins themselves. Notably, almost all of the recombinant proteins tested in these studies are produced in bacteria, so it would be expected that the possibility of LPS contamination is equal. As mentioned above, CD151 and TSPAN-2 showed no significant effect on *B.t*-induced fusion, although the LPS content in these protein preparations was higher compared to the amount in the CD9-EC2 protein as shown in figure 4.3.2 (John Palmer personal communication). In addition, CD63-EC2 produced in mammalian cells showed a similar   inhibitory effect to that observed with CD63-EC2 produced in bacteria in *B.t*-induced MNGC formation.
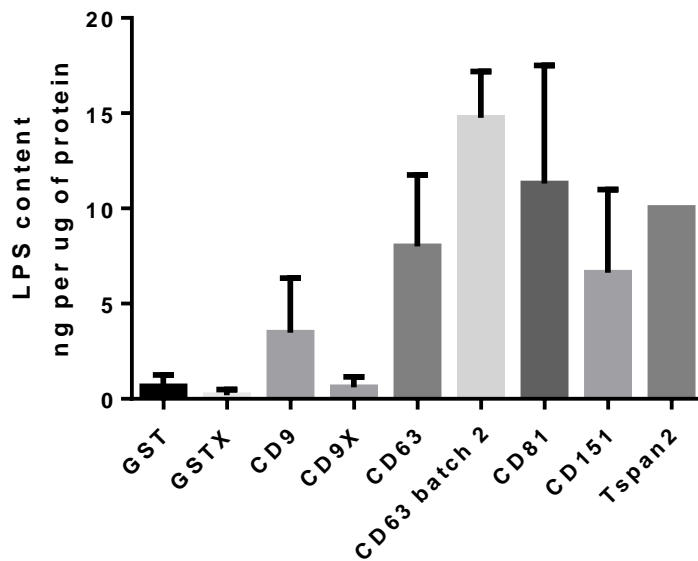
Figure 4.3.2 The concentration of LPS in recombinant EC2 proteins (determined by using a LAL Chromogenic Endotoxin Quantitation kit (Pierce). X refers to detergent treated proteins to reduce LPS concentration in EC2 proteins. This experiment was performed by John Palmer from our research group (J. Palmer, personal communication).

The effect of GST-EC2 recombinant proteins on overall cell number was examined by using the SRB assay (Skehan et al., 1990). Preliminary experiments revealed that this assay gave a linear correlation between the optical density and cell number. The experiments were performed in order to evaluate any possible anti-proliferative or cytotoxic effect of these proteins. Cells were treated with EC2 proteins for 1hr, and then washed and cultured for 16 hr in EC2-free medium. Alternatively, cells were incubated for 72hr in the presence of EC2 proteins. Interestingly, no effects were noted in cells pre-treated with EC2 compared to untreated cells, which indicates that the effects of GST-EC2s on *B.t*-induced MNGC formation are not due to anti-proliferative or cytotoxic activity. However, a longer incubation resulted in a significant reduction in cell number at higher concentrations, thus GST-EC2 proteins are likely to promote time- and dose-dependent anti-proliferative and/or cytotoxic activities or may affect cell adhesion. That was in contrast with the result that showed no effect of a long incubation with GST-CD9 and GST-CD63 proteins on the number of primary human monocytes. Also no effects on cell adhesion and aggregation were observed in that study (Parthasarathy et al 2009). Recent work in our group showed no effects of CD9, CD63, CD81 or CD151 on the adhesion of RBL2H3 cells treated overnight with the proteins (J. Palmer, PhD thesis University of Sheffield 2016).

Since GST-EC2CD9 showed inhibitory effects on *B.t*-induced cells fusion, the effects of EC2CD9 mutants on *B.t*-induced fusion were examined. GST-EC2CD9 proteins containing mutations at cysteine 153 (cysteine to alanine) and cysteine 152 (cysteine to alanine) were investigated. These mutants have been described previously (Higginbottom et al 2003) and are thought to be important for EC2 disulphide bond formation and conformation, as these mutants are not recognised by conformation-dependent antibodies. Interestingly, the GSTEC2CD9 mutants showed a significant decrease in fusion index but no effect on MNGC

size in cells infected with *B.t* CDC272, whereas no effect for these proteins observed in cells infected with *B.t* E264. Previous data showed that Cys152 and Cys153 mutated EC2 proteins can slightly inhibit sperm/oocyte fusion (Higginbottom et al., 2003), and the Cys153 mutation appeared to also have some inhibitory effect on Con A-induced cell fusion (Parthasarathy et al., 2009). These effects indicate that regions outside of the variable subloop region of CD9EC2 may be involved in the cell fusion process. Notably Higginbottom and co-workers showed that these mutants were unable to inhibit sperm/oocyte binding as strongly as wild type CD9EC2, demonstrating the importance of folding correct of CD9 EC2 in this process (Higginbottom et al., 2003).

We also attempted to identify the effective region of the EC2 CD9 protein that might promote cell fusion induced by *B.thailandensis* using short synthetic CD9-derived peptides. From preliminary data, none of the peptides tested had any effects on *B.t* E264-induced cell fusion. However, effects were observed with *B.t* CDC-infected cells or when peptides were incubated with cells after infection overnight (data not shown). We suggest that more effort should be attempted in these experiments, for example by using different concentrations of these peptides. These peptides have been shown to significantly reduce meningococcal and other bacterial pathogen adherence to an endometrial epithelial cell line (Daniel Cozens, personal communication) and *S. aureus* adhesion to human keratinocytes and a 3D model of human skin (Ventress et al., submitted to Journal of Infectious Disease).

4.3.3 Effects of tetraspanins on B.t uptake

Several studies indicate a role for tetraspanins in bacterial adhesion and entry into host cells, as discussed in more detail in Chapter 1. To investigate the role of tetraspanins in bacterial infection was also of interest to our research group. By utilizing anti-tetraspanin antibodies, EC2 proteins and gene knockdown by siRNA, the role of tetraspanins in bacterial attachment and entry has been demonstrated. Green and co-workers showed an inhibitory effect of anti tetraspanin CD9, CD63 and CD151 but not CD81 antibodies on bacterial adhesion to epithelial cells including adhesion of *Neisseria meningitides, Staphylococcus aureus and Escherichia coli* (Green et al., 2011). Previous and recent data from our group also showed a role for tetraspanins in Salmonella infection. Tetraspanins CD9, CD63, CD37 and CD151 have been shown to be involved in *Salmonella typhimurium* infection of human monocyte-derived macrophages at different stages (Noha Hassuna, PhD thesis 2010). A more recent finding showed that anti-CD9 and anti-CD81 antibodies inhibited *S. typhimurium* uptake by J774 cells whilst anti CD63 antibody had a slight effect. These effects seem to be cell line-dependent as anti-CD63, anti-CD81 and anti-CD151 showed a significant reduction in the bacterial infection in PMA-stimulated THP-1 cells with an insignificant effect for anti-CD9 (Fawwaz Ali personal communication). Recombinant CD9EC2 protein and short synthetic peptides mimicking CD9EC2 showed significant inhibitory effects on the adhesion of several bacterial isolates including meningococcal bacteria to human cells (Daniel Cozen, personal communication). The CD9-EC2 and peptides also inhibit *S.aureus* adhesion to human keratinocytes and a human skin model (Ventress et al., submitted to the Journal of Infectious Disease). In addition, anti tetraspanin CD9 and CD81 antibodies significantly inhibited the adhesion of *Pseudomonas earuoginosa* on U937 and HaCaT cell lines respectively (Jehan Alrahimi, personal communication). Based on these findings the effects of tetraspanin reagents on *B.t* uptake were examined.

Since the anti-tetraspanin antibodies and recombinant EC2 protein affected *B.t*-induced MNGC formation, the question was whether these finding was as a consequence of their effects on *B.t* uptake, resulting in the enhancement or the reduction in MNGC formation. The effect of pre-treatment of these reagents on cells infected at MOI 3:1 was examined, which were the same conditions used in the MNGC formation assays. There was a slight decrease in uptake of *B.t* CDC272 in anti-CD9 and anti-CD81-treated J774 cells relative to non-treated cells, but that was not significant compared to the effects of the isotype controls. In addition a slight increased invasion rate was observed in cell pre-treated with CD9EC2 protein. This suggests that the tetraspanins CD9 and CD81 (under these experimental conditions) are involved in *B.t*-induced cells fusion at the stage where MNGCs are produced, rather than the initial infection.

Chapter 5

Effects of CD9 deletion and CD82 deletion on *Burkholderia thailandensis*-induced multinucleated giant cell formation

5.1 Introduction

Results described in the previous chapter showed clearly that tetraspanin CD9 is involved in *Burkholderia thailandensis*-induced cell fusion and multinucleated giant cell formation. To gain insight into the role of CD9 in bacterial-induced cell fusion, the MNGC formation assay was performed using macrophage cell lines derived from CD9 knockout mice and corresponding wild type mice. The CD9 knockout mice were generated by Le Naour and co-workers. Briefly, the CD9 gene was disrupted by gene targeting in embryonic stem cells; the promoter and exon 1 were replaced by the neomycin resistance gene and the knock-out was confirmed at the DNA level by Southern blotting and cells from knockout mice showed no expression of CD9 by flow cytometry and immunohistology (Le Naour et al., 2000). CD9^{-/-} and wild-type macrophage cell lines were kindly provided by Dr. Gabriela Dveksler, Dept. Pathology, Uniformed Services University of Health Sciences, Bethesda, MD, US. The macrophage cell lines were derived from the CD9 knock-out or wild type mice by retroviral transformation of bone marrow-derived macrophages. These cells had been used in an investigation of the function of pregnancy-specific glycoprotein (PSG) and its association with CD9 (Ha et al., 2005). An attempt was made by a previous researcher in our group to induce MNGC formation in these cells using Con A and cytokine TNF-α; however no cell fusion from CD9WT and CD9KO cells was observed (Parthasarathy PhD thesis, University of Sheffield, 2005). Therefore, to take advantage of these cell lines, MNGC formation assays were performed using *B.thailandensis*.

CD82, also known as KAII, is a member of the tetraspanin superfamily that has been shown to be involved in a wide range of cell functions including cell dynamics and signalling (more details in Chapter 1). CD82 interacts with cell surface molecules including other tetraspanins, integrins, chemokine receptors and growth factor receptors; these interactions have been implicated in processes such as metastasis suppression (Sridhar and Miranti, 2006, Miranti, 2009). Since CD82 is involved in processes that affect cell fusion such as cell adhesion and migration, we hypothesised a possible role for CD82 in MNGC formation induced by *B.thailandensis*.

The CD82 gene has been disrupted using the recombination and cre-loxP deletion technique and the final recombination plasmid was then used for targeting embryonic stem cells, and by selective breeding CD82 null mice were obtained. CD82 knockout was confirmed by immunoblotting, immunohistochemistry, PCR, and qPCR (Risinger et al., 2014, Wei et al., 2014). Macrophage cell lines from CD82 -/- and corresponding wild type mice were kindly provided by Professor Jatin Vyas (Harvard University) for these studies. CD82 macrophage and corresponding wild type cell lines were also generated from bone marrow-derived macrophages by retroviral transformation (Jatin Vyas, personal communication).

5.1.1 Tetraspanin deficiency studies

The influence of gene disruption has been investigated for several tetraspanins, which have revealed tetraspanin functions and interactions in vivo, despite tetraspanin mutations resulting in few detectable abnormal phenotypes.

Although there was no obvious abnormal phenotype in CD63 null mice, CD63 deficiency was associated with altered water balance and kidney impairment (Schroder et al., 2009). The CD151-null mice exhibit varying phenotypes, with some mice developing glomerular kidney disease, depending on the mouse strain used to generate the knock-out (Baleato, RM et al 2008). Mutation of CD151 is also associated with renal disease in humans (Karamatic Crew et al, 2004). An absence of CD151 in mice also causes a minor abnormality in haemostasis, an increase in bleeding times and re-bleeding occurrences and also defects in wound healing due to poor migration of keratinocytes. In addition, mitogenic-stimulated CD151$^{-/-}$ T lymphocytes exhibit abnormal proliferative rates (Wright et al., 2004, Cowin et al., 2006). CD151-null mice also showed a reduction in cancer metastasis that is likely due to impaired tumour-endothelial interactions, and disorders in extracellular matrix production in mouse lung endothelial cell (Takeda et al., 2011).

CD37 lacking mice showed poor T-cell dependent antibody responses to antigen or viral infection; however this defect can be recovered by antigen-adjuvant administration (Knobeloch et al., 2000). CD81 null mice exhibited an increased number of microglia and astrocytes and subsequently an increase in brain size and weight, which demonstrated a role for CD81 in the regulation of proliferation of these cells (Geisert et al., 2002). Studying the effects of Tetraspanin 32 (Tssc6) deletion reveals the role of this tetraspanin in T-lymphocyte proliferation (Tarrant et al., 2002). As previously described in Chapter 1, CD9-defficient mouse studies indicated precise information about CD9 functional properties; CD9 was shown to be essential for fertilization as knockout mouse females displayed a severe inhibition of fertility due to defects in sperm-egg fusion (Le Naour et al., 2000). Alveolar macrophages and bone marrow cells derived from mice lacking CD9 formed large number of MNGC compared to those of wild-type (Takeda et al., 2003). Abnormal muscle regeneration with formation of large giant myofibres were found in mice lacking either CD9 or CD81; this data suggested that CD9 and CD81 control the regeneration of normal muscle (Charrin et al., 2013). CD81 knock-out also causes reduced fertility in female mice and CD9/CD81 double knockout mice are completely infertile (Rubinstein et al., 2006). Also CD9/CD81 double knockout show spontaneous MNGC formation in vivo and increased osteoclastogenesis (Takeda et al., 2003). Despite CD82 deficient mice exhibiting no phenotype abnormalities, gene ontology analysis revealed that the genes related to immune response, cell adhesion, proliferation and mitosis were those whose expression was most changed in the knock out animals (Risinger, Custer et al. 2014). Also recent data showed that CD82 knock-out mice have increased angiogenic responses, likely due to increased expression of adhesion-related molecules including CD44 (Wei et al., 2014).

5.1.2 Cell surface molecules involved in cell fusion processes

As mentioned previously in Chapters 1 and 4, a number of other cell surface molecules have been implicated MNGC formation. The properties of the proteins studied in this Chapter are described in more detail below.

5.1.2.1 CD36

CD36 is a membrane glycoprotein known as a member of the class B scavenger receptor family. CD36 is expressed on many cell types including monocytes (Talle et al., 1983), blood platelets and microvasculature endothelial cells (Swerlick et al., 1992). The main feature of CD36 is its capacity to recognize and bind to various ligands including bacterial lipopeptides, *Plasmodium falciparum* parasitized erythrocytes (PEs), oxidized low density lipoprotein (ox LDL), collagen and fatty acids (Moore and Freeman, 2006). Therefore CD36 has been implicated in immunity, lipid metabolism and angiogenesis (Silverstein and Febbraio, 2009). CD36 mediates the phagocytosis of *P.falciparum* and is thought to be involved in malaria clearance (McGilvray et al., 2000). In addition, CD36 functions as a phagocytic receptor for both gram-positive and gram-negative bacteria including *Salmonella typhimurium*, *Staphylococcus aureus, Klebsiella pneumoniae* and *Escherichia coli* (Baranova et al., 2008). CD36 is also involved in HIV-1 dissemination as anti-CD36 mAb block release of HIV from macrophages and virus transmission to CD4^{+} cells (Berre et al., 2013). Macrophage CD36 mediates the binding and internalization of ox LDL and thus contributes to foam cell formation and atherosclerotic plaques (Podrez et al., 2000, Febbraio et al., 2000). CD36 promotes apoptotic cell removal by macrophages by recognizing and binding to phosphatidylserine (PS) expressed on apoptotic cells (Ren et al., 1995). A role for CD36 in cell fusion has been demonstrated. Helming and co-workers showed that CD36 promotes cytokine-induced macrophage fusion; anti-CD36 antibodies significantly inhibited IL-4/GM-CSF-induced murine macrophage fusion. Cell fusion was also strongly impaired in macrophages from CD36KO compared to that of CD36WT mice. Although CD36 surface expression showed no change after IL-4 stimulation, CD36 was localized in the cell-cell contact zones, however M-CSF/RANKL-induced osteoclasts was not affected by anti-CD36 antibodies or CD36KO, thus CD36 seems to selectively contribute to MNGC formation but not osteoclastogenesis (Helming et al., 2009). CD36 recognises the lipid, phosphatidylserine (PS), which is transiently expressed on the membrane of fusing cells, Helming and co-workers showed that masking PS also blocked fusion and so hypothesised that the role of CD36 in fusion related to recognition of PS. Similarly, masking of CD36 prevented fusion of embryonic stem cells with microglial cells and neurones (Cusulin et al., 2012)

Recently CD36 has been shown to be involved in myoblast fusion during myogenic differentiation. The expression of CD36 was significantly up-regulated during myoblast differentiation and it was localized in multinucleated myotubes. CD36 knockdown markedly inhibited myotube formation suggesting that CD36 is essential for myogenic differentiation (Park et al., 2012).

CD36 is implicated in *Mycobacterium tuberculosis* infection. CD36 deficiency resulted in resistance to the infection in vivo and in vitro models. CD36 null mice showed a decrease in mycobacterial load in liver and spleen compared with wild-type animals, as well as reduction in granuloma formation which promotes bacterial dissemination. Mycobacterial growth and survival was also reduced in CD36KO macrophages (Hawkes et al., 2010).

5.1.2.2 CD44

CD44 is a transmembrane glycoprotein expressed broadly on a variety of cell types and exists as various isoforms. CD44 is implicated in a number of physiological and pathological processes such as cell-cell and cell-substrate adhesion. Several studies showed the involvement of CD44 in infectious disease and the inflammatory response; CD44 promotes

E.coli infection of the murine urinary tract, as CD44 deficient mice showed a decrease in *E.coli* intracellular proliferation (Rouschop et al., 2006). CD44 deficiency was also associated with reduction in proliferation and dissemination of *Klebsiella pneumoniae* accompanied by increased lung inflammation (van der Windt et al., 2010). In *Mycobacterium tuberculosis* it has been demonstrated that CD44 promotes bacterial phagocytosis, macrophage recruitment and immune response to pulmonary tuberculosis. The average number of bacteria binding and uptake by CD44 deficient macrophages was lower compared with wild-type and granuloma formation was reduced in CD44-/- mice (Leemans et al., 2003). In contrast, in *Cryptosporidium parvum* infection (an intracellular parasite), CD44 deficient mice showed increases in the number and size of granulomas formed after the infection compared to wild-type (Schmits et al., 1997).

CD44 has also been implicated in cell fusion including osteoclast and multinucleated giant cell formation. Sterling and co-workers reported that CD44 controls macrophage fusion as CD44 expression was up-regulated by macrophages under fusogenic conditions in vivo and in vitro. CD44 ligands strongly inhibited macrophage fusion and multinucleated giant cell formation and it was also reported that the recombinant extracellular domain of CD44 prevents macrophage fusion by interacting with a cell-surface binding site (Sterling et al., 1998). Kania and co-workers reported that monoclonal antibodies to CD44 inhibit osteoclast formation in a dose and time-dependent manner by blocking the development of osteoclast progenitor cells, and that this might due to cross-linking of CD44 molecules as Fab monomer fragments showed no effect on this process (Kania et al., 1997). CD44 associated with its ligand osteopontin (OPN, a glycoprotein that regulates mineral crystal growth) in osteoclast formation. Strong expression of CD44-OPN complexes was seen in processes including filopodia and pseudopodia during osteoclast formation; these processes were reduced and cell fusion was blocked in CD44 -/- and OPN -/- mice which suggested the involvement of CD44 in processes leading to cell fusion (Suzuki et al., 2002). CD44 has also been shown to be essential for the formation of multinucleated myofibers. CD44 deficiency delays muscle regeneration in vivo and myoblast fusion in vitro. This defect is linked with the negative effects of CD44 deletion on myoblast chemotaxis response and cell migration, which is thought to be essential for the fusion (Mylona et al., 2006).

In contrast with these finding, Vries and co-workers showed that the role of CD44 in fusion might be relate to the microenvironment of osteoclast formation. The effect of CD44 deficiency was investigated under three conditions: in vivo by analysis of the osteoclast formation in bones from CD44KO and wild-type mice and in vitro using bone marrow cells from CD44KO and wild-type on plastic or on bone. There was a significant increase in multinucleated osteoclast formation in CD44KO cells, however on bone and in vitro CD44 deficiency has no effect (de Vries et al., 2005).

5.1.2.3 CD47 and CD172a

CD47, an integrin-associated protein (IAP), is a transmembrane glycoprotein that belongs to the immunoglobulin superfamily and acts as a regulator of integrin function (Oldenborg, 2013). CD47 is reported to be important for macrophage fusion and multinucleation as monoclonal antibodies and a recombinant protein corresponding to the CD47 extracellular domain inhibit macrophage fusion and MNGC formation (Han et al., 2000). CD47 acts as a ligand for CD172a (also called macrophage fusion receptor MFR, signal regulator protein α SIRPα); a transmembrane glycoprotein which belongs to the immunoglobulin superfamily and its role in macrophage fusion has been reported (Saginario et al., 1998). CD47-CD172a

interaction promotes macrophage fusion processes (Han et al., 2000). One of proposed mechanisms of macrophage fusion has been constructed based upon the interaction between these proteins. First CD47 interacts with a long form of CD172a (via the amino-terminal immunoglobulin variable domain IgV loop) which stabilizes plasma membranes. Other molecules such as CD44 might be also associated with CD172a at this stage. Then the interaction of CD47 with the short form of CD172a brings the opposing plasma membranes to be close enough (down to 5-10 nm) to undergo fusion (Han et al., 2000, Saginario et al., 1998). This finding is supported by recent data reporting the involvement of the interaction of CD47 with its receptor CD172a in osteoclast formation. Koskinen and co-workers have reported that CD47 deficiency inhibits stromal cell CD172a signalling and thus impairs stromal cell differentiation and osteoclast formation (Koskinen et al., 2013).
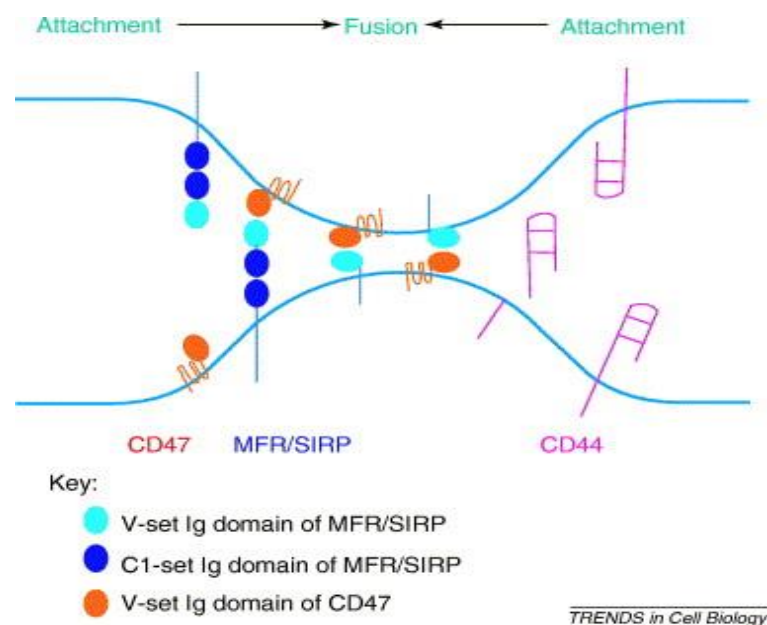
Figure 5.1.1 Hypothetical mechanism for homoptypic fusion of macrophage. Macrophage-macrophage adhesion is mediated by binding of MFR (CD172a) to CD47. Initial association with the long form of MFR followed by association with the short form (MFR-s, lacking 2 membrane proximal Ig domains) with CD47 reduces the distance between the plasma membranes. The distance could be reduced further to 5–10 nm if MFR-s and CD47 bend upon binding. Shedding of the extracellular domain of CD44 might facilitate closer interaction and fusion. Image courtesy of (Vignery, 2005).

5.1.2.4 CD98

CD98 is a type II transmembrane protein with a large, heavily glycosylated extracellular domain, and a short transmembrane domain and cytoplasmic tail. CD98 (also known as fusion regulatory protein-1 or FRP-1) has been implicated in adaptive immunity and cancer (reviewed by(Cantor and Ginsberg, 2012)). Monoclonal antibodies to CD98 induced MNGC formation in vitro without any other trigger of cell fusion, suggesting that MNGC formation might be induced in vivo by the interaction between FRP-1 and its ligand (Tabata et al.,

1994, Higuchi et al., 1998, Ohgimoto et al., 1995). Anti-CD98 mAbs also enhanced MNGC formation in HIV gp160 gene-transfected CD4⁺ U937 cell line (Ohgimoto et al., 1995). It has been reported that CD98 is expressed on the surface of eggs as part of a "tetraspanin web" that includes tetraspanins CD9 and CD81, ADAM 3 and integrins that promote sperm-egg adhesion and fusion (Takahashi et al., 2001).

5.1.2.5 DC-STAMP

DC-STAMP (dendritic cell-specific transmembrane protein) is a seven-transmembrane domain-containing protein originally identified in human monocyte-derived dendritic cells (Hartgers et al., 2000). It has been reported that DC-STAMP is critically involved in osteoclastogenesis. The expression of DC STAMP is upregulated in RANKL-stimulated cells and siRNA and specific antibody to DC-STAMP suppressed osteoclast formation, whereas DC-STAMP over expression enhanced RANKL-induced multinucleation of osteoclasts (Kukita et al., 2004). In DC-STAMP-deficient mice the osteoclast fusion and foreign body giant cell formation were abrogated, and this was restored by retroviral introduction of DC-STAMP (Yagi et al., 2005). Mensah and co-workers reported that DC-STAMP is internalized in some RANKL-stimulated osteoclasts precursors (DC-STAMP^{lo}), which following interaction with DC-STAMP ligand became "master fusogens". By contrast, cells that had not internalised DC-STAMP (DC-STAMP^{hi}) acted only as mononuclear donors. Interestingly gene expression analysis showed that the transcript levels of CD9 and CD47 were unregulated in the DC-STAMP^{lo} cells, whereas the levels of CD44 and CD172a were higher in DC-STAMP^{hi}. These findings suggested the possibility of the involvement of these molecules in DC-STAMP mediated osteoclast fusion (Mensah et al., 2010).

5.2 Aims of work in this Chapter

In this chapter the effects of CD9 and CD82 deletion on *B.thailandensis*-induced MNGC formation was investigated. Initially the loss of CD9 expression on CD9KO macrophages was confirmed by FACS analysis, immunoblotting and immunofluorescence microscopy. However, because anti-mouse antibodies to CD82 are not available, the loss of CD82 expression on CD82KO cells could not be confirmed in this study. To start with, the ability of *B.thailandensis* to invade these cells and promote cell fusion was investigated. A time course experiment was performed to determine the influence of CD9-deficiency on *B.thailandensis* -induced cell fusion.

As described previously, it is well known that tetraspanins act as membrane organizers, interacting with another membrane molecules including tetraspanins and forming TEM web. The possibility that the absence of one of the tetraspanins might affect the expression of other partners, especially those who have been involved in cells fusion, an event that is organized by cell membrane molecules was considered. Therefore the expression level of other molecules on CD9-/- and CD82-/- was investigated by FACS analysis, and for further investigation the effect of CD9 gene disruption on gene expression profile was examined by microarray analysis.

5.3 Results

5.3.1 Expression of CD9 on CD9 WT and CD9KO cells by flow cytometry

Initially CD9 expression level on CD9-deficient cells was compared with that on CD9 wild-type cells by flow cytometry as described in 2.2.3.2.1 There was a significant different in CD9 expression level in between wild type and CD9 KO cells. The results showed that about 80% wild type cells are highly expressing CD9. The mean of normalized median florescent intensity was 6.28±0.542 and 1.83±0.057 in wild type and CD9-/- respectively. Unexpectedly, about 2-7% of CD9KO cells showed a positive expression for CD9. Therefore further examination was required to confirm the loss of CD9 expression on CD9-/- macrophages (Figure 5.3.1).

A   B

C   D
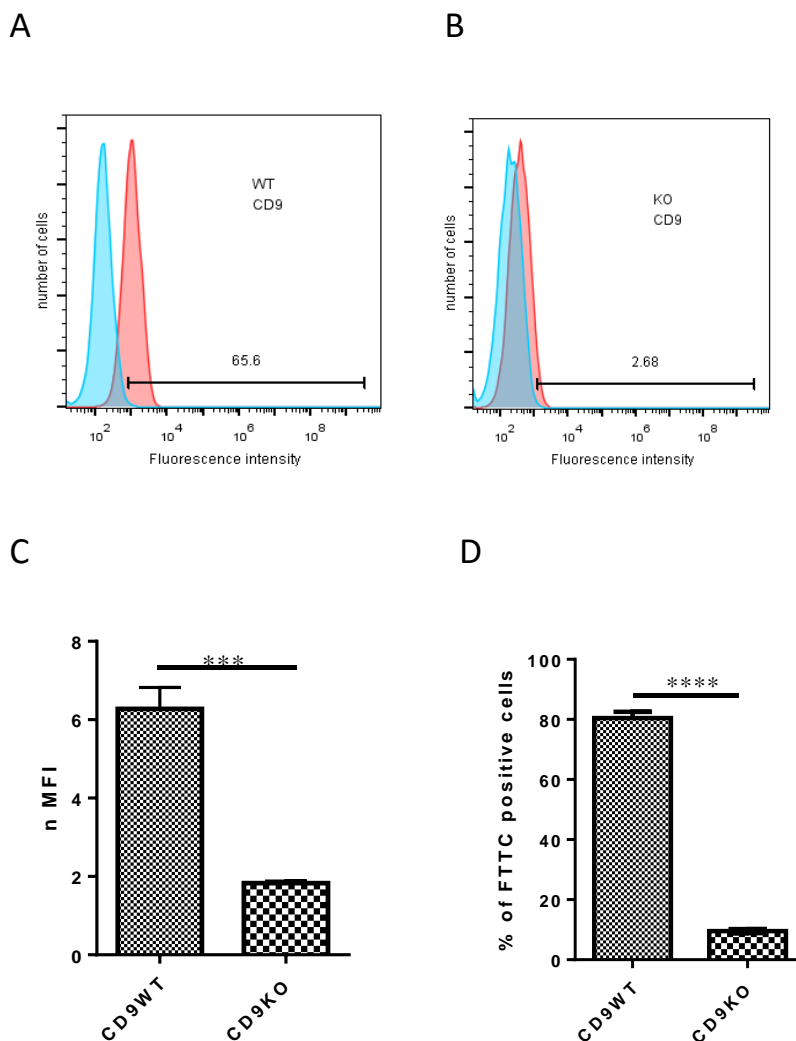
Figure 5.3.1 Expression of CD9 on CD9WT and CD9KO cells by flow cytometry. Cells were analysed using primary rat anti-mouse CD9, isotype control (rat IgG2a) and secondary anti-rat IgG-FITC. (A)(B) The overlying histogram of fluorescence intensity of CD9 on CD9WT and CD9KO cells respectively. (C) The normalized median fluorescence intensity of CD9 on CD9 KO cells compared to that on CD9WT cells. (D) Shows the percentage of positive cells in CD9KO cells compared to CD9WT cells. The experiment performed three time in duplicate and the significant was determined by using unpaired t test where ***significant at P<

0.001. n MFI= MFI of sample/ MFI of isotype control . % of positive cells = % of positive in sample - % of positive in the isotype control.

5.3.2 Confirmation of the loss CD9 expression on CD9-/- macrophages by immunofluorescence microscopy.

Since the flow cytometry experiment appeared to show slight positive expression of CD9 on CD9KO cells, immunofluorescence microscopy was used to determine the expression of CD9 on CD9KO cells and to compare that with its expression on CD9WT cell as described in 2.2.3.1. Images in Figure 4.4.2 showed the positive expression for CD9 on CD9WT, whereas no signal for CD9 stain was observed on CD9KO cells.
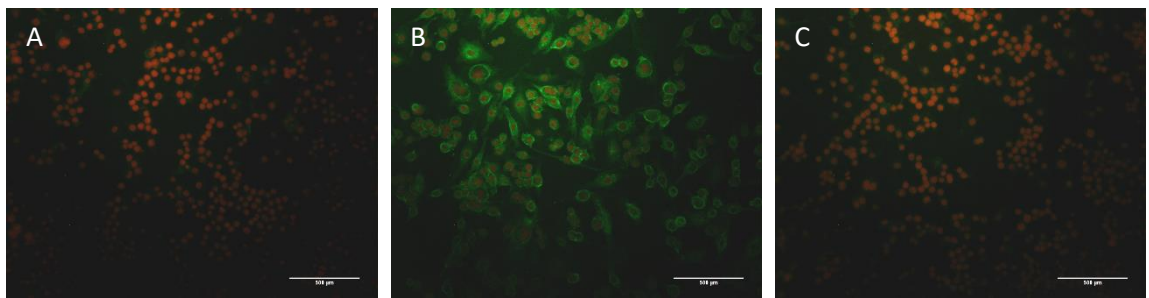
Figure 5.3.2 Immunofluorescence microscopy of CD9WT and CD9KO cells. Cells were cultured overnight in Lab-Tek™ chamber slides, then fixed and stained as described in 2.2.3.1. (A) Isotype control, (B) CD9WT cells. C CD9KO cells 20. The images were captured with a Nikon Eclipse E400 immunofluorescence microscope using 20X objective.

5.3.3 Western blot confirmed the loss of CD9 expression

CD9 deficiency was also confirmed by immunoblotting as described in 2.2.6 and 2.2.7. The result indicated a complete loss of CD9 protein expression on CD9KO cells with highly CD9 expression level on wild-type cells figure (5.3.3). The apparent low expression of CD9 on the CD9-/- cells observed in flow cytometry may have been due to slightly higher non-specific binding of the anti CD9 antibody relative to the isotype control.
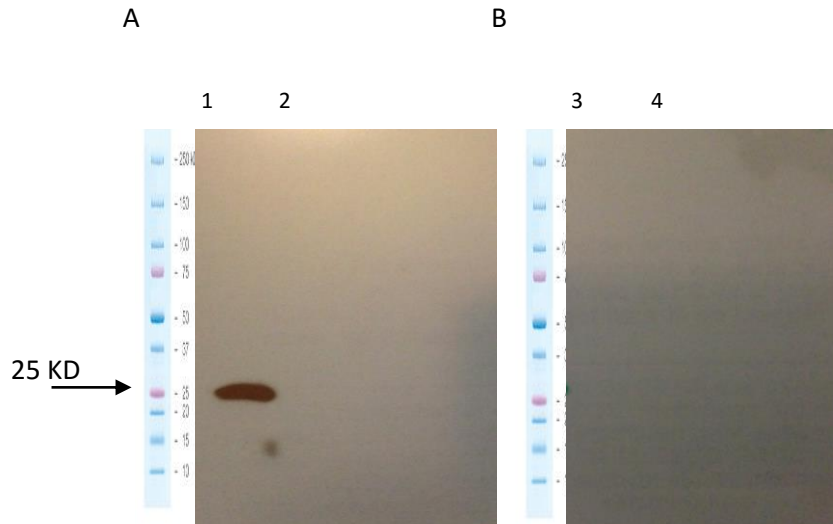
Figure 5.3.3 Western blot analysis of CD9WT and CD9KO cells. Proteins present in whole cell lysates were separated by SDS-PAGE, transferred to nitrocellulose membrane and then incubated with antibodies as described in 2.2.7. 1 and 3 lysates from CD9 wild type cells and 2 and 4 lysates from CD9 knock-out cells. (A) probed with anti-CD9 and (B) probed with isotype control.

5.3.4 Evaluation of intracellular *B.thailandensis* at different times of infection

To start with, the ability of *B.thailandensis* to infect and survive within CD9 deficient cell line (CD9KO) and in its corresponding wild type cells line (CD9WT) was investigated. Numbers of intracellular *B.thailandensis* CDC272were assessed in CD9WT and CD9KO cells at different time points after infection using kanamycin protection assay. The results showed that there was a significant difference in intracellular CDC272 in CD9KO compared to CD9WT cells after 30 and 60 min post infection. This difference was not significant after 90 and 120 min post infection. Therefore, the time of 120 min was chosen for carrying out MNGC formation assay in CD9WT and CD9KO cells. This is in line with the observation with J774 where anti CD9 antibodies showed no significant effect on B.t uptake after 2hr post infection (figure 5.3.4).
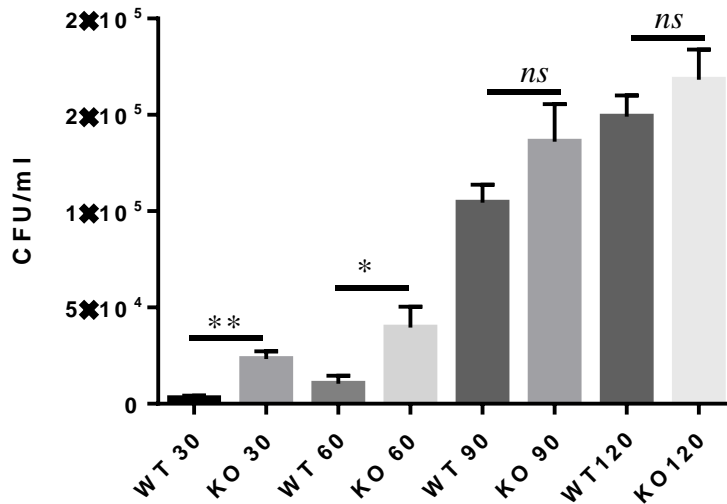
Figure 5.3.4 B.thailandensis uptake by mouse macrophage CD9WT and CD9KO cells. The number of intracellular bacteria was estimated at different time points as described in (2.2.10.1). The experiment was performed twice in duplicate. Significance of differences was tested by unpaired t test P<0.05.

5.3.5 Effect of CD9 deficiency on giant cell formation induced by *Burkholderia thailandensis*.

To investigate the effect of CD9knockout on *B.t*-induced cell fusion a MNGC formation assay was performed as described in 2.2.10.2.

5.3.5.1 Enhanced MNGC formation in CD9 KO mouse macrophage cell line

A considerably earlier onset of MNGC formation was noted in CD9 knockout cells (after approximately 4hr post infection) compared to CD9 wild type cells (figure 5.3.5 A). After 14hr post infection 60-80% of CD9KO cells were a part of MNGC, which was sevenfold more than those of CD9WT cells. Also, the size of these MNGCs was higher in CD9KO cells than CD9WT cells, which increased about threefold and sixfold in E264 and CDC272-infected cells, respectively (figure 5.3.5 B).

A

B
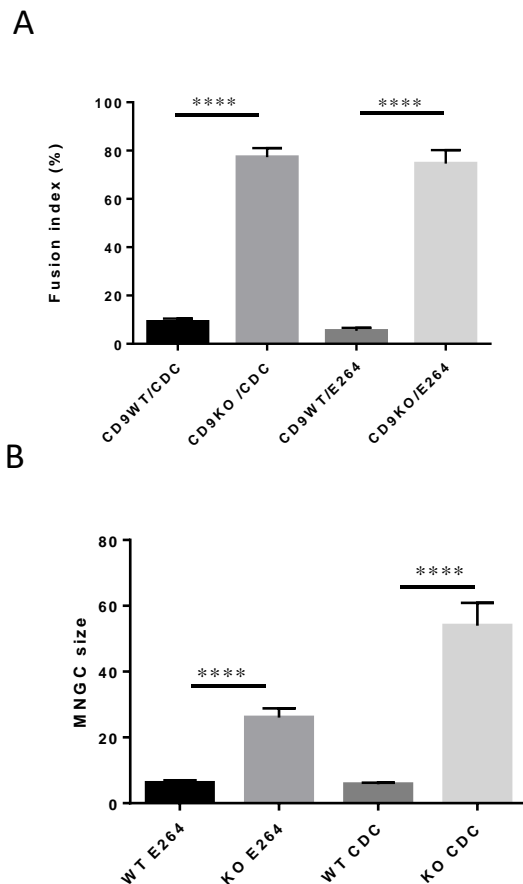
Figure 5.3.5 MNGC formation in macrophage CD9WT and CD9KO cells induced by *B.thailandensis*. Cells were cultured overnight in 24 well plates and then infected with CDC272 or E264 at MOI 3:1 as described in 2.2.11.2. MNGC formation was determined at 14 hr post infection. Cells were fixed and stained with Giemsa. The fusion index (A) and MNGC size (B) were assessed in 10 fields of view as described in 2.2.6.3.The experiment was done three times in duplicate. Significance of differences was tested by unpaired t test $P<0.05$.

5.3.5.2 The progress of MNGC formation is affected by CD9 deletion

Since the deletion of CD9 showed a considerable effect on *B.thailandensis* -induced MNGC formation, a time-course experiment was performed to track MNGC formation in CD9WT and CD9KO cells during the 23hr post infection period. At various time points post-infection, cells were fixed, stained and MNGC formation was assessed as before. Results in figure 5.3.6 A showed that after about 8hr more than 10% of CD9KO cells were part of MNGC, whereas less than 5% of CD9WT cells formed MNGC. A dramatic increase in MNGC formation was noted in CD9KO cells after 11hr post infection, and there was a significant difference in fusion index within CD9KO cells (60-80%) compared with that of wild type cells (about 10-15%) after 14 hr post infection. After 23 hr post infection more than 90% of CD9KO cells formed MNGC and less than 89% of CD9WT cells fused. At this stage there was no difference noted between CD9KO and CD9WT which were infected with CDC272; however the differences in MNGC formation was still significant between E264-infected cells. With regard to MNGC size in figure 5.3.6 B, CD9KO cells showed larger MNGC

compared with CD9WT cells. At 19 hr post infection an average of about 40 and 80 nuclei were present within CD9KO MNGC infected with E264 and CDC, respectively, with fewer in wild type MNGC (20 and 30 nuclei within E264 and CDC-infected cells, respectively).
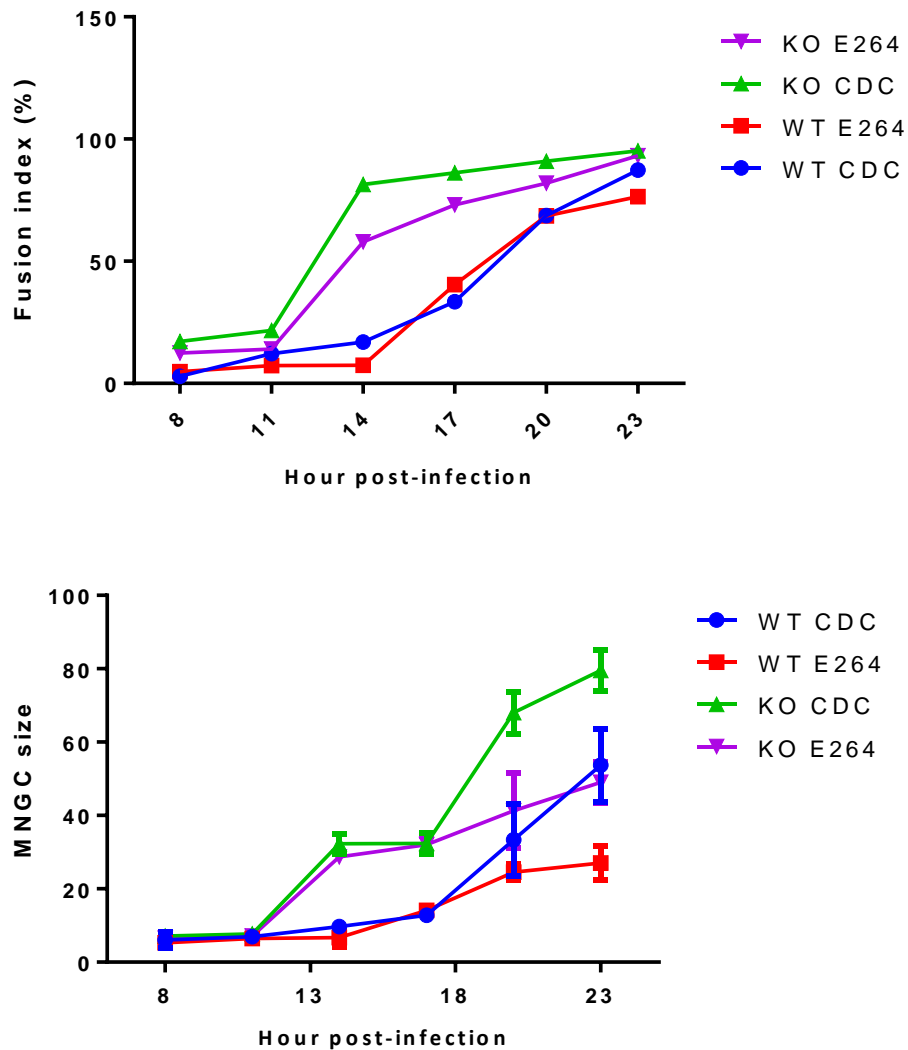
Figure 5.2.7 Progress of MNGC formation CD9WT and CD9KO macrophages induced by _B.thailandensis_. Cells were cultured overnight in 24 well plates and infected with CDC272 or E264 at MOI 1:1 as described in 2.2.10.2. MNGC formation was determined at various times post infection. Cells were fixed and stained with Giemsa. Fusion index (A) and MNGC size (B) were assessed in 10 fields of view as described in 2.2.10.3.

5.2.7 The expression levels of tetraspanins CD81 and CD63 markedly decrease upon CD9 deletion.

CD9 has been described as a cell membrane organiser and its interaction with tetraspanins and other molecules are involved in various cell functions. We therefore speculated that the disruption of the CD9 gene might affect the expression level of other partner molecules, which might be relevant to the mechanism by which CD9 deletion enhances macrophage fusion.

We started to examine whether deletion of CD9 affects the expression of tetraspanins CD81 and CD63, well-known CD9 tetraspanin partners. Initially their expression on CD9KO cells were compared with that on wild-type cells using immunofluorescence microscopy as described in 2.2.3.1 and FACS analysis technique as described in 2.2.3.2.2. Images in Figure 5.3.7 showed that the expression level of CD63 and CD81 was lower in CD9KO cells compared to their expression in CD9WT cells. However, poor staining was obtained with CD81 that might be due to the effect of the fixation on the CD81 epitope. Accordingly, flow cytometry analysis was performed to confirm the result, where all the staining process could be applied on live cells. Data obtained from the FACS analysis were normalized according to the appropriate isotype control in each experiment. The results revealed that CD81 expression was significantly decreased in CD9KO cells compared to that on wild type: the normalized median florescence intensity declined from 14.47±0.32 to 6.21±0.28 respectively (Figure 5.3.8). In both cell lines poor signals were detected for CD63 on the cell surface; however there was a small but significant decrease in cell surface CD63 expression in CD9KO compared to wild type cells (mean of nMFI 1.65±0.094 and 1.26±0.0219, respectively).

To determine the extracellular and intracellular expression of CD63, the experiment was performed using fixed and permeabilized cells as described in 2.2.3.2.2. The analysis revealed that the total expression of CD63 decreased on CD9KO relative to wild type (mean of nMFI 7.21±1.311 and 4.16±0.905, respectively), but this was not significant at p<0.05. (Figure 5.3.9).
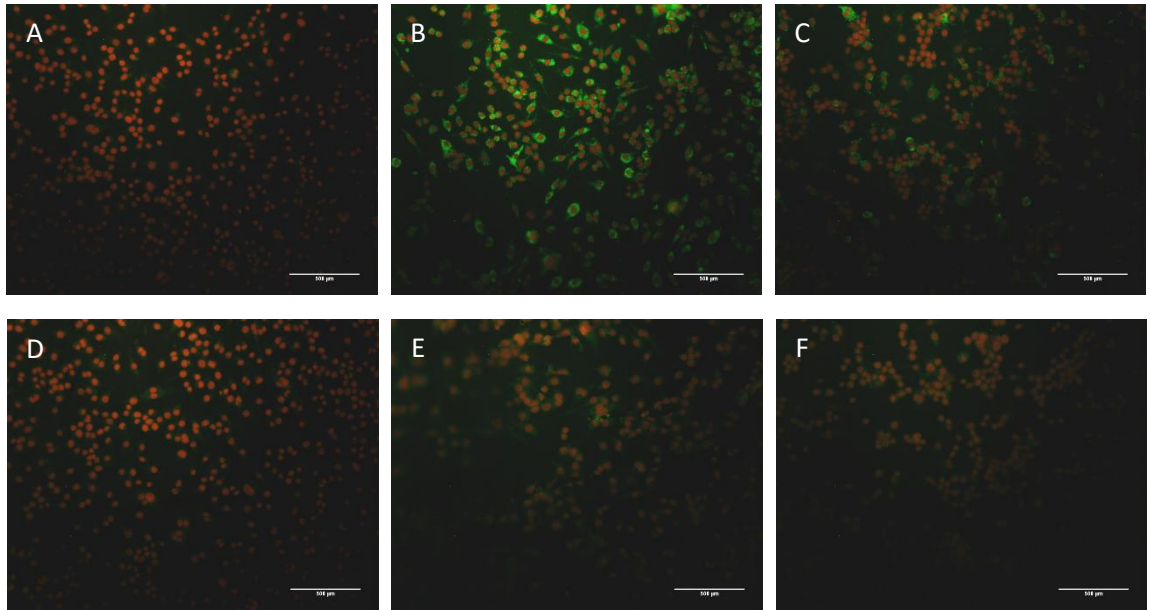
Figure 5.3.7 Effect of CD9 deletion on the expression level of CD63 and CD81. Cells were cultured overnight in Lab-Tek™ chamber slides. The cells were fixed and stained as described above using appropriate tetraspanin-specific antibodies or matched isotype controls. A and D isotype controls. B and C CD63 in CD9WT and CD9KO respectively. E and F CD81 on CD9WT and CD9KO respectively. The images were captured with a Nikon Eclipse E400 immunofluorescence microscope using 20X objective.
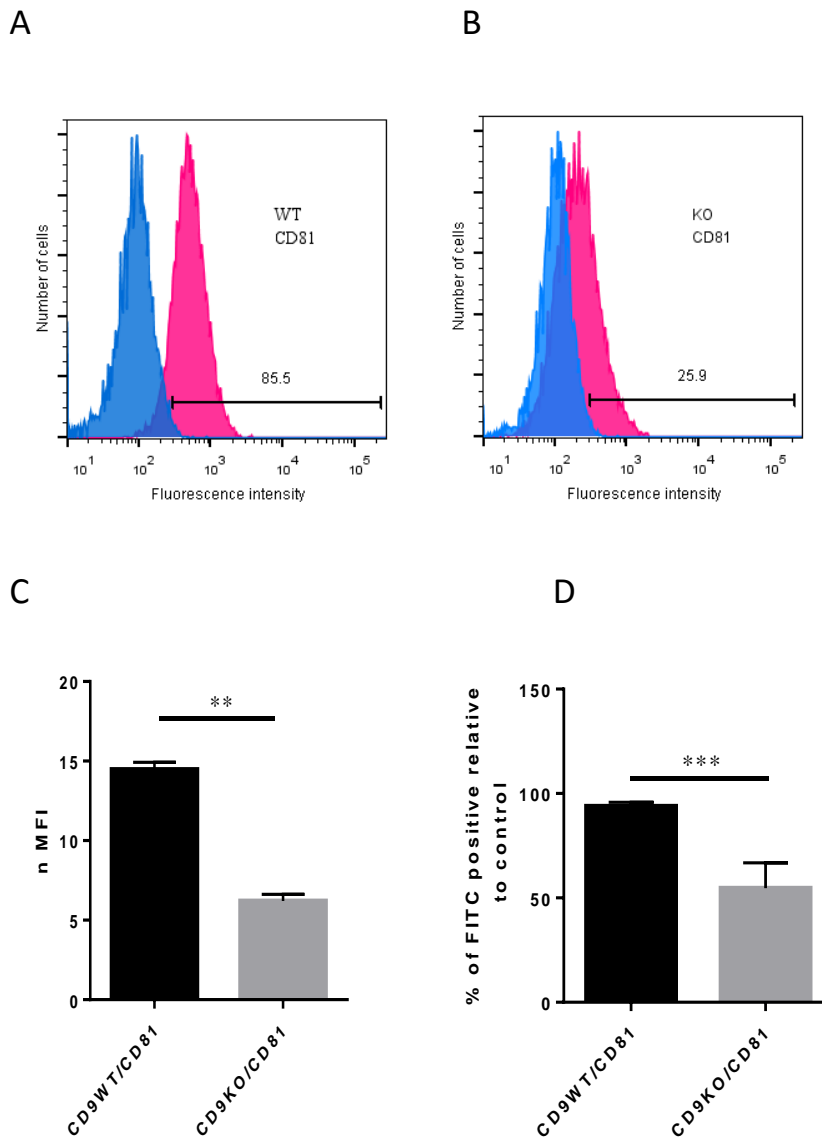
Figure 5.3.8 The expression of CD81 is decreased on CD9KO cells. The expression level of CD81 on CD9KO and CD9WT cells was tested by flow cytometry analysis. (A)(B) The overlying histogram of fluorescence intensity of CD81 on CD9WT and CD9KO cells respectively. (C) The normalized (to isotype control) median fluorescence intensity (nMFI) of CD81 on CD9 KO cells compared to that on CD9WT cells.(D) shows the percentage of cells that expressed CD81. The experiment was performed three times in duplicate and the significance of differences was determined by unpaired t test where ***significant at P< 0.001, ** significant at P< 0.05.
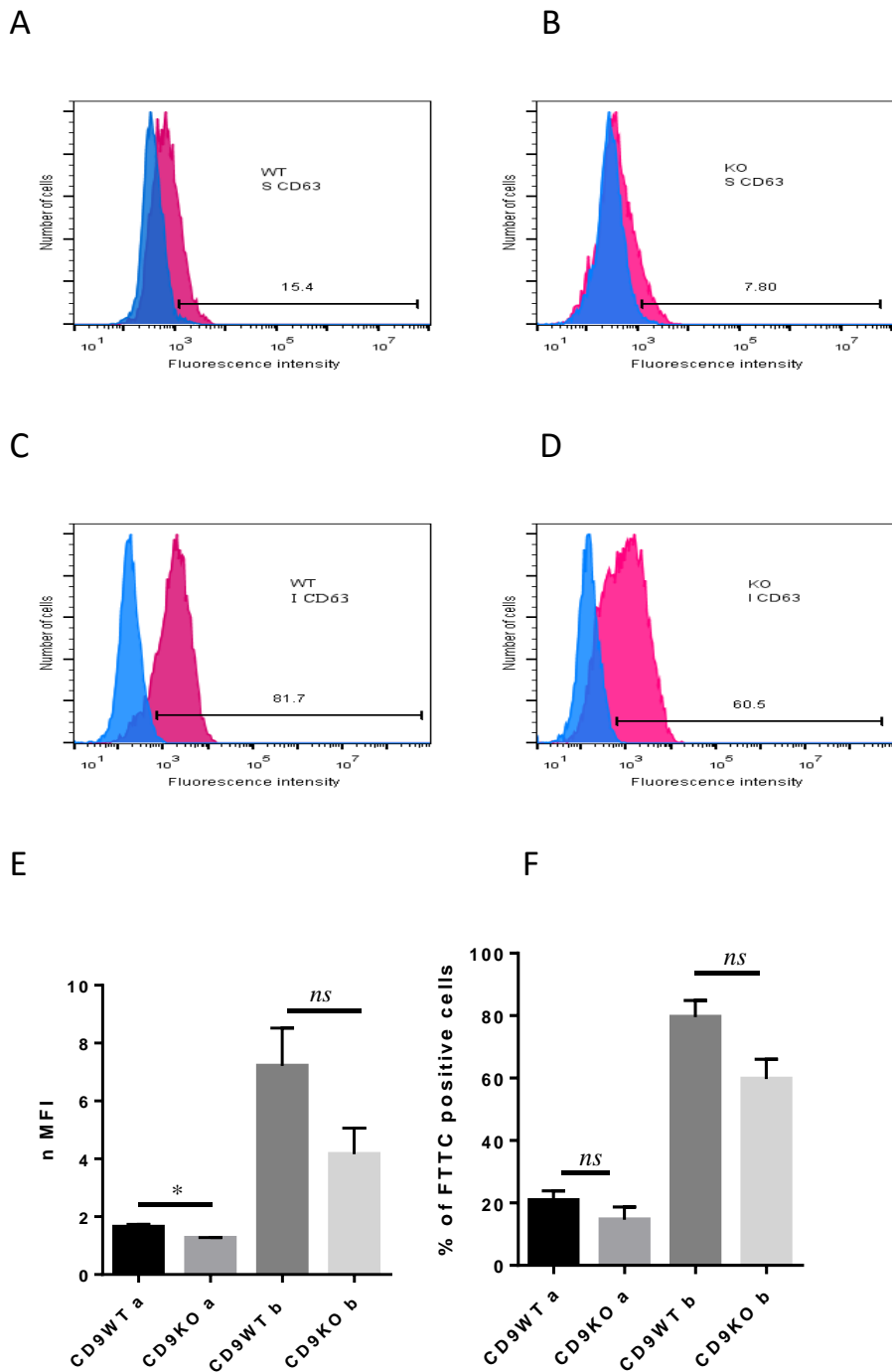
Figure 5.3.9 Decrease in the expression level of CD63 in CD9KO cells. The expression level of CD63 on CD9KO and CD9WT cells was tested by flow cytometry analysis. (A)(B) The overlying histogram of fluorescence intensity of CD63 expressed on the surface of CD9WT and CD9KO cells respectively. (C)(D) The overlying histogram of fluorescence intensity of total CD63 expressed in CD9WT and CD9KO cells respectively. (E and F) nMFI and the percentage of positive cells of extracellular CD63 (a) and all CD63 (b). The experiment performed three times in duplicate and the significance of differences was determined by unpaired t test where * significant at P< 0.05.

5.3.8 Several cell surface molecules are up- or down-regulated in the absence of CD9

To try to further elucidate the effect of CD9 deletion on cell fusion the expression level of other surface molecules that have been shown to promote cell fusion and MNGC formation was investigated by FACS analysis. Such information might explain the behaviour of CD9 deficient cells as well as illustrating the results of MNGC formation assays. The expression levels of scavenger receptor CD36, immunoglobulin superfamily member CD47 and its receptor CD172a, type II integral membrane protein CD98, integral membrane glycoprotein CD44, and dendritic cell-specific transmembrane protein DC STAMP were examined by FACS analysis in CD9KO cells in comparison with CD9WT cells as described in 2.2.3.2.1.

As shown in figures 5.3.8. a and 5.3.8 b, the expression level of several cell membrane proteins was affected by the absence of tetraspanin CD9. The expression level of scavenger receptor CD36 was significantly lower on CD9KO cells compared to that on wild type (MFI 2412 and 1238 in CD9 WT and CD9KO cells, respectively) and the percentage of cells that showed a positive expression for CD36 was also slightly lower in CD9KO macrophages. The expression level of CD44 was significantly lower on CD9KO compared to its level on wild type (MFI about 3848 on CD9WT and 1932 on CD9KO cells). The percentage of CD44 positive cells was also significantly decreased by about 10% in CD9KO. No significant effect was observed in the expression of CD47. Despite CD98 and CD172 being expressed at comparable level on both cell lines with respect to MFI, the parentage of positive cells for these molecules was significantly lower by about 10% and 6% respectively on CD9KO compared to wild type. Interestingly the expression level of DC STAMP was shown to be up-regulated in the absence of CD9 (MFI raised from about 1811 in CD9WT cells to about 2390 in CD9KO cells).

A: Expression of CD36 on CD9WT and CD9KO cells
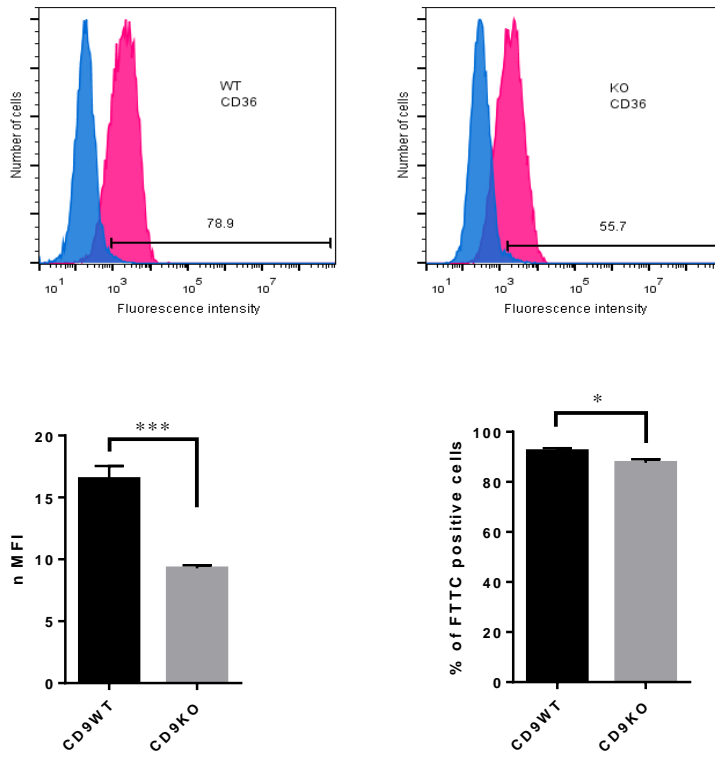
B: Expression of CD44 on CD9WT and CD9KO cells
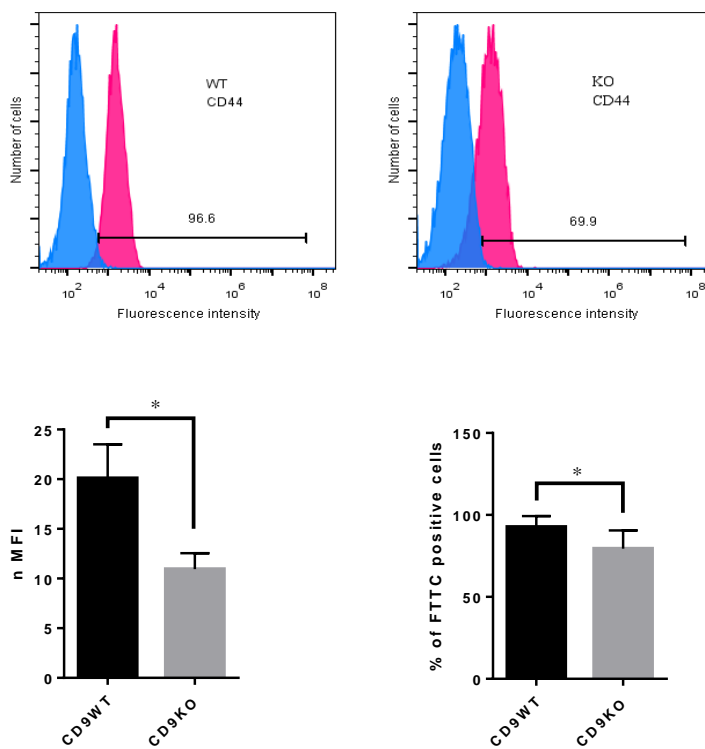
C: Expression of CD47 on CD9WT and CD9KO cells
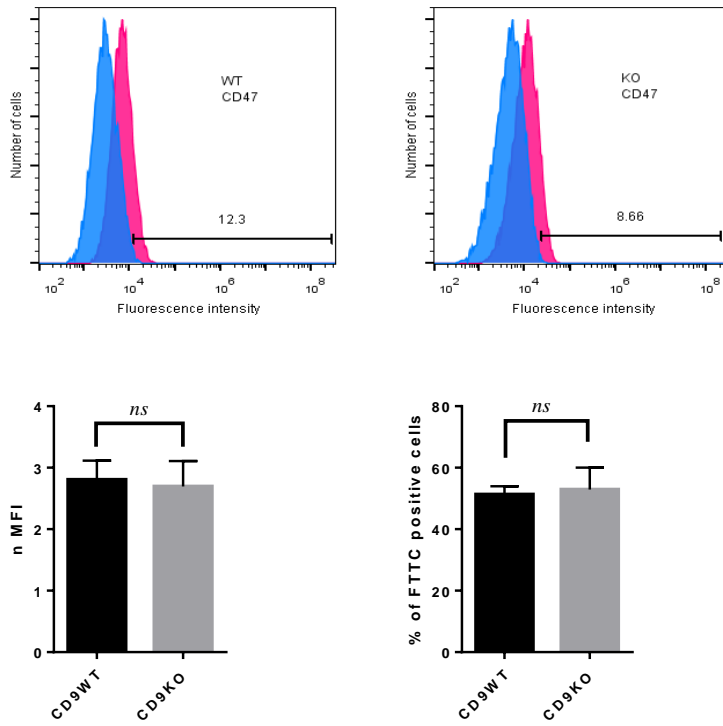
D: Expression of CD98 on CD9WT and CD9KO cells
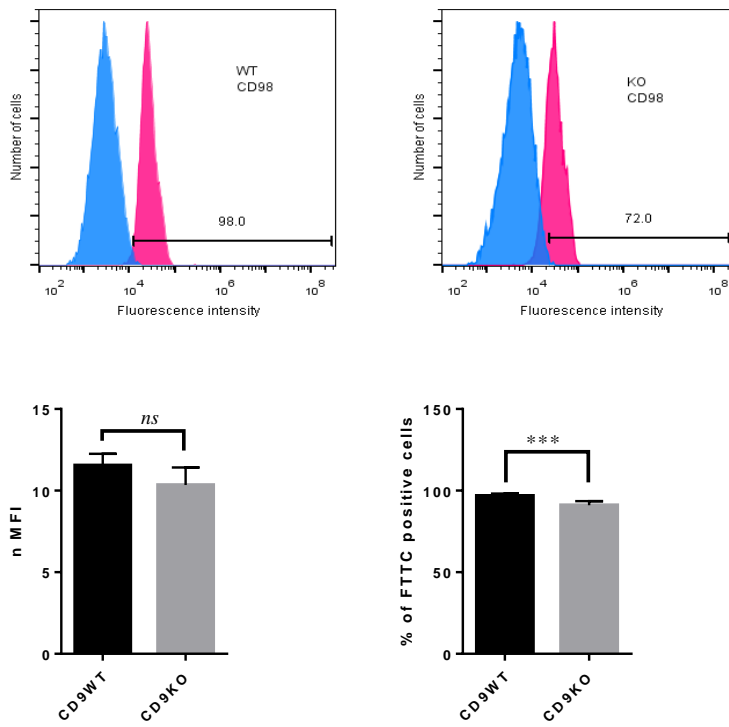
E: Expression of CD172a on CD9WT and CD9KO cells
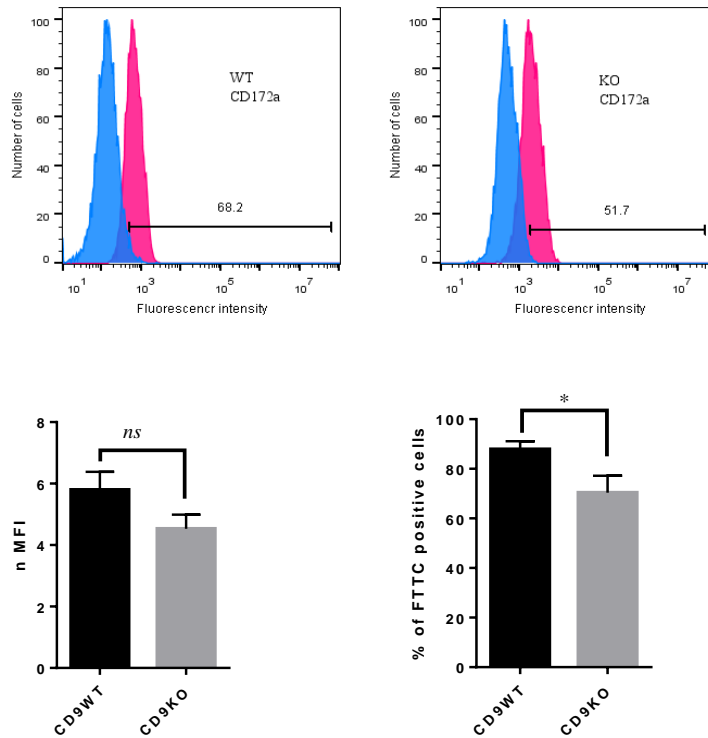
Figure 5.3.10a Expression of plasma membrane molecules on CD9 WT and CD9KO cells. FACS analysis was performed as described in 2.2.32.1 using specific monoclonal antibodies and isotype-matched controls. The mean fluorescence intensity (MFI) of each antigen (pink histogram) was normalized to the appropriate isotype control negative control (blue histogram). nMFI= MFI of sample/ MFI of isotype control. % of FITC positive cells = % of FITC positive of sample - % of FITC of isotype control. The significance of differences was tested by unpaired t-test $p < 0.05$.

F: Expression of DC STAMP on CD9WT and CD9KO cells
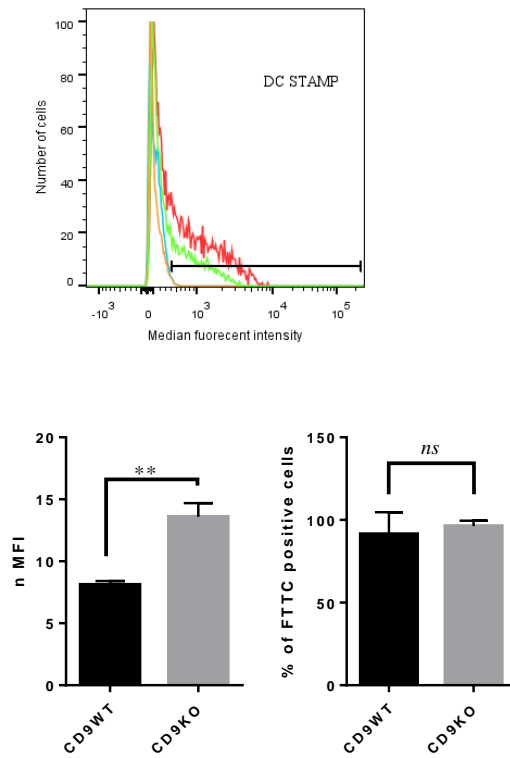
Figure 5.2.11b Expression of DC STAMP on CD9 WT and CD9KO cells. The histogram represents (blue and brown) CD9WT and CD9KO cells labelled with isotype control respectively, (green and red) CD9WT and CD9KO cells labelled with anti DC STAMP antibody respectively. nMFI= MFI of sample/ MFI of isotype control. % of FITC positive cells = % of FITC positive of sample - % of FITC of isotype control. The significance of differences was tested by unpaired t-test p<0.05.

5.3.9 Effects of disruption of tetraspanin CD82 on *B.thailandensis*- induced cell fusion

Generally the experiments performed in this work were carried out by Jocelyn Pinto (an undergraduate project student in this Department) with my collaboration and supervision. The aim of this project was to investigate the role of CD82 in *B.thailandensis*-induced MNGC formation using a macrophage cell line derived from mice in which CD82 gene was disrupted, and the corresponding wild type macrophages.

The effect of CD82 deficiency on *B.thailandensis* uptake and MNGC formation was investigated. Further experiments including FACS analysis, electron microscopy and analysis of adhesion under flow conditions using microfluidics were undertaken to try to elucidate the results of MNGC formation assays.

5.3.9.1 *B.thailandensis* uptake is reduced in CD82 deficient macrophages

The effect of CD82 deletion on CDC272 and E264 internalization was investigated. Cells were infected at MOI 1:1 or 3:1 and the number of intracellular bacteria was determined at 4hr post infection as described in 2.2.6.1. The results showed that *B.thailandensis* uptake decreased in CD82KO cells compared to CD82WT (Figure 4.2.12). The number of intracellular bacteria was significantly decreased in CD82KO cells infected with *CDC* at MOI 3:1 (the mean of intracellular bacteria in CD82WT and CD82KO was $3.97 \times 10^6 \pm 315$ and $2.74 \times 10^6 \pm 247$, respectively). This finding suggested that CD82 might be implicated in the process of *B.thailandensis* uptake. Notably, this result was in contrast with the result that was obtained in CD9 deficient cells, where CD9KO cells were significantly more susceptible to *B.t* infection compared with CD9WT.
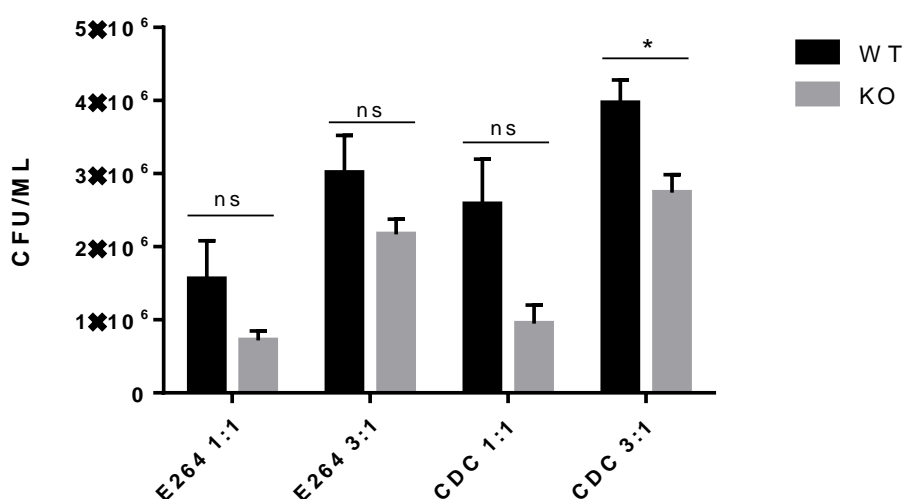
Figure 5.3.11 Effect of CD82 deficiency on *B.thailandensis* uptake. Cells were infected at MOI 1:1 or 3:1 and the number of intracellular bacteria was assessed as described in section (2.2.10.1). The experiment was performed three times in triplicate and significance of differences was tested at *P< 0.05 unpaired t-test.

5.3.9.2 CD82 negatively promotes *B.thailandensis* -induced cell fusion

In order to determine the time at which cells start to form MNGC, after 2, 4, 6, 8, 10 post infections CD82WT and CD82KO cells were fixed, stained and MNGC formation was evaluated as described in 2.2.10.3. Obvious MNGC was noted after 6hr post infection and this increased with time. At 10-12 hr post infection fused and unfused cells appeared to undergo apoptosis leading to cell death, which caused cell loss in washing and staining processes. Therefore, 9hr post infection was the optimal time for assessing *B.thailandensis* - induced MNGC formation in these cell lines**.**

Across all conditions tested it was clear that CD82KO cells had undergone fusion extensively compared to CD82WT. The fusion index in CD82 deficient cells was about 5-8 fold higher

than that in CD82WT cells and this was significant statistically (e.g. in *B.t E264*-infected cells at MOI of 3:1 the mean of fusion index was 4.44±1.64 and 25.13±3.82 in CD82WT and CD82KO, respectively). However, no statistical differences were apparent in comparison between different MOIs and different strains (Figure 5.3.13).
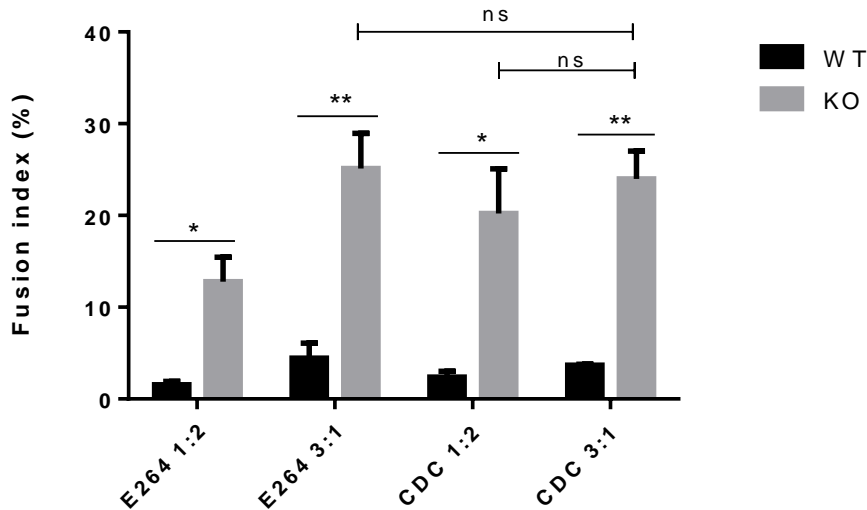
Figure 5.3.12 Effects of CD82 deficiency on *B.thailandensis*-induced MNGC formation. Cells were infected at MOI 1:2 or 3:1 and at appropriate times post-infection cells were fixed, stained and fusion index was assessed as described in 2.2.10.1. The experiment was performed three times in triplicate and significance of differences was tested by unpaired t-test at *P< 0.05.

Despite the extensive differences noted in fusion index between CD82WT and CD82KO cells, the increase in MNGC size in CD82KO cells compared to CD82WT across all conditions was statistically insignificant (e.g. the mean of MNGC size in E264-infected cells was 4.53±0.47 and 5.637±0.47 in CD82WT and CD82KO cells, respectively)(Figure 5.3.13).
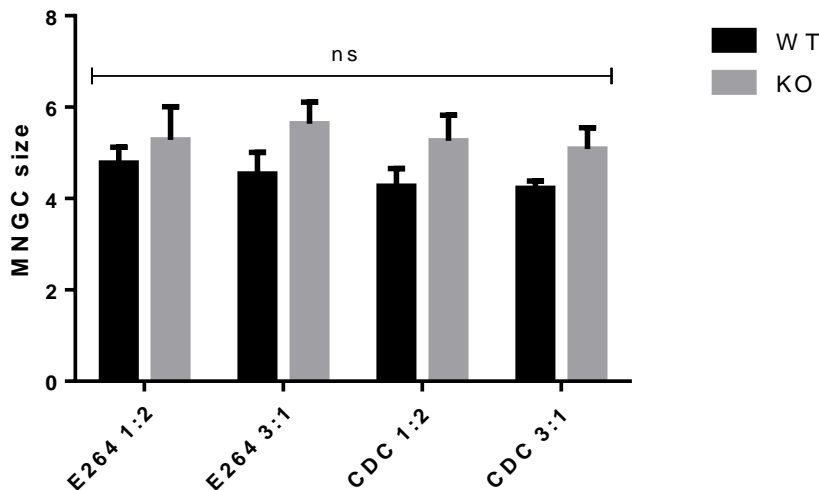
Figure 5.3.13 Effects of CD82 deficiency on *B.thailandensis*-induced MNGC formation. Cells were infected at MOI 1:2 or 3:1 and at appropriate times post-infection cells were fixed, stained and MNGC size was assessed as described in 2.2.6.2. The experiment was performed three times in triplicate and significance of differences was tested by unpaired t-test at *P< 0.05.

5.3.10 Several cell surface molecules up or down regulated in CD82 deficient macrophages

Since the absence of CD9 affects the expression level of other cell surface proteins that have been implicated in cell-cell fusion, this experiment aimed to investigate a possible effect for CD82 deletion on the expression level of the surface molecules mentioned above (section 5.3.8). Expression levels were determined using FACS analysis as described in 2.2.3.2.1. These experiments were performed by myself.

The results revealed that CD44, CD47, CD98 and CD172a were differently expressed on CD82KO compared to cells wild type. The mean nMFI of these molecules was 14.74±3.28, 3.53±22, 13.82±1.50 and 5.82±0.9, respectively, on wild type and this decreased in CD82 -/-cells (mean of nMFI was 5.65±1.95, 2.93±0.34, 6.07±1.52 and 3.08±.56 respectively). However, unpaired t-tests showed only significant differences in the expression levels of CD98 and CD172a at P< 0.05. Significant decreases in the percentage of positive CD82KO cells compared to wild type was found only for CD44 and CD172a. Finally, despite the increase in the intensity of DC STAMP in CD82KO compared to CD82WT (mean of nMFI was 5.87±1.4 in WT and 7.18±2.23 in CD82KO) this increase was not proved statistically.
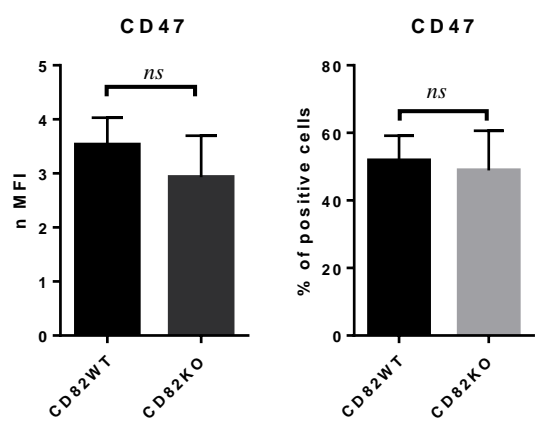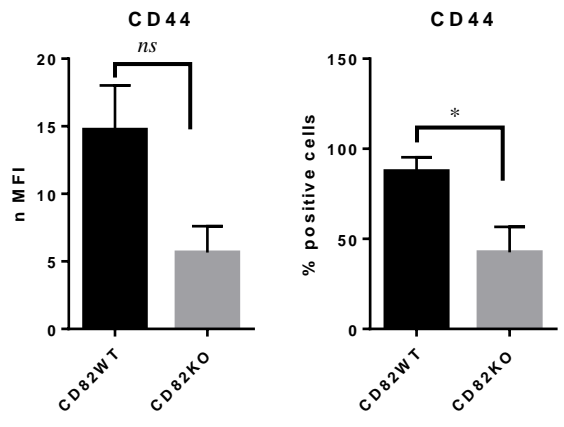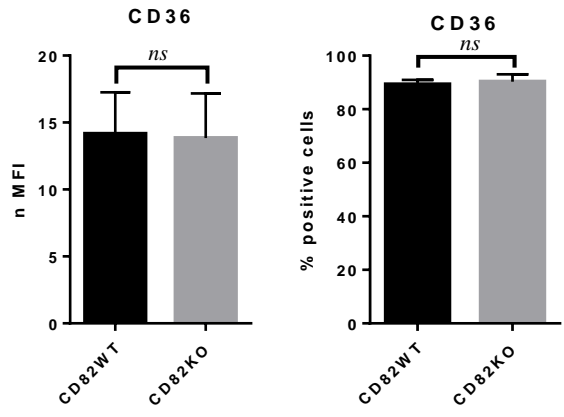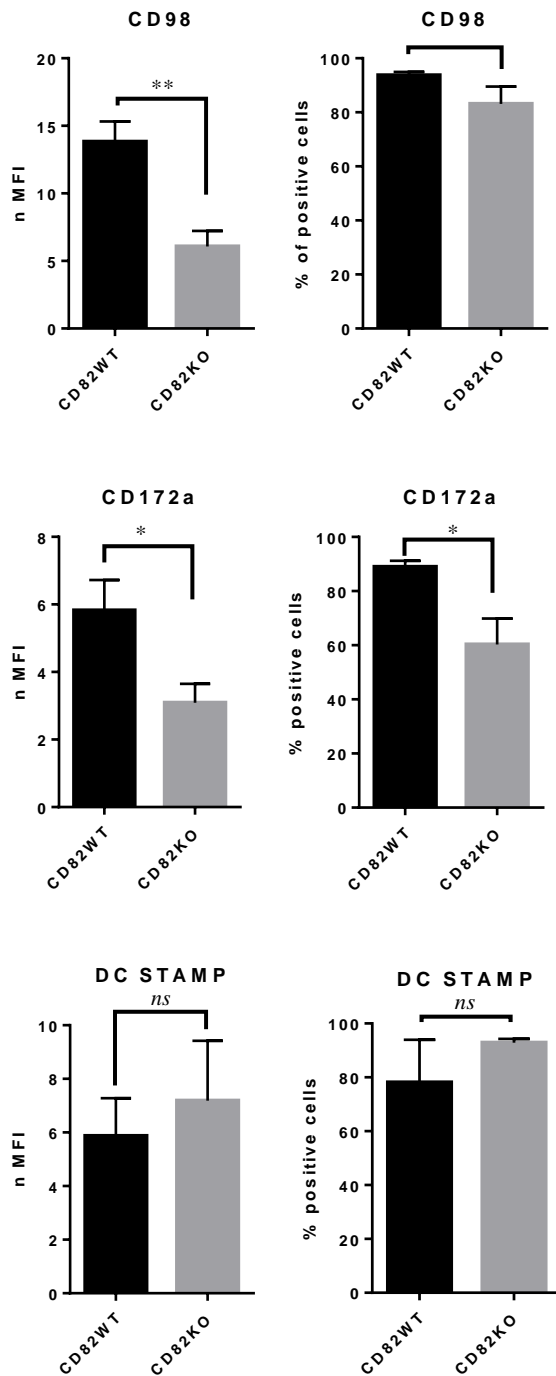
Figure 5.3.14 Expression levels of cell surface molecules on CD82WT and CD82KO. FACS analysis was performed as described in (2.2.3.2.1) using specific monoclonal antibodies and isotype-matched controls. The experiment was performed at least three times in duplicate. The mean fluorescence intensity of each antigen was normalized to appropriate isotype control (negative control) n MFI= MFI of sample/ MFI of isotype, % of positive cells= % of positive sample- % of positive isotype control.

5.3.11 Effect of CD82 ablation on cell adhesion

From the observations of the MNGC assay there was a notable difference between CD82KO and CD82WT cells in the number of cells that remained adherent during washing processes, which suggested that CD82 might be involved in cell adhesion. Therefore, cell adherence was examined under flow conditions using a microfluidic assay. This work was carried out by Jocelyn Pinto in collaboration with Dr Cecile Perrault (Dept. Mechanical Engineering, University of Sheffield). A three-flow channel microfluidic device was used to examine the susceptibility of cells to comparatively low flow rates. CD82KO cells appeared to be more susceptible to detachment than CD82WT as an average of 53.7±8.4% reduction in cell number was recorded under flow conditions in wild type cells and 74.3±0.9 percent reduction in CD82KO; however the different between two cell lines was not statistically significant. (Figure 5.3.15).
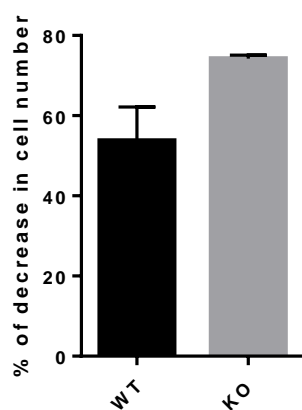
Figure 5.3.15 Effect of CD82 knockout on cell adhesion under flow conditions. A three-flow channel microfluidic device of polydimethylsiloxane was constructed using soft-lithography and photoligraphy techniques. Three channels were used for each cell type in each experiment. The channels were coated with CD82WT or CD82KO cells and left to adhere for 2hr. Thereafter RPMI medium was injected through the inlets of sample 1 and sample 2 (sample 3 was a control) at 1µl/min for 45 min. to equilibrate with the external flow rate. The flow rate was increased to 15µl/min Cell migration was recorded at several pre-determined positions every 3 min for 2hr using a time-lapse microscopy and Metamorph Microscopy Automation and Image Analysis Software. Strength of adhesion of each type was then quantified by obtaining the percentage difference in cell count after 1hr under 15µl/min flow conditions.

5.3.12 Electron microscopy analysis of *B.thailandensis* infection and cell-cell interaction in CD9 and CD82 knock-out and wild type cells

This work aimed to provide a qualitative analysis of phenotypes related to *B.thailandensis* infection in CD9-/- and CD82-/- macrophage cells and the corresponding wild types at high magnification. The experiment was performed as described in 2.2.16 using fixed pellets of

infected cells. *B.thailandensis* E264-infected CD9WT and CD9KO as well as CD82WT and CD82KO were examined at 6hr and 9hr post-infection, respectively, which is the prospective time of MNGC onset in these cell lines. The observation of cells at magnification 690x-4900x showed detailed characteristic features that are associated with *B.thailandensis* uptake, life cycle, bacterial transmission and cell interactions that may lead to cell fusion.

Some bacteria were observed at the cell surface, having apparently just been enclosed within a phagosome (Fig. 5.3.16 (A, B)), also bacteria can be seen within phagosome (Fig. 5.3.16 (C)). In addition, actively replicating bacteria also can be observed (Fig. 5.3.16 (D)). Interestingly, bacteria can be detected in the junction area where two adjacent cells were joined ((Fig. 5.3.16 (E)), which may represent an early stage of *B.thailandensis* cell-cell spreading. Bacterial cells were also located free in the cytosol where no phagosomal membrane can be detected (Fig. 5.3.16 (F)) whereas; other damaged bacteria could be observed within phagolysosomes (Fig. 5.3.16 (G)). Bacteria located at the edge of cells observed in ((Fig. 5.3.16 (H)). Intact bacteria were also observed within an extracellular vesicle, which suggests another mechanism for bacterial transmigration and survival ((Fig. 5.3.16 (I)).

Moreover, electron micrographs of infected macrophages reveal phenotypes associated with their responses to the *B.thailandensis* infection. A primary contact between macrophage pseudopodia can be detected (Fig. 5.3.17 (A)). In some micrographs, close contacts between cells were clear, and discontinuous plasma membrane between two adjacent cells could also be observed, indicating cell fusion ((Fig. 5.3.17 (C, B)), and MNGC can be observed ((Fig. 5.3.17 (d)). Morphological aspects of apoptosis and necrosis at early and advanced stages were noted in all infected cell lines used, such as nuclear condensation, cytoplasmic vacuolization, induction of apoptotic bodies and destruction of intracellular cytoplasmic membranes ((Fig. 5.2.18 (E, F)).

Infected CD82WT 1900X

Infected CD82WT 1200X

Infected CD82WT 1900X

Infected CD9KO 1900X

Infected CD9WT 1400X

1 μm

Infected CD82WT 1900X

1 μm

G

1 μm

Infected CD82WT 1900X

H

Infected CD82WT 4900X

0.2 μm
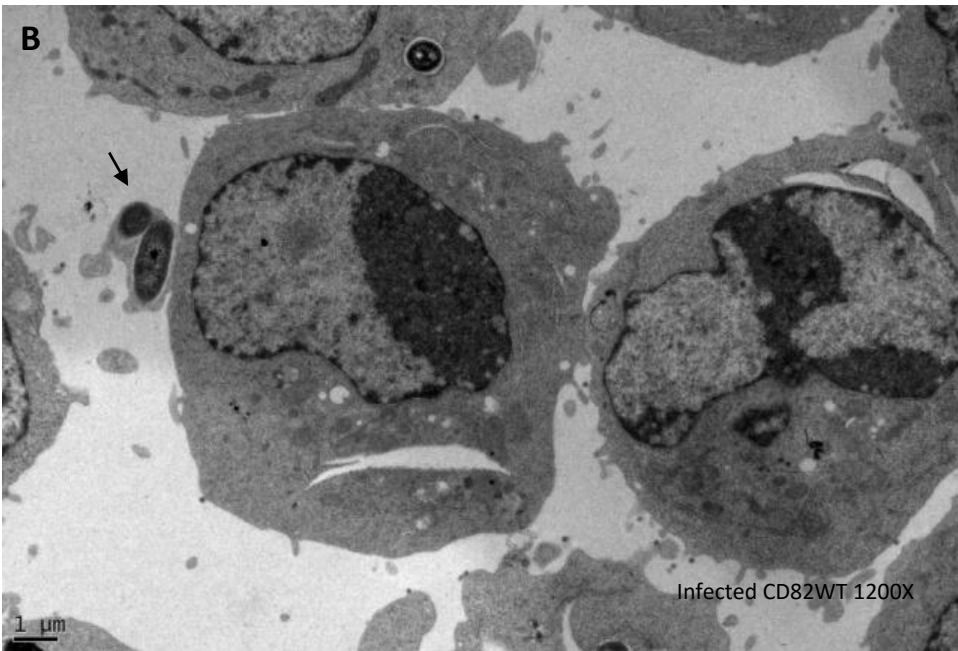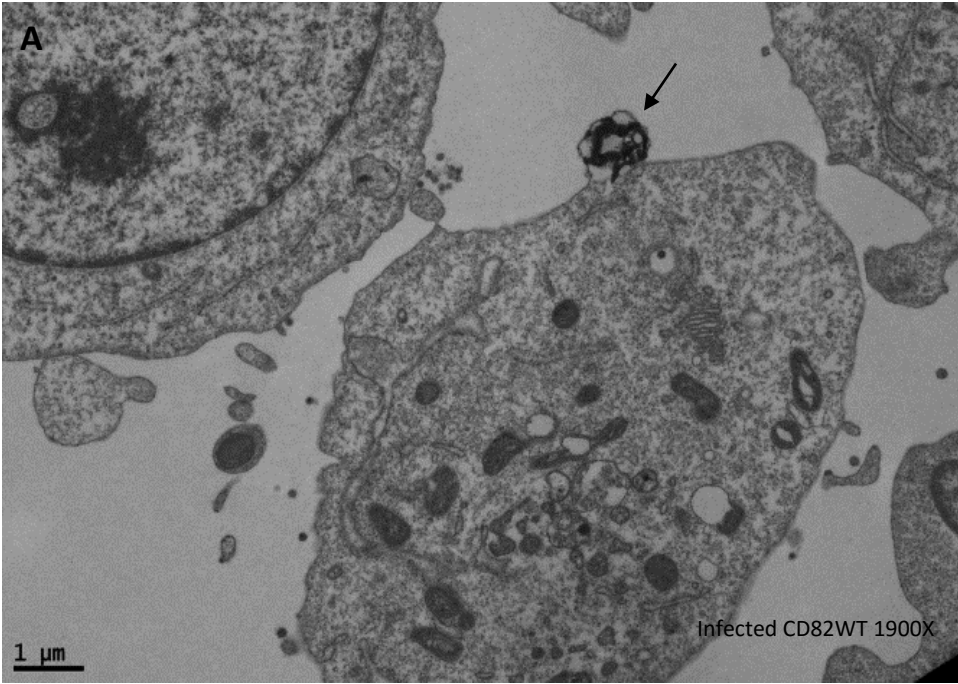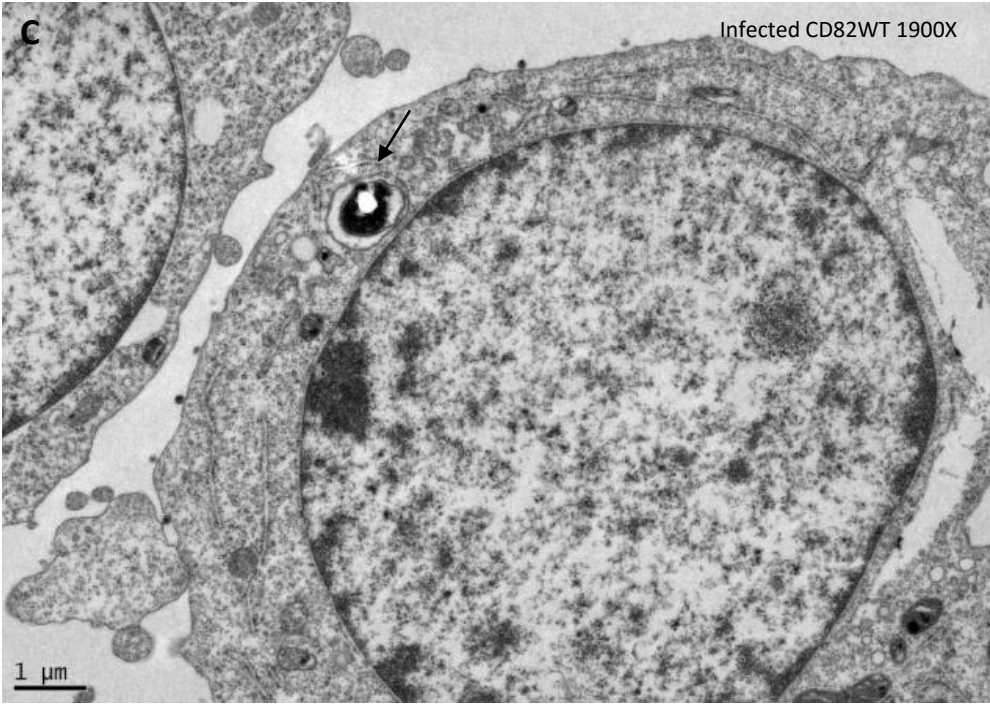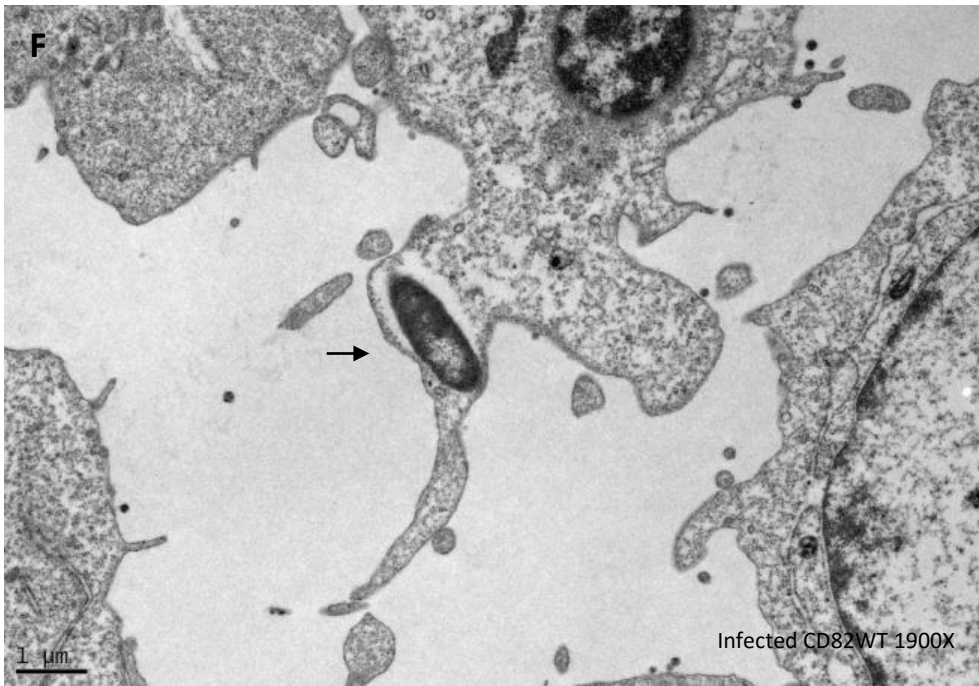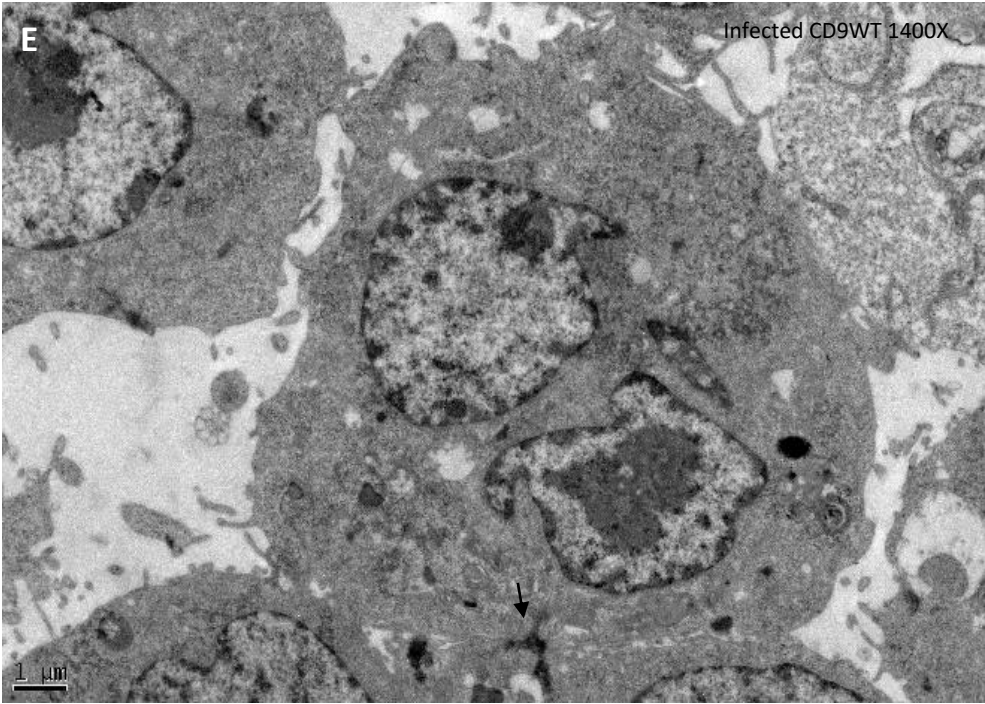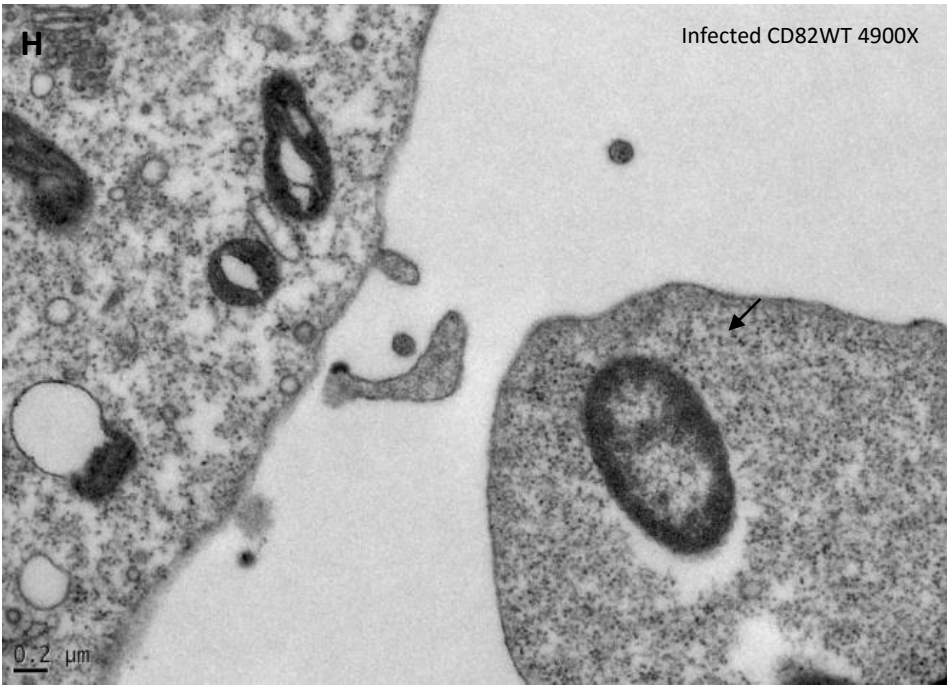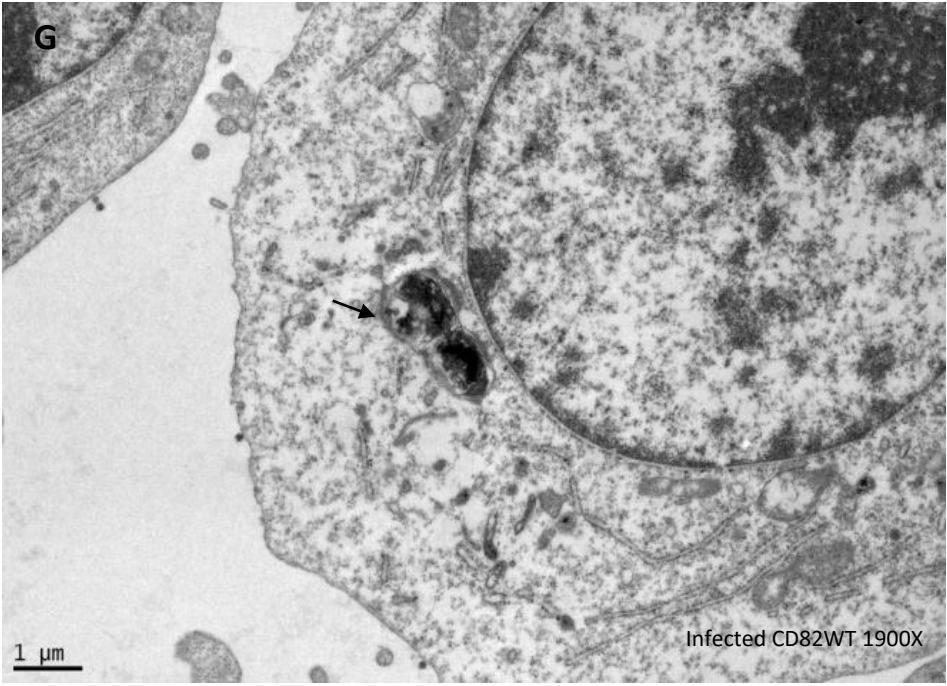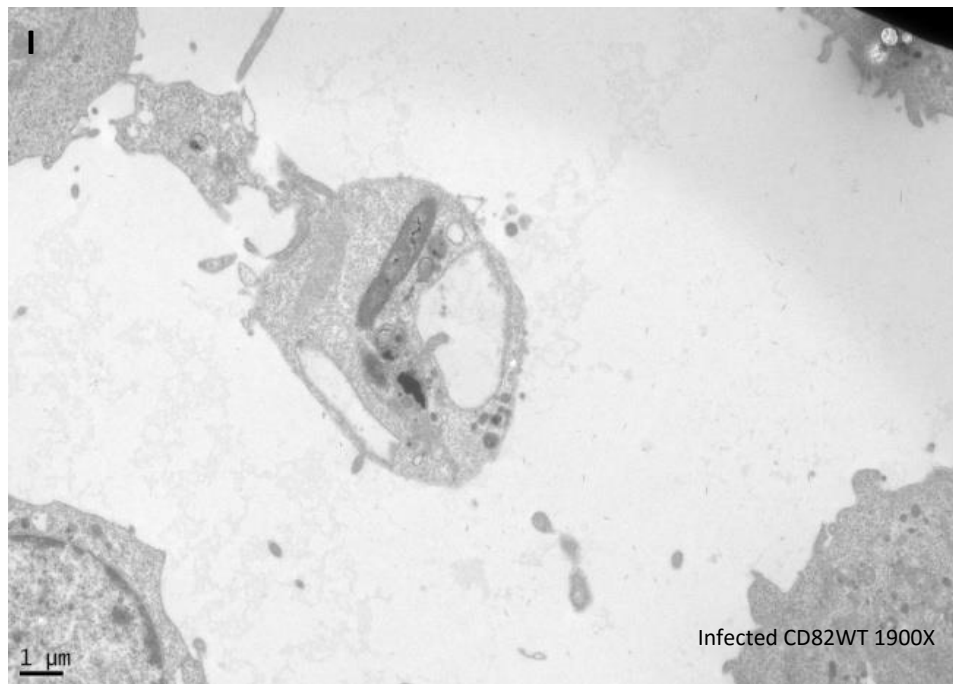
Figure 5.2.17 Intracellular *B.thailandensis* observed by electron microscopy. A and B show B.t within a phagosomal membrane near the cell surface. C shows intracellular vacuoles containing B.t. D show surviving bacilli. F indicates channels initiated between a giant cell and its neighbours and a possible route of B.t cell-cell transmission. F shows intracellular bacteria within the cytosol no phagosome membrane can be distinguished. G shows phagolysosomes containing destroyed bacteria near the nuclear region. G shows surviving B.t located at the edge of two cells. I show B.t surviving within extracellular vesicles, which might represent another mechanism for bacterial cell-cell transmission.

A

0.5 µm

Infected CD82WT 2900X

B

1 µm

Infected CD9WT 1900X

C

0.5 μm

Infected CD9WT 2900X

D

1 μm

Infected CD82WT 1200X
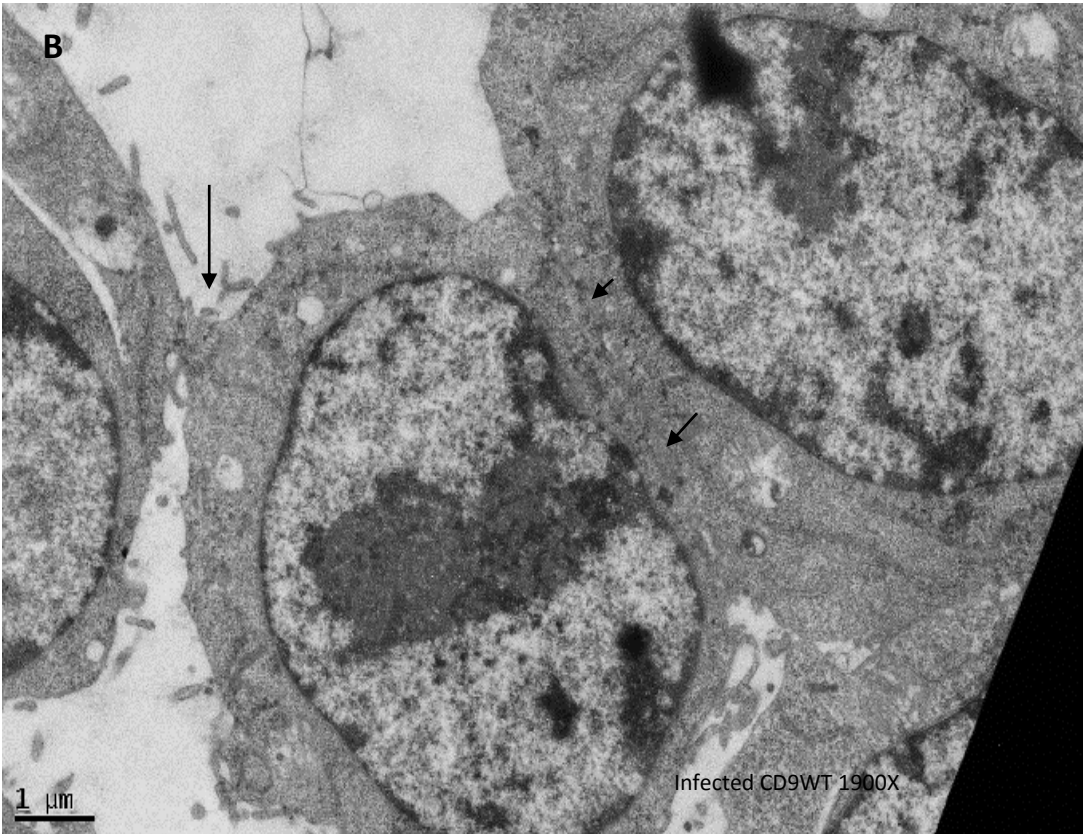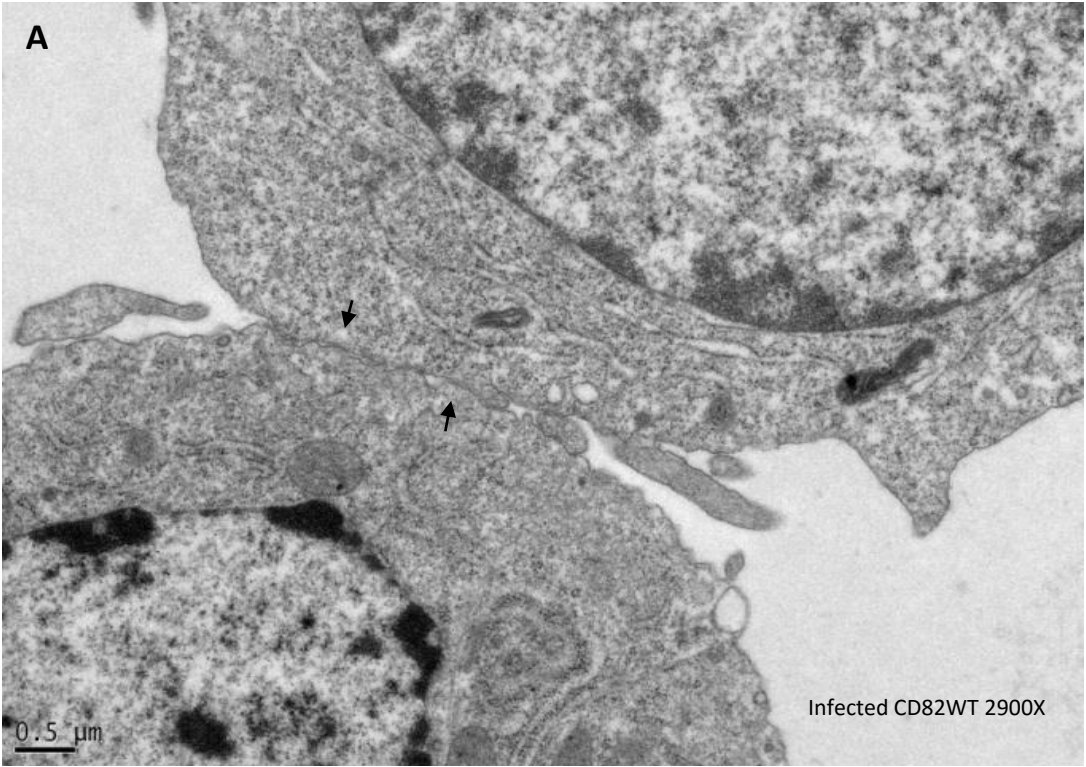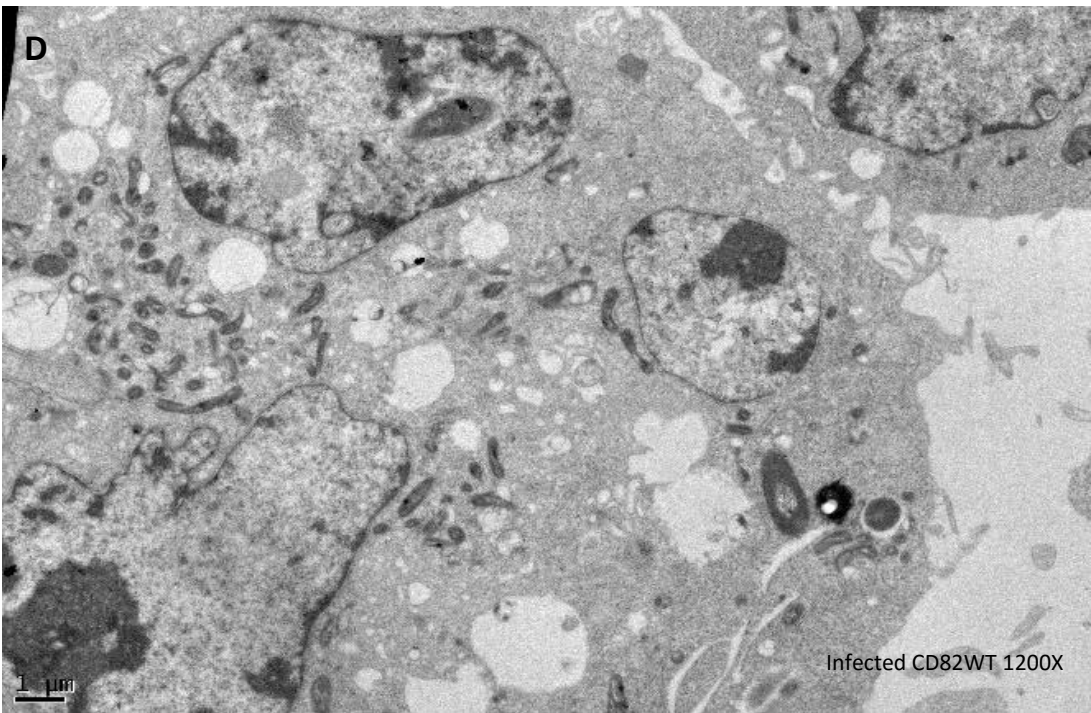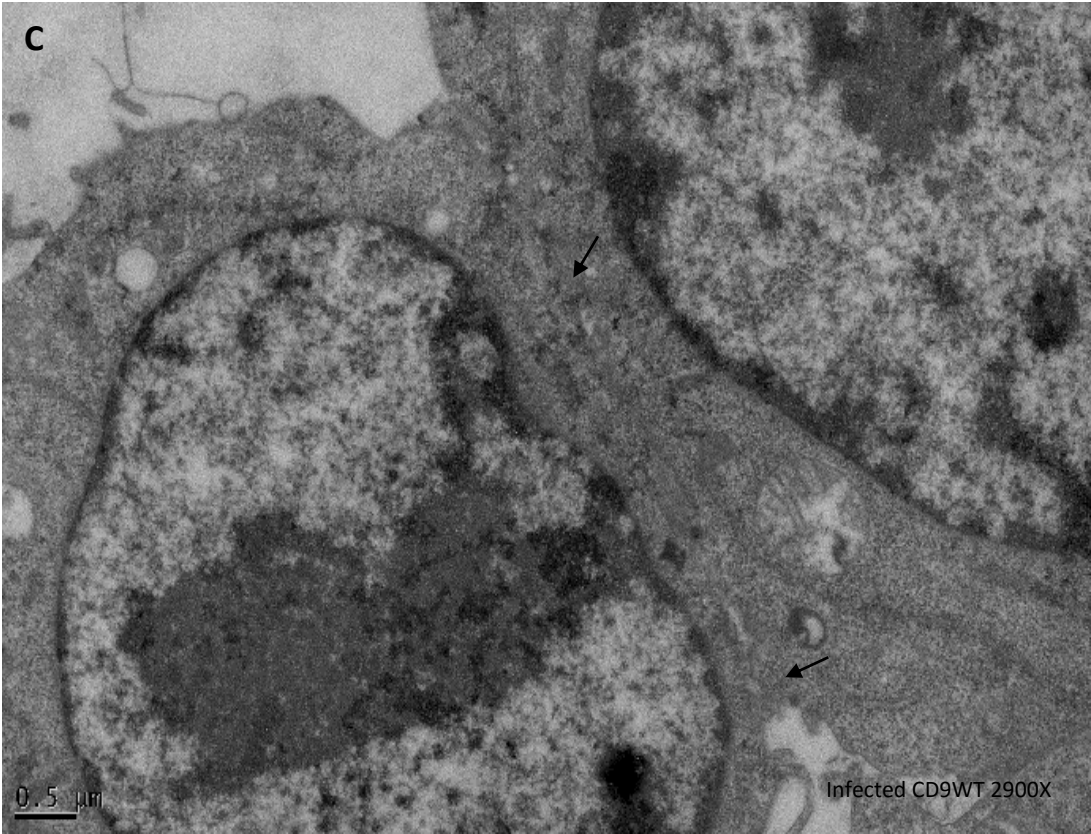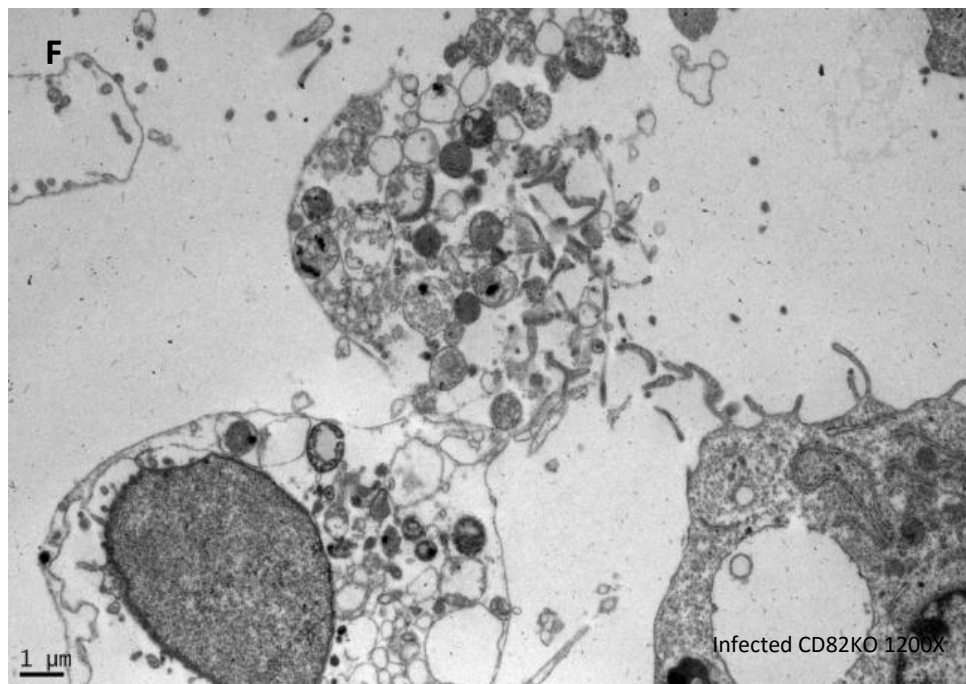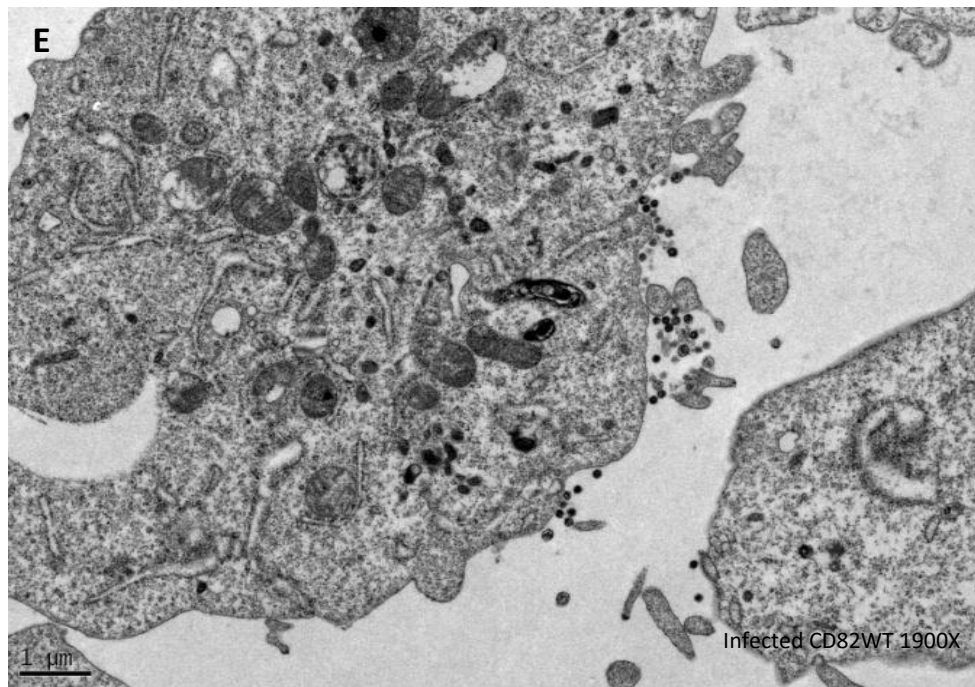
Figure 5.2.18 Electron microscopy analysis of WT and KO B.t-infected cells. A shows unfused cells, their cell membranes can be distinguished. B and C Cells in close contact at different magnifications. D and E MNGCs show morphological aspects of apoptosis. F indicates necrotic cells.

5.3.14 Determination of the localisation of CD9 on *B.thailandensis* -infected cells by confocal microscopy

According to the above results that have shown that CD9 negatively promoted *B.t*-induced cell fusion, it was speculated that its cell surface expression might change under the

conditions of fusion that are promoted by *B.thailandensis*. Therefore, the localization of CD9 in *B.thailandensis* -infected cells was investigated using confocal microscopy.

Initially, to visualise *B.thailandensis,* the bacteria were transfected with plasmids encoding green fluorescent protein (GFP) or *Discosoma* red fluorescent protein (DS RED) as described in section 2.2.4.5. J774 cells were co-cultured with transfected bacteria and at different time points, cells were fixed and stained as described in 2.2.15.

The confocal image in Figure 5.3.18 shows the distribution of CD9 on uninfected and *B.thailandensis* (E264) infected J774.2 which formed MNGC. CD9 is densely and quite evenly expressed at the cell periphery on uninfected cells, whilst on MNGC CD9 is restricted to patches on the cell membrane with relatively weak staining on other areas. It seems that there is no co-localization of CD9 with the bacteria.
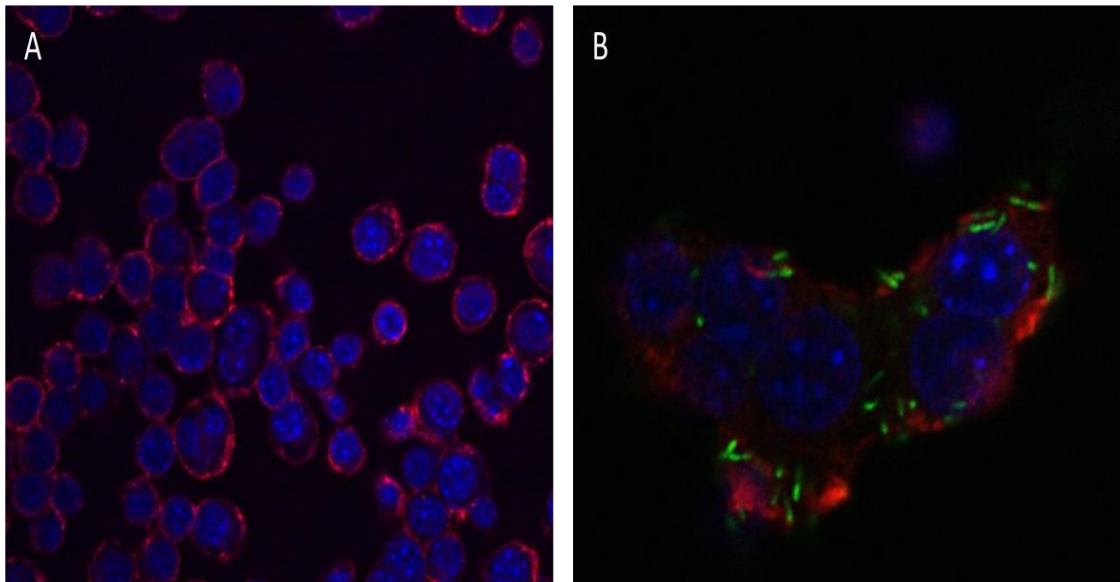
Figure 5.3.18 Confocal images of CD9 expression on uninfected and *B.thailandensis* E264 infected J774.2 cells. (A) uninfected J774.2 and (B) E264- GFP-infected J774 cells. Cells were fixed and stained after 6hr post infection as described in 2.2.14. Cells were incubated with primary rat anti mouse-CD9 antibody followed by anti- rat Alexa fluor secondary antibody. Nuclei were counter-stained with DAPI.

Images in figure 5.3.19 show the localization of CD9 on *B.thailandensis* CDC-infected cells. Again, the distribution of CD9 is patchy compared to that of uninfected cells (A and B), with some areas of the membrane having little CD9. Interestingly CD9 seems to be clustered in cell-cell contact sites where unfused cells adhere to large MNGC (C, D).

Images using Widefield microscope equipped with fluorescence and phase contrast in figure 5.3.20 also show the distribution of CD9 on infected J774.2 cells. Notably, CD9 shows intracellular distribution in MNGC cells which may explain the decrease in its extracellular level after the infection and under fusion conditions as described previously. Another important observation is t the localisation of CD9 at the cell-cell contact area in figure

5.3.21 where to cells seem to be undergoing fusion processes (maybe at the hemifusion or fusion pore opening stage). Also CD9 seems to co-localise with the bacteria in this area.
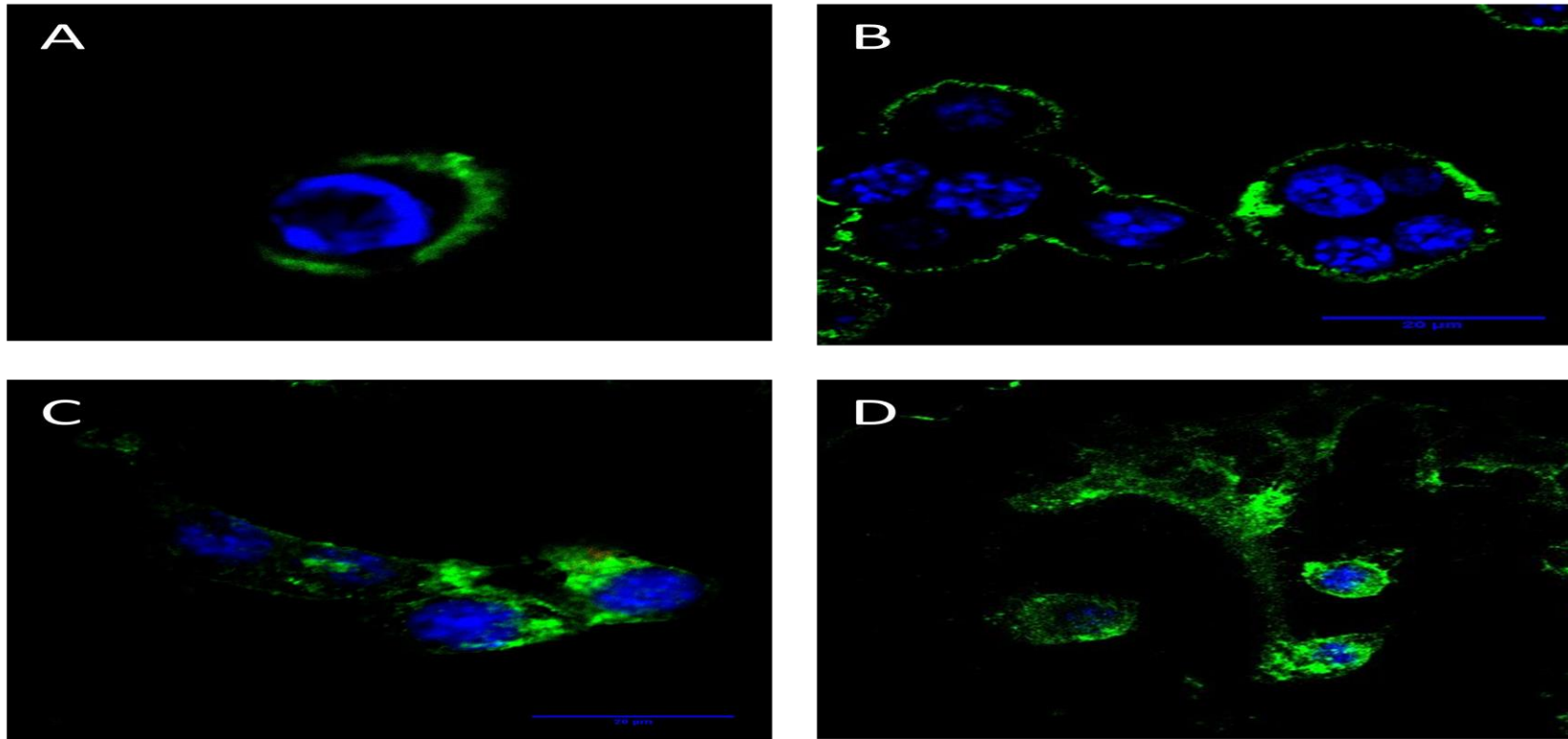
Figure 5.3.19 Confocal images of the distribution of CD9 on infected and uninfected J774 cells. Cells were fixed and stained after 4hr post infection as shown in 2.2.14. Non infected and infected cells were incubated with anti-CD9 antibody for 1hr. Cells were then incubated with FITC-conjugated antibody Nuclei were counter-stained with DAPI. (A) un-infected J774 and (B) *B.t* CDC-infected J774 cells (C and D) the localisation of CD9 in cell- cell contact region.
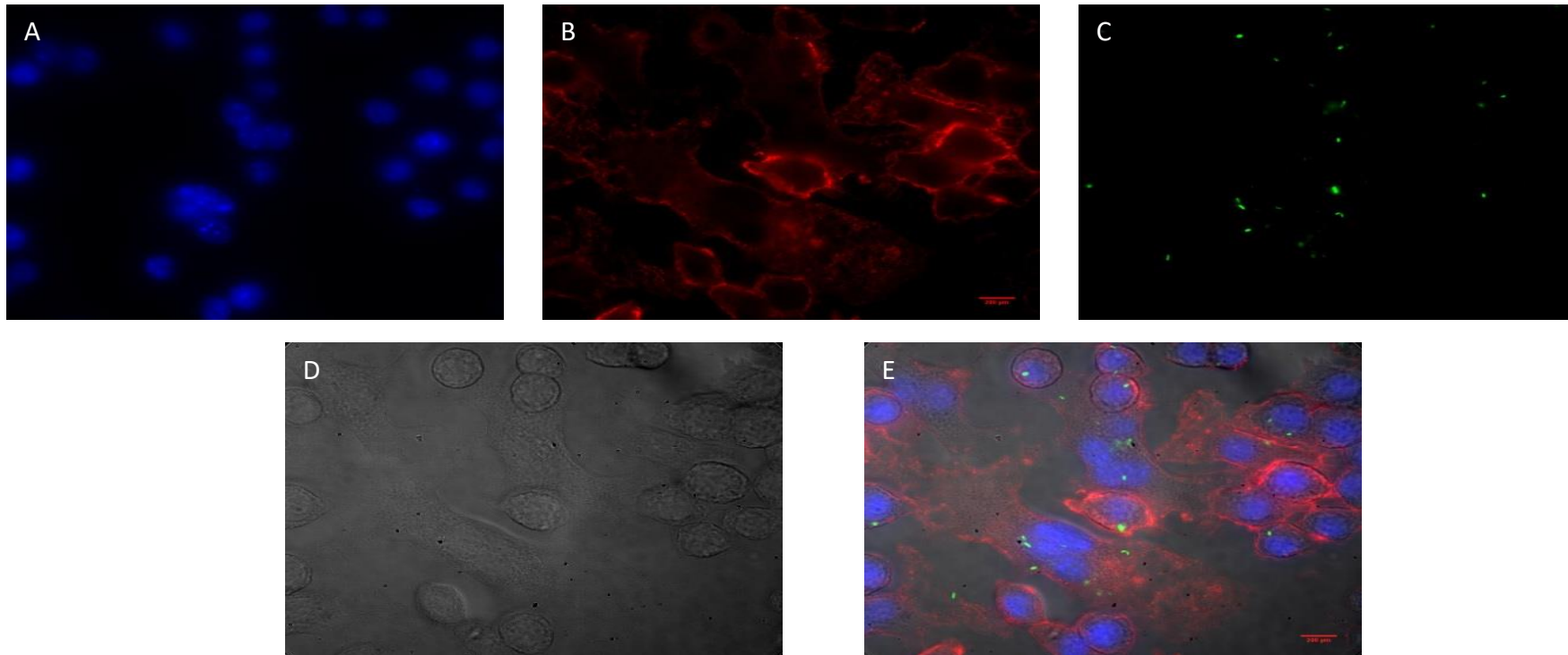
Figure 5.2.20. Widefield images of CD9 localization on *B.thailandensis* (E264 GFP) infected J774 cells. The images are single optical section from deconvolved sets obtained under identical conditions using a Deltavision widefield microscope (objective 60x oil). (A) nuclei stained with DAPI. (B) cells were immunostained with anti-CD9 mAb, followed by staining with Alexa fluor-conjugated anti-rat antibody. (C) *B.t*-GFP. (D) phase contrast. (D) merge.
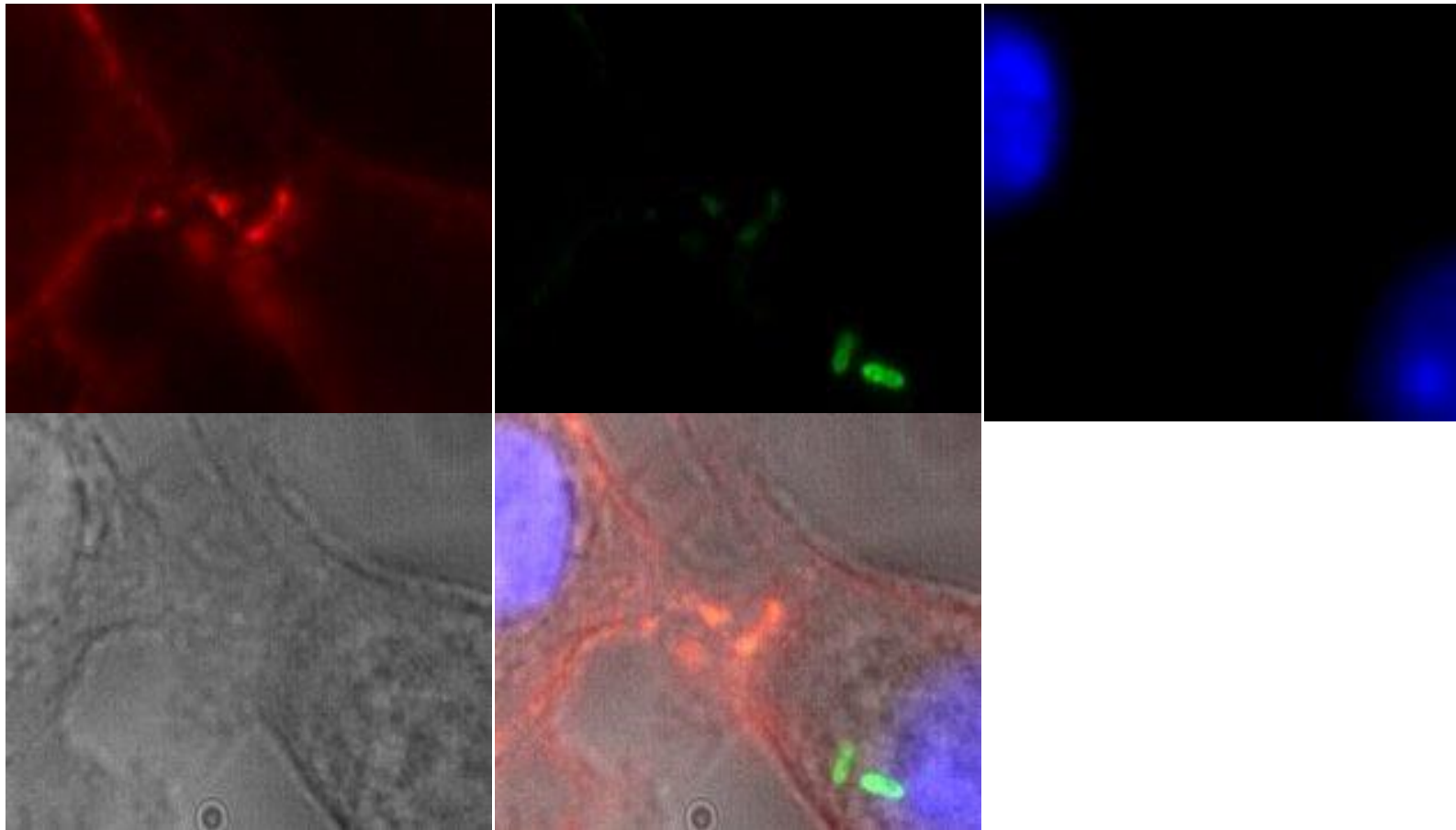
Figure 5.2.21. Widefield images of CD9 localization on *B.thailandensis* (E264 GFP) infected J774 cells. The images are single optical section from deconvolved sets obtained under identical conditions using a Deltavision widefield microscope (objective 60x oil). CD9 distributions (red), *B.t* E264 (green), nuclei (blue), phase contrast (grey).

5.3.15 Gene expression profile of CD9 deficient macrophages

As described in section 5.3.7 and 5.3.8, the cell surface expression levels of several molecules other than CD9 were altered in CD9KO cells compared to wild type. To try to further understand the influence of CD9 gene deletion on cell behaviour, we therefore investigated the gene expression profile of CD9KO cells using microarray analysis, and the variations in gene expression levels were compared with their expression levels in wild type cells.

This work was carried out with the collaboration with Dr Paul Heath; Sheffield Institute for Translation Neuroscience University of Sheffield (SITranN). Initially the extracted RNA yield and RNA quality were examined as described in 2.2.13.1 and 2.2.13.2 respectively, confirming that the RNA was of high quality with no DNA contamination. All RNA preparations were shown to have an RNA integrity number (RIN) of greater than 9 based on their electrophoretic mobility (Schroeder et al., 2006). Microarray analysis was then carried out using the GeneChip 3'IVT Expression Kit, as described in 2.2.13.3. Three independent analyses were performed.

The signal values were determined and analysed using the Affymetrix Expression Console using the MAS5 algorithm for normalisation. Affymetrix CEL file data were analysed using QLUCORE OMICS EXPLORER to obtain a list of genes that were differentially regulated in CD9KO cells compared to CD9WT cells. Principle component analysis (PCA) of the expression levels of all probe sets on the array data (in three independent experiments) showed that the data clustered in two goups according to the similarity of the data in each group (Figure 5.3.21). All statistical calculations were carried out using logarithmic values of signals to base 2 (Bayatti et al., 2014). Further analysis was carried out using the bioinformatics tool DAVID (Huang da et al., 2009). About 45,000 transcripts that were detected at least in these arrays were included in this analysis. Differentially expressed genes between CD9 knockout and wild type were determined by Two Group Comparison (t-test). There were 788 down-regulated and 263 up-regulated transcripts showing a one fold change at p-value <0.05, whereas there were 147 down-regulated and 48 upregulated transcripts showing one fold change at p<0.01 in CD9KO cells relative to CDWT cells. At p<0.05 with a fold change of 1.5 there were only 6 down-regulated and 3 upregulated genes.
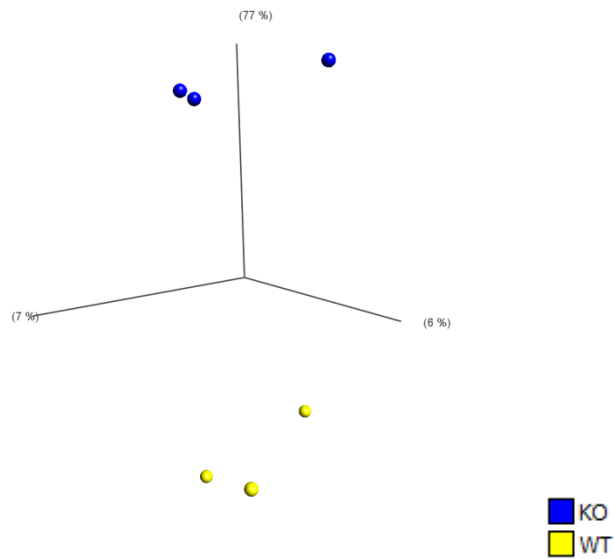
Figure 5.3.21 Principal component analysis (PCA) of the expression levels of probe sets of three independent experiments. The analysis was performed using QLUCORE OMICS Explorer. The dots represent the arrays that are clustered in two groups.

Five genes in addition to CD9 were shown to be down-regulated in CD9 knockout cells; X-inactive specific transcripts, Smpi3a (sphingomyelin phosphodiesterase, acid-like 3A) and Cdkn2a (cyclin-dependent kinase inhibitor 2A). Three genes were showed to be up-regulated in CD9KO: PVL3 (poliovirus receptor-related 3) and SPINK5 (serine peptidase inhibitor kaza type5) Figure 5.3.22, table 5.3.1.
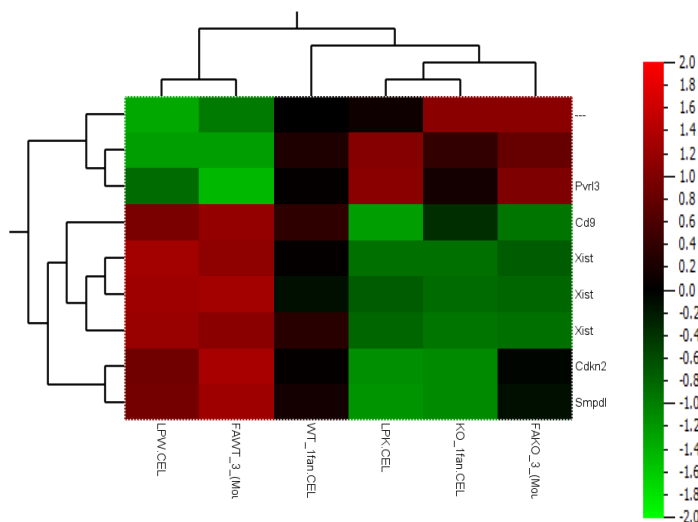
Figure 5.3.22 Genes that are differentially expressed in CD9KO cells compared to wild type. Red represents up-regulated genes, green represents down-regulated genes, at p< 0.05 t-test and fold change 1.5.

Gene ID	Gene Symbol	Gene Title	p-value	Difference
1427263_at	Xist	inactive X specific transcripts	0.003409	-1.28359
1416066_at	Cd9	CD9 antigen	0.009066	-0.83892
1436936_s_at	Xist	inactive X specific transcripts	0.014853	-0.85036
1427262_at	Xist	inactive X specific transcripts	0.025858	-1.21228
1416635_at	Smpdl3a	sphingomyelin phosphodiesterase, acid-like 3A	0.028011	-0.91719
1437534_at	---	---	0.039206	0.707157
1450140_a_at	Cdkn2a	cyclin-dependent kinase inhibitor 2A	0.041312	-0.84293
1423331_a_at	Pvrl3	poliovirus receptor-related 3	0.045487	0.762419
1430567_at	Spink 5	Serine peptidase inhibitor kaza type5	0.045807	0.663089

Table 5.3.1 Differentially expressed genes (up- or down-regulated) by CD9 ablation in macrophages derived from CD9-/- mice compared to wild type cells. The list shows statistical analysis of normalized data log 2 and the significance was at p< 0.05 and fold change 1.5.

Gene ontology analysis of the genes up- or down-regulated by 1.5 fold at p<0.05 showed that genes related to protein metabolism and cell adhesion were those up-regulated gene in CD9KO cells, whilst genes related to leukocyte activation, cell growth and immune response were amongst the down-regulated genes in these cells (Table 5.3.2).

ID	Gene Name	Biological process
1416066_at	CD9 antigen	Membrane fusion, cell-cell junction assembly, cell adhesion, single fertilization, fusion of sperm to egg plasma membrane, negative regulation of cell proliferation, cellular component assembly involved in morphogenesis, membrane organization.

1450140_a_at	cyclin-dependent kinase inhibitor 2A	Regulation of cyclin-dependent protein kinase activity, regulation of cell growth, negative regulation of immune system process, regulation of leukocyte activation.
1427263_at, 1427262_at, 1436936_s_at	inactive X specific transcripts	Inactivation of X chromosome, regulation of gene expression
1430567_at	Serine peptidase inhibitor, Kazal type 5	Negative regulation of macromolecule metabolic process, regulation of cell adhesion, negative regulation of cellular protein metabolic process, negative regulation of proteolysis.
1416635_at	sphingomyelin phosphodiesterase, acid-like 3A	Membrane lipid metabolic process, phospholipid metabolic process, sphingolipid metabolic process.

Table 5.3.2 Biological processes associated with up/down-regulated genes in CD9-/-macrophages.
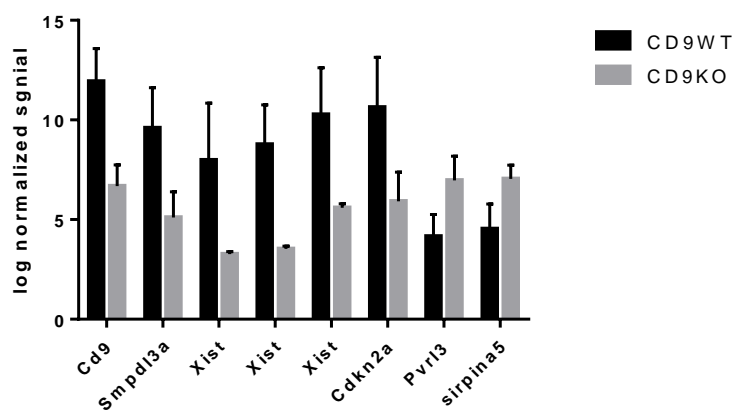
Figure 5.3.23 Histogram illustrating the expression levels (mRNA) of genes that are up/down-regulated significantly in CD9KO macrophage.

Although cell surface protein expression profiles for tetraspanins and for several fusion-associated molecules showed differences between CD9-/- and wild type cells, the gene profile analysis of these molecules showed no significant differences between the cell types (Figure 5.3.24).

A
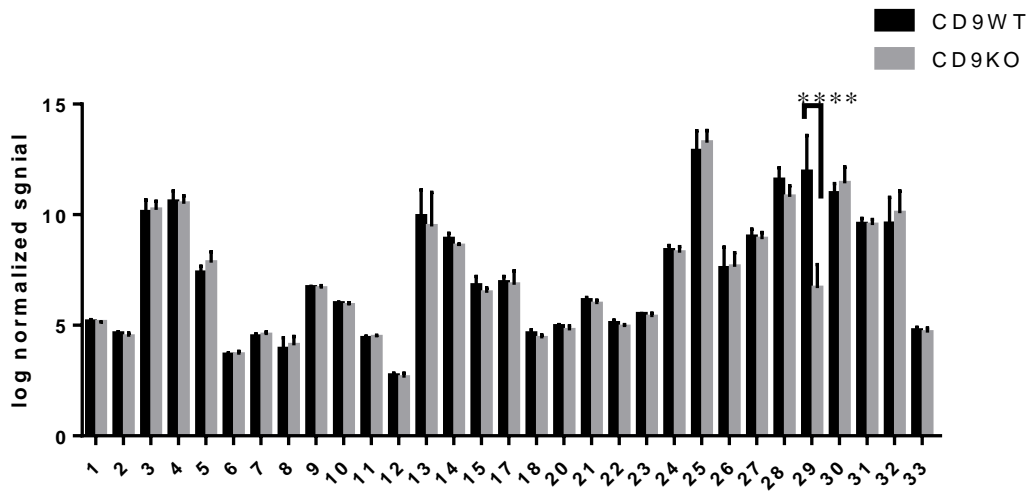
B
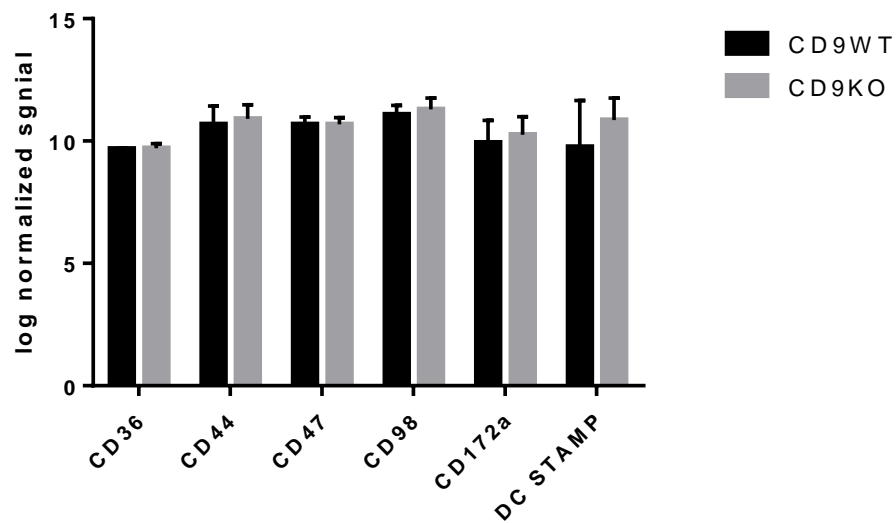
Figure 5.3.24 The expression levels (mRNA) of tetraspanins A, and fusion molecules B in CD9KO macrophages and wild type. In (A) the Tspan nomenclature (Tspan1 – Tspan33) is used rather than CD nomenclature (Tspan 29 = CD9).

5.4 Discussion

The results in this chapter provided more evidence for the role of tetraspanin CD9 in MNGC formation induced by *Burkholderia thailandensis*. We examined the effect of CD9 deficiency on bacterial invasion and MNGC formation. We also showed the involvement of CD82 in *B.t*-induced cell fusion.

5.4.1 Effect of CD9 knock-out on *Burkholderia thailandensis* uptake.

Initially the effects of the absence of CD9 on the number of intracellular bacteria within the infected CD9WT and CD9KO cells at MOI 3:1 was examined at different time points. The results revealed that the number of intracellular bacteria was higher in CD9KO compared with that within CD9WT cells. However, these increased numbers in CD9KO cells was only significant after 30 and 60 min post infection. In a comparable study, the infection rate of *Salmonellas typhimurium* at MOI 5:1 and 30 min post infection was found to be higher in CD9KO cells compared with CD9WT cells (Fawwaz Ali, personal communication). However, after 90 and 120 min post infection the differences in the number of internalized *B.t* become insignificant, suggesting that the effect of CD9 deletion on *B.t* uptake is time-dependent. However it may also suggest that the bacteria are initially taken up more readily by the CD9KO cells, but are then able to survive similarly in both cells. This result was in line with the results obtained with anti-CD9 antibodies and CD9EC2 proteins, where no significant difference was observed in the number of intracellular bacteria within untreated and treated J774 cells after 120min post infection (chapter 4), the time chosen as standard for the MNGC assay. To try to minimise effects caused by the variable load of bacteria in cell fusion 120min post infection was used to investigate the effect of CD9KO on *B.t*-induced MNGC formation.

5.4.2 Enhanced MNGC formation in CD9 Knock-out macrophages

The effect of CD9 deletion on *Burkholderia thailandensis*- induced cell fusion was investigated. Fusion index and MNGC size were both significantly higher in CD9KO cells relative to those of CD9WT cells. According to these result, a time course assay was performed and MNGC formation were assessed at different time points. The results showed a considerably earlier onset of MNGC formation in CD9 knockout cells compared with wild type cells. CD9KO cells showed a dramatic increase in MNGC formation after 11hr post infection; at 14hr post-infection the fusion index was about 6-fold higher in CD9KO cells and the MNGC were about four times larger in CD9KO cells relative to CD9WT cells. This data showed clearly that CD9 is involved in *B.t*-induced cell fusion leading MNGC formation. The early MNGC formation in CD9KO cells compared to CD9WT cells suggested that CD9 down regulation might be essential for the early onset of cell fusion induced by *B.thailandensis*. This data is in agreement with the previous findings of Takeda and co-workers, who showed enhanced MNGC formation in the absence of CD9 in vivo in response to *Propionibacterium acnes* and in vitro in response to Con A (Takeda, Tachibana et al. 2003). These finding suggested that CD9 negatively regulated MNGC formation. In contrast, CD9 was shown to be a positive regulator for sperm/oocyte fusion, as the fertility of CD9 null mice is reduced due to the reduction in sperm-egg fusion (Le Naour et al., 2000).

5.4.3 CD9 abrogation affected the expression level of other fusion-related proteins

To gain insight into the function of CD9 in cell fusion and MNGC formation, the effect of CD9 deletion on the expression level of several cell membrane proteins that have been associated with cell fusion was examined using flow cytometry analysis. The expression level of these molecules on CD9KO cells were compared with their expression level on wild type cells. Two parameters were used to assess the level of the expression; the intensity of staining of the antigen on cell surface and the percentage of cells that positively expressed the antigen, with the data were normalized relative to the isotype control for each antigen. The results showed a significant decrease in the level of CD81 on CD9KO cells relative to its expression on CD9WT cells, while CD63 showed a comparable extra/intracellular expression levels in both cell lines. This data indicated that the deletion of CD9 gene influences the expression of CD81 at the protein level. These two molecules are known to be relatively close and have been linked and associated with several biological processes. A similar role for CD9 and CD81 in cell fusion and MNGC formation has been demonstrated; MNGCs were spontaneously induced in CD9/CD81 double-null mice (Takeda et al., 2003). Although myoblasts isolated from CD9 or CD81 null mice showed normal fusion, those form CD9/CD81 double null mice showed greatly enhanced fusion, suggesting an integrated role for CD9 and CD81 in this process (Charrin et al., 2013). In addition, the deletion of CD9 or CD81 severely or partly inhibited sperm-oocyte fusion respectively, however, fusion was completely inhibited in mice lacking both CD9 and CD81 (Le Naour et al., 2000, Rubinstein et al., 2006). The comparable role for CD9 and CD81 in these fusion process are likely due to their highly identity and their ability to interact with same partner proteins including EWI-1 and CD9P-1 (Stipp et al., 2001, Charrin et al., 2001). Charrin and co-workers showed that CD9P-1 and EWI-1 associated with CD9 and CD81 on primary myoblasts and this interaction was thought to regulate the fusion of myoblast (Charrin et al., 2013). Also the interaction of CD9 and CD81 regulated CD9P-1 induced cell motility through a β1-integrin dependent mechanism (Chambrion and Le Naour, 2010). With regard to monocyte fusion, Takeda and co-workers showed that CD9 and CD81 form a complex with β1 and β2 integrins in freshly isolated blood monocytes and this complex was up-regulated in normal condition; however under fusogenic conditions this complex was down regulated, suggested significance of this complex in regulating MNGC formation (Takeda et al., 2003).

For further investigation, the expression levels of scavenger receptor CD36, immunoglobulin superfamily member CD47 and its receptor CD172a, type II integral membrane protein CD98, integral membrane glycoprotein CD44, and dendritic cell-specific transmembrane protein DC STAMP were also examined by FACS analysis in CD9KO cells in comparison with their levels on CD9WT cells. These molecules have been implicated in cell fusion (reviewed in 5.1.2). The data revealed that CD36 and CD44 showed lower expression levels in CD9KO cells relative to their expression on CD9WT cells, whereas DC-STAMP showed an increased expression level in CD9KO cell compared to that of CD9WT. CD47, CD98 and CD172a have a comparable expression level on both cell lines, despite the percentage of positive cells that expressed CD172 being lower on CD9KO cells. This data suggested that the absence of CD9 on cell fusion could influence the levels of cell surface molecules that facilitate cell fusion and MNGC formation.

CD9 has been associated with CD44 (Jones et al., 1996, Toyo-oka et al., 1999, Yashiro-Ohtani et al., 2000) and with CD47 (Longhurst et al., 1999). The interaction between CD9 and CD98 has been implicated in sperm-oocyte adhesion and fusion, by promoting sperm

ADAMs and multiple egg β1 integrins interactions leading to sperm-egg binding and fusion (Takahashi et al., 2001). CD9 has also been shown to associate with CD36 (Miao et al., 2001, Kazerounian et al., 2011). On macrophages the loss of this association by deletion of CD9 led to significant decrease in CD36-mediated foam cell formation (Huang et al., 2011).

CD9 has been linked with DC-STAMP in osteoclast formation. It has been shown that DC-STAMP is internalized in some RANKL-stimulated osteoclasts precursors (DC-STAMP[lo]), which following interaction with DC-STAMP ligand and became "master fusogens". By contrast, cells that had not internalised DC-STAMP (DC-STAMP[hi]) acted only as mononuclear donors. Interestingly gene expression analysis showed that the transcript levels of CD9 and CD47 were upregulated in the DC-STAMP^{lo} cells, whereas the levels of CD44 and CD172a were higher in DC-STAMP[hi]. These findings suggested the possibility of the involvement of these molecules in DC-STAMP-mediated osteoclast fusion (Mensah et al., 2010).

5.4.4 Gene expression profile of CD9WT and CD9KO cells

Since the deletion of CD9 gene affected the expression of several cell surface molecules at the protein level, we aimed to investigate its possible effects on the expression at gene level. Therefore, the gene expression profiles of CD9 wild type cells and CD9 deficient cells were examined using microarray analysis and differentially expressed genes between CD9KO and wild type were determined. The results revealed that none of the molecules that are expressed differentially on CD9KO cells relative to CD9WT cells at protein level was expressed differentially at gene level. The reduction or increase in the surface expression of these molecules was therefore not because of changes in gene expression, but more likely to be due to changes protein processing or trafficking. This is perhaps not surprising, as tetraspanins have often been shown to regulate trafficking of cell surface expression of proteins they interact with. For example, tetraspanins have been shown to modulate expression of membrane type-1 matrix metalloproteinase (Schroder et al., 2013) and CD81 is known to regulate expression of the B cell marker CD19 (Shoham et al., 2003).

However, there were several genes including CD9 found to up/down regulated in CD9KO cells compared to WT cells at p<0.05 (t.test) and by 1.5 fold change. In addition to CD9, X-inactive specific transcripts, Smpi3a (sphingomyelin phosphodiesterase, acid-like 3A) and Cdkn2a (cyclin-dependent kinase inhibitor 2A) were found to be down-regulated in CD9 KO cells. PVL3 (poliovirus receptor-related 3) and SPINK5 (serine peptidase inhibitor kaza type5) were found to be up-regulated in CD9KO relative to that of CD9WT cells.

Smpdl3a has been identified as a cholesterol-regulated gene and encodes Sphingomyelin Phosphodiesterase Acid-Like 3A (SMPDL3A) protein. Its mRNA, intracellular expression protein and secretion are up-regulated in response to increased cholesterol levels in macrophages and also to liver X receptor ligand (LXR) in monocytes and macrophages, suggesting a role in lipid metabolic processes (Traini et al., 2014, Noto et al., 2012).

The Cdkn2a is an important tumour suppressor gene that arrests cell cycle in G1 phase; this gene encodes the p14/ARF and p16/INK4A proteins that are expressed from related mRNAs that differ in exon-1 and exon-2 and are subsequently translated in distinct reading frames (Jennings et al., 2015). P14 and p16 belong to the family of cyclin dependent kinase inhibitors (CDKIs) that modulate the activity of cyclin dependent kinase (CDK) cell cycle regulators, for instance the expression of p16/INK4A results in inhibition of CDK-4/6 activity

at the G1/S checkpoint in the cell cycle (Burke et al, 2014). The disruption of CDKN2a is often associated with more aggressive tumours, while reconstitution of their expression in tumour cell lines results in cell cycle arrest; this evidence suggests they function as tumour suppressors (Tanner et al., 2000, Wong et al., 2002, Serrano, 1997, Agarwal et al., 2013, DeInnocentes et al., 2009).

The Pvrl3 gene encodes poliovirus receptor-related 3 protein, which is also known as nectin-3 or CD113. Nectin-3 is member of immunoglobulin superfamily which also includes nectin-1 and nectin-2. Nectins have been essentially described as cell adhesion molecules that promote the formation of adhesion and tight junctions in epithelial cells (Takai et al., 2003, Takai and Nakanishi, 2003). Nectins are involved in cell processes such as migration, proliferation and polarization though their interactions with adhesion-molecules including integrins, cadherins and growth factor receptors (reviewed in (Takai et al., 2008)). These molecules have also been associated with tetraspanins. Recently studies reported that the expression of nectin-3 can be an a prognostic factor for lung adenocinoma and pancreatic cancer (Izumi et al., 2015).

The Spink 5 gene, encodes the serine peptidase inhibitor kaza type5, also known as Lympho-epithelial Kazal-type-related inhibitor (LEKTI), which controls the homeostasis of epithelial tissue (Galliano et al., 2005). Spink 5 has been identified as the gene defective in Netherton syndrome, a severe autosomal recessive skin disorder (Chavanas et al., 2000, Judge et al., 1994). The effect of recombinant LEKTI protein in inhibiting the activity of plasmin, trypsin, subtilisin A, cathepsin G, and elastase suggested its role in functions associated with tissue homeostasis and disorders (Mitsudo et al., 2003, Descargues et al., 2005).

The interaction of tetraspanins with these molecules has not to our knowledge been reported. With the exception pg Pvrl3 these genes have no obvious link to cell fusion.

5.4.5 Tetraspanin CD82 negatively regulate B.t-induced MNGC formation

CD82/ KAI1 is a metastasis suppressor in various tumour cells and its role in this process has been widely studied. However, a role for CD82 in MNGC formation has not to our knowledge been reported. It was of interest to examine the effect of knock-out of another tetraspanin apart from CD9 and here we aimed a preliminary characterisation of the role of CD82 in *B.t*-induced cell fusion.

Initially the effect of CD82 knock-out on *B.t* uptake was examined, and data in general showed that the efficiency of bacteria uptake was higher in CD82WT cells than in CD82KO cells. A significant reduction in the number of intercellular *B.t* CDC was shown within CD82KO compared to that of CD82 cells, while the reduced of *B.t* E264 uptake by CD82KO cell was insignificant. Notably, in a comparable study, the absence of CD82 showed no effect on *Salmonella typhimurium* uptake (Fawwaz Ali, personal communication). This data may suggest some selective involvement of CD82 in *B.t* CDC uptake by macrophages. CD82 has been linked with the infection of HIV and HTLV-1 and has also been shown to be recruited to the phagosome after uptake of fungal pathogens including *Cryptococcus neoformans, Candida albicans* and *Aspergillus fumigatus*, as well as bacterial pathogens including; *Staphylococcus aureus* and *Escherichia coli* (Artavanis-Tsakonas et al., 2011). Based on our results it would be interesting to perform further investigations on the involvement of CD82 in *B.t* uptake, which was not the main aim in this present study.

The next step was to investigate the effect of the loss of CD82 on *B.t*-induced MNGC formation. The result indicated a contribution of CD82 to the formation of MNGC, as CD82KO cells were found to undergo MNGC formation earlier and more rapidly than CD82WT cells. Despite CD82KO being less efficient in bacterial uptake, they were about 10 times more active in the formation of giant cells in response to *B.t* infection. This indicates that CD82 may be positively involved in bacteria uptake, however may also negatively be involved in *B.t*-induced MNGC formation. This data also suggested that the induction of cell fusion in such cell lines does not depend directly on the load of intracellular bacteria. Our finding is in line with previous results showing that CD82 negatively regulates cell fusion. CD82 has specifically been implicated in HTLV-1-induced syncytium formation (Fukudome et al., 1992, Imai et al., 1992, Imai and Yoshie, 1993). The co-expression of CD82 proteins with HTLV-1 envelope glycoproteins inhibited the syncytium formation, whereas CD82 proteins had no effect on HIV-1 envelope protein-induced syncytium formation (Pique et al., 2000). . CD82 also suppressed cell-to-cell transmission of HTLV-1 (Pique et al., 2000).

CD82 was identified as a metastasis suppressor gene (Dong et al., 1995). Down-regulation of CD82 expression is widely associated with the advanced stages of many types of cancer (Tonoli and Barrett, 2005, Miranti, 2009). CD82 suppression of metastasises likely due to the inhibition of multiple processes including proliferation, motility, invasion and apoptosis by modulating the activity and the trafficking of molecules essential for metastasis (Tsai and Weissman, 2011). CD82 organizes E-cadherin-mediated intercellular adhesion of cancer cells, thus preventing the migration of cancer cells from the primary site of the tumour (Abe et al., 2008). The expression of CD82 was showed to attenuate the integrin α6-mediated cell adhesion in prostate cancer cell lines; upon the expression of CD82 the surface expression of integrin α6 was reduced and that was in conjunction with the enhanced internalization of α6 (He et al., 2005). CD82 has also been found to regulate integrin α4β1-medated erythroblasts adhesion; anti CD82 antibody enhanced the adhesion of proerythroblasts to Vascular Cell Adhesion Molecule-1 (VCAM-1) on macrophages and extracellular matrix fibronectin (Spring et al., 2013). CD82 was found to enhance the adhesion of hematopoietic stem cells (HSPC) to the marrow microenvironment, by utilizing super resolution microscope, CD82 was found to regulate the membrane organization of α4 integrin; CD82 over-expression enhanced the density of α4 within the cell membrane leading to increased cell adhesion (Termini et al., 2014). These findings suggest a variable mechanisms of CD82 in regulating integrin- mediated cell adhesion.

To gain deeper insight into the effect of the absence of CD82 on the cells characters and behaviour, the expression of cell surface proteins (CD36, CD47, CD44, CD98, CD172a and DC-STAMP) were assessed in comparison with that of wild type. Flow cytometry analysis showed that, in regard of staining intensities, the level of CD98 and CD172a were significantly lower in CD82KO. The reduction in the level of CD44 and the increased level of DC-STAMP were insignificant, although it should be noted that these experiments were only performed three times in duplicate due to time constraints. CD36 showed comparable levels in both cell lines. In addition the percentage of cells that expressed CD44 and CD172 were also reduced by 50% and 30% respectively in CD82KO cells compared to wild type. CD82 has been found to interact with cell adhesion molecules including CD44; endothelial cells lacking CD82 showed enhanced migration and invasion, due to the increased levels of cell adhesion molecules including integrins and CD44 on the cell surface, in contrast to the preliminary data presented here (Wei et al., 2014). CD9 and CD82 were found to be down-

regulated in metastatic cell lines compared to their level on primary tumour cells; despite CD44 being associated with the tetraspanin web on these cells its expression levels showed no change here (Le Naour et al., 2006). The effect of CD82 on expression of CD44 (and other molecules) may therefore vary between cell types.

5.3.6 Electron microscopy

For further investigation the phenotype associated with infected CD9-/- and CD82-/- was examined at high magnification using electron microscopy. The observation of micrographs revealed bacteria located at different stages of uptake and cellular events. Bacteria were found to be within phagosomes, where some damaged bacteria can be detected and other free bacteria were observed in the cytosol. In addition intracellular actively replicating bacteria can also be noted. The bacteria within vacuoles which were adjacent to the cell membrane were observed, which may be in the process of endocytosis or exocytosis. Notably intact bacteria were also observed within extracellular vesicles suggesting another mechanism for bacteria transmigration and survival. It has been demonstrated that *B.t* as well as *B.p* promote escape from endosomes using T3SS-3 (Haraga et al., 2008, Galyov et al., 2010, French et al., 2011).The analysis of *B.p*-infected RAW by EM microscopy showed that T3SS-3 mutant bacteria are significantly less efficient in the phagosome escape compared to wild type (Gong et al., 2015). It has also been shown that *B.p* remain viable within macrophages due to a reduced level of phagosome-lysosomal fusion (Puthucheary and Nathan, 2006); this EM study showed that efficient in phagosome-lysosomal fusion was reduced in macrophages of melioidosis patients, suggesting the importance of these mechanisms in bacterial clearance.

Close contact of adjacent cells was observed and in some regions the discontinued plasma membrane between two adjacent cells can be distinguished where two cells seem to share the same cytosol, suggests that macrophage fusion induced by *B.t* is likely to be in processes. The mechanism is similar to that proposed by Takito, which revealed that the attachment of two macrophages is followed by a delay before fusion and this delay is thought to be required for forming of a temporary actin superstructure named the zipper-like structure at the contact site. This structure disappears from a small area where the site of fusion was initiated and with time the gap is expanded in parallel with plasma membrane deformation following membrane fusion, resulting in the fusion of podosome belts of distinct osteoclasts (Takito and Nakamura, 2012).

5.3.7 The distribution of CD9 on MNGCs

The confocal images showed that the CD9 is densely and quite evenly expressed at the cell periphery on uninfected cells, whilst on MNGC CD9 is restricted to patches on the cell membrane with relatively weak staining on other areas. Interestingly, the confocal images showed that the distribution of CD9 on MNGCs was more obvious in two areas; at perinuclear and at the region of MNGC-unfused cell contact. Widefield images also confirmed these observations. These finding are in line with Takeda and co-workers observations, where CD9 staining on murine macrophages was shown to be weak under fusogenic condition (Takeda et al., 2003). Our observations indicate that although CD9 shows less even distribution on cell membrane of MNGC, it is also more condensed in cell-

cell connect area suggesting the involvement of CD9 in processes that precede the fusion for instance cell movement and/or cell adhesion. Interestingly CD9 has been shown to control the clustering of membrane proteins including integrin α 6 β1 involved in sperm-egg fusion (Ziyyat et al., 2006) It would be interesting in future to examine the co-localisation of CD9 and integrins on infected cells. Widefield microscope images showed that CD9 clustered near cell-cell contact area that are likely to correspond to the pore opening stage and showed co-localisation with the bacteria. Symeonides and co-workers suggested that the over expression of CD9 and CD63 inhibited HIV-1-induced cell-cell fusion at a post-hemifusion stage, and tetraspanin may interact with host cell or viral factors that control fusion pore stabilisation and/or expansion (Symeonides et al., 2014). In our case of *B.t*-induce fusion we found that CD9 deficiency resulted in enhancement in cell-cell fusion. It might be tempting to speculate that if CD9 is a negative regulator of fusion, infection induces clustering of CD9 away from areas of the membrane where fusion is initiated, but future studies would be necessary to understand the mechanism by which CD9 is involved in *B.t*-induced fusion.

Chapter 6 General discussion

Tetraspanins are cell membrane proteins that facilitate various cell functions such as activation, trafficking and adhesion. Their role in different fusion processes has also been demonstrated including sperm-egg fusion (Le Naour et al., 2000, Miyado et al., 2000a, Kaji et al., 2002, Ziyyat et al., 2006, Zhou et al., 2009, Jankovicova et al., 2015), muscle fusion (Tachibana and Hemler, 1999, Charrin et al., 2013), virus-host cell fusion and virus-induced cell-cell fusion (Fukudome et al., 1992, Imai et al., 1992, Gordon-Alonso et al., 2006, Weng et al., 2009, Nydegger et al., 2006, Singethan et al., 2008, Symeonides et al., 2014)and monocyte/macrophage fusion (Takeda et al., 2003, Parthasarathy et al., 2009, Ishii et al., 2006, Yi et al., 2006, Hulme et al., 2014).

Monocyte/ macrophage fusion is a feature of granulomatous inflammation associated with chronic infections; for instance tuberculosis, fungal infection and HIV, as reviewed in (Kumar et al., 2013). However, the exact role of MNGCs in infection remains unknown. Although it has been suggested that MNGCs may limit the cell-cell spread of infection, they may cause inflammatory damage in infected tissues (Byrd, 1998). *Burkholderia pseudomallei* the causative agent of melioidosis, induces cell-cell fusion leading to multinucleated giant cell formation; however in this case MNGC formation is correlated with pathogenesis and appears to be used by the bacterium as means of cell-cell spreading (Wong et al., 1995). However, the mechanism of these processes is not fully understood.

In this study the role of tetraspanins in *Burkholderia thailandensis*-induced MNGC formation has been investigated. (*B.t.)* is a non pathogenic species that relatively closely related to *Burkholderia pseudomallei* (*B.p*.).

Initially, as described in chapter 3 the susceptibility of mouse and human cell lines to the infection with *B.t* was confirmed, and the appropriate conditions for *B.t*-induced MNGC formation in mouse macrophage cell lines J774.2 and RAW264.7 was optimized. The ability of *B.t* to induce cell fusion was examined in human monocyte cell lines THP1 and U937, in order to take advantage of the availability of anti human tetraspanin antibodies and these cells showed positive expression of several tetraspanin which was increased upon PMA stimulation. However, unfortunately the results obtained with these cells were not sufficient to assess MNGC formation by either the parameter of fusion index or MNGC size. After PMA stimulation U937 cells formed cell aggregates and thus it was difficult to determine whether these cells were fused or not. In addition, few MNGC were formed in infected THP1 cells, with only about five nuclei /MNGC, even when cells were incubated for up to 24hr. Therefore, the project was carried out using mouse macrophage cell lines. Notably, only a few antibodies against mouse tetraspanins were available at the time of performing this study, but these included anti CD9, anti CD63 and anti CD81. Flow cytometry analysis showed high expression levels of CD9 and CD81 on J774.2 and RAW264.7 cells with weak surface expression of CD63.

Previously Takeda and co-workers demonstrated roles for CD9 and CD81 in Con A-induced MNGC formation; anti CD9 and anti CD81 antibodies enhanced MNGC formation, whereas recombinant proteins representing CD9 EC2 inhibited cell fusion (Takeda et al., 2003). Similar results were also obtained by our research group; Parthasarathy and co-workers showed also the involvement of CD63￼ in this process as anti CD63 antibodies and recombinant CD63 EC2 proteins inhibited Con A-induced cell fusion. By contrast , CD81 and

CD151 GST-EC2 showed no effect (Parthasarathy et al., 2009) (Parthasarathy, PhD thesis, University of Sheffield, 2006). The results described in chapter 4 on the effect of tetraspanin-based reagents on MNGC formation induced by *B.t.* in the mouse macrophage cell lines were partly in line with these findings. The effects of anti-tetraspanin antibodies were compared with untreated cell or cells treated with corresponding isotype controls. The effects were tested by pre-treating cells with the antibodies before the infection and also by examining the effect of longer incubation with these antibodies during and after the infection. (The latter conditions more closely follow those used previously to investigate the role of tetraspanins in Con A induced MNGC formation of human monocytes.) In both cases, antibodies to CD9 and CD81 enhanced *B.t*-induced MNGC formation, as shown by a significant increase in fusion index and MNGC size. Pre-treatment of cells with anti CD63 showed no effect, whilst longer treatment with the antibody resulted in inhibition of MNGC formation. Pre-treatment of J774 cells with GST-EC2 proteins of CD9, CD63 and CD81 suppressed *B.t*-induced MNGC formation, whereas GST-EC2 proteins of CD151 and Tspan-2 had no effect. These data therefore suggests negative regulatory roles for CD9 and CD81 in *B.t*-induced MNGC formation. Despite the poor expression level of CD63, significant reduction was noted with long incubation with anti CD63 and pre-treatment with GST-EC2 CD63 proteins. The inhibition of fusion likely resulted from interaction with a molecule other than CD63, which could be another tetraspanin or another molecule of a different family. CD63 is known to interact with tetraspanins such as CD9, CD81, CD82 and CD151 and with other proteins including integrins such as β1 integrin, syntenin-1 and TIMP-1 (Berditchevski, 2001, Jung et al., 2006, Latysheva et al., 2006). Previous work in our group showed that CD9EC2 and CD63EC2 can bind specifically to Con A-stimulated monocyte which express relatively low levels of CD63 (Parthasarathy et al., 2009). In this case immunoprecipitation and pull-down assays may reveal the molecules that the tetraspanin EC2s are associating with.

Further investigation on the effect of EC2 proteins on *B.t*-induced MNGC formation were performed as discussed in chapter 4. Some previous work indicated that the inhibitory effect of CD9 EC2 protein in monocyte fusion was due to the contamination with LPS rather than direct effect of the EC2 protein (Marzieh Fanaei PhD thesis 2013). In fact there are contradictory reports about the activity of bacterial products on cell fusion, with some indicating that LPS could inhibit the monocyte fusion induced by Con A (Takashima et al., 1993) whereas other studies showed that bacterial cell wall proteins can stimulate MNGC formation (Tanaka and Emori, 1980) and enhance Con A-induced monocyte fusion(Mizuno et al., 2001a, Mizuno et al., 2001b, Parthasarathy et al., 2009). Other recent data showed an insignificant effect for LPS on Con A-induced MNGC formation(Hulme et al., 2014). Here we tested different batches of EC2 proteins (GST-CD9 and GST-CD9X where LPS in the protein was reduced).

Both GST-CD9 and GST-CD9X significant inhibited *B.t*-induced cell fusion, and there was no significant difference between the effects of GST-CD9 and GST-CD9X when cells were pre-treated with these reagents before the infection. However, long incubation with these proteins after the infection resulted in some inhibitory effect on MNGC formation with the GST control, as well for GST-CD9. This effect was reduced in GSTX; thus the difference between the effects of GST-CD9X and GSTX was statically significant. These results suggested a small and time dependent effect for LPS on EC2 activity. Pure LPS showed a slight effect on *B.t* CD272-induced cell fusion but not with *B.t* E264. Notably, almost all of the recombinant proteins tested in these studies are produced in bacteria, so it would be

expected that the possibility of LPS contamination is equal. As mentioned above, CD151 and TSPAN-2 had no effect on *B.t*-induced fusion, although the LPS content in these protein preparations was higher compared to the amount in the CD9-EC2 protein. In addition, CD63-EC2 produced in mammalian cells showed a similar inhibitory effect to that observed with CD63-EC2 produced in bacteria in *B.t*-induced MNGC formation. Overall, the data suggests that LPS has little contribution to the recombinant protein activity and the inhibition in *B.t*-induced MNGC formation is due to the EC2 proteins themselves.

It has been reported that human CD9 EC2 (where the GST tag has been removed) was slightly less active than GST-CD9 EC2, suggesting that GST contributes to the stability/activity of CD9 EC2 or that GST alone has weakly inhibitory effects in sperm-egg fusion (Higginbottom et al., 2003). However, Parthasarathy and co-workers reported similarly significant inhibitory effects for cleaved CD63 EC2, and highly purified his-tagged CD9 EC2 and CD63 EC2 compared to GST-CD63EC2 in Con A-induced cell fusion (Parthasarathy et al., 2009). It would be of interest to examine cleaved CD9 in the *B.t*-induced cell fusion assay.

It was important to determine whether the inhibitory effect of EC2 proteins was due to any cytotoxic/cytostatic effects. This was investigated using the SRB cytotoxicity assay. Pre-treatment of J774 cells with EC2 proteins for 2hr had no effect on the number of cells, however long incubation resulted in reduction in cell number at higher concentrations. This suggests that the long-term incubation with EC2s may affect cell functions shuch as adhesion or and proliferation which may affect the activity of these protein in cell fusion. Hovever other data from our research group showed no effect of EC2 proteins over 72hr incubation on human moncyte adhesion or cell number (Parthasarathy et al., 2009).

The effect of synthetic peptides corresponding to different regions of the CD9 EC2 have previously been shown to have activity similar to the intact EC2 in some biological assays (Daniel Cozens, Jenny Ventress, personal communication). Since the GST-CD9 EC2 proteins inhibited *B.t*-induced fusion, the effect of these peptides was also examined. Preliminary data showed no significant effect for these peptides on *B.t*-induced cell fusion. This suggests that the whole EC2 is needed to cause inhibition of fusion or that the regions of the EC2 that these peptides represent are not involved. However, these experiments were preliminary and it would be interesting to perform more investigations for example using different concentrations or combining the peptides.

A previous study showed that *B.p* but not *B.t* induced MNGCs are analogous to osteoclasts. *B.p* infected RAW 264 cells expressed osteoclast markers similar to those induced by RANKL, a stimulator of osteoclastogenesis, whereas the level of these markers in *B.t*-induced cells was similar to that of uninfected cells. The change in the level of these markers is correlated with the activation of *lfpA*, the gene for lactonase family protein A, which is absent in *B.t* (Boddey et al., 2007). CD9 has been found to positively regulate osteoclastogenesis; anti CD9 antibodies inhibit osteoclast formation whereas over expression of CD9 enhances this process (Yi et al., 2006, Ishii et al., 2006). Herein, CD9 was found to negatively regulate *B.t*-induced MNGC formation, which is similar to its role in Con A-induced monocyte fusion. It has been reported that Con A induced MNGC formation have characteristics that mimic Langhans giant cells (Parthasarathy et al., 2009). *B.p* and *B.t* infection caused a similar cytokine production profile in human monocyte-derived dendritic cells (Horton et al., 2012). The cytokine response to *B.t* infection in the presence or absence of tetraspanins has not been investigated in this study, nevertheless, Takeda and co-

workers noted that anti CD9 and anti CD81 antibodies had no effect on the production of cytokines by Con A-stimulated monocytes (Takeda et al., 2003). In conclusion, whether tetraspanins could have similar or different effects on *B.p*-induced MNGC formation would be interesting to investigate, but that would require category 3 containment facilities.

Our data suggests that CD9 and CD81 negatively regulate cell fusion induced by *B.t,* since anti CD9 and anti CD81 enhance MNGC formation while EC2 proteins of CD9 and CD81 inhibited this process. More evidence for the role of CD9 was obtained from the examining *B.t*-induced fusion in macrophages derived from CD9-/- mice. The data appear to confirm that CD9 negatively regulates MNGC formation induced by *B.t.*, as discussed in chapter 5. CD9KO cells showed enhanced MNGC formation compared to the wild type control cell line. A time course experiment showed that the fusion event started earlier in infected CD9KO cells and there was a dramatic increase in fusion index and MNGC in these cells with the time compared to WT cells. This is in agreement with Takeda and co-workers, where alveolar and bone-marrow derived macrophages from CD9 null mice and CD81 null mice showed enhanced MNGC formation in response to *Propionibacterium acnes* in vivo and in vitro. In addition CD9/CD81 double knockout mice exhibited spontaneous MNGCs in the lung and enhanced osteoclastogenesis in the bone. In contrast, the same group noted that CD9 appeared to be essential for *P.acnes*-promoted hepatic granuloma formation in vivo, as CD9 null mice showed bacterial dissemination and a reduction in the number and size of granulomas compared to wild type (Yamane et al., 2005). In addition, the induction of granuloma-inducing cytokines, TNF-alpha and IFN-gamma, was delayed and chemotactic activity for macrophages was inhibited in the liver of CD9 null mice. CD9 expression was-upregulated on *P.acnes*-infected hepatocytes in wild type mice, although its expression levels on monocyte recruited into granulomas was low (Yamane et al., 2005). It would be interesting to perform in vivo studies to find out the role of CD9 in such immune responses to *Burkholderia* infection.

Observations of CD9 distribution in *B.t.* infected cells by confocal microscope and widefield microscopy revealed that, on uninfected cells CD9 was densely and quite evenly expressed at the cell periphery, whilst on MNGC CD9 is restricted to patches on the cell membrane with relatively weak staining on other areas. CD9 did not appear to co-localise with the bacteria at the cell periphery. Notably, the distribution of CD9 on MNGCs was more obvious in two areas; at perinuclear and at the region of MNGC-unfused cell contact. These finding are in line with Takeda and co-workers observations, where CD9 staining on murine macrophages was shown to be weak under fusogenic condition and they noted that CD9 stain was weak in cell-cell contact regions (Takeda et al., 2003). In contrast, our observations indicate that although CD9 shows less even distribution on cell membrane of MNGC, it is also more condensed in cell-cell connect area suggesting the involvement of CD9 in processes that precede the fusion for instance cell movement and/or cell adhesion. Interestingly CD9 has been shown to control the clustering of membrane proteins including integrin α 6 β1 involved in sperm-egg fusion (Ziyyat et al., 2006). It would be interesting in future to examine co-localisation of CD9 and integrins on infected cells. It is tempting to speculate that if CD9 is a negative regulator of fusion, *B.t.* infection induces clustering of CD9 away from areas of the membrane where fusion is initiated, but further image analysis is necessary.

A role for CD82 in *B.t*-induced fusion has also been shown, using macrophages derived from CD82 null mice and corresponding wild type cells. Initially, the rate of bacteria uptake was tested and wild type cells were found to be more susceptible to the infection than

CD82KO cells. CD82 has been linked with the infection of HIV and HTLV-1 and has also been shown to be recruited to the phagosome after uptake of fungal pathogens including *Cryptococcus neoformans, Candida albicans* and *Aspergillus fumigatus*, as well as bacterial pathogens including *Staphylococcus aureus* and *Escherichia coli* (Artavanis-Tsakonas et al., 2011). It would be interesting to perform further investigations on the involvement of CD82 in *B.t* uptake. With regard to MNGC formation, CD82KO cells were found to undergo cell-cell fusion more readily than wild type cells, suggesting that CD82 also negatively regulates *B.t*-induced MNGC formation. CD82 has specifically been implicated in HTLV-1-induced syncytium formation (Fukudome et al., 1992, Imai et al., 1992, Imai and Yoshie, 1993). The co-expression of CD82 with HTLV-1 envelope glycoproteins inhibited the syncytium formation, although CD82 expression had no effect on HIV-1 envelope protein-induced syncytium formation (Pique et al., 2000). CD82 expression also suppressed cell-to-cell transmission of HTLV-1 (Pique et al., 2000).

The effects shown with anti-tetraspanin antibodies and EC2 proteins on *B.t*-induced MNGC formation in J774 cells was not due effects on bacterial uptake, as these reagent showed slight or no effect on the number of intracellular bacteria under the conditions used in MNGC formation assay. CD9KO cells showed greater uptake of bacteria at 30 and 60 minutes post infection compared to wild type, however after 90 and 120 minutes post infection the number of intracellular in CD9KO cells and WT cells was comparable. In contrast, CD82WT cells were shown to be more susceptible to the infection; after 120 minutes post infection the number of intracellular bacteria in WT cells was significantly higher compared to CD82KO cells, suggesting the importance of CD82 in bacteria uptake. The role of tetraspanins in infectious disease has been demonstrated (Monk and Partridge, 2012). The effect of tetraspanins in bacterial adhesion and internalisation is of interest to our research group: Green and co-workers showed an inhibitory effect of anti tetraspanin CD9, CD63 and CD151 but not CD81 antibodies on bacterial adhesion to epithelial cells including adhesion of *Neisseria meningitides, Staphylococcus aureus and Escherichia coli* (Green et al., 2011) as discussed in greater detail in Chapter 3.

Electron micrographs of infected cells revealed the bacteria in different stages of phagosomal maturation. Morphologically-appearing live bacteria were located within phagosomes, some of them were damaged and others free in the cytosol. In addition intracellular actively replicating bacteria can also be observed. The bacteria also are seen within vacuoles that adjacent to the cell membrane, which might be in the process of endocytosis or exocytosis. Notably intact bacteria were also observed within extracellular vesicles suggesting another mechanism for bacteria transmigration and survival. *B.t* as well as *B.p* promote escape from endosomes using T3SS-3 (Haraga et al., 2008, Galyov et al., 2010, French et al., 2011).The analysis of *B.p*-infected RAW by EM microscopy showed that T3SS-3 mutant bacteria are significantly less efficient in the phagosome escape compared to wild type (Gong et al., 2015). *B.p* was shown to remain viable within macrophages due to a reduced level of phagosome-lysosomal fusion (Puthucheary and Nathan, 2006); this EM study showed that efficient phagosome-lysosomal fusion was reduced in macrophages of melioidosis patients, suggesting the importance of these mechanisms in bacterial clearance. It has also been showed that *B.p* are able to evade autophagy, a multifunctional, intracellular process that is important for protecting eukaryotic cells and maintaining intracellular homoeostasis (Devenish and Lai, 2015).

We noted that CD9KO and CD82KO cells seemed to be more sensitive to the infection as they showed apoptotic and necrotic cell characteristics more often compared to the wild type (data not shown), which may indicate a contribution of these proteins to the bacterial life cycle. Further investigation is needed to elucidate this phenomena using immunogold labelling for CD9 and CD82 and that would provide obvious details.

Close contact of adjacent cells was observed and in some regions the discontinued plasma membrane between two adjacent cells can be distinguished where two cells seem to share the same cytosol, suggesting that macrophage fusion induced by *B.t* is likely to be in process. The mechanism is similar to that proposed by Takito, which revealed that the attachment of two macrophages is followed by a delay before fusion and this delay is thought to be required for forming of a temporary actin superstructure named the zipper-like structure at the contact site. This structure disappears from a small area where the site of fusion was initiated and with time the gap is expanded in parallel with plasma membrane deformation following membrane fusion, resulting in the fusion of podosome belts of distinct osteoclasts (Takito and Nakamura, 2012).

We found that the deletion of CD9 as well as the deletion of CD82 affects the expression level of cell surface molecules that have been implicated in cell-cell fusion (discussed in chapter 5). CD9KO cells showed lower levels of CD81, CD36 and CD44, and higher levels of DC-STAMP relative to their level on wild type cells. These molecules have been associated with CD9 in fusion and other cell function (discussed in chapter5). Takeda and co-workers showed that CD9 and CD81 form a complex with β1 and β2 integrins in freshly isolated blood monocytes and this complex was up-regulated in normal conditions. However, under fusogenic conditions this complex was down regulated (Takeda et al., 2003), suggesting the significance of this complex in regulating MNGC formation. It would be interesting to look at the effect of CD9 deletion on the cell surface expression of these proteins. The interaction between CD9 and CD98 has been implicated in sperm-oocyte adhesion and fusion, by promoting sperm ADAMs and multiple egg β1 integrins interactions leading to sperm-egg binding and fusion (Takahashi et al., 2001). CD9 is also involved in DC-STAMP-mediated osteoclast fusion (Mensah et al., 2010).

The gene expression profiles of CD9KO and wild type showed that none of the molecules that are expressed differentially on CD9KO cells relative to CD9WT cells at the protein level was expressed differentially at gene level. The reduction or increase in the surface expression of these molecules was therefore not because of changes in gene expression, but more likely to be due to changes in protein processing or trafficking. This is expected, as tetraspanins have often been shown to regulate trafficking of cell surface expression of proteins they interact with. For example, tetraspanins have been shown to modulate expression of membrane type-1 matrix metalloproteinase (Schroder et al., 2013) and CD81 is known to regulate expression of the B cell marker CD19 (Shoham et al., 2003).

A role for several cell surface molecules including CD47, CD89 and CD172a in *B.p*-induced MNGC formation in human U937 cells has been suggested (Suparak et al., 2011). Monoclonal antibodies to these molecules inhibited MNGC formation whereas anti-CD44 had no effect. The expression levels of CD47 and CD98 was upregulated in infected cells, with the comparable levels of CD44 and CD172a. Our preliminary data showed that *B.t*-induced MNGC formation in J774 cells was also inhibited in cells treated with anti CD47 and anti DC-STAMP antibodies, whereas anti CD44 antibody enhanced *B.t*-MNGC. The expression level of CD9, CD81 and CD44 was down regulated after 3hr post infection,

whereas the level of DC-STAMP was upregulated. CD47 expression was at similar levels on infected and uninfected cells. It might be interesting to look at the effect of infection of fusion defective variants of *B.t* on the expression of these molecules to see if the changes relate to fusion. Suparak and colleagues propose that specific cell surface molecules of *B.p* infected-cells undergoing fusion may promote the attachment of cells and bring cell membranes into close contact and it is likely that *B.p* may facilitate this process by altering the surface expression of these molecules (Suparak et al., 2011).

The importance of T6SS-5 in *Burkholderia* induced cell fusion is well established (Schell et al., 2007, Shalom et al., 2007, Schwarz et al., 2010, French et al., 2011, Burtnick et al., 2011). Recently *B.p* has been shown to facilitate membrane fusion and intercellular spread, using the T6SS-5 spike protein VgrG5 (valine-glycine repeat protein). VgrG5 was found to be conserved and functionally interchangeable among *Burkholderia* species including *B.t*, *B.m* suggesting that they share a similar mechanism of cell-cell spread (Toesca et al., 2014). This group proposed a hypothesis for this mechanism: bacterial movement by flagella or actin polymerization generates the force needed to bring the membrane of infected cells into close position with adjacent cells, and then by membrane attachment or some of the T6SS-5 proteins the resulting energy drives the VgrG5 across the cell membranes, resulting a disordered zone then merging of the membranes. Although VgrG is required, they proposed that it is likely to be insufficient for fusion and additional bacterial effectors and cell membrane proteins are also required for perfecting this process (Toesca et al., 2014). Our work suggests that tetraspanins are amongst the host cell proteins that regulate the *B.t*- induced fusion. The fusion mechanisms of *B.t* and *B.p* are believed to be similar. Our finding that tetraspanins are involved in this processes, which related to *B.p* pathogenesis and spread may therefore relative to melioidosis disease.

Conclusion and Future Directions

This work was the first study that explored the involvement of tetraspanins in cell fusion induced by bacteria. Our data provide advances for the role of tetraspanins CD9, CD81 and CD82 in *B.thailandensis*-induced multinucleated giant cell formation. Further work might be performed following the results that have been shown in this thesis:

- Investigate the region of CD9EC2 that may be involved in the fusion process by using peptide fragments of CD9EC2.
- Investigate cell response to *B.t* infection by testing the cytokines produced in the presence and the absences of tetraspanins CD9 and CD82.
- In vivo assays using tetraspanins mutant mice would provide more detail about the involvement of tetraspanins in *B.t*-induced cell fusion.
- Further investigation is needed to elucidate the localization of CD9, CD82 and CD82 by EM using immunogold labelling for CD9, CD81 and CD82 and that would provide greater details.
- Investigating whether tetraspanins could have similar or different effects on *B.p*-induced MNGC formation would be interesting.
- Investigate the involvement of CD82 in *B.t* uptake and its possible role in bacterial pathogenesis.

- Investigate the mechanism by which tetraspanins involve in *B.t*-induced cell fusion for example study the interaction with cell membrane fusion molecules, which could be performed by using pull down assays, confocal microscopy or/and high resolution microscope.

References

ABE, E., SHIINA, Y., MIYAURA, C., TANAKA, H., HAYASHI, T., KANEGASAKI, S., SAITO, M., NISHII, Y., DELUCA, H. F. & SUDA, T. 1984. Activation and fusion induced by 1 alpha,25-dihydroxyvitamin D3 and their relation in alveolar macrophages. *Proc Natl Acad Sci U S A,* 81**,** 7112-6.

ABE, M., SUGIURA, T., TAKAHASHI, M., ISHII, K., SHIMODA, M. & SHIRASUNA, K. 2008. A novel function of CD82/KAI-1 on E-cadherin-mediated homophilic cellular adhesion of cancer cells. *Cancer Lett,* 266**,** 163-70.

AGARWAL, P., SANDEY, M., DEINNOCENTES, P. & BIRD, R. C. 2013. Tumor suppressor gene p16/INK4A/CDKN2A-dependent regulation into and out of the cell cycle in a spontaneous canine model of breast cancer. *J Cell Biochem,* 114**,** 1355-63.

AHMED, K., ENCISO, H. D., MASAKI, H., TAO, M., OMORI, A., THARAVICHIKUL, P. & NAGATAKE, T. 1999. Attachment of Burkholderia pseudomallei to pharyngeal epithelial cells: a highly pathogenic bacteria with low attachment ability. *Am J Trop Med Hyg,* 60**,** 90-3.

ALLWOOD, E. M., DEVENISH, R. J., PRESCOTT, M., ADLER, B. & BOYCE, J. D. 2011. Strategies for Intracellular Survival of Burkholderia pseudomallei. *Front Microbiol,* 2**,** 170.

ANDERSON, J. M. 2000. Multinucleated giant cells. *Curr Opin Hematol,* 7**,** 40-7.

ANGELISOVA, P., HILGERT, I. & HOREJSI, V. 1994. Association of four antigens of the tetraspans family (CD37, CD53, TAPA-1, and R2/C33) with MHC class II glycoproteins. *Immunogenetics,* 39**,** 249-56.

ANUNTAGOOL, N., INTACHOTE, P., WUTHIEKANUN, V., WHITE, N. J. & SIRISINHA, S. 1998. Lipopolysaccharide from nonvirulent Ara+ Burkholderia pseudomallei isolates is immunologically indistinguishable from lipopolysaccharide from virulent Ara- clinical isolates. *Clin Diagn Lab Immunol,* 5**,** 225-9.

ARJCHAROEN, S., WIKRAIPHAT, C., PUDLA, M., LIMPOSUWAN, K., WOODS, D. E., SIRISINHA, S. & UTAISINCHAROEN, P. 2007. Fate of a Burkholderia pseudomallei lipopolysaccharide mutant in the mouse macrophage cell line RAW 264.7: possible role for the O-antigenic polysaccharide moiety of lipopolysaccharide in internalization and intracellular survival. *Infect Immun,* 75**,** 4298-304.

ARTAVANIS-TSAKONAS, K., KASPERKOVITZ, P. V., PAPA, E., CARDENAS, M. L., KHAN, N. S., VAN DER VEEN, A. G., PLOEGH, H. L. & VYAS, J. M. 2011. The tetraspanin CD82 is specifically recruited to fungal and bacterial phagosomes prior to acidification. *Infect Immun,* 79**,** 1098-106.

AUWERX, J. 1991. The human leukemia cell line, THP-1: a multifacetted model for the study of monocyte-macrophage differentiation. *Experientia,* 47**,** 22-31.

AZORSA, D. O., HYMAN, J. A. & HILDRETH, J. E. 1991. CD63/Pltgp40: a platelet activation antigen identical to the stage-specific, melanoma-associated antigen ME491. *Blood,* 78**,** 280-4.

BALDER, R., LIPSKI, S., LAZARUS, J. J., GROSE, W., WOOTEN, R. M., HOGAN, R. J., WOODS, D. E. & LAFONTAINE, E. R. 2010. Identification of Burkholderia mallei and Burkholderia pseudomallei adhesins for human respiratory epithelial cells. *BMC Microbiol,* 10**,** 250.

BARANOVA, I. N., KURLANDER, R., BOCHAROV, A. V., VISHNYAKOVA, T. G., CHEN, Z., REMALEY, A. T., CSAKO, G., PATTERSON, A. P. & EGGERMAN, T. L. 2008. Role of human CD36 in bacterial recognition, phagocytosis, and pathogen-induced JNK-mediated signaling. *J Immunol,* 181**,** 7147-56.

BARREIRO, O., ZAMAI, M., YANEZ-MO, M., TEJERA, E., LOPEZ-ROMERO, P., MONK, P. N., GRATTON, E., CAIOLFA, V. R. & SANCHEZ-MADRID, F. 2008. Endothelial adhesion

receptors are recruited to adherent leukocytes by inclusion in preformed tetraspanin nanoplatforms. *J Cell Biol,* 183**,** 527-42.

BAYATTI, N., COOPER-KNOCK, J., BURY, J. J., WYLES, M., HEATH, P. R., KIRBY, J. & SHAW, P. J. 2014. Comparison of blood RNA extraction methods used for gene expression profiling in amyotrophic lateral sclerosis. *PLoS One,* 9**,** e87508.

BEATTY, W. L. 2006. Trafficking from CD63-positive late endocytic multivesicular bodies is essential for intracellular development of Chlamydia trachomatis. *J Cell Sci,* 119**,** 350-9.

BEATTY, W. L. 2008. Late endocytic multivesicular bodies intersect the chlamydial inclusion in the absence of CD63. *Infect Immun,* 76**,** 2872-81.

BENANTI, E. L., NGUYEN, C. M. & WELCH, M. D. 2015. Virulent Burkholderia species mimic host actin polymerases to drive actin-based motility. *Cell,* 161**,** 348-60.

BERDITCHEVSKI, F. 2001. Complexes of tetraspanins with integrins: more than meets the eye. *J Cell Sci,* 114**,** 4143-51.

BERDITCHEVSKI, F. & ODINTSOVA, E. 2007. Tetraspanins as regulators of protein trafficking. *Traffic,* 8**,** 89-96.

BERDITCHEVSKI, F., ZUTTER, M. M. & HEMLER, M. E. 1996. Characterization of novel complexes on the cell surface between integrins and proteins with 4 transmembrane domains (TM4 proteins). *Mol Biol Cell,* 7**,** 193-207.

BERRE, S., GAUDIN, R., CUNHA DE ALENCAR, B., DESDOUITS, M., CHABAUD, M., NAFFAKH, N., RABAZA-GAIRI, M., GOBERT, F. X., JOUVE, M. & BENAROCH, P. 2013. CD36-specific antibodies block release of HIV-1 from infected primary macrophages and its transmission to T cells. *J Exp Med,* 210**,** 2523-38.

BISHOP, B. L., DUNCAN, M. J., SONG, J., LI, G., ZAAS, D. & ABRAHAM, S. N. 2007. Cyclic AMP-regulated exocytosis of Escherichia coli from infected bladder epithelial cells. *Nat Med,* 13**,** 625-30.

BODDEY, J. A., DAY, C. J., FLEGG, C. P., ULRICH, R. L., STEPHENS, S. R., BEACHAM, I. R., MORRISON, N. A. & PEAK, I. R. 2007. The bacterial gene lfpA influences the potent induction of calcitonin receptor and osteoclast-related genes in Burkholderia pseudomallei-induced TRAP-positive multinucleated giant cells. *Cell Microbiol,* 9**,** 514-31.

BOUCHEIX, C., DUC, G. H., JASMIN, C. & RUBINSTEIN, E. 2001. Tetraspanins and malignancy. *Expert Rev Mol Med,* 2001**,** 1-17.

BOUCHEIX, C. & RUBINSTEIN, E. 2001. Tetraspanins. *Cell Mol Life Sci,* 58**,** 1189-205.

BOYLE, W. J., SIMONET, W. S. & LACEY, D. L. 2003. Osteoclast differentiation and activation. *Nature,* 423**,** 337-42.

BRETT, P. J., BURTNICK, M. N. & WOODS, D. E. 2003. The wbiA locus is required for the 2-O-acetylation of lipopolysaccharides expressed by Burkholderia pseudomallei and Burkholderia thailandensis. *FEMS Microbiol Lett,* 218**,** 323-8.

BRETT, P. J., DESHAZER, D. & WOODS, D. E. 1997. Characterization of Burkholderia pseudomallei and Burkholderia pseudomallei-like strains. *Epidemiol Infect,* 118**,** 137-48.

BRETT, P. J., DESHAZER, D. & WOODS, D. E. 1998. Burkholderia thailandensis sp. nov., a Burkholderia pseudomallei-like species. *Int J Syst Bacteriol,* 48 Pt 1**,** 317-20.

BRODBECK, W. G. & ANDERSON, J. M. 2009. Giant cell formation and function. *Curr Opin Hematol,* 16**,** 53-7.

BURTNICK, M. N., BRETT, P. J., HARDING, S. V., NGUGI, S. A., RIBOT, W. J., CHANTRATITA, N., SCORPIO, A., MILNE, T. S., DEAN, R. E., FRITZ, D. L., PEACOCK, S. J., PRIOR, J. L., ATKINS, T. P. & DESHAZER, D. 2011. The cluster 1 type VI secretion system is a major virulence determinant in Burkholderia pseudomallei. *Infect Immun,* 79**,** 1512-25.

BYRD, T. F. 1998. Multinucleated giant cell formation induced by IFN-gamma/IL-3 is associated with restriction of virulent Mycobacterium tuberculosis cell to cell invasion in human monocyte monolayers. *Cell Immunol,* 188**,** 89-96.

CANTOR, J. M. & GINSBERG, M. H. 2012. CD98 at the crossroads of adaptive immunity and cancer. *J Cell Sci,* 125**,** 1373-82.

CAO, X. Q., LIU, T. Y. & NAKHASI, H. L. 1992. The cis-acting 3'-element of rubella virus RNA has DNA promoter activity. *Gene,* 114**,** 251-6.

CHAMBRION, C. & LE NAOUR, F. 2010. The tetraspanins CD9 and CD81 regulate CD9P1-induced effects on cell migration. *PLoS One,* 5**,** e11219.

CHANPUT, W., MES, J. J. & WICHERS, H. J. 2014. THP-1 cell line: an in vitro cell model for immune modulation approach. *Int Immunopharmacol,* 23**,** 37-45.

CHANTRATITA, N., RHOLL, D. A., SIM, B., WUTHIEKANUN, V., LIMMATHUROTSAKUL, D., AMORNCHAI, P., THANWISAI, A., CHUA, H. H., OOI, W. F., HOLDEN, M. T., DAY, N. P., TAN, P., SCHWEIZER, H. P. & PEACOCK, S. J. 2011. Antimicrobial resistance to ceftazidime involving loss of penicillin-binding protein 3 in Burkholderia pseudomallei. *Proc Natl Acad Sci U S A,* 108**,** 17165-70.

CHAOWAGUL, W., CHIERAKUL, W., SIMPSON, A. J., SHORT, J. M., STEPNIEWSKA, K., MAHARJAN, B., RAJCHANUVONG, A., BUSARAWONG, D., LIMMATHUROTSAKUL, D., CHENG, A. C., WUTHIEKANUN, V., NEWTON, P. N., WHITE, N. J., DAY, N. P. & PEACOCK, S. J. 2005. Open-label randomized trial of oral trimethoprim-sulfamethoxazole, doxycycline, and chloramphenicol compared with trimethoprim-sulfamethoxazole and doxycycline for maintenance therapy of melioidosis. *Antimicrob Agents Chemother,* 49**,** 4020-5.

CHARLES, J. F. & ALIPRANTIS, A. O. 2014. Osteoclasts: more than 'bone eaters'. *Trends Mol Med,* 20**,** 449-59.

CHAROENSAP, J., UTAISINCHAROEN, P., ENGERING, A. & SIRISINHA, S. 2009. Differential intracellular fate of Burkholderia pseudomallei 844 and Burkholderia thailandensis UE5 in human monocyte-derived dendritic cells and macrophages. *BMC Immunol,* 10**,** 20.

CHARRIN, S., LATIL, M., SOAVE, S., POLESSKAYA, A., CHRETIEN, F., BOUCHEIX, C. & RUBINSTEIN, E. 2013. Normal muscle regeneration requires tight control of muscle cell fusion by tetraspanins CD9 and CD81. *Nat Commun,* 4**,** 1674.

CHARRIN, S., LE NAOUR, F., OUALID, M., BILLARD, M., FAURE, G., HANASH, S. M., BOUCHEIX, C. & RUBINSTEIN, E. 2001. The major CD9 and CD81 molecular partner. Identification and characterization of the complexes. *J Biol Chem,* 276**,** 14329-37.

CHARRIN, S., LE NAOUR, F., SILVIE, O., MILHIET, P. E., BOUCHEIX, C. & RUBINSTEIN, E. 2009. Lateral organization of membrane proteins: tetraspanins spin their web. *Biochem J,* 420**,** 133-54.

CHARRIN, S., MANIE, S., OUALID, M., BILLARD, M., BOUCHEIX, C. & RUBINSTEIN, E. 2002. Differential stability of tetraspanin/tetraspanin interactions: role of palmitoylation. *FEBS Lett,* 516**,** 139-44.

CHAVANAS, S., BODEMER, C., ROCHAT, A., HAMEL-TEILLAC, D., ALI, M., IRVINE, A. D., BONAFE, J. L., WILKINSON, J., TAIEB, A., BARRANDON, Y., HARPER, J. I., DE PROST, Y. & HOVNANIAN, A. 2000. Mutations in SPINK5, encoding a serine protease inhibitor, cause Netherton syndrome. *Nat Genet,* 25**,** 141-2.

CHEN, C. & FOLCH, A. 2006. A high-performance elastomeric patch clamp chip. *Lab Chip,* 6**,** 1338-45.

CHENG, A. C. & CURRIE, B. J. 2005. Melioidosis: epidemiology, pathophysiology, and management. *Clin Microbiol Rev,* 18**,** 383-416.

CHOUDHARY, K. S., HUDAIBERDIEV, S., GELENCSER, Z., GONCALVES COUTINHO, B., VENTURI, V. & PONGOR, S. 2013. The organization of the quorum sensing luxI/R family genes in Burkholderia. *Int J Mol Sci,* 14**,** 13727-47.

CLASSON, B. J., WILLIAMS, A. F., WILLIS, A. C., SEED, B. & STAMENKOVIC, I. 1990. The primary structure of the human leukocyte antigen CD37, a species homologue of the rat MRC OX-44 antigen. *J Exp Med,* 172**,** 1007.

COWIN, A. J., ADAMS, D., GEARY, S. M., WRIGHT, M. D., JONES, J. C. & ASHMAN, L. K. 2006. Wound healing is defective in mice lacking tetraspanin CD151. *J Invest Dermatol,* 126**,** 680-9.

CRUZ-MIGONI, A., HAUTBERGUE, G. M., ARTYMIUK, P. J., BAKER, P. J., BOKORI-BROWN, M., CHANG, C. T., DICKMAN, M. J., ESSEX-LOPRESTI, A., HARDING, S. V., MAHADI, N. M., MARSHALL, L. E., MOBBS, G. W., MOHAMED, R., NATHAN, S., NGUGI, S. A., ONG, C., OOI, W. F., PARTRIDGE, L. J., PHILLIPS, H. L., RAIH, M. F., RUZHEINIKOV, S., SARKAR-TYSON, M., SEDELNIKOVA, S. E., SMITHER, S. J., TAN, P., TITBALL, R. W., WILSON, S. A. & RICE, D. W. 2011. A Burkholderia pseudomallei toxin inhibits helicase activity of translation factor eIF4A. *Science,* 334**,** 821-4.

CULLINANE, M., GONG, L., LI, X., LAZAR-ADLER, N., TRA, T., WOLVETANG, E., PRESCOTT, M., BOYCE, J. D., DEVENISH, R. J. & ADLER, B. 2008. Stimulation of autophagy suppresses the intracellular survival of Burkholderia pseudomallei in mammalian cell lines. *Autophagy,* 4**,** 744-53.

CURRIE, B. J., FISHER, D. A., ANSTEY, N. M. & JACUPS, S. P. 2000. Melioidosis: acute and chronic disease, relapse and re-activation. *Trans R Soc Trop Med Hyg,* 94**,** 301-4.

CUSULIN, C., MONNI, E., AHLENIUS, H., WOOD, J., BRUNE, J. C., LINDVALL, O. & KOKAIA, Z. 2012. Embryonic stem cell-derived neural stem cells fuse with microglia and mature neurons. *Stem Cells,* 30**,** 2657-71.

DALGLEISH, A. G., BEVERLEY, P. C., CLAPHAM, P. R., CRAWFORD, D. H., GREAVES, M. F. & WEISS, R. A. 1984. The CD4 (T4) antigen is an essential component of the receptor for the AIDS retrovirus. *Nature,* 312**,** 763-7.

DANCE, D. A. 1991. Melioidosis: the tip of the iceberg? *Clin Microbiol Rev,* 4**,** 52-60.

DANCE, D. A., WUTHIEKANUN, V., NAIGOWIT, P. & WHITE, N. J. 1989. Identification of Pseudomonas pseudomallei in clinical practice: use of simple screening tests and API 20NE. *J Clin Pathol,* 42**,** 645-8.

DE VRIES, T. J., SCHOENMAKER, T., BEERTSEN, W., VAN DER NEUT, R. & EVERTS, V. 2005. Effect of CD44 deficiency on in vitro and in vivo osteoclast formation. *J Cell Biochem,* 94**,** 954-66.

DEFIFE, K. M., JENNEY, C. R., MCNALLY, A. K., COLTON, E. & ANDERSON, J. M. 1997. Interleukin-13 induces human monocyte/macrophage fusion and macrophage mannose receptor expression. *J Immunol,* 158**,** 3385-90.

DEINNOCENTES, P., AGARWAL, P. & BIRD, R. C. 2009. Phenotype-rescue of cyclin-dependent kinase inhibitor p16/INK4A defects in a spontaneous canine cell model of breast cancer. *J Cell Biochem,* 106**,** 491-505.

DELAGUILLAUMIE, A., LAGAUDRIERE-GESBERT, C., POPOFF, M. R. & CONJEAUD, H. 2002. Rho GTPases link cytoskeletal rearrangements and activation processes induced via the tetraspanin CD82 in T lymphocytes. *J Cell Sci,* 115**,** 433-43.

DESCARGUES, P., DERAISON, C., BONNART, C., KREFT, M., KISHIBE, M., ISHIDA-YAMAMOTO, A., ELIAS, P., BARRANDON, Y., ZAMBRUNO, G., SONNENBERG, A. & HOVNANIAN, A. 2005. Spink5-deficient mice mimic Netherton syndrome through degradation of desmoglein 1 by epidermal protease hyperactivity. *Nat Genet,* 37**,** 56-65.

DEVENISH, R. J. & LAI, S. C. 2015. Autophagy and burkholderia. *Immunol Cell Biol,* 93**,** 18-24.

DONG, J. T., LAMB, P. W., RINKER-SCHAEFFER, C. W., VUKANOVIC, J., ICHIKAWA, T., ISAACS, J. T. & BARRETT, J. C. 1995. KAI1, a metastasis suppressor gene for prostate cancer on human chromosome 11p11.2. *Science,* 268**,** 884-6.

DOORBAR, J. 2006. Molecular biology of human papillomavirus infection and cervical cancer. *Clin Sci (Lond),* 110**,** 525-41.

DUELLI, D. & LAZEBNIK, Y. 2003. Cell fusion: a hidden enemy? *Cancer Cell,* 3**,** 445-8.

DURAND, E., CAMBILLAU, C., CASCALES, E. & JOURNET, L. 2014. VgrG, Tae, Tle, and beyond: the versatile arsenal of Type VI secretion effectors. *Trends Microbiol,* 22**,** 498-507.

EASTON, A., HAQUE, A., CHU, K., LUKASZEWSKI, R. & BANCROFT, G. J. 2007. A critical role for neutrophils in resistance to experimental infection with Burkholderia pseudomallei. *J Infect Dis,* 195**,** 99-107.

EKCHARIYAWAT, P., PUDLA, S., LIMPOSUWAN, K., ARJCHAROEN, S., SIRISINHA, S. & UTAISINCHAROEN, P. 2005. Burkholderia pseudomallei-induced expression of suppressor of cytokine signaling 3 and cytokine-inducible src homology 2-containing protein in mouse macrophages: a possible mechanism for suppression of the response to gamma interferon stimulation. *Infect Immun,* 73**,** 7332-9.

ENELOW, R. I., SULLIVAN, G. W., CARPER, H. T. & MANDELL, G. L. 1992. Induction of multinucleated giant cell formation from in vitro culture of human monocytes with interleukin-3 and interferon-gamma: comparison with other stimulating factors. *Am J Respir Cell Mol Biol,* 6**,** 57-62.

ENGERING, A. & PIETERS, J. 2001. Association of distinct tetraspanins with MHC class II molecules at different subcellular locations in human immature dendritic cells. *Int Immunol,* 13**,** 127-34.

ESCOLA, J. M., KLEIJMEER, M. J., STOORVOGEL, W., GRIFFITH, J. M., YOSHIE, O. & GEUZE, H. J. 1998. Selective enrichment of tetraspan proteins on the internal vesicles of multivesicular endosomes and on exosomes secreted by human B-lymphocytes. *J Biol Chem,* 273**,** 20121-7.

ESSEX-LOPRESTI, A. E., BODDEY, J. A., THOMAS, R., SMITH, M. P., HARTLEY, M. G., ATKINS, T., BROWN, N. F., TSANG, C. H., PEAK, I. R., HILL, J., BEACHAM, I. R. & TITBALL, R. W. 2005. A type IV pilin, PilA, Contributes To Adherence of Burkholderia pseudomallei and virulence in vivo. *Infect Immun,* 73**,** 1260-4.

EVANS, M. J., VON HAHN, T., TSCHERNE, D. M., SYDER, A. J., PANIS, M., WOLK, B., HATZIIOANNOU, T., MCKEATING, J. A., BIENIASZ, P. D. & RICE, C. M. 2007. Claudin-1 is a hepatitis C virus co-receptor required for a late step in entry. *Nature,* 446**,** 801-5.

FEBBRAIO, M., PODREZ, E. A., SMITH, J. D., HAJJAR, D. P., HAZEN, S. L., HOFF, H. F., SHARMA, K. & SILVERSTEIN, R. L. 2000. Targeted disruption of the class B scavenger receptor CD36 protects against atherosclerotic lesion development in mice. *J Clin Invest,* 105**,** 1049-56.

FIGDOR, C. G. & VAN SPRIEL, A. B. 2010. Fungal pattern-recognition receptors and tetraspanins: partners on antigen-presenting cells. *Trends Immunol,* 31**,** 91-6.

FLINT, M., MAIDENS, C., LOOMIS-PRICE, L. D., SHOTTON, C., DUBUISSON, J., MONK, P., HIGGINBOTTOM, A., LEVY, S. & MCKEATING, J. A. 1999. Characterization of hepatitis C virus E2 glycoprotein interaction with a putative cellular receptor, CD81. *J Virol,* 73**,** 6235-44.

FREED, E. O. & MARTIN, M. A. 1995. The role of human immunodeficiency virus type 1 envelope glycoproteins in virus infection. *J Biol Chem,* 270**,** 23883-6.

FRENCH, C. T., TOESCA, I. J., WU, T. H., TESLAA, T., BEATY, S. M., WONG, W., LIU, M., SCHRODER, I., CHIOU, P. Y., TEITELL, M. A. & MILLER, J. F. 2011. Dissection of the Burkholderia intracellular life cycle using a photothermal nanoblade. *Proc Natl Acad Sci U S A,* 108**,** 12095-100.

FUKUDOME, K., FURUSE, M., IMAI, T., NISHIMURA, M., TAKAGI, S., HINUMA, Y. & YOSHIE, O. 1992. Identification of membrane antigen C33 recognized by monoclonal antibodies inhibitory to human T-cell leukemia virus type 1 (HTLV-1)-induced syncytium formation: altered glycosylation of C33 antigen in HTLV-1-positive T cells. *J Virol,* 66**,** 1394-401.

GALLIANO, M. F., ROCCASECCA, R. M., DESCARGUES, P., MICHELONI, A., LEVY, E., ZAMBRUNO, G., D'ALESSIO, M. & HOVNANIAN, A. 2005. Characterization and expression analysis of the Spink5 gene, the mouse ortholog of the defective gene in Netherton syndrome. *Genomics,* 85**,** 483-92.

GALYOV, E. E., BRETT, P. J. & DESHAZER, D. 2010. Molecular insights into Burkholderia pseudomallei and Burkholderia mallei pathogenesis. *Annu Rev Microbiol,* 64**,** 495-517.

GAN, Y. H. 2005. Interaction between Burkholderia pseudomallei and the host immune response: sleeping with the enemy? *J Infect Dis,* 192**,** 1845-50.

GARCIA-ESPANA, A., CHUNG, P. J., SARKAR, I. N., STINER, E., SUN, T. T. & DESALLE, R. 2008. Appearance of new tetraspanin genes during vertebrate evolution. *Genomics,* 91**,** 326-34.

GASSER, A. & MOST, J. 1999. Generation of multinucleated giant cells in vitro by culture of human monocytes with Mycobacterium bovis BCG in combination with cytokine-containing supernatants. *Infect Immun,* 67**,** 395-402.

GINTHER, J. L., MAYO, M., WARRINGTON, S. D., KAESTLI, M., MULLINS, T., WAGNER, D. M., CURRIE, B. J., TUANYOK, A. & KEIM, P. 2015. Identification of Burkholderia pseudomallei Near-Neighbor Species in the Northern Territory of Australia. *PLoS Negl Trop Dis,* 9**,** e0003892.

GLASS, M. B., GEE, J. E., STEIGERWALT, A. G., CAVUOTI, D., BARTON, T., HARDY, R. D., GODOY, D., SPRATT, B. G., CLARK, T. A. & WILKINS, P. P. 2006. Pneumonia and septicemia caused by Burkholderia thailandensis in the United States. *J Clin Microbiol,* 44**,** 4601-4.

GONCALVES, D. U., PROIETTI, F. A., RIBAS, J. G., ARAUJO, M. G., PINHEIRO, S. R., GUEDES, A. C. & CARNEIRO-PROIETTI, A. B. 2010. Epidemiology, treatment, and prevention of human T-cell leukemia virus type 1-associated diseases. *Clin Microbiol Rev,* 23**,** 577-89.

GONG, L., LAI, S. C., TREERAT, P., PRESCOTT, M., ADLER, B., BOYCE, J. D. & DEVENISH, R. J. 2015. Burkholderia pseudomallei type III secretion system cluster 3 ATPase BsaS, a chemotherapeutic target for small-molecule ATPase inhibitors. *Infect Immun,* 83**,** 1276-85.

GORDON-ALONSO, M., YANEZ-MO, M., BARREIRO, O., ALVAREZ, S., MUNOZ-FERNANDEZ, M. A., VALENZUELA-FERNANDEZ, A. & SANCHEZ-MADRID, F. 2006. Tetraspanins CD9 and CD81 modulate HIV-1-induced membrane fusion. *J Immunol,* 177**,** 5129-37.

GORDON, S., PLUDDEMANN, A. & MARTINEZ ESTRADA, F. 2014. Macrophage heterogeneity in tissues: phenotypic diversity and functions. *Immunol Rev,* 262**,** 36-55.

GORDON, S. & TAYLOR, P. R. 2005. Monocyte and macrophage heterogeneity. *Nat Rev Immunol,* 5**,** 953-64.

GORI, A. H., AHMED, K., MARTINEZ, G., MASAKI, H., WATANABE, K. & NAGATAKE, T. 1999. Mediation of attachment of Burkholderia pseudomallei to human pharyngeal epithelial cells by the asialoganglioside GM1-GM2 receptor complex. *Am J Trop Med Hyg,* 61**,** 473-5.

GREEN, L. R., MONK, P. N., PARTRIDGE, L. J., MORRIS, P., GORRINGE, A. R. & READ, R. C. 2011. Cooperative role for tetraspanins in adhesin-mediated attachment of bacterial species to human epithelial cells. *Infect Immun,* 79**,** 2241-9.

GROVE, J., HUBY, T., STAMATAKI, Z., VANWOLLEGHEM, T., MEULEMAN, P., FARQUHAR, M., SCHWARZ, A., MOREAU, M., OWEN, J. S., LEROUX-ROELS, G., BALFE, P. & MCKEATING, J. A. 2007. Scavenger receptor BI and BII expression levels modulate hepatitis C virus infectivity. *J Virol,* 81**,** 3162-9.

HA, C. T., WATERHOUSE, R., WESSELLS, J., WU, J. A. & DVEKSLER, G. S. 2005. Binding of pregnancy-specific glycoprotein 17 to CD9 on macrophages induces secretion of IL-10, IL-6, PGE2, and TGF-beta1. *J Leukoc Biol,* 77**,** 948-57.

HAIKO, J. & WESTERLUND-WIKSTROM, B. 2013. The role of the bacterial flagellum in adhesion and virulence. *Biology (Basel),* 2**,** 1242-67.

HAN, X., STERLING, H., CHEN, Y., SAGINARIO, C., BROWN, E. J., FRAZIER, W. A., LINDBERG, F. P. & VIGNERY, A. 2000. CD47, a ligand for the macrophage fusion receptor, participates in macrophage multinucleation. *J Biol Chem,* 275**,** 37984-92.

HARAGA, A., WEST, T. E., BRITTNACHER, M. J., SKERRETT, S. J. & MILLER, S. I. 2008. Burkholderia thailandensis as a model system for the study of the virulence-associated type III secretion system of Burkholderia pseudomallei. *Infect Immun,* 76**,** 5402-11.

HARLEY, V. S., DANCE, D. A., DRASAR, B. S. & TOVEY, G. 1998. Effects of Burkholderia pseudomallei and other Burkholderia species on eukaryotic cells in tissue culture. *Microbios,* 96**,** 71-93.

HARTGERS, F. C., VISSERS, J. L., LOOMAN, M. W., VAN ZOELEN, C., HUFFINE, C., FIGDOR, C. G. & ADEMA, G. J. 2000. DC-STAMP, a novel multimembrane-spanning molecule preferentially expressed by dendritic cells. *Eur J Immunol,* 30**,** 3585-90.

HATTORI, T., PACK, M., BOUGNOUX, P., CHANG, Z. L. & HOFFMAN, T. 1983. Interferon-induced differentiation of U937 cells. Comparison with other agents that promote differentiation of human myeloid or monocytelike cell lines. *J Clin Invest,* 72**,** 237-44.

HAWKES, M., LI, X., CROCKETT, M., DIASSITI, A., FINNEY, C., MIN-OO, G., LILES, W. C., LIU, J. & KAIN, K. C. 2010. CD36 deficiency attenuates experimental mycobacterial infection. *BMC Infect Dis,* 10**,** 299.

HE, B., LIU, L., COOK, G. A., GRGUREVICH, S., JENNINGS, L. K. & ZHANG, X. A. 2005. Tetraspanin CD82 attenuates cellular morphogenesis through down-regulating integrin alpha6-mediated cell adhesion. *J Biol Chem,* 280**,** 3346-54.

HEIDECKER, G., LLOYD, P. A., FOX, K., NAGASHIMA, K. & DERSE, D. 2004. Late assembly motifs of human T-cell leukemia virus type 1 and their relative roles in particle release. *J Virol,* 78**,** 6636-48.

HEISS, C., BURTNICK, M. N., BLACK, I., AZADI, P. & BRETT, P. J. 2012. Detailed structural analysis of the O-polysaccharide expressed by Burkholderia thailandensis E264. *Carbohydr Res,* 363**,** 23-8.

HELMING, L. & GORDON, S. 2007. Macrophage fusion induced by IL-4 alternative activation is a multistage process involving multiple target molecules. *Eur J Immunol,* 37**,** 33-42.

HELMING, L. & GORDON, S. 2009. Molecular mediators of macrophage fusion. *Trends Cell Biol,* 19**,** 514-22.

HELMING, L., TOMASELLO, E., KYRIAKIDES, T. R., MARTINEZ, F. O., TAKAI, T., GORDON, S. & VIVIER, E. 2008. Essential role of DAP12 signaling in macrophage programming into a fusion-competent state. *Sci Signal,* 1**,** ra11.

HELMING, L., WINTER, J. & GORDON, S. 2009. The scavenger receptor CD36 plays a role in cytokine-induced macrophage fusion. *J Cell Sci,* 122**,** 453-9.

HEMLER, M. E. 2003. Tetraspanin proteins mediate cellular penetration, invasion, and fusion events and define a novel type of membrane microdomain. *Annu Rev Cell Dev Biol,* 19**,** 397-422.

HEMLER, M. E. 2005. Tetraspanin functions and associated microdomains. *Nat Rev Mol Cell Biol,* 6**,** 801-11.

HEMLER, M. E. 2014. Tetraspanin proteins promote multiple cancer stages. *Nat Rev Cancer,* 14**,** 49-60.

HIGGINBOTTOM, A., QUINN, E. R., KUO, C. C., FLINT, M., WILSON, L. H., BIANCHI, E., NICOSIA, A., MONK, P. N., MCKEATING, J. A. & LEVY, S. 2000. Identification of amino acid residues in CD81 critical for interaction with hepatitis C virus envelope glycoprotein E2. *J Virol,* 74**,** 3642-9.

HIGGINBOTTOM, A., TAKAHASHI, Y., BOLLING, L., COONROD, S. A., WHITE, J. M., PARTRIDGE, L. J. & MONK, P. N. 2003. Structural requirements for the inhibitory action of the CD9 large extracellular domain in sperm/oocyte binding and fusion. *Biochem Biophys Res Commun,* 311**,** 208-14.

HIGUCHI, S., TABATA, N., TAJIMA, M., ITO, M., TSURUDOME, M., SUDO, A., UCHIDA, A. & ITO, Y. 1998. Induction of human osteoclast-like cells by treatment of blood monocytes with anti-fusion regulatory protein-1/CD98 monoclonal antibodies. *J Bone Miner Res,* 13**,** 44-9.

HO, S. H., MARTIN, F., HIGGINBOTTOM, A., PARTRIDGE, L. J., PARTHASARATHY, V., MOSELEY, G. W., LOPEZ, P., CHENG-MAYER, C. & MONK, P. N. 2006. Recombinant extracellular domains of tetraspanin proteins are potent inhibitors of the infection of macrophages by human immunodeficiency virus type 1. *J Virol,* 80**,** 6487-96.

HORTON, R. E., MORRISON, N. A., BEACHAM, I. R. & PEAK, I. R. 2012. Interaction of Burkholderia pseudomallei and Burkholderia thailandensis with human monocyte-derived dendritic cells. *J Med Microbiol,* 61**,** 607-14.

HOTTA, H., ROSS, A. H., HUEBNER, K., ISOBE, M., WENDEBORN, S., CHAO, M. V., RICCIARDI, R. P., TSUJIMOTO, Y., CROCE, C. M. & KOPROWSKI, H. 1988. Molecular cloning and characterization of an antigen associated with early stages of melanoma tumor progression. *Cancer Res,* 48**,** 2955-62.

HUANG DA, W., SHERMAN, B. T. & LEMPICKI, R. A. 2009. Bioinformatics enrichment tools: paths toward the comprehensive functional analysis of large gene lists. *Nucleic Acids Res,* 37**,** 1-13.

HUANG, S., YUAN, S., DONG, M., SU, J., YU, C., SHEN, Y., XIE, X., YU, Y., YU, X., CHEN, S., ZHANG, S., PONTAROTTI, P. & XU, A. 2005. The phylogenetic analysis of tetraspanins projects the evolution of cell-cell interactions from unicellular to multicellular organisms. *Genomics,* 86**,** 674-84.

HUANG, W., FEBBRAIO, M. & SILVERSTEIN, R. L. 2011. CD9 tetraspanin interacts with CD36 on the surface of macrophages: a possible regulatory influence on uptake of oxidized low density lipoprotein. *PLoS One,* 6**,** e29092.

HULME, R. S., HIGGINBOTTOM, A., PALMER, J., PARTRIDGE, L. J. & MONK, P. N. 2014. Distinct regions of the large extracellular domain of tetraspanin CD9 are involved in the control of human multinucleated giant cell formation. *PLoS One,* 9**,** e116289.

IMAI, T., FUKUDOME, K., TAKAGI, S., NAGIRA, M., FURUSE, M., FUKUHARA, N., NISHIMURA, M., HINUMA, Y. & YOSHIE, O. 1992. C33 antigen recognized by monoclonal antibodies inhibitory to human T cell leukemia virus type 1-induced syncytium formation is a member of a new family of transmembrane proteins including CD9, CD37, CD53, and CD63. *J Immunol,* 149**,** 2879-86.

IMAI, T. & YOSHIE, O. 1993. C33 antigen and M38 antigen recognized by monoclonal antibodies inhibitory to syncytium formation by human T cell leukemia virus type 1 are both members of the transmembrane 4 superfamily and associate with each other and with CD4 or CD8 in T cells. *J Immunol,* 151**,** 6470-81.

INGLIS, T. J., RIGBY, P., ROBERTSON, T. A., DUTTON, N. S., HENDERSON, M. & CHANG, B. J. 2000. Interaction between Burkholderia pseudomallei and Acanthamoeba species

results in coiling phagocytosis, endamebic bacterial survival, and escape. *Infect Immun,* 68**,** 1681-6.

ISHII, M., IWAI, K., KOIKE, M., OHSHIMA, S., KUDO-TANAKA, E., ISHII, T., MIMA, T., KATADA, Y., MIYATAKE, K., UCHIYAMA, Y. & SAEKI, Y. 2006. RANKL-induced expression of tetraspanin CD9 in lipid raft membrane microdomain is essential for cell fusion during osteoclastogenesis. *J Bone Miner Res,* 21**,** 965-76.

IWAI, K., ISHII, M., OHSHIMA, S., MIYATAKE, K. & SAEKI, Y. 2008. Abundant expression of tetraspanin CD9 in activated osteoclasts in ovariectomy-induced osteoporosis and in bone erosions of collagen-induced arthritis. *Rheumatol Int,* 28**,** 225-31.

IWAMOTO, R., HIGASHIYAMA, S., MITAMURA, T., TANIGUCHI, N., KLAGSBRUN, M. & MEKADA, E. 1994. Heparin-binding EGF-like growth factor, which acts as the diphtheria toxin receptor, forms a complex with membrane protein DRAP27/CD9, which up-regulates functional receptors and diphtheria toxin sensitivity. *EMBO J,* 13**,** 2322-30.

IZUMI, H., HIRABAYASHI, K., NAKAMURA, N. & NAKAGOHRI, T. 2015. Nectin expression in pancreatic adenocarcinoma: nectin-3 is associated with a poor prognosis. *Surg Today,* 45**,** 487-94.

JACOBS, A. T. & IGNARRO, L. J. 2001. Lipopolysaccharide-induced expression of interferon-beta mediates the timing of inducible nitric-oxide synthase induction in RAW 264.7 macrophages. *J Biol Chem,* 276**,** 47950-7.

JANKOVICOVA, J., SIMON, M., ANTALIKOVA, J., CUPPEROVA, P. & MICHALKOVA, K. 2015. Role of tetraspanin CD9 molecule in fertilization of mammals. *Physiol Res,* 64**,** 279-93.

JENNINGS, C. J., MURER, B., O'GRADY, A., HEARN, L. M., HARVEY, B. J., KAY, E. W. & THOMAS, W. 2015. Differential p16/INK4A cyclin-dependent kinase inhibitor expression correlates with chemotherapy efficacy in a cohort of 88 malignant pleural mesothelioma patients. *Br J Cancer,* 113**,** 69-75.

JI, C., LIU, Y., PAMULAPATI, C., BOHINI, S., FERTIG, G., SCHRAEML, M., RUBAS, W., BRANDT, M., RIES, S., MA, H. & KLUMPP, K. 2015. Prevention of hepatitis C virus infection and spread in human liver chimeric mice by an anti-CD81 monoclonal antibody. *Hepatology,* 61**,** 1136-44.

JONES, D., GLIMCHER, L. H. & ALIPRANTIS, A. O. 2011a. Osteoimmunology at the nexus of arthritis, osteoporosis, cancer, and infection. *J Clin Invest,* 121**,** 2534-42.

JONES, E. L., DEMARIA, M. C. & WRIGHT, M. D. 2011b. Tetraspanins in cellular immunity. *Biochem Soc Trans,* 39**,** 506-11.

JONES, P. H., BISHOP, L. A. & WATT, F. M. 1996. Functional significance of CD9 association with beta 1 integrins in human epidermal keratinocytes. *Cell Adhes Commun,* 4**,** 297-305.

JUDGE, M. R., MORGAN, G. & HARPER, J. I. 1994. A clinical and immunological study of Netherton's syndrome. *Br J Dermatol,* 131**,** 615-21.

JUNG, K. K., LIU, X. W., CHIRCO, R., FRIDMAN, R. & KIM, H. R. 2006. Identification of CD63 as a tissue inhibitor of metalloproteinase-1 interacting cell surface protein. *EMBO J,* 25**,** 3934-42.

KAJI, K., ODA, S., MIYAZAKI, S. & KUDO, A. 2002. Infertility of CD9-deficient mouse eggs is reversed by mouse CD9, human CD9, or mouse CD81; polyadenylated mRNA injection developed for molecular analysis of sperm-egg fusion. *Dev Biol,* 247**,** 327-34.

KAJI, K., ODA, S., SHIKANO, T., OHNUKI, T., UEMATSU, Y., SAKAGAMI, J., TADA, N., MIYAZAKI, S. & KUDO, A. 2000. The gamete fusion process is defective in eggs of Cd9-deficient mice. *Nat Genet,* 24**,** 279-82.

KAJI, K., TAKESHITA, S., MIYAKE, K., TAKAI, T. & KUDO, A. 2001. Functional association of CD9 with the Fc gamma receptors in macrophages. *J Immunol,* 166**,** 3256-65.

KANIA, J. R., KEHAT-STADLER, T. & KUPFER, S. R. 1997. CD44 antibodies inhibit osteoclast formation. *J Bone Miner Res,* 12**,** 1155-64.

KARAMATIC CREW, V., BURTON, N., KAGAN, A., GREEN, C. A., LEVENE, C., FLINTER, F., BRADY, R. L., DANIELS, G. & ANSTEE, D. J. 2004. CD151, the first member of the tetraspanin (TM4) superfamily detected on erythrocytes, is essential for the correct assembly of human basement membranes in kidney and skin. *Blood,* 104**,** 2217-23.

KAZEROUNIAN, S., DUQUETTE, M., REYES, M. A., LAWLER, J. T., SONG, K., PERRUZZI, C., PRIMO, L., KHOSRAVI-FAR, R., BUSSOLINO, F., RABINOVITZ, I. & LAWLER, J. 2011. Priming of the vascular endothelial growth factor signaling pathway by thrombospondin-1, CD36, and spleen tyrosine kinase. *Blood,* 117**,** 4658-66.

KESPICHAYAWATTANA, W., INTACHOTE, P., UTAISINCHAROEN, P. & SIRISINHA, S. 2004. Virulent Burkholderia pseudomallei is more efficient than avirulent Burkholderia thailandensis in invasion of and adherence to cultured human epithelial cells. *Microb Pathog,* 36**,** 287-92.

KESPICHAYAWATTANA, W., RATTANACHETKUL, S., WANUN, T., UTAISINCHAROEN, P. & SIRISINHA, S. 2000. Burkholderia pseudomallei induces cell fusion and actin-associated membrane protrusion: a possible mechanism for cell-to-cell spreading. *Infect Immun,* 68**,** 5377-84.

KITADOKORO, K., BORDO, D., GALLI, G., PETRACCA, R., FALUGI, F., ABRIGNANI, S., GRANDI, G. & BOLOGNESI, M. 2001. CD81 extracellular domain 3D structure: insight into the tetraspanin superfamily structural motifs. *EMBO J,* 20**,** 12-8.

KNOBELOCH, K. P., WRIGHT, M. D., OCHSENBEIN, A. F., LIESENFELD, O., LOHLER, J., ZINKERNAGEL, R. M., HORAK, I. & ORINSKA, Z. 2000. Targeted inactivation of the tetraspanin CD37 impairs T-cell-dependent B-cell response under suboptimal costimulatory conditions. *Mol Cell Biol,* 20**,** 5363-9.

KOO, G. C. & GAN, Y. H. 2006. The innate interferon gamma response of BALB/c and C57BL/6 mice to in vitro Burkholderia pseudomallei infection. *BMC Immunol,* 7**,** 19.

KOSKINEN, C., PERSSON, E., BALDOCK, P., STENBERG, A., BOSTROM, I., MATOZAKI, T., OLDENBORG, P. A. & LUNDBERG, P. 2013. Lack of CD47 impairs bone cell differentiation and results in an osteopenic phenotype in vivo due to impaired signal regulatory protein alpha (SIRPalpha) signaling. *J Biol Chem,* 288**,** 29333-44.

KOTHA, J., LONGHURST, C., APPLING, W. & JENNINGS, L. K. 2008. Tetraspanin CD9 regulates beta 1 integrin activation and enhances cell motility to fibronectin via a PI-3 kinase-dependent pathway. *Exp Cell Res,* 314**,** 1811-22.

KREMENTSOV, D. N., WENG, J., LAMBELE, M., ROY, N. H. & THALI, M. 2009. Tetraspanins regulate cell-to-cell transmission of HIV-1. *Retrovirology,* 6**,** 64.

KUDO, Y. & BOYD, C. A. 2004. RNA interference-induced reduction in CD98 expression suppresses cell fusion during syncytialization of human placental BeWo cells. *FEBS Lett,* 577**,** 473-7.

KUIJPERS, T. W., TOOL, A. T., VAN DER SCHOOT, C. E., GINSEL, L. A., ONDERWATER, J. J., ROOS, D. & VERHOEVEN, A. J. 1991. Membrane surface antigen expression on neutrophils: a reappraisal of the use of surface markers for neutrophil activation. *Blood,* 78**,** 1105-11.

KUKITA, T., WADA, N., KUKITA, A., KAKIMOTO, T., SANDRA, F., TOH, K., NAGATA, K., IIJIMA, T., HORIUCHI, M., MATSUSAKI, H., HIESHIMA, K., YOSHIE, O. & NOMIYAMA, H. 2004. RANKL-induced DC-STAMP is essential for osteoclastogenesis. *J Exp Med,* 200**,** 941-6.

KUMAR, S. N., PRASAD, T. S., NARAYAN, P. A. & MURUGANANDHAN, J. 2013. Granuloma with langhans giant cells: An overview. *J Oral Maxillofac Pathol,* 17**,** 420-3.

LATYSHEVA, N., MURATOV, G., RAJESH, S., PADGETT, M., HOTCHIN, N. A., OVERDUIN, M. & BERDITCHEVSKI, F. 2006. Syntenin-1 is a new component of tetraspanin-enriched microdomains: mechanisms and consequences of the interaction of syntenin-1 with CD63. *Mol Cell Biol,* 26**,** 7707-18.

LAY, G., POQUET, Y., SALEK-PEYRON, P., PUISSEGUR, M. P., BOTANCH, C., BON, H., LEVILLAIN, F., DUTEYRAT, J. L., EMILE, J. F. & ALTARE, F. 2007. Langhans giant cells from M. tuberculosis-induced human granulomas cannot mediate mycobacterial uptake. *J Pathol,* 211**,** 76-85.

LAZAR ADLER, N. R., GOVAN, B., CULLINANE, M., HARPER, M., ADLER, B. & BOYCE, J. D. 2009. The molecular and cellular basis of pathogenesis in melioidosis: how does Burkholderia pseudomallei cause disease? *FEMS Microbiol Rev,* 33**,** 1079-99.

LAZARUS, D., YAMIN, M., MCCARTHY, K., SCHNEEBERGER, E. E. & KRADIN, R. 1990. Anti-RMA, a murine monoclonal antibody, activates rat macrophages: II. Induction of DNA synthesis and formation of multinucleated giant cells. *Am J Respir Cell Mol Biol,* 3**,** 103-11.

LE NAOUR, F., ANDRE, M., GRECO, C., BILLARD, M., SORDAT, B., EMILE, J. F., LANZA, F., BOUCHEIX, C. & RUBINSTEIN, E. 2006. Profiling of the tetraspanin web of human colon cancer cells. *Mol Cell Proteomics,* 5**,** 845-57.

LE NAOUR, F., RUBINSTEIN, E., JASMIN, C., PRENANT, M. & BOUCHEIX, C. 2000. Severely reduced female fertility in CD9-deficient mice. *Science,* 287**,** 319-21.

LEEMANS, J. C., FLORQUIN, S., HEIKENS, M., PALS, S. T., VAN DER NEUT, R. & VAN DER POLL, T. 2003. CD44 is a macrophage binding site for Mycobacterium tuberculosis that mediates macrophage recruitment and protective immunity against tuberculosis. *J Clin Invest,* 111**,** 681-9.

LENGWEHASATIT, I., NUCHTAS, A., TUNGPRADABKUL, S., SIRISINHA, S. & UTAISINCHAROEN, P. 2008. Involvement of B. pseudomallei RpoS in apoptotic cell death in mouse macrophages. *Microb Pathog,* 44**,** 238-45.

LERTPATANASUWAN, N., SERMSRI, K., PETKASEAM, A., TRAKULSOMBOON, S., THAMLIKITKUL, V. & SUPUTTAMONGKOL, Y. 1999. Arabinose-positive Burkholderia pseudomallei infection in humans: case report. *Clin Infect Dis,* 28**,** 927-8.

LEVY, S., NGUYEN, V. Q., ANDRIA, M. L. & TAKAHASHI, S. 1991. Structure and membrane topology of TAPA-1. *J Biol Chem,* 266**,** 14597-602.

LEVY, S. & SHOHAM, T. 2005. Protein-protein interactions in the tetraspanin web. *Physiology (Bethesda),* 20**,** 218-24.

LIMMATHUROTSAKUL, D., WONGRATANACHEEWIN, S., TEERAWATTANASOOK, N., WONGSUVAN, G., CHAISUKSANT, S., CHETCHOTISAKD, P., CHAOWAGUL, W., DAY, N. P. & PEACOCK, S. J. 2010. Increasing incidence of human melioidosis in Northeast Thailand. *Am J Trop Med Hyg,* 82**,** 1113-7.

LIU, Z., TIAN, Y., MACHIDA, K., LAI, M. M., LUO, G., FOUNG, S. K. & OU, J. H. 2012. Transient activation of the PI3K-AKT pathway by hepatitis C virus to enhance viral entry. *J Biol Chem,* 287**,** 41922-30.

LONGHURST, C. M., WHITE, M. M., WILKINSON, D. A. & JENNINGS, L. K. 1999. A CD9, alphaIIbbeta3, integrin-associated protein, and GPIb/V/IX complex on the surface of human platelets is influenced by alphaIIbbeta3 conformational states. *Eur J Biochem,* 263**,** 104-11.

LUNDBERG, P., KOSKINEN, C., BALDOCK, P. A., LOTHGREN, H., STENBERG, A., LERNER, U. H. & OLDENBORG, P. A. 2007. Osteoclast formation is strongly reduced both in vivo and in vitro in the absence of CD47/SIRPalpha-interaction. *Biochem Biophys Res Commun,* 352**,** 444-8.

MACLAUCHLAN, S., SKOKOS, E. A., MEZNARICH, N., ZHU, D. H., RAOOF, S., SHIPLEY, J. M., SENIOR, R. M., BORNSTEIN, P. & KYRIAKIDES, T. R. 2009. Macrophage fusion, giant

cell formation, and the foreign body response require matrix metalloproteinase 9. *J Leukoc Biol,* 85**,** 617-26.

MAECKER, H. T. & LEVY, S. 1997. Normal lymphocyte development but delayed humoral immune response in CD81-null mice. *J Exp Med,* 185**,** 1505-10.

MAECKER, H. T., TODD, S. C. & LEVY, S. 1997. The tetraspanin superfamily: molecular facilitators. *FASEB J,* 11**,** 428-42.

MAHENTHIRALINGAM, E., BALDWIN, A. & VANDAMME, P. 2002. Burkholderia cepacia complex infection in patients with cystic fibrosis. *J Med Microbiol,* 51**,** 533-8.

MARTIN, F., ROTH, D. M., JANS, D. A., POUTON, C. W., PARTRIDGE, L. J., MONK, P. N. & MOSELEY, G. W. 2005. Tetraspanins in viral infections: a fundamental role in viral biology? *J Virol,* 79**,** 10839-51.

MARTINEZ, F. O. & GORDON, S. 2014. The M1 and M2 paradigm of macrophage activation: time for reassessment. *F1000Prime Rep,* 6**,** 13.

MARTINEZ, F. O., HELMING, L. & GORDON, S. 2009. Alternative activation of macrophages: an immunologic functional perspective. *Annu Rev Immunol,* 27**,** 451-83.

MASCIOPINTO, F., GIOVANI, C., CAMPAGNOLI, S., GALLI-STAMPINO, L., COLOMBATTO, P., BRUNETTO, M., YEN, T. S., HOUGHTON, M., PILERI, P. & ABRIGNANI, S. 2004. Association of hepatitis C virus envelope proteins with exosomes. *Eur J Immunol,* 34**,** 2834-42.

MAZUROV, D., HEIDECKER, G. & DERSE, D. 2006. HTLV-1 Gag protein associates with CD82 tetraspanin microdomains at the plasma membrane. *Virology,* 346**,** 194-204.

MCGILVRAY, I. D., SERGHIDES, L., KAPUS, A., ROTSTEIN, O. D. & KAIN, K. C. 2000. Nonopsonic monocyte/macrophage phagocytosis of Plasmodium falciparum-parasitized erythrocytes: a role for CD36 in malarial clearance. *Blood,* 96**,** 3231-40.

MCNALLY, A. K. & ANDERSON, J. M. 1995. Interleukin-4 induces foreign body giant cells from human monocytes/macrophages. Differential lymphokine regulation of macrophage fusion leads to morphological variants of multinucleated giant cells. *Am J Pathol,* 147**,** 1487-99.

MCNALLY, A. K. & ANDERSON, J. M. 2002. Beta1 and beta2 integrins mediate adhesion during macrophage fusion and multinucleated foreign body giant cell formation. *Am J Pathol,* 160**,** 621-30.

MCNALLY, A. K. & ANDERSON, J. M. 2005. Multinucleated giant cell formation exhibits features of phagocytosis with participation of the endoplasmic reticulum. *Exp Mol Pathol,* 79**,** 126-35.

MCNALLY, A. K., DEFIFE, K. M. & ANDERSON, J. M. 1996. Interleukin-4-induced macrophage fusion is prevented by inhibitors of mannose receptor activity. *Am J Pathol,* 149**,** 975-85.

MCNALLY, A. K., MACEWAN, S. R. & ANDERSON, J. M. 2007. alpha subunit partners to beta1 and beta2 integrins during IL-4-induced foreign body giant cell formation. *J Biomed Mater Res A,* 82**,** 568-74.

MEERLOO, T., PARMENTIER, H. K., OSTERHAUS, A. D., GOUDSMIT, J. & SCHUURMAN, H. J. 1992. Modulation of cell surface molecules during HIV-1 infection of H9 cells. An immunoelectron microscopic study. *AIDS,* 6**,** 1105-16.

MEERTENS, L., BERTAUX, C. & DRAGIC, T. 2006. Hepatitis C virus entry requires a critical postinternalization step and delivery to early endosomes via clathrin-coated vesicles. *J Virol,* 80**,** 11571-8.

MENSAH, K. A., RITCHLIN, C. T. & SCHWARZ, E. M. 2010. RANKL induces heterogeneous DC-STAMP(lo) and DC-STAMP(hi) osteoclast precursors of which the DC-STAMP(lo) precursors are the master fusogens. *J Cell Physiol,* 223**,** 76-83.

MEULENBERG, J. J., BOS-DE RUIJTER, J. N., WENSVOORT, G. & MOORMANN, R. J. 1998. An infectious cDNA clone of porcine reproductive and respiratory syndrome virus. *Adv Exp Med Biol,* 440**,** 199-206.

MEYER-WENTRUP, F., FIGDOR, C. G., ANSEMS, M., BROSSART, P., WRIGHT, M. D., ADEMA, G. J. & VAN SPRIEL, A. B. 2007. Dectin-1 interaction with tetraspanin CD37 inhibits IL-6 production. *J Immunol,* 178**,** 154-62.

MIAO, W. M., VASILE, E., LANE, W. S. & LAWLER, J. 2001. CD36 associates with CD9 and integrins on human blood platelets. *Blood,* 97**,** 1689-96.

MILES, A. A., MISRA, S. S. & IRWIN, J. O. 1938. The estimation of the bactericidal power of the blood. *J Hyg (Lond),* 38**,** 732-49.

MIRANTI, C. K. 2009. Controlling cell surface dynamics and signaling: how CD82/KAI1 suppresses metastasis. *Cell Signal,* 21**,** 196-211.

MITAMURA, T., IWAMOTO, R., UMATA, T., YOMO, T., URABE, I., TSUNEOKA, M. & MEKADA, E. 1992. The 27-kD diphtheria toxin receptor-associated protein (DRAP27) from vero cells is the monkey homologue of human CD9 antigen: expression of DRAP27 elevates the number of diphtheria toxin receptors on toxin-sensitive cells. *J Cell Biol,* 118**,** 1389-99.

MITSUDO, K., JAYAKUMAR, A., HENDERSON, Y., FREDERICK, M. J., KANG, Y., WANG, M., EL-NAGGAR, A. K. & CLAYMAN, G. L. 2003. Inhibition of serine proteinases plasmin, trypsin, subtilisin A, cathepsin G, and elastase by LEKTI: a kinetic analysis. *Biochemistry,* 42**,** 3874-81.

MIYADO, K., MEKADA, E. & KOBAYASHI, K. 2000a. [A crucial role of tetraspanin, CD9 in fertilization]. *Tanpakushitsu Kakusan Koso,* 45**,** 1728-34.

MIYADO, K., YAMADA, G., YAMADA, S., HASUWA, H., NAKAMURA, Y., RYU, F., SUZUKI, K., KOSAI, K., INOUE, K., OGURA, A., OKABE, M. & MEKADA, E. 2000b. Requirement of CD9 on the egg plasma membrane for fertilization. *Science,* 287**,** 321-4.

MIYAMOTO, H., KATSUYAMA, E., MIYAUCHI, Y., HOSHI, H., MIYAMOTO, K., SATO, Y., KOBAYASHI, T., IWASAKI, R., YOSHIDA, S., MORI, T., KANAGAWA, H., FUJIE, A., HAO, W., MORIOKA, H., MATSUMOTO, M., TOYAMA, Y. & MIYAMOTO, T. 2012. An essential role for STAT6-STAT1 protein signaling in promoting macrophage cell-cell fusion. *J Biol Chem,* 287**,** 32479-84.

MIYATA, S. T., BACHMANN, V. & PUKATZKI, S. 2013. Type VI secretion system regulation as a consequence of evolutionary pressure. *J Med Microbiol,* 62**,** 663-76.

MIYAZAKI, T., MULLER, U. & CAMPBELL, K. S. 1997. Normal development but differentially altered proliferative responses of lymphocytes in mice lacking CD81. *EMBO J,* 16**,** 4217-25.

MIZUNO, K., OKAMOTO, H. & HORIO, T. 2001a. Heightened ability of monocytes from sarcoidosis patients to form multi-nucleated giant cells in vitro by supernatants of concanavalin A-stimulated mononuclear cells. *Clin Exp Immunol,* 126**,** 151-6.

MIZUNO, K., OKAMOTO, H. & HORIO, T. 2001b. Muramyl dipeptide and mononuclear cell supernatant induce Langhans-type cells from human monocytes. *J Leukoc Biol,* 70**,** 386-94.

MOLLINEDO, F., FONTAN, G., BARASOAIN, I. & LAZO, P. A. 1997. Recurrent infectious diseases in human CD53 deficiency. *Clin Diagn Lab Immunol,* 4**,** 229-31.

MONK, P. N. & PARTRIDGE, L. J. 2012. Tetraspanins: gateways for infection. *Infect Disord Drug Targets,* 12**,** 4-17.

MOORE, K. J. & FREEMAN, M. W. 2006. Scavenger receptors in atherosclerosis: beyond lipid uptake. *Arterioscler Thromb Vasc Biol,* 26**,** 1702-11.

MOORE, R. A., RECKSEIDLER-ZENTENO, S., KIM, H., NIERMAN, W., YU, Y., TUANYOK, A., WARAWA, J., DESHAZER, D. & WOODS, D. E. 2004. Contribution of gene loss to the

pathogenic evolution of Burkholderia pseudomallei and Burkholderia mallei. *Infect Immun,* 72**,** 4172-87.

MORENO, J. L., MIKHAILENKO, I., TONDRAVI, M. M. & KEEGAN, A. D. 2007. IL-4 promotes the formation of multinucleated giant cells from macrophage precursors by a STAT6-dependent, homotypic mechanism: contribution of E-cadherin. *J Leukoc Biol,* 82**,** 1542-53.

MORTENSEN, K., LICHTENBERG, J., THOMSEN, P. D. & LARSSON, L. I. 2004. Spontaneous fusion between cancer cells and endothelial cells. *Cell Mol Life Sci,* 61**,** 2125-31.

MOSSER, D. M. & EDWARDS, J. P. 2008. Exploring the full spectrum of macrophage activation. *Nat Rev Immunol,* 8**,** 958-69.

MUELLER, C. A., BROZ, P. & CORNELIS, G. R. 2008. The type III secretion system tip complex and translocon. *Mol Microbiol,* 68**,** 1085-95.

MUELLER, O., HAHNENBERGER, K., DITTMANN, M., YEE, H., DUBROW, R., NAGLE, R. & ILSLEY, D. 2000. A microfluidic system for high-speed reproducible DNA sizing and quantitation. *Electrophoresis,* 21**,** 128-34.

MYLONA, E., JONES, K. A., MILLS, S. T. & PAVLATH, G. K. 2006. CD44 regulates myoblast migration and differentiation. *J Cell Physiol,* 209**,** 314-21.

NGAUY, V., LEMESHEV, Y., SADKOWSKI, L. & CRAWFORD, G. 2005. Cutaneous melioidosis in a man who was taken as a prisoner of war by the Japanese during World War II. *J Clin Microbiol,* 43**,** 970-2.

NOTO, P. B., BUKHTIYAROV, Y., SHI, M., MCKEEVER, B. M., MCGEEHAN, G. M. & LALA, D. S. 2012. Regulation of sphingomyelin phosphodiesterase acid-like 3A gene (SMPDL3A) by liver X receptors. *Mol Pharmacol,* 82**,** 719-27.

NYDEGGER, S., KHURANA, S., KREMENTSOV, D. N., FOTI, M. & THALI, M. 2006. Mapping of tetraspanin-enriched microdomains that can function as gateways for HIV-1. *J Cell Biol,* 173**,** 795-807.

O'QUINN, A. L., WIEGAND, E. M. & JEDDELOH, J. A. 2001. Burkholderia pseudomallei kills the nematode Caenorhabditis elegans using an endotoxin-mediated paralysis. *Cell Microbiol,* 3**,** 381-93.

OHGIMOTO, S., TABATA, N., SUGA, S., NISHIO, M., OHTA, H., TSURUDOME, M., KOMADA, H., KAWANO, M., WATANABE, N. & ITO, Y. 1995. Molecular characterization of fusion regulatory protein-1 (FRP-1) that induces multinucleated giant cell formation of monocytes and HIV gp160-mediated cell fusion. FRP-1 and 4F2/CD98 are identical molecules. *J Immunol,* 155**,** 3585-92.

OHNAMI, N., NAKAMURA, A., MIYADO, M., SATO, M., KAWANO, N., YOSHIDA, K., HARADA, Y., TAKEZAWA, Y., KANAI, S., ONO, C., TAKAHASHI, Y., KIMURA, K., SHIDA, T., MIYADO, K. & UMEZAWA, A. 2012. CD81 and CD9 work independently as extracellular components upon fusion of sperm and oocyte. *Biol Open,* 1**,** 640-7.

OLDENBORG, P. A. 2013. CD47: A Cell Surface Glycoprotein Which Regulates Multiple Functions of Hematopoietic Cells in Health and Disease. *ISRN Hematol,* 2013**,** 614619.

OP DE BEECK, A., VOISSET, C., BARTOSCH, B., CICZORA, Y., COCQUEREL, L., KECK, Z., FOUNG, S., COSSET, F. L. & DUBUISSON, J. 2004. Characterization of functional hepatitis C virus envelope glycoproteins. *J Virol,* 78**,** 2994-3002.

OREN, R., TAKAHASHI, S., DOSS, C., LEVY, R. & LEVY, S. 1990. TAPA-1, the target of an antiproliferative antibody, defines a new family of transmembrane proteins. *Mol Cell Biol,* 10**,** 4007-15.

PAPPENHEIMER, A. M., JR. 1977. Diphtheria toxin. *Annu Rev Biochem,* 46**,** 69-94.

PARK, S. Y., YUN, Y. & KIM, I. S. 2012. CD36 is required for myoblast fusion during myogenic differentiation. *Biochem Biophys Res Commun,* 427**,** 705-10.

PARRISH, N. M., DICK, J. D. & BISHAI, W. R. 1998. Mechanisms of latency in Mycobacterium tuberculosis. *Trends Microbiol,* 6**,** 107-12.

PARTHASARATHY, V., MARTIN, F., HIGGINBOTTOM, A., MURRAY, H., MOSELEY, G. W., READ, R. C., MAL, G., HULME, R., MONK, P. N. & PARTRIDGE, L. J. 2009. Distinct roles for tetraspanins CD9, CD63 and CD81 in the formation of multinucleated giant cells. *Immunology,* 127**,** 237-48.

PEACOCK, S. J., LIMMATHUROTSAKUL, D., LUBELL, Y., KOH, G. C., WHITE, L. J., DAY, N. P. & TITBALL, R. W. 2012. Melioidosis vaccines: a systematic review and appraisal of the potential to exploit biodefense vaccines for public health purposes. *PLoS Negl Trop Dis,* 6**,** e1488.

PILERI, P., UEMATSU, Y., CAMPAGNOLI, S., GALLI, G., FALUGI, F., PETRACCA, R., WEINER, A. J., HOUGHTON, M., ROSA, D., GRANDI, G. & ABRIGNANI, S. 1998. Binding of hepatitis C virus to CD81. *Science,* 282**,** 938-41.

PIQUE, C., LAGAUDRIERE-GESBERT, C., DELAMARRE, L., ROSENBERG, A. R., CONJEAUD, H. & DOKHELAR, M. C. 2000. Interaction of CD82 tetraspanin proteins with HTLV-1 envelope glycoproteins inhibits cell-to-cell fusion and virus transmission. *Virology,* 276**,** 455-65.

PIZARRO-CERDA, J., PAYRASTRE, B., WANG, Y. J., VEIGA, E., YIN, H. L. & COSSART, P. 2007. Type II phosphatidylinositol 4-kinases promote Listeria monocytogenes entry into target cells. *Cell Microbiol,* 9**,** 2381-90.

PLOSS, A., EVANS, M. J., GAYSINSKAYA, V. A., PANIS, M., YOU, H., DE JONG, Y. P. & RICE, C. M. 2009. Human occludin is a hepatitis C virus entry factor required for infection of mouse cells. *Nature,* 457**,** 882-6.

PODREZ, E. A., FEBBRAIO, M., SHEIBANI, N., SCHMITT, D., SILVERSTEIN, R. L., HAJJAR, D. P., COHEN, P. A., FRAZIER, W. A., HOFF, H. F. & HAZEN, S. L. 2000. Macrophage scavenger receptor CD36 is the major receptor for LDL modified by monocyte-generated reactive nitrogen species. *J Clin Invest,* 105**,** 1095-108.

PUISSEGUR, M. P., LAY, G., GILLERON, M., BOTELLA, L., NIGOU, J., MARRAKCHI, H., MARI, B., DUTEYRAT, J. L., GUERARDEL, Y., KREMER, L., BARBRY, P., PUZO, G. & ALTARE, F. 2007. Mycobacterial lipomannan induces granuloma macrophage fusion via a TLR2-dependent, ADAM9- and beta1 integrin-mediated pathway. *J Immunol,* 178**,** 3161-9.

PUTHUCHEARY, S. D. & NATHAN, S. A. 2006. Comparison by electron microscopy of intracellular events and survival of Burkholderia pseudomallei in monocytes from normal subjects and patients with melioidosis. *Singapore Med J,* 47**,** 697-703.

QI, J. C., WANG, J., MANDADI, S., TANAKA, K., ROUFOGALIS, B. D., MADIGAN, M. C., LAI, K., YAN, F., CHONG, B. H., STEVENS, R. L. & KRILIS, S. A. 2006. Human and mouse mast cells use the tetraspanin CD9 as an alternate interleukin-16 receptor. *Blood,* 107**,** 135-42.

RACHKOVSKY, M., SODI, S., CHAKRABORTY, A., AVISSAR, Y., BOLOGNIA, J., MCNIFF, J. M., PLATT, J., BERMUDES, D. & PAWELEK, J. 1998. Melanoma x macrophage hybrids with enhanced metastatic potential. *Clin Exp Metastasis,* 16**,** 299-312.

RAJESH, S., SRIDHAR, P., TEWS, B. A., FENEANT, L., COCQUEREL, L., WARD, D. G., BERDITCHEVSKI, F. & OVERDUIN, M. 2012. Structural basis of ligand interactions of the large extracellular domain of tetraspanin CD81. *J Virol,* 86**,** 9606-16.

RALPH, P. & NAKOINZ, I. 1975. Phagocytosis and cytolysis by a macrophage tumour and its cloned cell line. *Nature,* 257**,** 393-4.

RALPH, P. & NAKOINZ, I. 1977. Antibody-dependent killing of erythrocyte and tumor targets by macrophage-related cell lines: enhancement by PPD and LPS. *J Immunol,* 119**,** 950-54.

RAPPA, G., GREEN, T. M., KARBANOVA, J., CORBEIL, D. & LORICO, A. 2015. Tetraspanin CD9 determines invasiveness and tumorigenicity of human breast cancer cells. *Oncotarget,* 6**,** 7970-91.

RECKSEIDLER-ZENTENO, S. L., DEVINNEY, R. & WOODS, D. E. 2005. The capsular polysaccharide of Burkholderia pseudomallei contributes to survival in serum by reducing complement factor C3b deposition. *Infect Immun,* 73**,** 1106-15.

RECKSEIDLER, S. L., DESHAZER, D., SOKOL, P. A. & WOODS, D. E. 2001. Detection of bacterial virulence genes by subtractive hybridization: identification of capsular polysaccharide of Burkholderia pseudomallei as a major virulence determinant. *Infect Immun,* 69**,** 34-44.

REICHELT, P., SCHWARZ, C. & DONZEAU, M. 2006. Single step protocol to purify recombinant proteins with low endotoxin contents. *Protein Expr Purif,* 46**,** 483-8.

REN, Y., SILVERSTEIN, R. L., ALLEN, J. & SAVILL, J. 1995. CD36 gene transfer confers capacity for phagocytosis of cells undergoing apoptosis. *J Exp Med,* 181**,** 1857-62.

RHEE, I., DAVIDSON, D., SOUZA, C. M., VACHER, J. & VEILLETTE, A. 2013. Macrophage fusion is controlled by the cytoplasmic protein tyrosine phosphatase PTP-PEST/PTPN12. *Mol Cell Biol,* 33**,** 2458-69.

RISINGER, J. I., CUSTER, M., FEIGENBAUM, L., SIMPSON, R. M., HOOVER, S. B., WEBSTER, J. D., CHANDRAMOULI, G. V., TESSAROLLO, L. & BARRETT, J. C. 2014. Normal viability of Kai1/Cd82 deficient mice. *Mol Carcinog,* 53**,** 610-24.

ROBB, L., TARRANT, J., GROOM, J., IBRAHIM, M., LI, R., BOROBAKAS, B. & WRIGHT, M. D. 2001. Molecular characterisation of mouse and human TSSC6: evidence that TSSC6 is a genuine member of the tetraspanin superfamily and is expressed specifically in haematopoietic organs. *Biochim Biophys Acta,* 1522**,** 31-41.

ROUSCHOP, K. M., SYLVA, M., TESKE, G. J., HOEDEMAEKER, I., PALS, S. T., WEENING, J. J., VAN DER POLL, T. & FLORQUIN, S. 2006. Urothelial CD44 facilitates Escherichia coli infection of the murine urinary tract. *J Immunol,* 177**,** 7225-32.

RUBINSTEIN, E., ZIYYAT, A., PRENANT, M., WROBEL, E., WOLF, J. P., LEVY, S., LE NAOUR, F. & BOUCHEIX, C. 2006. Reduced fertility of female mice lacking CD81. *Dev Biol,* 290**,** 351-8.

RUNGE, K. E., EVANS, J. E., HE, Z. Y., GUPTA, S., MCDONALD, K. L., STAHLBERG, H., PRIMAKOFF, P. & MYLES, D. G. 2007. Oocyte CD9 is enriched on the microvillar membrane and required for normal microvillar shape and distribution. *Dev Biol,* 304**,** 317-25.

SAGINARIO, C., STERLING, H., BECKERS, C., KOBAYASHI, R., SOLIMENA, M., ULLU, E. & VIGNERY, A. 1998. MFR, a putative receptor mediating the fusion of macrophages. *Mol Cell Biol,* 18**,** 6213-23.

SAKAI, H., OKAFUJI, I., NISHIKOMORI, R., ABE, J., IZAWA, K., KAMBE, N., YASUMI, T., NAKAHATA, T. & HEIKE, T. 2012. The CD40-CD40L axis and IFN-gamma play critical roles in Langhans giant cell formation. *Int Immunol,* 24**,** 5-15.

SANDOR, M., WEINSTOCK, J. V. & WYNN, T. A. 2003. Granulomas in schistosome and mycobacterial infections: a model of local immune responses. *Trends Immunol,* 24**,** 44-52.

SAUNDERS, B. M., FRANK, A. A. & ORME, I. M. 1999. Granuloma formation is required to contain bacillus growth and delay mortality in mice chronically infected with Mycobacterium tuberculosis. *Immunology,* 98**,** 324-8.

SCHELL, M. A., ULRICH, R. L., RIBOT, W. J., BRUEGGEMANN, E. E., HINES, H. B., CHEN, D., LIPSCOMB, L., KIM, H. S., MRAZEK, J., NIERMAN, W. C. & DESHAZER, D. 2007. Type VI secretion is a major virulence determinant in Burkholderia mallei. *Mol Microbiol,* 64**,** 1466-85.

SCHICK, M. R. & LEVY, S. 1993. The TAPA-1 molecule is associated on the surface of B cells with HLA-DR molecules. *J Immunol,* 151**,** 4090-7.

SCHMITS, R., FILMUS, J., GERWIN, N., SENALDI, G., KIEFER, F., KUNDIG, T., WAKEHAM, A., SHAHINIAN, A., CATZAVELOS, C., RAK, J., FURLONGER, C., ZAKARIAN, A., SIMARD, J. J., OHASHI, P. S., PAIGE, C. J., GUTIERREZ-RAMOS, J. C. & MAK, T. W. 1997. CD44 regulates hematopoietic progenitor distribution, granuloma formation, and tumorigenicity. *Blood,* 90**,** 2217-33.

SCHRODER, H. M., HOFFMANN, S. C., HECKER, M., KORFF, T. & LUDWIG, T. 2013. The tetraspanin network modulates MT1-MMP cell surface trafficking. *Int J Biochem Cell Biol,* 45**,** 1133-44.

SCHRODER, J., LULLMANN-RAUCH, R., HIMMERKUS, N., PLEINES, I., NIESWANDT, B., ORINSKA, Z., KOCH-NOLTE, F., SCHRODER, B., BLEICH, M. & SAFTIG, P. 2009. Deficiency of the tetraspanin CD63 associated with kidney pathology but normal lysosomal function. *Mol Cell Biol,* 29**,** 1083-94.

SCHROEDER, A., MUELLER, O., STOCKER, S., SALOWSKY, R., LEIBER, M., GASSMANN, M., LIGHTFOOT, S., MENZEL, W., GRANZOW, M. & RAGG, T. 2006. The RIN: an RNA integrity number for assigning integrity values to RNA measurements. *BMC Mol Biol,* 7**,** 3.

SCHWARZ, S., SINGH, P., ROBERTSON, J. D., LEROUX, M., SKERRETT, S. J., GOODLETT, D. R., WEST, T. E. & MOUGOUS, J. D. 2014. VgrG-5 is a Burkholderia type VI secretion system-exported protein required for multinucleated giant cell formation and virulence. *Infect Immun,* 82**,** 1445-52.

SCHWARZ, S., WEST, T. E., BOYER, F., CHIANG, W. C., CARL, M. A., HOOD, R. D., ROHMER, L., TOLKER-NIELSEN, T., SKERRETT, S. J. & MOUGOUS, J. D. 2010. Burkholderia type VI secretion systems have distinct roles in eukaryotic and bacterial cell interactions. *PLoS Pathog,* 6**,** e1001068.

SCHWEIZER, H. P. 2012. Mechanisms of antibiotic resistance in Burkholderia pseudomallei: implications for treatment of melioidosis. *Future Microbiol,* 7**,** 1389-99.

SEGOVIA-SILVESTRE, T., NEUTZSKY-WULFF, A. V., SORENSEN, M. G., CHRISTIANSEN, C., BOLLERSLEV, J., KARSDAL, M. A. & HENRIKSEN, K. 2009. Advances in osteoclast biology resulting from the study of osteopetrotic mutations. *Hum Genet,* 124**,** 561-77.

SEIGNEURET, M., DELAGUILLAUMIE, A., LAGAUDRIERE-GESBERT, C. & CONJEAUD, H. 2001. Structure of the tetraspanin main extracellular domain. A partially conserved fold with a structurally variable domain insertion. *J Biol Chem,* 276**,** 40055-64.

SERRANO, M. 1997. The tumor suppressor protein p16INK4a. *Exp Cell Res,* 237**,** 7-13.

SHALOM, G., SHAW, J. G. & THOMAS, M. S. 2007. In vivo expression technology identifies a type VI secretion system locus in Burkholderia pseudomallei that is induced upon invasion of macrophages. *Microbiology,* 153**,** 2689-99.

SHANMUKHAPPA, K., KIM, J. K. & KAPIL, S. 2007. Role of CD151, A tetraspanin, in porcine reproductive and respiratory syndrome virus infection. *Virol J,* 4**,** 62.

SHEARER, M., BARTKOVA, J., BARTEK, J., BERDICHEVSKY, F., BARNES, D., MILLIS, R. & TAYLOR-PAPADIMITRIOU, J. 1992. Studies of clonal cell lines developed from primary breast cancers indicate that the ability to undergo morphogenesis in vitro is lost early in malignancy. *Int J Cancer,* 51**,** 602-12.

SHILAGARDI, K., LI, S., LUO, F., MARIKAR, F., DUAN, R., JIN, P., KIM, J. H., MURNEN, K. & CHEN, E. H. 2013. Actin-propelled invasive membrane protrusions promote fusogenic protein engagement during cell-cell fusion. *Science,* 340**,** 359-63.

SHOHAM, T., RAJAPAKSA, R., BOUCHEIX, C., RUBINSTEIN, E., POE, J. C., TEDDER, T. F. & LEVY, S. 2003. The tetraspanin CD81 regulates the expression of CD19 during B cell

development in a postendoplasmic reticulum compartment. *J Immunol,* 171**,** 4062-72.

SILVERSTEIN, R. L. & FEBBRAIO, M. 2009. CD36, a scavenger receptor involved in immunity, metabolism, angiogenesis, and behavior. *Sci Signal,* 2**,** re3.

SILVIE, O., CHARRIN, S., BILLARD, M., FRANETICH, J. F., CLARK, K. L., VAN GEMERT, G. J., SAUERWEIN, R. W., DAUTRY, F., BOUCHEIX, C., MAZIER, D. & RUBINSTEIN, E. 2006a. Cholesterol contributes to the organization of tetraspanin-enriched microdomains and to CD81-dependent infection by malaria sporozoites. *J Cell Sci,* 119**,** 1992-2002.

SILVIE, O., GRECO, C., FRANETICH, J. F., DUBART-KUPPERSCHMITT, A., HANNOUN, L., VAN GEMERT, G. J., SAUERWEIN, R. W., LEVY, S., BOUCHEIX, C., RUBINSTEIN, E. & MAZIER, D. 2006b. Expression of human CD81 differently affects host cell susceptibility to malaria sporozoites depending on the Plasmodium species. *Cell Microbiol,* 8**,** 1134-46.

SILVIE, O., RUBINSTEIN, E., FRANETICH, J. F., PRENANT, M., BELNOUE, E., RENIA, L., HANNOUN, L., ELING, W., LEVY, S., BOUCHEIX, C. & MAZIER, D. 2003. Hepatocyte CD81 is required for Plasmodium falciparum and Plasmodium yoelii sporozoite infectivity. *Nat Med,* 9**,** 93-6.

SIM, B. M., CHANTRATITA, N., OOI, W. F., NANDI, T., TEWHEY, R., WUTHIEKANUN, V., THAIPADUNGPANIT, J., TUMAPA, S., ARIYARATNE, P., SUNG, W. K., SEM, X. H., CHUA, H. H., RAMNARAYANAN, K., LIN, C. H., LIU, Y., FEIL, E. J., GLASS, M. B., TAN, G., PEACOCK, S. J. & TAN, P. 2010. Genomic acquisition of a capsular polysaccharide virulence cluster by non-pathogenic Burkholderia isolates. *Genome Biol,* 11**,** R89.

SIMONET, W. S., LACEY, D. L., DUNSTAN, C. R., KELLEY, M., CHANG, M. S., LUTHY, R., NGUYEN, H. Q., WOODEN, S., BENNETT, L., BOONE, T., SHIMAMOTO, G., DEROSE, M., ELLIOTT, R., COLOMBERO, A., TAN, H. L., TRAIL, G., SULLIVAN, J., DAVY, E., BUCAY, N., RENSHAW-GEGG, L., HUGHES, T. M., HILL, D., PATTISON, W., CAMPBELL, P., SANDER, S., VAN, G., TARPLEY, J., DERBY, P., LEE, R. & BOYLE, W. J. 1997. Osteoprotegerin: a novel secreted protein involved in the regulation of bone density. *Cell,* 89**,** 309-19.

SINCOCK, P. M., FITTER, S., PARTON, R. G., BERNDT, M. C., GAMBLE, J. R. & ASHMAN, L. K. 1999. PETA-3/CD151, a member of the transmembrane 4 superfamily, is localised to the plasma membrane and endocytic system of endothelial cells, associates with multiple integrins and modulates cell function. *J Cell Sci,* 112 (Pt 6)**,** 833-44.

SINGETHAN, K., MULLER, N., SCHUBERT, S., LUTTGE, D., KREMENTSOV, D. N., KHURANA, S. R., KROHNE, G., SCHNEIDER-SCHAULIES, S., THALI, M. & SCHNEIDER-SCHAULIES, J. 2008. CD9 clustering and formation of microvilli zippers between contacting cells regulates virus-induced cell fusion. *Traffic,* 9**,** 924-35.

SITTHIDET, C., KORBSRISATE, S., LAYTON, A. N., FIELD, T. R., STEVENS, M. P. & STEVENS, J. M. 2011. Identification of motifs of Burkholderia pseudomallei BimA required for intracellular motility, actin binding, and actin polymerization. *J Bacteriol,* 193**,** 1901-10.

SKEHAN, P., STORENG, R., SCUDIERO, D., MONKS, A., MCMAHON, J., VISTICA, D., WARREN, J. T., BOKESCH, H., KENNEY, S. & BOYD, M. R. 1990. New colorimetric cytotoxicity assay for anticancer-drug screening. *J Natl Cancer Inst,* 82**,** 1107-12.

SMITH, D. B. & JOHNSON, K. S. 1988. Single-step purification of polypeptides expressed in Escherichia coli as fusions with glutathione S-transferase. *Gene,* 67**,** 31-40.

SPODEN, G., FREITAG, K., HUSMANN, M., BOLLER, K., SAPP, M., LAMBERT, C. & FLORIN, L. 2008. Clathrin- and caveolin-independent entry of human papillomavirus type 16--involvement of tetraspanin-enriched microdomains (TEMs). *PLoS One,* 3**,** e3313.

SPRING, F. A., GRIFFITHS, R. E., MANKELOW, T. J., AGNEW, C., PARSONS, S. F., CHASIS, J. A. & ANSTEE, D. J. 2013. Tetraspanins CD81 and CD82 facilitate alpha4beta1-mediated

adhesion of human erythroblasts to vascular cell adhesion molecule-1. *PLoS One,* 8**,** e62654.

SRIDHAR, S. C. & MIRANTI, C. K. 2006. Tetraspanin KAI1/CD82 suppresses invasion by inhibiting integrin-dependent crosstalk with c-Met receptor and Src kinases. *Oncogene,* 25**,** 2367-78.

STERLING, H., SAGINARIO, C. & VIGNERY, A. 1998. CD44 occupancy prevents macrophage multinucleation. *J Cell Biol,* 143**,** 837-47.

STEVENS, J. M., ULRICH, R. L., TAYLOR, L. A., WOOD, M. W., DESHAZER, D., STEVENS, M. P. & GALYOV, E. E. 2005a. Actin-binding proteins from Burkholderia mallei and Burkholderia thailandensis can functionally compensate for the actin-based motility defect of a Burkholderia pseudomallei bimA mutant. *J Bacteriol,* 187**,** 7857-62.

STEVENS, M. P., FRIEBEL, A., TAYLOR, L. A., WOOD, M. W., BROWN, P. J., HARDT, W. D. & GALYOV, E. E. 2003. A Burkholderia pseudomallei type III secreted protein, BopE, facilitates bacterial invasion of epithelial cells and exhibits guanine nucleotide exchange factor activity. *J Bacteriol,* 185**,** 4992-6.

STEVENS, M. P., HAQUE, A., ATKINS, T., HILL, J., WOOD, M. W., EASTON, A., NELSON, M., UNDERWOOD-FOWLER, C., TITBALL, R. W., BANCROFT, G. J. & GALYOV, E. E. 2004. Attenuated virulence and protective efficacy of a Burkholderia pseudomallei bsa type III secretion mutant in murine models of melioidosis. *Microbiology,* 150**,** 2669-76.

STEVENS, M. P., STEVENS, J. M., JENG, R. L., TAYLOR, L. A., WOOD, M. W., HAWES, P., MONAGHAN, P., WELCH, M. D. & GALYOV, E. E. 2005b. Identification of a bacterial factor required for actin-based motility of Burkholderia pseudomallei. *Mol Microbiol,* 56**,** 40-53.

STIPP, C. S., KOLESNIKOVA, T. V. & HEMLER, M. E. 2001. EWI-2 is a major CD9 and CD81 partner and member of a novel Ig protein subfamily. *J Biol Chem,* 276**,** 40545-54.

STIPP, C. S., KOLESNIKOVA, T. V. & HEMLER, M. E. 2003. Functional domains in tetraspanin proteins. *Trends Biochem Sci,* 28**,** 106-12.

SUAREZ-MORENO, Z. R., CABALLERO-MELLADO, J., COUTINHO, B. G., MENDONCA-PREVIATO, L., JAMES, E. K. & VENTURI, V. 2012. Common features of environmental and potentially beneficial plant-associated Burkholderia. *Microb Ecol,* 63**,** 249-66.

SUN, G. W. & GAN, Y. H. 2010. Unraveling type III secretion systems in the highly versatile Burkholderia pseudomallei. *Trends Microbiol,* 18**,** 561-8.

SUN, T. T., ZHAO, H., PROVET, J., AEBI, U. & WU, X. R. 1996. Formation of asymmetric unit membrane during urothelial differentiation. *Mol Biol Rep,* 23**,** 3-11.

SUNDSTROM, C. & NILSSON, K. 1976. Establishment and characterization of a human histiocytic lymphoma cell line (U-937). *Int J Cancer,* 17**,** 565-77.

SUPARAK, S., KESPICHAYAWATTANA, W., HAQUE, A., EASTON, A., DAMNIN, S., LERTMEMONGKOLCHAI, G., BANCROFT, G. J. & KORBSRISATE, S. 2005. Multinucleated giant cell formation and apoptosis in infected host cells is mediated by Burkholderia pseudomallei type III secretion protein BipB. *J Bacteriol,* 187**,** 6556-60.

SUPARAK, S., MUANGSOMBUT, V., RIYAPA, D., STEVENS, J. M., STEVENS, M. P., LERTMEMONGKOLCHAI, G. & KORBSRISATE, S. 2011. Burkholderia pseudomallei-induced cell fusion in U937 macrophages can be inhibited by monoclonal antibodies against host cell surface molecules. *Microbes Infect,* 13**,** 1006-11.

SUZUKI, K., ZHU, B., RITTLING, S. R., DENHARDT, D. T., GOLDBERG, H. A., MCCULLOCH, C. A. & SODEK, J. 2002. Colocalization of intracellular osteopontin with CD44 is associated with migration, cell fusion, and resorption in osteoclasts. *J Bone Miner Res,* 17**,** 1486-97.

SUZUKI, M., TACHIBANA, I., TAKEDA, Y., HE, P., MINAMI, S., IWASAKI, T., KIDA, H., GOYA, S., KIJIMA, T., YOSHIDA, M., KUMAGAI, T., OSAKI, T. & KAWASE, I. 2009. Tetraspanin CD9 negatively regulates lipopolysaccharide-induced macrophage activation and lung inflammation. *J Immunol,* 182**,** 6485-93.

SWERLICK, R. A., LEE, K. H., WICK, T. M. & LAWLEY, T. J. 1992. Human dermal microvascular endothelial but not human umbilical vein endothelial cells express CD36 in vivo and in vitro. *J Immunol,* 148**,** 78-83.

SYMEONIDES, M., LAMBELE, M., ROY, N. H. & THALI, M. 2014. Evidence showing that tetraspanins inhibit HIV-1-induced cell-cell fusion at a post-hemifusion stage. *Viruses,* 6**,** 1078-90.

SZOLLOSI, J., HOREJSI, V., BENE, L., ANGELISOVA, P. & DAMJANOVICH, S. 1996. Supramolecular complexes of MHC class I, MHC class II, CD20, and tetraspan molecules (CD53, CD81, and CD82) at the surface of a B cell line JY. *J Immunol,* 157**,** 2939-46.

TABATA, N., ITO, M., SHIMOKATA, K., SUGA, S., OHGIMOTO, S., TSURUDOME, M., KAWANO, M., MATSUMURA, H., KOMADA, H., NISHIO, M. & ET AL. 1994. Expression of fusion regulatory proteins (FRPs) on human peripheral blood monocytes. Induction of homotypic cell aggregation and formation of multinucleated giant cells by anti-FRP-1 monoclonal antibodies. *J Immunol,* 153**,** 3256-66.

TACHIBANA, I. & HEMLER, M. E. 1999. Role of transmembrane 4 superfamily (TM4SF) proteins CD9 and CD81 in muscle cell fusion and myotube maintenance. *J Cell Biol,* 146**,** 893-904.

TAKAHASHI, Y., BIGLER, D., ITO, Y. & WHITE, J. M. 2001. Sequence-specific interaction between the disintegrin domain of mouse ADAM 3 and murine eggs: role of beta1 integrin-associated proteins CD9, CD81, and CD98. *Mol Biol Cell,* 12**,** 809-20.

TAKAI, Y., IRIE, K., SHIMIZU, K., SAKISAKA, T. & IKEDA, W. 2003. Nectins and nectin-like molecules: roles in cell adhesion, migration, and polarization. *Cancer Sci,* 94**,** 655-67.

TAKAI, Y., MIYOSHI, J., IKEDA, W. & OGITA, H. 2008. Nectins and nectin-like molecules: roles in contact inhibition of cell movement and proliferation. *Nat Rev Mol Cell Biol,* 9**,** 603-15.

TAKAI, Y. & NAKANISHI, H. 2003. Nectin and afadin: novel organizers of intercellular junctions. *J Cell Sci,* 116**,** 17-27.

TAKASHIMA, T., OHNISHI, K., TSUYUGUCHI, I. & KISHIMOTO, S. 1993. Differential regulation of formation of multinucleated giant cells from concanavalin A-stimulated human blood monocytes by IFN-gamma and IL-4. *J Immunol,* 150**,** 3002-10.

TAKEDA, Y., LI, Q., KAZAROV, A. R., EPARDAUD, M., ELPEK, K., TURLEY, S. J. & HEMLER, M. E. 2011. Diminished metastasis in tetraspanin CD151-knockout mice. *Blood,* 118**,** 464-72.

TAKEDA, Y., TACHIBANA, I., MIYADO, K., KOBAYASHI, M., MIYAZAKI, T., FUNAKOSHI, T., KIMURA, H., YAMANE, H., SAITO, Y., GOTO, H., YONEDA, T., YOSHIDA, M., KUMAGAI, T., OSAKI, T., HAYASHI, S., KAWASE, I. & MEKADA, E. 2003. Tetraspanins CD9 and CD81 function to prevent the fusion of mononuclear phagocytes. *J Cell Biol,* 161**,** 945-56.

TAKITO, J. & NAKAMURA, M. 2012. Precursors linked via the zipper-like structure or the filopodium during the secondary fusion of osteoclasts. *Commun Integr Biol,* 5**,** 453-7.

TAKITO, J., NAKAMURA, M., YODA, M., TOHMONDA, T., UCHIKAWA, S., HORIUCHI, K., TOYAMA, Y. & CHIBA, K. 2012. The transient appearance of zipper-like actin superstructures during the fusion of osteoclasts. *J Cell Sci,* 125**,** 662-72.

TALBOT, P., SHUR, B. D. & MYLES, D. G. 2003. Cell adhesion and fertilization: steps in oocyte transport, sperm-zona pellucida interactions, and sperm-egg fusion. *Biol Reprod,* 68**,** 1-9.

TALLE, M. A., RAO, P. E., WESTBERG, E., ALLEGAR, N., MAKOWSKI, M., MITTLER, R. S. & GOLDSTEIN, G. 1983. Patterns of antigenic expression on human monocytes as defined by monoclonal antibodies. *Cell Immunol,* 78**,** 83-99.

TAN, G. Y., LIU, Y., SIVALINGAM, S. P., SIM, S. H., WANG, D., PAUCOD, J. C., GAUTHIER, Y. & OOI, E. E. 2008. Burkholderia pseudomallei aerosol infection results in differential inflammatory responses in BALB/c and C57Bl/6 mice. *J Med Microbiol,* 57**,** 508-15.

TANAKA, A. & EMORI, K. 1980. Epithelioid granuloma formation by a synthetic bacterial cell wall component, muramyl dipeptide (MDP). *Am J Pathol,* 98**,** 733-48.

TANNER, F. C., BOEHM, M., AKYUREK, L. M., SAN, H., YANG, Z. Y., TASHIRO, J., NABEL, G. J. & NABEL, E. G. 2000. Differential effects of the cyclin-dependent kinase inhibitors p27(Kip1), p21(Cip1), and p16(Ink4) on vascular smooth muscle cell proliferation. *Circulation,* 101**,** 2022-5.

TARRANT, J. M., GROOM, J., METCALF, D., LI, R., BOROBOKAS, B., WRIGHT, M. D., TARLINTON, D. & ROBB, L. 2002. The absence of Tssc6, a member of the tetraspanin superfamily, does not affect lymphoid development but enhances in vitro T-cell proliferative responses. *Mol Cell Biol,* 22**,** 5006-18.

TARRANT, J. M., ROBB, L., VAN SPRIEL, A. B. & WRIGHT, M. D. 2003. Tetraspanins: molecular organisers of the leukocyte surface. *Trends Immunol,* 24**,** 610-7.

TEITELBAUM, S. L. 2006. Osteoclasts; culprits in inflammatory osteolysis. *Arthritis Res Ther,* 8**,** 201.

TERMINI, C. M., COTTER, M. L., MARJON, K. D., BURANDA, T., LIDKE, K. A. & GILLETTE, J. M. 2014. The membrane scaffold CD82 regulates cell adhesion by altering alpha4 integrin stability and molecular density. *Mol Biol Cell,* 25**,** 1560-73.

THAM, T. N., GOUIN, E., RUBINSTEIN, E., BOUCHEIX, C., COSSART, P. & PIZARRO-CERDA, J. 2010. Tetraspanin CD81 is required for Listeria monocytogenes invasion. *Infect Immun,* 78**,** 204-9.

TIMPE, J. M. & MCKEATING, J. A. 2008. Hepatitis C virus entry: possible targets for therapy. *Gut,* 57**,** 1728-37.

TITBALL, R. W., RUSSELL, P., CUCCUI, J., EASTON, A., HAQUE, A., ATKINS, T., SARKAR-TYSON, M., HARLEY, V., WREN, B. & BANCROFT, G. J. 2008. Burkholderia pseudomallei: animal models of infection. *Trans R Soc Trop Med Hyg,* 102 Suppl 1**,** S111-6.

TODD, S. C., LIPPS, S. G., CRISA, L., SALOMON, D. R. & TSOUKAS, C. D. 1996. CD81 expressed on human thymocytes mediates integrin activation and interleukin 2-dependent proliferation. *J Exp Med,* 184**,** 2055-60.

TODRES, E., NARDI, J. B. & ROBERTSON, H. M. 2000. The tetraspanin superfamily in insects. *Insect Mol Biol,* 9**,** 581-90.

TOESCA, I. J., FRENCH, C. T. & MILLER, J. F. 2014. The Type VI secretion system spike protein VgrG5 mediates membrane fusion during intercellular spread by pseudomallei group Burkholderia species. *Infect Immun,* 82**,** 1436-44.

TONOLI, H. & BARRETT, J. C. 2005. CD82 metastasis suppressor gene: a potential target for new therapeutics? *Trends Mol Med,* 11**,** 563-70.

TOYO-OKA, K., YASHIRO-OHTANI, Y., PARK, C. S., TAI, X. G., MIYAKE, K., HAMAOKA, T. & FUJIWARA, H. 1999. Association of a tetraspanin CD9 with CD5 on the T cell surface: role of particular transmembrane domains in the association. *Int Immunol,* 11**,** 2043-52.

TRAINI, M., QUINN, C. M., SANDOVAL, C., JOHANSSON, E., SCHRODER, K., KOCKX, M., MEIKLE, P. J., JESSUP, W. & KRITHARIDES, L. 2014. Sphingomyelin

phosphodiesterase acid-like 3A (SMPDL3A) is a novel nucleotide phosphodiesterase regulated by cholesterol in human macrophages. *J Biol Chem,* 289**,** 32895-913.

TSAI, Y. C. & WEISSMAN, A. M. 2011. Dissecting the diverse functions of the metastasis suppressor CD82/KAI1. *FEBS Lett,* 585**,** 3166-73.

TSITSIKOV, E. N., GUTIERREZ-RAMOS, J. C. & GEHA, R. S. 1997. Impaired CD19 expression and signaling, enhanced antibody response to type II T independent antigen and reduction of B-1 cells in CD81-deficient mice. *Proc Natl Acad Sci U S A,* 94**,** 10844-9.

TSUCHIYA, S., YAMABE, M., YAMAGUCHI, Y., KOBAYASHI, Y., KONNO, T. & TADA, K. 1980. Establishment and characterization of a human acute monocytic leukemia cell line (THP-1). *Int J Cancer,* 26**,** 171-6.

UFIMTSEVA, E. 2015. Mycobacterium-Host Cell Relationships in Granulomatous Lesions in a Mouse Model of Latent Tuberculous Infection. *Biomed Res Int,* 2015**,** 948131.

ULETT, G. C., CURRIE, B. J., CLAIR, T. W., MAYO, M., KETHEESAN, N., LABROOY, J., GAL, D., NORTON, R., SMITH, C. A., BARNES, J., WARNER, J. & HIRST, R. G. 2001. Burkholderia pseudomallei virulence: definition, stability and association with clonality. *Microbes Infect,* 3**,** 621-31.

ULETT, G. C., KETHEESAN, N., CLAIR, T. W., MCELNEA, C. L., BARNES, J. L. & HIRST, R. G. 2002. Analogous cytokine responses to Burkholderia pseudomallei strains contrasting in virulence correlate with partial cross-protection in immunized mice. *Infect Immun,* 70**,** 3953-8.

UTAISINCHAROEN, P., ARJCHAROEN, S., LIMPOSUWAN, K., TUNGPRADABKUL, S. & SIRISINHA, S. 2006. Burkholderia pseudomallei RpoS regulates multinucleated giant cell formation and inducible nitric oxide synthase expression in mouse macrophage cell line (RAW 264.7). *Microb Pathog,* 40**,** 184-9.

UTAISINCHAROEN, P., TANGTHAWORNCHAIKUL, N., KESPICHAYAWATTANA, W., CHAISURIYA, P. & SIRISINHA, S. 2001. Burkholderia pseudomallei interferes with inducible nitric oxide synthase (iNOS) production: a possible mechanism of evading macrophage killing. *Microbiol Immunol,* 45**,** 307-13.

VAN DER WINDT, G. J., FLORQUIN, S., DE VOS, A. F., VAN'T VEER, C., QUEIROZ, K. C., LIANG, J., JIANG, D., NOBLE, P. W. & VAN DER POLL, T. 2010. CD44 deficiency is associated with increased bacterial clearance but enhanced lung inflammation during Gram-negative pneumonia. *Am J Pathol,* 177**,** 2483-94.

VAN SPRIEL, A. B. & FIGDOR, C. G. 2010. The role of tetraspanins in the pathogenesis of infectious diseases. *Microbes Infect,* 12**,** 106-12.

VAN SPRIEL, A. B., SOFI, M., GARTLAN, K. H., VAN DER SCHAAF, A., VERSCHUEREN, I., TORENSMA, R., RAYMAKERS, R. A., LOVELAND, B. E., NETEA, M. G., ADEMA, G. J., WRIGHT, M. D. & FIGDOR, C. G. 2009. The tetraspanin protein CD37 regulates IgA responses and anti-fungal immunity. *PLoS Pathog,* 5**,** e1000338.

VAN ZELM, M. C., SMET, J., ADAMS, B., MASCART, F., SCHANDENE, L., JANSSEN, F., FERSTER, A., KUO, C. C., LEVY, S., VAN DONGEN, J. J. & VAN DER BURG, M. 2010. CD81 gene defect in humans disrupts CD19 complex formation and leads to antibody deficiency. *J Clin Invest,* 120**,** 1265-74.

VERGUNST, A. C., MEIJER, A. H., RENSHAW, S. A. & O'CALLAGHAN, D. 2010. Burkholderia cenocepacia creates an intramacrophage replication niche in zebrafish embryos, followed by bacterial dissemination and establishment of systemic infection. *Infect Immun,* 78**,** 1495-508.

VIGNERY, A. 2005. Macrophage fusion: are somatic and cancer cells possible partners? *Trends Cell Biol,* 15**,** 188-93.

VISCHER, U. M. & WAGNER, D. D. 1993. CD63 is a component of Weibel-Palade bodies of human endothelial cells. *Blood,* 82**,** 1184-91.

VON LINDERN, J. J., ROJO, D., GROVIT-FERBAS, K., YERAMIAN, C., DENG, C., HERBEIN, G., FERGUSON, M. R., PAPPAS, T. C., DECKER, J. M., SINGH, A., COLLMAN, R. G. & O'BRIEN, W. A. 2003. Potential role for CD63 in CCR5-mediated human immunodeficiency virus type 1 infection of macrophages. *J Virol,* 77**,** 3624-33.

WAND, M. E., MULLER, C. M., TITBALL, R. W. & MICHELL, S. L. 2011. Macrophage and Galleria mellonella infection models reflect the virulence of naturally occurring isolates of B. pseudomallei, B. thailandensis and B. oklahomensis. *BMC Microbiol,* 11**,** 11.

WANG, R., SUN, X., WANG, C. Y., HU, P., CHU, C. Y., LIU, S., ZHAU, H. E. & CHUNG, L. W. 2012. Spontaneous cancer-stromal cell fusion as a mechanism of prostate cancer androgen-independent progression. *PLoS One,* 7**,** e42653.

WARAWA, J. & WOODS, D. E. 2005. Type III secretion system cluster 3 is required for maximal virulence of Burkholderia pseudomallei in a hamster infection model. *FEMS Microbiol Lett,* 242**,** 101-8.

WEI, Q., ZHANG, F., RICHARDSON, M. M., ROY, N. H., RODGERS, W., LIU, Y., ZHAO, W., FU, C., DING, Y., HUANG, C., CHEN, Y., SUN, Y., DING, L., HU, Y., MA, J. X., BOULTON, M. E., PASULA, S., WREN, J. D., TANAKA, S., HUANG, X., THALI, M., HAMMERLING, G. J. & ZHANG, X. A. 2014. CD82 restrains pathological angiogenesis by altering lipid raft clustering and CD44 trafficking in endothelial cells. *Circulation,* 130**,** 1493-504.

WENG, J., KREMENTSOV, D. N., KHURANA, S., ROY, N. H. & THALI, M. 2009. Formation of syncytia is repressed by tetraspanins in human immunodeficiency virus type 1-producing cells. *J Virol,* 83**,** 7467-74.

WEST, T. E., ERNST, R. K., JANSSON-HUTSON, M. J. & SKERRETT, S. J. 2008. Activation of Toll-like receptors by Burkholderia pseudomallei. *BMC Immunol,* 9**,** 46.

WIERSINGA, W. J., CURRIE, B. J. & PEACOCK, S. J. 2012. Melioidosis. *N Engl J Med,* 367**,** 1035-44.

WIERSINGA, W. J., DE VOS, A. F., DE BEER, R., WIELAND, C. W., ROELOFS, J. J., WOODS, D. E. & VAN DER POLL, T. 2008. Inflammation patterns induced by different Burkholderia species in mice. *Cell Microbiol,* 10**,** 81-7.

WIERSINGA, W. J., VAN DER POLL, T., WHITE, N. J., DAY, N. P. & PEACOCK, S. J. 2006. Melioidosis: insights into the pathogenicity of Burkholderia pseudomallei. *Nat Rev Microbiol,* 4**,** 272-82.

WIERSINGA, W. J., WIELAND, C. W., DESSING, M. C., CHANTRATITA, N., CHENG, A. C., LIMMATHUROTSAKUL, D., CHIERAKUL, W., LEENDERTSE, M., FLORQUIN, S., DE VOS, A. F., WHITE, N., DONDORP, A. M., DAY, N. P., PEACOCK, S. J. & VAN DER POLL, T. 2007. Toll-like receptor 2 impairs host defense in gram-negative sepsis caused by Burkholderia pseudomallei (Melioidosis). *PLoS Med,* 4**,** e248.

WILLETT, B., HOSIE, M., SHAW, A. & NEIL, J. 1997. Inhibition of feline immunodeficiency virus infection by CD9 antibody operates after virus entry and is independent of virus tropism. *J Gen Virol,* 78 (Pt 3)**,** 611-8.

WITTEVELDT, J., EVANS, M. J., BITZEGEIO, J., KOUTSOUDAKIS, G., OWSIANKA, A. M., ANGUS, A. G., KECK, Z. Y., FOUNG, S. K., PIETSCHMANN, T., RICE, C. M. & PATEL, A. H. 2009. CD81 is dispensable for hepatitis C virus cell-to-cell transmission in hepatoma cells. *J Gen Virol,* 90**,** 48-58.

WONG, K. T., PUTHUCHEARY, S. D. & VADIVELU, J. 1995. The histopathology of human melioidosis. *Histopathology,* 26**,** 51-5.

WONG, L., ZHOU, J., ANDERSON, D. & KRATZKE, R. A. 2002. Inactivation of p16INK4a expression in malignant mesothelioma by methylation. *Lung Cancer,* 38**,** 131-6.

WRIGHT, M. D., GEARY, S. M., FITTER, S., MOSELEY, G. W., LAU, L. M., SHENG, K. C., APOSTOLOPOULOS, V., STANLEY, E. G., JACKSON, D. E. & ASHMAN, L. K. 2004.

Characterization of mice lacking the tetraspanin superfamily member CD151. *Mol Cell Biol,* 24**,** 5978-88.

WRIGHT, M. D. & TOMLINSON, M. G. 1994. The ins and outs of the transmembrane 4 superfamily. *Immunol Today,* 15**,** 588-94.

WU, X. R., SUN, T. T. & MEDINA, J. J. 1996. In vitro binding of type 1-fimbriated Escherichia coli to uroplakins Ia and Ib: relation to urinary tract infections. *Proc Natl Acad Sci U S A,* 93**,** 9630-5.

XIE, B., ZHOU, G., CHAN, S. Y., SHAPIRO, E., KONG, X. P., WU, X. R., SUN, T. T. & COSTELLO, C. E. 2006. Distinct glycan structures of uroplakins Ia and Ib: structural basis for the selective binding of FimH adhesin to uroplakin Ia. *J Biol Chem,* 281**,** 14644-53.

YAGI, M., MIYAMOTO, T., SAWATANI, Y., IWAMOTO, K., HOSOGANE, N., FUJITA, N., MORITA, K., NINOMIYA, K., SUZUKI, T., MIYAMOTO, K., OIKE, Y., TAKEYA, M., TOYAMA, Y. & SUDA, T. 2005. DC-STAMP is essential for cell-cell fusion in osteoclasts and foreign body giant cells. *J Exp Med,* 202**,** 345-51.

YAGI, M., NINOMIYA, K., FUJITA, N., SUZUKI, T., IWASAKI, R., MORITA, K., HOSOGANE, N., MATSUO, K., TOYAMA, Y., SUDA, T. & MIYAMOTO, T. 2007. Induction of DC-STAMP by alternative activation and downstream signaling mechanisms. *J Bone Miner Res,* 22**,** 992-1001.

YALAOUI, S., ZOUGBEDE, S., CHARRIN, S., SILVIE, O., ARDUISE, C., FARHATI, K., BOUCHEIX, C., MAZIER, D., RUBINSTEIN, E. & FROISSARD, P. 2008. Hepatocyte permissiveness to Plasmodium infection is conveyed by a short and structurally conserved region of the CD81 large extracellular domain. *PLoS Pathog,* 4**,** e1000010.

YAMANE, H., TACHIBANA, I., TAKEDA, Y., SAITO, Y., TAMURA, Y., HE, P., SUZUKI, M., SHIMA, Y., YONEDA, T., HOSHINO, S., INOUE, K., KIJIMA, T., YOSHIDA, M., KUMAGAI, T., OSAKI, T., EISHI, Y. & KAWASE, I. 2005. Propionibacterium acnes-induced hepatic granuloma formation is impaired in mice lacking tetraspanin CD9. *J Pathol,* 206**,** 486-92.

YAN, J., WU, B., HUANG, B., HUANG, S., JIANG, S. & LU, F. 2014. Dectin-1-CD37 association regulates IL-6 expression during Toxoplasma gondii infection. *Parasitol Res,* 113**,** 2851-60.

YANEZ-MO, M., BARREIRO, O., GORDON-ALONSO, M., SALA-VALDES, M. & SANCHEZ-MADRID, F. 2009. Tetraspanin-enriched microdomains: a functional unit in cell plasma membranes. *Trends Cell Biol,* 19**,** 434-46.

YASHIRO-OHTANI, Y., ZHOU, X. Y., TOYO-OKA, K., TAI, X. G., PARK, C. S., HAMAOKA, T., ABE, R., MIYAKE, K. & FUJIWARA, H. 2000. Non-CD28 costimulatory molecules present in T cell rafts induce T cell costimulation by enhancing the association of TCR with rafts. *J Immunol,* 164**,** 1251-9.

YAUCH, R. L., KAZAROV, A. R., DESAI, B., LEE, R. T. & HEMLER, M. E. 2000. Direct extracellular contact between integrin alpha(3)beta(1) and TM4SF protein CD151. *J Biol Chem,* 275**,** 9230-8.

YI, T., KIM, H. J., CHO, J. Y., WOO, K. M., RYOO, H. M., KIM, G. S. & BAEK, J. H. 2006. Tetraspanin CD9 regulates osteoclastogenesis via regulation of p44/42 MAPK activity. *Biochem Biophys Res Commun,* 347**,** 178-84.

YU, Y., KIM, H. S., CHUA, H. H., LIN, C. H., SIM, S. H., LIN, D., DERR, A., ENGELS, R., DESHAZER, D., BIRREN, B., NIERMAN, W. C. & TAN, P. 2006. Genomic patterns of pathogen evolution revealed by comparison of Burkholderia pseudomallei, the causative agent of melioidosis, to avirulent Burkholderia thailandensis. *BMC Microbiol,* 6**,** 46.

ZHOU, G., MO, W. J., SEBBEL, P., MIN, G., NEUBERT, T. A., GLOCKSHUBER, R., WU, X. R., SUN, T. T. & KONG, X. P. 2001. Uroplakin Ia is the urothelial receptor for

uropathogenic Escherichia coli: evidence from in vitro FimH binding. *J Cell Sci,* 114**,** 4095-103.

ZHOU, G. B., LIU, G. S., MENG, Q. G., LIU, Y., HOU, Y. P., WANG, X. X., LI, N. & ZHU, S. E. 2009. Tetraspanin CD9 in bovine oocytes and its role in fertilization. *J Reprod Dev,* 55**,** 305-8.

ZHU, G. Z., MILLER, B. J., BOUCHEIX, C., RUBINSTEIN, E., LIU, C. C., HYNES, R. O., MYLES, D. G. & PRIMAKOFF, P. 2002. Residues SFQ (173-175) in the large extracellular loop of CD9 are required for gamete fusion. *Development,* 129**,** 1995-2002.

ZIYYAT, A., RUBINSTEIN, E., MONIER-GAVELLE, F., BARRAUD, V., KULSKI, O., PRENANT, M., BOUCHEIX, C., BOMSEL, M. & WOLF, J. P. 2006. CD9 controls the formation of clusters that contain tetraspanins and the integrin alpha 6 beta 1, which are involved in human and mouse gamete fusion. *J Cell Sci,* 119**,** 416-24.

ZUGHAIER, S. M., RYLEY, H. C. & JACKSON, S. K. 1999. Lipopolysaccharide (LPS) from Burkholderia cepacia is more active than LPS from Pseudomonas aeruginosa and Stenotrophomonas maltophilia in stimulating tumor necrosis factor alpha from human monocytes. *Infect Immun,* 67**,** 1505-7.

ZUIDSCHERWOUDE, M., GOTTFERT, F., DUNLOCK, V. M., FIGDOR, C. G., VAN DEN BOGAART, G. & VAN SPRIEL, A. B. 2015. The tetraspanin web revisited by super-resolution microscopy. *Sci Rep,* 5**,** 12201.